

**Decellularisation of the Dental Pulp for Use as a
Scaffold in Regenerative Endodontics**

Manal Matoug-Elwerfelli

Submitted in accordance with the requirements for the degree of Doctor
of Philosophy

The University of Leeds

School of Dentistry

November 2017

The candidate confirms that the work submitted is their own, except where work which has formed part of jointly authored publications has been included. The contribution of the candidate and the other authors to this work has been explicitly indicated below. The candidate confirms that appropriate credit has been given within the thesis where reference has been made to the work of others.

This thesis contains work from a jointly-authored publication:

Matoug-Elwerfelli, M., Duggal, M.S., Nazzal, H., Esteves, F. & Raïf, E. A biocompatible decellularized pulp scaffold for regenerative endodontics. *International Endodontic Journal*, 2018; DOI: 10.1111/iej.12882.

I was responsible for all the laboratory work and drafting a publication manuscript. The remaining co-authors provided guidance on the final editing and layout of the publication.

This copy has been supplied on the understanding that it is copyright material and that no quotation from the thesis may be published without proper acknowledgement.

The right of Manal Matoug-Elwerfelli to be identified as Author of this work has been asserted by her in accordance with the Copyright, Designs and Patents Act 1988.

© 2017 The University of Leeds and Manal Matoug-Elwerfelli

Acknowledgements

Foremost, I am very grateful to GOD who gave me blessing, strength, and patience to complete this work.

I would like to offer my sincere gratitude and appreciation to my supervisors Professor Monty Duggal, Dr El-Mostafa Raif, and Dr Hani Nazzal for their advice, guidance, and continuous support throughout my journey. I am grateful for your motivation and the opportunities you gave me to fulfil my full academic potential.

I would also like to extend my sincere gratitude and appreciation to Dr Stacy-Paul Wilshaw and Dr Filomena Esteves, who have offered me unconditional support during this journey. Dr Wilshaw, I would like to thank you for sharing with me your vast knowledge in regards to tissue decellularisation, cytotoxicity assays, the use of the polarised and inverted microscope in your laboratory. Dr Esteves, I would like to thank you for the immunohistochemistry training, trouble shooting techniques, and many more. The experience, knowledge and critical advice you both gave me will always be with me.

Extended thanks goes to Mrs Jaqueline Hudson for the training in several aspects including; general laboratory usage, histology, scanning electron, and confocal microscope. As a clinician, this was not easy, thank you for your patience. I would like to thank Dr. Matthew Thomlinson for his training on the extraction of human pulp tissue and dental pulp stem cells. Thanks to all patients for their consent and to all tissue bank staff who are involved in the collection and distribution of human teeth from the chair side to the laboratory. I would also like to thank Dr Steve Brookes for

his training on the extraction of rat pulp tissue. Thanks to all staff from the Animal House, Central Science Building, Mr Lan Chung, Mr Neil Crossley for providing me with the Wistar rats.

Extended thank and appreciation all staff and students at School of Dentistry, University of Leeds, you have all assisted me and made me feel very welcome.

Within the Oral Biology department, special thanks to Mrs Claire Godfrey, Mrs Ruth Kyman, Mrs Julie McDermott, Miss Sarah Myers, Mr Gregory Baugh for all their assistance in several areas including obtaining all documents required for ethical approval and teeth collection, consumable purchasing, conference booking, and many more. A big thank you to Prof David Wood, I will never forget the lost USB day!, thanks for helping me with my search. Dr Xubien Yang and Dr Simon wood for their supportive role as Postgraduate Tutors. Prof Jennifer Kirkham for her ongoing support and being their when needed.

From the Paediatric department, special thanks to Mrs Jinous Tahmassebi for her unlimited kindness and support. Thanks are also due to Mr Tim Zoltie, Mr Tom Archer, and all staff at the Photography department (School of dentistry, University of Leeds) for their continuous assistance.

I am also indebted to all my colleagues from both the Oral biology and Paediatric department for the great memories we have together. Especially Miss Jennifer Graham, Mrs. Aseel, Al-Jaboori, Miss Lucia Pontiroli, Miss Monika Naginyt, Mrs Shabnum Rashuid, Mrs Rasha Albannaa, Mr Kenny Man, Mrs Rina Osman Basah, Miss Claire Gabe, Mrs Hayat Alghutaimel, and many more, please forgive me if your

name is not here. Special thanks to Mr Ali Maria, Dr Liam Lawlor, Dr Alban Smith, Dr Reem El-Gendy, and Miss Rachel bell for their laboratory help and technology assistance.

I am also very grateful to the Libyan Government for the financial support to undertake my postgraduate studies.

Last but not least, special thanks to my parents, my husband, and sons for their continuous love and support at all times. I could not have accomplished this without you all.

Dedication

To my Mum and Dad

To my Husband (Abduraawf) and Sons (Laith and Sanad)

To my late Grandma, may her soul rest in peace

Abstract

Background: Endodontic management of immature necrotic permanent teeth is currently undergoing a paradigm shift from the conventional apexification and apical plug techniques to biological based regenerative procedures. The shift towards a tissue engineered clinical based procedure is highly attractive. However, the ideal scaffold to support pulp-dentine complex regeneration is yet to be identified.

Aim: The primary aim of this work was to develop, characterise, and assess the biocompatibility of an acellular extracellular matrix scaffold developed through decellularisation of rat and human dental pulp tissues. The secondary aim was to assess the ability of the scaffold to support human dental pulp stem cells attachment, viability, and differentiation.

Methods: Following ethical approval, rat and human dental pulps were retrieved and decellularised. The efficiency of the decellularised protocol was assessed using histology and immunohistochemistry staining methods, scanning electron microscopy, and DNA quantification assays. Contact and extract cytotoxicity assays were performed to determine the biocompatibility of the developed scaffold. Decellularised scaffolds were recellularised with human dental pulp stem cells and cell viability was assessed, for up to 14 days, in culture. Expression of odontoblastic markers and molecular proteins within the recellularised scaffold were also investigated. Quantitative data were analysed using Student's *t*-test and one-way analysis of variance using GraphPad Prism (Version 6).

Results: Assessment of decellularised scaffolds revealed an acellular matrix with preservation of the connective tissue architecture and composition. Acellular scaffolds were biocompatible with normal cell growth in direct contact with the acellular scaffold. No difference in cellular activity was found following incubation in acellular scaffold extracts ($p > 0.05$). Live/Dead[®] confocal imaging

showed high majority of viable cells. Furthermore, the scaffold was able to support human dental pulp stem cells viability and attachment following recellularisation. Immunolabelling of dental pulp stem cells within the recellularised scaffold revealed a positive expression against several tested odontoblastic markers and molecular proteins.

Conclusion: The decellularisation protocol used showed promising results following decellularisation of rat and human dental pulp tissues in terms of developing an acellular biological scaffold with preserved extracellular structural components required for tissue specific regeneration.

Table of Contents

Acknowledgements	iii
Dedication.....	vi
Abstract	vii
Table of Contents.....	ix
List of Figures	xiv
List of Tables.....	xviii
List of Abbreviations	xix
Chapter 1 Literature review.....	1
Introduction:	1
1.1 The dental pulp:.....	3
1.1.1 Dental pulp composition:.....	5
1.2 Pulpal necrosis in the developing child:.....	11
1.3 Endodontic management of immature teeth with pulpal necrosis:..	12
1.3.1 Calcium hydroxide apexification:.....	12
1.3.2 Apical plug techniques:	14
1.3.3 Regenerative endodontic procedures:	16
1.4 Tissue engineering of the dental pulp:.....	21
1.4.1 Stem cells for dental pulp tissue regeneration:.....	22
1.4.2 Signalling molecules for dental pulp tissue regeneration:	26
1.4.3 Scaffolds for dental pulp tissue regeneration:	27
1.5 Tissue decellularisation:	39
1.5.1 Tissue decellularisation process:	40
1.6 In summary:.....	45

1.7	Aim and objectives:	46
Chapter 2 General Materials and Methods		47
2.1	General materials:	47
2.1.1	Equipment and consumables:	47
2.1.2	Chemicals, reagents and kits:	50
2.1.3	Antibodies:	52
2.1.4	Isotype controls:	55
2.2	General methods:	56
2.2.1	Tissue procurement:	56
2.2.2	Tissue decellularisation:	57
2.2.3	General histological technique:	60
2.2.4	Histological staining methods:	62
2.2.5	Immunohistochemical labelling:	65
2.2.6	DNA quantification assay:	67
2.2.7	Scanning electron microscope:	69
2.2.8	Cell culture techniques:	69
2.2.9	Cytotoxicity evaluation:	73
2.2.10	Recellularisation of decellularised scaffold with dental pulp stem cells:	76
2.2.11	Cell viability assay:	77
2.2.12	Statistical analysis:	78
Chapter 3 Decellularisation of the dental pulp tissues.....		79
3.1	Introduction:	79
3.2	Aim and objectives:	83
3.2.1	Aim:	83

3.2.2	Objectives:	83
3.3	Methods and experimental approaches:.....	84
3.3.1	Experiment 1:.....	84
3.3.2	Experiment 2:.....	86
3.4	Results:	89
3.4.1	Results of experiment 1:	89
3.4.2	Results of experiment 2:	93
3.5	Discussion:	98
Chapter 4 Characterisation of the developed decellularised dental pulp tissue		103
4.1	Introduction:.....	103
4.2	Aim and objectives:	107
4.2.1	Aim:.....	107
4.2.2	Objectives:	107
4.3	Methods and experimental approaches:.....	108
4.3.1	Histology characterisation of rat and human pulp tissues: ..	108
4.3.2	Immunohistochemical labelling of rat and human pulp tissues:	
	108	
4.3.3	Scanning electron microscope evaluation:.....	109
4.4	Results:	110
4.4.1	Histological evaluation of native and decellularised dental pulp tissues:.....	110
4.4.2	Immunohistochemical evaluation of native and decellularised dental pulp tissues:	117
4.4.3	Scanning electron microscope evaluation:.....	132
4.5	Discussion:	135

Chapter 5 Cytotoxicity assessment and recellularisation of the decellularised scaffold	140
5.1 Introduction:.....	140
5.2 Aim and objectives:	145
5.2.1 Aim:.....	145
5.2.2 Objectives:	145
5.3 Methods and experimental approaches:.....	146
5.3.1 Cytotoxicity evaluation of decellularised rat and human scaffolds:.....	146
5.3.2 Cell seeding density:	148
5.3.3 Cell viability assay of rat and human scaffolds:.....	149
5.3.4 Recellularisation of rat scaffolds using DPSCs:	149
5.4 Results:	151
5.4.1 Cytotoxicity evaluation of decellularised rat and human scaffolds:.....	151
5.4.2 Cell viability assay of rat and human scaffolds:.....	155
5.4.3 Recellularisation of rat scaffolds using DPSCs:	157
5.5 Discussion:	170
Chapter 6 General discussion, future work, and conclusions	175
6.1 General discussion:.....	175
6.2 Conclusions:.....	189
6.3 Recommendations for future work and clinical translation:.....	190

References.....	197
Appendices.....	224
Appendix (A): Tissue bank approval form for teeth collection and the use of dental pulp stem cells.....	224
Appendix (B): Percentage of pulp tissue water content.....	225
Appendix (C): National and international poster/oral presentations and awards achieved.....	226

List of Figures

Figure 1.1: Histological zones of the native dental pulp.	4
Figure 1.2: Schematic illustration of tissue engineering elements.....	22
Figure 1.3: Schematic illustration of tooth derived stem cells.	25
Figure 2.1: DNA extraction protocol.	68
Figure 2.2: Seeding rotator apparatus.	77
Figure 3.1: Process flow diagram of decellularisation experiment 1.	85
Figure 3.2: Representative images of decellularised human pulp tissues....	86
Figure 3.3: Process flow diagram of decellularisation experiment 2.	88
Figure 3.4: Representative images of H&E stained human tissues viewed under the light microscope.	91
Figure 3.5: Representative images of DAPI stained human pulp tissues viewed under the fluorescent microscope.	92
Figure 3.6: Representative images of H&E stained rat pulp tissues viewed under the light microscope.	94
Figure 3.7: Representative images of DAPI stained rat pulp tissues viewed under the fluorescent microscope.	94
Figure 3.8: Representative images of H&E stained human pulp tissues viewed under the light microscope.	95
Figure 3.9: Representative images of DAPI stained human pulp tissues viewed under the fluorescent microscope.	95
Figure 3.10: DNA content of native and decellularised rat pulp tissue following DNA extraction determined by NanoDrop™ 2000 spectrophotometer.	97

Figure 3.11: DNA content of native and decellularised human pulp tissues following DNA extraction determined by NanoDrop™ 2000 spectrophotometer.....	97
Figure 4.1: Representative images of Alcian blue stained rat pulp tissues viewed under the light microscope.....	111
Figure 4.2: Representative images of Alcian blue stained human pulp tissues viewed under the light microscope.....	112
Figure 4.3: Representative images of Picrosirius red stained rat pulp tissues viewed under the light microscope.....	114
Figure 4.4: Representative images of Picrosirius red stained human pulp tissues viewed under the light microscope.....	114
Figure 4.5: Representative images of Picrosirius red stained rat pulp tissues viewed under polarised microscope.....	115
Figure 4.6: Representative images of Picrosirius red stained human pulp tissues viewed under the polarised microscope.....	116
Figure 4.7: Representative images of rat pulp tissues labelled with collagen type I antigen viewed under the light microscope.	118
Figure 4.8: Representative images of human pulp tissues labelled with collagen type I antigen viewed under the light microscope.	119
Figure 4.9: Representative images of rat pulp tissues labelled with collagen type III antigen viewed under the light microscope.	121
Figure 4.10: Representative images of human pulp tissues labelled with collagen type III antigen viewed under the light microscope.	122
Figure 4.11: Representative images of rat pulp tissues labelled with fibronectin antigen and viewed under the light microscope.....	124
Figure 4.12: Representative images of human pulp tissues labelled with fibronectin antigen and viewed under the light microscope.....	125

Figure 4.13: Representative images of rat pulp tissues labelled with laminin antigen viewed under the light microscope.	127
Figure 4.14: Representative images of human pulp tissues labelled with laminin antigen viewed under the light microscope.....	128
Figure 4.15: Representative images of rat pulp tissues labelled major histocompatibility complex class II antigen and viewed under the light microscope.....	130
Figure 4.16: Representative images of human pulp tissues labelled major histocompatibility complex class II antigen and viewed under the light microscope.....	131
Figure 4.17: Representative images of rat pulp tissues viewed using the scanning electron microscope.....	133
Figure 4.18: Representative images of human pulp tissues viewed using the scanning electron microscope.....	134
Figure 5.1: Optimisation of cell seeding density.....	149
Figure 5.2: Contact cytotoxicity assays of decellularised rat scaffolds cultured with L-929 cell line for 48 hours, stained with Giemsa stain and viewed under brightfield illumination.	152
Figure 5.3: Contact cytotoxicity assays of decellularised human scaffolds cultured with L-929 cell line for 48 hours, stained with Giemsa stain and viewed under brightfield illumination.	152
Figure 5.4: Controls used for contact cytotoxicity assays cultured with L-929 cell line for 48 hours, stained with Giemsa stain and viewed under brightfield illumination.	153
Figure 5.5: Extract cytotoxicity assay measuring the relative cellular ATP content of decellularised rat extracts following 24 hour culture.	154
Figure 5.6: Extract cytotoxicity assay measuring the relative cellular ATP content of decellularised human extracts following 24 hour culture.	155

Figure 5.7: Cell viability assay of decellularised rat scaffolds seeded with DPSCs and analysed with Live/Dead [®] stain using laser confocal microscopy.	156
Figure 5.8: Cell viability assay of decellularised human scaffolds seeded with DPSCs and analysed with Live/Dead [®] stain using laser confocal microscope.	156
Figure 5.9: Representative images of H&E stained recellularised rat scaffolds seeded with DPSCs following 7 days culture viewed under the light microscope.....	158
Figure 5.10: Representative images of H&E stained recellularised rat scaffolds seeded with DPSCs following 14 days culture viewed under the light microscope.	159
Figure 5.11: Representative images of recellularised rat scaffolds labelled with DSPP antigen and viewed under the light microscope.	161
Figure 5.12: Representative images of recellularised rat scaffolds labelled with DMP-1 antigen and viewed under the light microscope.....	162
Figure 5.13: Representative images of recellularised rat scaffolds labelled with ALP antigen and viewed under the light microscope.	163
Figure 5.14: Representative images of recellularised rat scaffolds labelled with vimentin antigen and viewed under the light microscope.	164
Figure 5.15: Representative images of recellularised rat scaffolds labelled with nestin antigen and viewed under the light microscope.	165
Figure 5.16: Representative images of recellularised rat scaffolds labelled with α -SMA antigen and viewed under the light microscope.....	166
Figure 5.17: Representative images of recellularised rat scaffolds labelled with VEGF-A antigen and viewed under the light microscope.	168
Figure 5.18: Representative images of recellularised rat scaffolds labelled with VEGFR-2 antigen and viewed under the light microscope.	169

List of Tables

Table 1.1: Classification of stem cells	24
Table 1.2: Classification of tooth derived stem cells	25
Table 1.3: Scaffold performance used for pulp-dentine complex regeneration	31
Table 2.1: General laboratory equipment used throughout the study	47
Table 2.2: General laboratory consumables used throughout the study	49
Table 2.3: Chemicals, reagents and kits used throughout the study	50
Table 2.4: Details of primary antibodies, the corresponding antigen retrieval method and isotypes used throughout the study.....	53
Table 2.5: Isotype controls used throughout the study.....	55
Table 2.6: Tissue processor protocol	61
Table 2.7: Cell types used throughout the study	70

List of Abbreviations

%	Percentage
°C	Degree Celsius
μ	Micron
μg	Microgram
μL	Microliter
μm	Micrometer
ALP	Alkaline phosphatase
ANOVA	Analysis of variance
Ca(OH)₂	Calcium hydroxide
Ca²⁺	Calcium
CO₂	Carbon dioxide
DAB	3,3` -diaminobenzidine
DAPI	4',6-diamidino-2-phenylindole
DMEM	Dulbecco's modified Eagle's medium
DMP-1	Dentine matrix protein-1
DMSO	Dimethyl sulfoxide
DNA	Deoxyribonucleic acid
DNase	Deoxyribonuclease
DPSCs	Dental pulp stem/stromal cells
DSPP	Dentine sialophosphoprotein
ECM	Extracellular matrix
EDTA	Ethylene-diamine-tetra-acetic acid
FBS	Foetal bovine serum

GAG	Glycosaminoglycan
H&E	Haematoxylin and eosin
HERS	Hertwig's epithelial root sheath
KIU	Kallikrein inhibitor unit
mg	Milligram
Mg²⁺	Magnesium
MHC	Major histocompatibility
mL	Milliliter
MTA	Mineral trioxide aggregate
PBS	Phosphate-buffered saline
RNA	Ribonucleic acid
RNase	Ribonuclease
rpm	Revolutions per minute
SAPs	Self-assembling peptides
SCAP	Stem cells from apical papilla
SDS	Sodium dodecyl sulphate
SEM	Scanning electron microscope
SHED	Stem cells from human exfoliated deciduous teeth
TBS	Tris-buffered saline
U	Units
VEGF	Vascular endothelial growth factor
VEGFR-2	Vascular endothelial growth factor receptor-2
α-gal	Alpha-1,3 Galactose
α-SMA	Alpha-smooth muscle actin

Chapter 1

Literature review

Introduction:

Endodontic management of immature permanent teeth with necrotic (non-vital) pulps is one of the challenging fields in paediatric dentistry. The clinical management of these teeth has evolved throughout the years. Conventional management included promoting a calcific apical barrier through the use of calcium hydroxide apexification or creating an artificial apical barrier using mainly Mineral Trioxide Aggregate (Duggal et al., 2017). Despite the clinical success of these techniques in the short term, these techniques do not contribute to any quantitative increase in root length or thickening of root dentinal walls (Petrino et al., 2010; Torabinejad and Abu-Tahun, 2010).

Recently, the field of dental tissue regeneration has emerged as a new area of research with huge potentials for dental pulp regeneration. Regenerative endodontic (revitalisation) procedures are increasingly used in the treatment of immature necrotic permanent teeth (Galler, 2016). Clinically this treatment involves root canal disinfection followed by inducing apical bleeding within the root canal space (Iwaya et al., 2001; Banchs and Trope, 2004). Unfortunately, the early optimism for using regenerative endodontic procedures in the management of immature necrotic teeth has now faded, due to the unpredictability in promoting continuation of root development and non-specific tissue formation (Jung et al., 2008; Chen et al., 2012; Nosrat et al., 2012).

Several reasons for these unpredictable results were suggested (Nazzal and Duggal, 2017) such as the effect of disinfectant on stem cells, effect of intracanal medicaments on stem cells, the lack of specific growth factors, and the controversial use of a blood clot as a scaffold (Ding et al., 2009; Petrino et al., 2010; Lenzi and Trope, 2012).

Therefore, development of regenerative endodontic procedures utilising more advanced tissue engineering principles has been recommended (Nör, 2006; Cordeiro et al., 2008; Garcia-Godoy and Murray, 2012; Conde et al., 2015) in order to guide cells for targeted regeneration of pulp tissues rather than healing as seen with the current procedures.

The selection of an appropriate scaffold is vital for successful tissue engineering. These scaffolds provide sites for cell adhesion, proliferation and differentiation. Various natural and synthetic scaffold materials have been tested in an attempt to regenerate the pulp-dentine complex, however, limited success has been reported. Limited control over newly formed tissue, low cell survival following implantation, toxicity and biocompatibility concerns still exists (Murray et al., 2007). To overcome previous material limitations, biological scaffolds composed of an acellular extracellular matrix developed through the process of decellularisation has been advocated (Gilbert et al., 2006; Crapo et al., 2011). The extracellular matrix is a vital and dynamic tissue component composed of structural and functional proteins and regarded as the ideal scaffold for tissue engineering (Badylak, 2002; Badylak et al., 2009).

1.1 The dental pulp:

Tooth formation occurs as a result of interaction between epithelium derived from the first branchial arch and ectomesenchymal cells of neural crest origin. Developmentally, tooth formation originates from the tooth germ. The tooth germ consists of two components: (i) The ectodermal component (enamel organ) which consequently forms enamel; (ii) The ectomesenchymal component (dental papilla and dental follicle). The dental papilla is responsible for dentine and pulp formation, while the dental follicle forms cementum and tooth supporting structures, the periodontal ligament (Kumar, 2014). Following formation, a dental tooth consists of three mineralised outer layers (enamel, dentine and cementum) surrounding a non-mineralised vital pulp tissue (Veis and Goldberg, 2014).

Structurally the dental pulp is a rich cellular, highly vascularised and innervated connective tissue. This unique structure contributes to several functions (Yu and Abbott, 2007; Pashley et al., 2008). Specialised cells of the pulp, the odontoblasts, have a unique ability to form dentine throughout life. These specialised cells together with the underlying blood supply provide nutrition to the dentine structure (Yu and Abbott, 2007). The pulp tissue also contains defence cells with the ability to initiate an immune reaction when required (Yu and Abbott, 2007).

Histologically and microscopically, the dental pulp is classically described as four zones or regions (Figure 1.1): (i) The odontoblastic (or more precisely the sub-odontoblastic) zone is the outermost layer adjacent to dentine and composed of cell bodies of the odontoblasts, capillaries, nerve fibres and

dendritic cells; (ii) The so-called cell free (Weil's) zone (now recognised as a fixation artefact) is located adjacent to the sub-odontoblastic zone, devoid of cells and transversed by plexuses of capillaries and nerve fibres; (iii) The cell rich zone is a highly cellular area located between the cell free zone and pulp core; (iv) The central pulp core (pulp proper) zone contains the principal support system namely large blood vessels, unmyelinated nerve trunks with collagen and ground substances forming the main connective tissue components of this zone (Pashley et al., 2008; Goldberg, 2014b; Goldberg, 2014a; Kumar, 2014).

The dental pulp is described as a specialised loose areolar connective tissue, principally composed of cells that secrete and organise its collagen rich extracellular matrix (ECM). Additional supportive elements include blood supply, lymphatic supply and nerve fibre bundles (Pashley et al., 2008; Goldberg, 2014b; Goldberg, 2014a; Kumar, 2014).

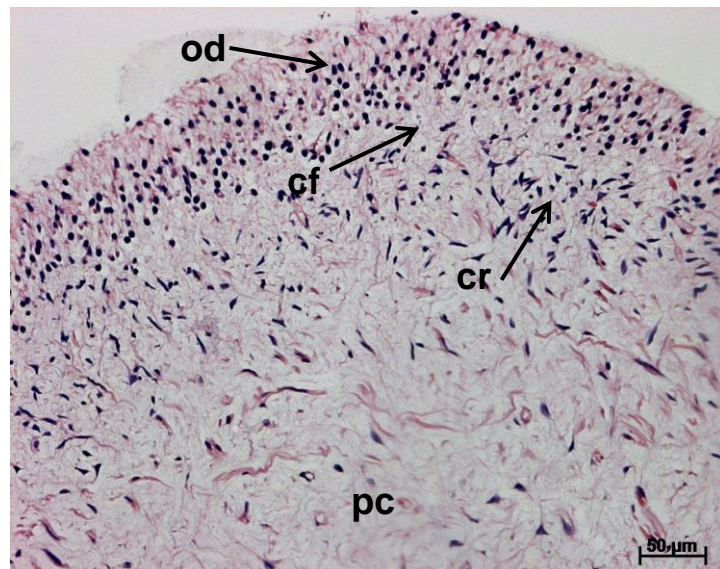


Figure 1.1: Histological zones of the native dental pulp. (od) Sub-odontoblastic layer, (cf) Cell free zone, (cr) Cell rich zone and (pc) Pulp core. Scale bar at 50 μm.

1.1.1 Dental pulp composition:

1.1.1.1 Cells of the dental pulp:

The pulpal tissue is occupied by two types of cells known as resident and non-resident cells. Non-resident cells form the minority of cells within the dental pulp. These originate or migrate from distant tissues and enter the pulp tissue through its apical part. In contrast, resident cells are considered the main type of pulp cells due to their important structural role in shaping the pulp tissue construction (Goldberg, 2014b), through the formation and turnover of the non-mineralised matrix (Goldberg and Smith, 2004).

Pulp fibroblasts (pulpoblasts) are the most abundant cell type of the dental pulp and are largely involved in the synthesis and secretion of collagen fibres and ECM components. Fibroblast cells are elongated spindle shaped cells with a large ovoid nucleus. They contain long protracted processes that connect with other fibroblasts through intercellular junctions, desmosome-like and gap junctions facilitating cellular communications (Goldberg and Smith, 2004; Pashley et al., 2008; Goldberg, 2014b; Kumar, 2014).

Odontoblastic cells are the second most numerous cell type of the dental pulp and are known to be involved in production of the dentine matrix, dentinogenesis. The odontoblasts' are consistently located in the odontoblastic region of the dental pulp and consist of cell bodies and cell processes. The cell processes extend across the pre-dentine and enter the dentinal tubules (Pashley et al., 2008; Goldberg, 2014b; Kumar, 2014).

Defence cells are equally important and present in the dental pulp, they are known to express major histocompatibility complex class II molecules (Jontell et al., 1987; Ohshima et al., 1999; Goldberg, 2014a). In the normal healthy pulp, these cells mainly include macrophages (histiocytes), dendritic cells and T-lymphocytes playing an important role in immune-surveillance of the pulp tissue. These immune cells phagocytose and eliminate bacteria and apoptotic bodies from the pulp tissue (Goldberg, 2014a).

A limited number of B-lymphocytes, eosinophils and mast cells are also present in the healthy pulp (Goldberg and Smith, 2004). Following pulp injury and inflammation a considerable change in the types of defence cells occurs. Increase numbers of B-lymphocytes, eosinophils, mast cells with the appearance of neutrophils and plasma cells become present in the inflamed pulp (Goldberg and Smith, 2004; Pashley et al., 2008; Goldberg, 2014b; Kumar, 2014).

Progenitor cells have also been isolated from the dental pulp tissue. Within the dental pulp, these cells represent a small population of undifferentiated stem cells accounting for approximately 1 – 2 % of total cell population (Sloan and Waddington, 2009; Goldberg, 2014a). In the adult dental pulp, these cells were identified by Gronthos et al. (2000) and termed dental pulp stem cells (DPSCs). These mesenchymal derived stem cells are characterised as undifferentiated cells with the ability to differentiate into multilineage cells (Sloan and Waddington, 2009; Egusa et al., 2012; Lee et al., 2014).

1.1.1.2 Extracellular matrix of the dental pulp:

1.1.1.2.1 Collagen:

Collagen fibres are a family of fibrous proteins and regarded as the most abundant proteins in the ECM of all connective tissues (Gelse et al., 2003). They play an essential part in constructing and maintaining the histoarchitecture of tissues and organs (Linde, 1985; Goldberg and Smith, 2004) and regarded as the fibrillar backbone of the ECM (Gelse et al., 2003). Collagen fibres are synthesised and maintained by resident cells, predominately fibroblasts (Gelse et al., 2003; Ricard-Blum and Ruggiero, 2005).

On a molecular level, several types of collagen fibres have been identified. These fibres are characterised by a triple helix structure consisting of three polypeptide chains (Gelse et al., 2003; Ricard-Blum and Ruggiero, 2005). The triple helix structure, in collagen type I, is known to be a heteropolymer chain consisting of two identical alpha1-chains and one alpha2-chain. In contrast, collagen type III is a homopolymer chain consisting of three alpha1-chains (Linde, 1985; Gelse et al., 2003; Ricard-Blum and Ruggiero, 2005).

The main types of collagen fibres present within the dental pulp include collagen type I and type III which account for 56 % and 41 % of total collagen, respectively (van Amerongen et al., 1984; Goldberg and Smith, 2004). Collagen type V (2 %) and VI (0.5 %) are also present at lesser amounts (Goldberg and Smith, 2004).

1.1.1.2.2 Fibronectin:

Fibronectin is a non-collagenous adhesive protein present in the pulp matrix (Linde et al., 1982; Veis and Goldberg, 2014). They are a class of high-molecular weight structures with an approximate size of 500 kilodaltons (Hynes, 1985). On a molecular level, fibronectin is composed of two large subunits joined by disulfide bonds (Hynes, 1985; Martinez et al., 2000). Fibronectin exists either in a soluble form, present in blood, or an insoluble form, present in the ECM (Hynes, 1985). Fibronectin proteins are known to mediate cell-cell and cell-matrix interactions (Linde et al., 1982). These interactions have profound effects on a variety of cell functions including adhesion, migration, growth, and differentiation (Hynes, 1985; Linde, 1985).

1.1.1.2.3 Laminin:

Laminin is a major basement membrane adhesive protein with a large molecular size of 400 to 900 kilodaltons (Aumailley et al., 2005). On a molecular level, over 15 laminin isoforms have been identified. They are structured as multidomain heterotrimers consisting of alpha (α), beta (β) and gamma (γ) chain subunits (Colognato and Yurchenco, 2000; Aumailley et al., 2005). Laminin proteins provide unique cellular interactions mediated through cell surface receptors and integrin's. These interactions contribute towards cell adhesion, differentiation, and migration (Aumailley et al., 2005). During tooth formation, laminin proteins regulate peripheral nerve fibres development and maturation (Fried et al., 2005).

1.1.1.2.4 Proteoglycans and glycosaminoglycans:

The ground substance of the pulp tissue is largely composed of proteoglycans, glycosaminoglycans (GAGs) and water. On a molecular level, proteoglycans consist of a central protein core covalently linked to side chains of GAGs present within the ECM (Linde, 1985). Based on their molecular weight, small (biglycan and decorin) and large (versican) proteoglycans occupy the pulp tissue (Goldberg and Smith, 2004; Veis and Goldberg, 2014).

GAGs, also known as acidic mucopolysaccharides, are linear polymers consisting of repeating disaccharides. Within the pulp tissue matrix, GAGs attach to proteoglycans and constitute approximately 50 % to 90 % of their molecular weight (Linde, 1985). Several types of GAGs are present within the dental pulp including chondroitin 4- and 6-sulphate, dermatan sulphate, heparan sulphate, hyaluronan and keratan sulphate (Linde, 1985; Goldberg and Smith, 2004). GAGs play important roles in several tissue functions. They regulate water flow and retention, protect against high tissue pressure, transport nutrients and waste, and provide binding sites for several cell surface receptors and growth factors (Linde, 1973; Kumar, 2014).

1.1.1.3 Supportive elements of the dental pulp:

In addition to the above cellular and structural elements, the pulp tissue is a vital organ composed of a complex rich network of nerve fibres, lymphatics, and blood vascularisation (Goldberg, 2014a).

The blood supply of the highly vascularised pulp tissue arises from the superior or inferior alveolar artery (Kumar, 2014). Due to the small size of the pulp tissue, the blood vessels mainly consist of arterioles branching into terminal arterioles and capillaries. This pulpal blood flow system is regulated by vasoconstriction and vasodilatation actions (Pashley et al., 2008; Goldberg, 2014b; Kumar, 2014).

The lymphatic system is implicated in tissue fluid balance and as an immune barrier. They consist of lymphatic capillaries that coalesce with each other forming collecting vessels (Pashley et al., 2008; Goldberg, 2014b; Kumar, 2014).

The pulp tissue is well innervated with sensory afferent fibres arising from the trigeminal ganglion penetrating the root apex into the dental pulp. The majority of nerve fibre bundles, approximately 70 %, contain axons of nonmyelinated nerve sheaths that are mainly sympathetic in nature. Myelinated sensory nerve sheaths, approximately 20 – 30 %, that mediate pain sensation are also present (Goldberg, 2014a). These large myelinated fibres branch peripherally in the cell-rich zone forming a parietal layer of nerves termed plexus of Raschkow (Pashley et al., 2008; Kumar, 2014; Veis and Goldberg, 2014).

1.2 Pulpal necrosis in the developing child:

On average, root formation in the permanent dentition usually completes three years following emergence of the tooth in the oral cavity (Kumar, 2014). Unfortunately, during this early age, loss of vitality (pulp necrosis) is not uncommon. Several factors including developmental anomalies, dental caries and dental trauma can consequently lead to pulp necrosis therefore arresting further root development (Diogenes et al., 2013). The United Kingdom's child dental health survey, carried out in 2003, reported 5 % of 8 year old children suffering dental trauma of their anterior teeth with 52 % showing obvious decay experience (Lader et al., 2003). Failure to seal permanent teeth with developmental defects such as dens invaginatus and dens evaginatus, although to a lesser extent in United Kingdom, can lead to pulpal necrosis. Loss of pulpal vitality prior to root completion results in immature permanent teeth with compromised crown to root ratio, thin dentinal walls, and wide open apices (Cvek, 1992; Andreasen et al., 2002; Al Ansary et al., 2009). Indeed, these teeth are associated with poor long term survival rates (Cvek, 1992; Jeeruphan et al., 2012).

The early loss of a permanent tooth, especially an anterior tooth, in a growing child leads to lifelong consequences (Diogenes et al., 2016). These consequences include malocclusion, altered bone development, and interference with speech and masticatory functions (Diogenes et al., 2014; Diogenes et al., 2016). Within the anterior region, changes in dental aesthetics including tooth position or colour change is associated with detrimental effects on the child's social and psychological aspects (Traebert et al., 2012).

1.3 Endodontic management of immature teeth with pulpal

necrosis:

Endodontic management of immature permanent teeth with necrotic pulps remains a challenge in clinical dentistry. Conventional root canal treatment is the therapy of choice for most necrotic permanent teeth with complete root formation. While the outcome of conventional endodontic treatment is usually excellent in mature teeth, high risks of cervical root fractures are associated with endodontically treated immature permanent teeth (Cvek, 1992).

The two main conventional techniques widely used include calcium hydroxide apexification and mineral trioxide aggregate apical plug technique. More recently, newer treatment strategies based on the regenerative ability of the pulp tissue are increasingly being used.

1.3.1 Calcium hydroxide apexification:

Calcium hydroxide [Ca(OH)₂] apexification is defined as a clinical method to induce apical closure of the open apex by means of a calcified hard tissue barrier formation against which a permanent obturation material can be placed (Glossary of Endodontic Terms 9th edition, 2016.). Chemically, Ca(OH)₂ is classified as a strong base with high pH (approximately 12.5 - 12.8). This characteristic feature plays an important role in the production of a calcified barrier and hard tissue formation when used in apexification cases (Rafter, 2005; Mohammadi and Dummer, 2011).

Clinically the use of Ca(OH)_2 for the treatment of immature teeth has been regarded as a reliable technique with consistent clinical results (Rafter, 2005; Duggal et al., 2017). However, the formation of the apical barrier requires multiple visits of repeated root canal dressing requiring prolonged treatment periods (Rafter, 2005; Duggal et al., 2017). Variation exists in the literature with regards to the required time for formation of the hard tissue barrier, with an average between 6 to 24 months (Dominguez Reyes et al., 2005; Rafter, 2005; Moule and Moule, 2007; Mohammadi and Dummer, 2011). Observational analysis under the scanning electron microscope revealed the formation of a calcified barrier with a porous irregular layered structure (Walia et al., 2001).

Furthermore, the frequency of cervical root fracture in immature teeth treated with Ca(OH)_2 apexification was increasingly documented. A retrospective clinical study with a 4 year follow-up of traumatised non-vital maxillary teeth following Ca(OH)_2 apexification reported a high frequency of cervical root fracture (Cvek, 1992). The fractures were more commonly associated with immature teeth compared to mature teeth (28 % to 77 % depending on root development stage). The fractures were associated with weak forces, suggesting that prolonged contact between Ca(OH)_2 and the root dentine may increase the brittleness of dentine (Cvek, 1992).

This assumption was confirmed by several studies which reported a decrease in the mechanical properties of root dentine following long term placement of intracanal Ca(OH)_2 dressing such as that used in the apexification technique (Andreasen et al., 2002; Doyon et al., 2005; Twati et al., 2009b). The

underlying mechanism of reduced dentine fracture resistance is possibly linked to changes in the physical properties of dentine (Andreasen et al., 2002). More recently, a systematic review of the literature concluded that long term usage of Ca(OH)_2 within the root canals of immature teeth should be discouraged, (Al Ansary et al., 2009; Duggal et al., 2017).

1.3.2 Apical plug techniques:

Apical plug techniques consist of packing a biocompatible material into the apical end of the immature root. The packed material acts as an artificial apical barrier against which root canal filling, gutta-percha, is condensed (Al Ansary et al., 2009). To overcome Ca(OH)_2 limitations, the use of mineral trioxide aggregate (MTA) as an apical barrier plug has been advocated (Torabinejad and Chivian, 1999; Torabinejad and Abu-Tahun, 2010).

Recently MTA has gained large usage popularity for treatment of immature teeth. Sarris et al. (2008) reported a high clinical success rate of 94.1 % following 12 months follow-up period (Sarris et al., 2008). Similar high success rates have also been reported following either one-visit (93.5 %) or two-visit (90.5 %) clinical application (Witherspoon et al., 2008). This was also in agreement with the work of Simon et al. (2007) showing single visit MTA apical plug technique to be the preferred treatment approach (Simon et al., 2007). Currently, MTA apical plug technique, is considered the gold standard treatment option for immature non-vital teeth (Nicoloso et al., 2017).

The MTA powder contains fine hydrophilic particles with calcium, silica and bismuth oxide as the main elemental components. MTA sets in the presence of

moisture with a final pH ranging between 12 to 13 (Torabinejad et al., 1995a). MTA material benefits from antimicrobial and biocompatible properties (Parirokh and Torabinejad, 2010; Marão et al., 2012). However, material drawbacks include difficult handling properties, long setting time and high material cost (Parirokh and Torabinejad, 2010; Marão et al., 2012).

Comparative studies evaluating the use of Ca(OH)_2 and MTA for treatment of immature teeth have been performed. Results of these studies concluded higher clinical and radiographic success rates and shorter treatment times following the use of MTA apical plug technique (El Meligy and Avery, 2006; Pradhan et al., 2006). However, the majority of reported MTA apical plug technique studies are based on a small sample size with the need for controlled studies of larger sample size and extended follow-up periods. In similarity with Ca(OH)_2 , MTA has a high pH and similar mechanism of action to Ca(OH)_2 (Marão et al., 2012). Indeed, a preliminary *in vitro* study found comparable weakening effect of Ca(OH)_2 and MTA on human dentine tooth slices (Twati et al., 2009a). Therefore, further clinical studies to ascertain the effect of MTA on the fracture resistance of dentinal walls are needed.

Despite periapical healing in most of the cases treated with either prolonged placement of Ca(OH)_2 or MTA apical plug technique, these conventional techniques do not restore the natural pulp tissue function (Diogenes et al., 2016). The lost tissue functions, due to pulp necrosis, include the lack of pulp/s defence ability and pain receptors (Diogenes et al., 2016). Furthermore, conventional techniques do not contribute to any quantitative increase in root

lengths or thickening of root dentinal walls (Petrino et al., 2010; Torabinejad and Abu-Tahun, 2010).

1.3.3 Regenerative endodontic procedures:

To overcome the limitations of conventional endodontic techniques, regenerative procedures have been proposed. These procedures aim to induce pulp tissue regeneration, dentine formation and subsequent root development (Wigler et al., 2013; Galler, 2016). This shift towards regenerative therapy is regarded as a biological based treatment method (Galler, 2016) and the ideal approach in the management of these compromised teeth (Torabinejad and Abu-Tahun, 2010; Nakashima and Iohara, 2011).

According to the American Association of Endodontists, regenerative endodontics is considered one of the most exciting developments in dentistry at the present time. The American Association of Endodontists also published a position statement (2013) formally acknowledging regenerative endodontics as one of the techniques accepted within the scopes of endodontic practice (American Association of Endodontists, 2013). Regenerative endodontic procedures in their current format are non-expensive, technically simple and accomplished with daily used instruments (Murray et al., 2007; European Society of Endodontology, 2016). Furthermore, the use of patients own blood reduces the risk of immune rejection or pathogen transmitted diseases is highly advantageous (Murray et al., 2007).

The concept of pulp regeneration dates back to as early as 1960`s following the novel work of Nygaard-Östby (1961) reporting new tissue ingrowth in an empty

pulp space following introduction of a blood clot (Östby, 1961). His work showed limited tissue ingrowth and no pulpal regeneration (Galler, 2016). The high regenerative potential of the pulp tissue was later demonstrated by revascularisation of the dental pulp reported by Iwaya et al. (2001) as an alternative treatment for non-vital immature permanent teeth. Their work involved treatment of a necrotic immature mandibular second premolar with a chronic apical abscess in a 13 year old patient. On the first visit an intracanal antibiotic dressing was placed in the canal. Induction of bleeding through insertion of a sharp instrument beyond the root apex was performed on the second visit. Apical closure, thickening of the root canal walls and increased root length were visible radiographically 30 months following treatment (Iwaya et al., 2001).

Subsequently, Banchs and Trope (2004) reported successful revascularisation of an immature permanent tooth in an 11 year old patient with apical periodontitis. At 24 months follow-up the tooth was asymptomatic, responded positively to cold test and showed radiographic evidence of apical closure with thickening of the dentinal walls. The authors further emphasised on this new treatment approach in selected cases (Banchs and Trope, 2004).

One of the main steps in applying regenerative endodontic procedures involves evoking bleeding from the periapical tissues. The formed blood clot, subsequently, attracts stem cells from the periapical area and acts as a scaffold assisting new tissue formation (Trope, 2008; Lovelace et al., 2011; Diogenes and Ruparel, 2017).

The introduced blood clot is known to contain a rich supply of stem cells originated from the apical papilla termed stem cells of the apical papilla (SCAP) (Sonoyama et al., 2006; Sonoyama et al., 2008). This is in agreement with molecular analysis studies of the blood collected inside the root canal. Their results identified a large delivery of undifferentiated mesenchymal stem cells in the collected blood samples (Lovelace et al., 2011).

1.3.3.1 Treatment outcome of regenerative endodontic procedures in their current format:

More than 65 case reports, case series, retrospective and prospective clinical trials treating over 320 teeth have been published in the dental literature (Galler, 2016). In general, these clinical studies reported favourable treatment outcomes in terms of periodontal healing and resolution of periapical infection (Thibodeau and Trope, 2007; Jung et al., 2008; Thomson and Kahler, 2010; Cehreli et al., 2011; Chen et al., 2012; Miller et al., 2012). Furthermore, positive response to sensibility tests at follow-up appointment has been reported (Banchs and Trope, 2004; Thomson and Kahler, 2010; Cehreli et al., 2011; Miller et al., 2012).

However, variable results in regards to continuation of root development and thickening of the canal walls have been reported following regenerative endodontic procedures. Jeeruphan et al. (2012) in a retrospective clinical study involving 20 treated teeth reported only 28.2 % and 14.9 % increase in root width and root length, respectively (Jeeruphan et al., 2012). Lower success rates of 26.5 % increase in root width and 7.7 % increase in root length were

reported by Cehrelli et al. (2011) following treatment of six teeth with pulp necrosis as a result of caries. Of these six treated teeth, only two responded positively to sensibility testing at 12 months follow-up (Cehrelli et al., 2011). Furthermore, variable treatment outcome with higher success rates were reported by Jung et al. (2008) and Chen et al. (2012). Despite periapical healing in all treated cases, evidence of continued root development was reported in 75 % of treated cases (Jung et al., 2008; Chen et al., 2012). No root development following a six year follow-up has also been reported in two traumatised non-vital teeth (Nosrat et al., 2012).

To further understand the nature of the regenerated tissue, histological analysis of extracted human and animal teeth treated with regenerative endodontic procedures revealed poor resemblance of the developed tissues to the native pulp tissues. The new tissue ingrowth was described, in most studies, as a well mineralised cementum- or bone-like tissue within the canal space and at the apical ends (Wang et al., 2010b; Shimizu et al., 2013; Becerra et al., 2014; Lin et al., 2014).

Unfortunately, most of the evidence from which regenerative endodontic procedures have progressed is stemmed from a large number of case reports and case series of low level of evidence (Kontakiotis et al., 2014). Moreno-Hidalgo et al. (2013) reported substantial heterogeneity in terms of study types, treatments, evaluation periods, and species (animals and human) evaluated (Moreno-Hidalgo et al., 2014).

Recently, more randomised controls trials, systematic reviews and meta-analysis have been published (Kahler et al., 2017; Tong et al., 2017; Torabinejad et al., 2017). These reviews concluded inconsistent treatment outcomes, mainly in regards to continued root development and apical closure following regenerative endodontic procedures.

Several hypotheses were made with regards to the reasons for such inconsistent results such as: (i) The use of a blood clot as a scaffold; (ii) Damage to Hertwig's epithelial root sheath secondary to traumatic injuries or infection; (iii) Lack of radiographic standardisation and root measurement techniques (Nazzal and Duggal, 2017).

Regenerative endodontic procedures in their current format rely on the formation of a blood clot. The formed blood clot is a composed of undefined components including immune cells (Palma et al., 2017). The concentration and type of cells incorporated in the blood clot is unpredictable leading to an uncontrolled environment which directly affects both quality and quantity of the newly generated tissue (Murray et al., 2007; Nazzal and Duggal, 2017).

Developmentally, the epithelial cells of Hertwig's epithelial root sheath guide the apical papilla cells to form pulp and dentine structure through complex epithelial-mesenchymal interactions (Huang et al., 2010). Therefore, the presence of Hertwig's epithelial root sheath is considered necessary for true pulp regeneration (European Society of Endodontology, 2016). According to Sonoyama et al. (2007) cells from Hertwig's epithelial root sheath guide the differentiation of periodontal ligament stem cells and form cementum-like tissue

in vivo (Sonoyama et al., 2007). Consequently, damage to Hertwig's epithelial root sheath following trauma may affect the required cell lineage differentiation (cementoblasts), hence prevent further root development (Nagata et al., 2014; Saoud et al., 2014; Nazzal and Duggal, 2017). Therefore, to improve the clinical outcome, the incorporation of tissue engineering principles within the clinical management of these compromised teeth was proposed.

1.4 Tissue engineering of the dental pulp:

Tissue engineering is defined as an interdisciplinary field that aims to restore and maintain tissue function using the principles of engineering and life sciences (Langer and Vacanti, 1993). Utilising tissue engineering principles namely the appropriate cells, a supporting scaffold material and the correct morphogenic signals provides a more controlled approach over tissue response and new tissue formation (European Society of Endodontology, 2016; Duggal et al., 2017).

Although the maintenance of a vital pulp is the ultimate goal in restorative and paediatric dentistry (European Society of Endodontology, 2016; Duggal et al., 2017), pulp preservation is not always possible and presents a treatment challenge especially in young patients with immature teeth. Such patients might benefit from a tissue engineered treatment strategy, if clinically available (Nazzal and Duggal, 2017). This treatment strategy, if successful, could potentially allow the completion of lateral and vertical root surfaces, therefore, improving the long-term prognosis of these compromised teeth (Nör, 2006; Cordeiro et al., 2008; Garcia-Godoy and Murray, 2012; Conde et al., 2015;

Nazzal and Duggal, 2017). To achieve the desired clinical success, the combined presence of cells, scaffolds and signalling molecules within a disinfected pulp canal system is required (Figure 1.2). The use of 1.5 – 3 % sodium hypochlorite followed by physiological saline and a final irrigation with 17 % EDTA is clinically recommended in achieving disinfection of the root canal system prior to revitalisation / regeneration procedures (Martin et al., 2014; European Society of Endodontology, 2016).

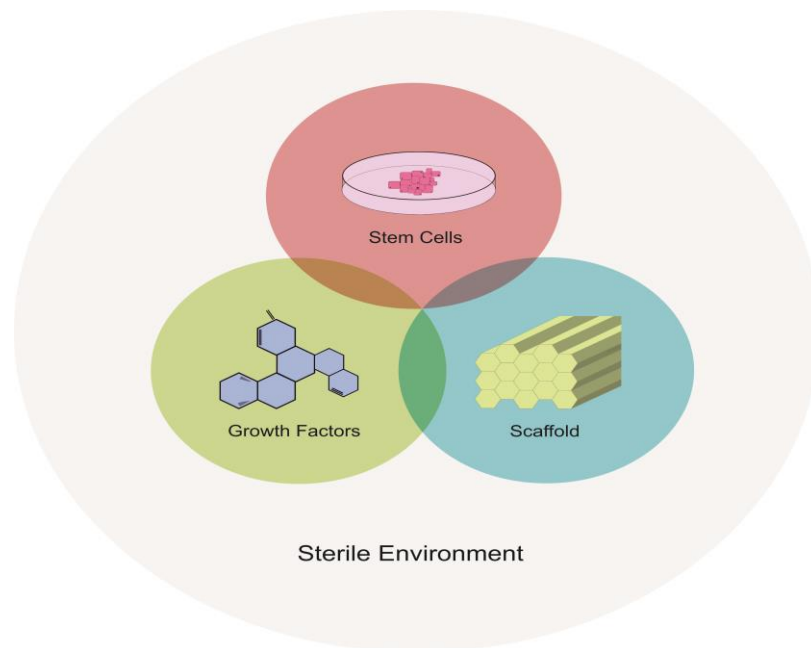


Figure 1.2: Schematic illustration of tissue engineering elements. The triad of stem cells, scaffolds and growth factors within a disinfected pulp canal system is required for successful pulp tissue engineering.

1.4.1 Stem cells for dental pulp tissue regeneration:

Although pulp-derived fibroblastic cells have been investigated for pulp tissue engineering (Mooney et al., 1996), within the past decade, stem cells have gained considerable attention as a preferred candidate for stem-cell based therapies. Stem cells are defined as immature, unspecialised and

undifferentiated cells that have an ability to continuously divide into different cell lineages (Egusa et al., 2012). Stem cells reside in a specific area of each tissue called stem cell niche, where the regulation of stem cell activity occurs (Sloan and Waddington, 2009).

According to the Mesenchymal and Tissue Stem Cell Committee of the International Society for Cellular Therapy (2006) a minimal standard criteria for human mesenchymal stem cells has been proposed (Dominici et al., 2006). The current set criteria include: (i) Ability to adhere to plastic tissue culture flasks under normal tissue culture procedures; (ii) Expression of specific surface antigens. More than 95 % of the isolated mesenchymal stem cells should positively express CD105 (endoglin), CD73 (ecto 5' nucleotidase) and CD90 (Thy-1). Furthermore, the isolated mesenchymal stem cells should negatively express (less than 2 % positive) a panel of antigens. These antigens include CD45 (pan-leukocyte marker), CD34 (hematopoietic progenitor and endothelial cell marker), CD14 and CD11b (macrophages and monocytes marker), CD79 α and CD19 (B cell marker) and human leukocyte antigens class II (HLA-DR) molecules in an unstimulated state. (iii) Ability to differentiate *in vitro* into adipocytes, chondroblasts, and osteoblasts lineages (Dominici et al., 2006). Their characteristic feature to differentiate into a wide range of specialised cells is termed plasticity (Sloan and Waddington, 2009; Galler et al., 2010). Stem cells are classified based on their origin, source, and plasticity (Murray et al., 2007; Galler et al., 2010; Egusa et al., 2012) as listed in Table 1.1.

Table 1.1: Classification of stem cells

Origin	Embryonic (foetal)
	Postnatal (adult)
Plasticity	Totipotent: unlimited potency to divide and give rise to all cell types of the body
	Pluripotent: cells can differentiate into any (over 200) cell types except extraembryonic (placenta)
	Multipotent: cells can differentiate into a limited number of cell types (most postnatal stem cells fall into this category)
Source	Autologous: donor cells are from the same individual
	Allogenic: donor cells are from the same species
	Xenogenic: donor cells are from different species

Embryonic stem cells are derived from totipotent cells in the inner cell mass of the developing embryo during the blastocyst stage (Thomson et al., 1998). However, despite their totipotent ability their use is afflicted with both legal and ethical issues which restrict their future usage (Murray et al., 2007; Galler et al., 2010). On the other hand, postnatal stem cells have been identified and isolated from a wide range of different tissues including various oral and maxillofacial regions. These tooth derived mesenchymal stem cells are increasingly being studied and are classified as potent self-renewal cells with multipotent differentiation capabilities (Sloan and Waddington, 2009; Egusa et al., 2012; Lee et al., 2014). They are categorised based on the tissue and location from which they are isolated. The commonly isolated tooth derived stem cells are listed in Table 1.2 and schematically illustrated in Figure 1.3.

Table 1.2: Classification of tooth derived stem cells

Tissue source	Stem cell terminology
Pulp tissue of permanent dentition	Dental pulp stem cells (DPSCs) (Gronthos et al., 2000)
Pulp tissue of primary dentition	Stem cells from human exfoliated deciduous teeth (SHED) (Miura et al., 2003)
Periodontal tissue	Periodontal ligament stem cells (PDLSCs) (Seo et al., 2004)
Apical papilla tissue	Stem cells from apical papilla (SCAP) (Sonoyama et al., 2006)
Dental follicle of an un-erupted tooth	Dental follicle progenitor cells (DFPCs) (Morsczech et al., 2005)
Gingival tissue	Gingiva-derived mesenchymal stem cells (GMSCs) (Zhang et al., 2009)

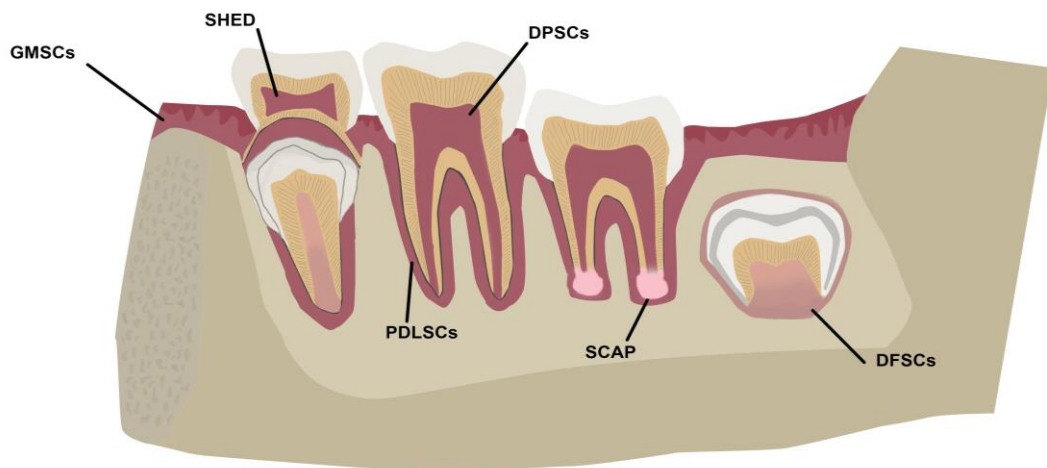


Figure 1.3: Schematic illustration of tooth derived stem cells. GMSCs (gingiva-derived mesenchymal stem cells), SHED (stem cells from human exfoliated deciduous teeth), PDLSCs (periodontal ligament stem cells), DPSCs (dental pulp stem cells), SCAP (stem cells from apical papilla) and DFPCs (dental follicle progenitor cells).

These tooth derived stem cells are regarded as a viable cell source for regeneration of both tooth and non-tooth structures (Lee et al., 2014). Within the context of pulp-dentine engineering several studies have reported favourable results following *in vitro* and *in vivo* use of DPSCs (Gronthos et al., 2000; Gronthos et al., 2002; El-Backly et al., 2008; Prescott et al., 2008; Kodonas et al., 2012), stem cells from human exfoliated deciduous teeth (Miura et al., 2003; Cordeiro et al., 2008; Sakai et al., 2010), and stem cells from apical papilla (Sonoyama et al., 2006; Abe et al., 2008; Huang et al., 2008) for pulp and dentine tissue engineering.

1.4.2 Signalling molecules for dental pulp tissue regeneration:

Signalling molecules, growth factors and cytokines are also regarded as an essential element for tissue engineering (Langer and Vacanti, 1993). They are defined as peptide molecules controlling tissue growth during epithelial-mesenchymal interactions (Nakashima and Reddi, 2003; Nakashima and Akamine, 2005). At a molecular level, these interactions involve a complex network consisting of signals, receptors and transcriptional control systems (Thesleff and Sharpe, 1997). It is these crucial interactions between cells and tissue elements that regulate future tissue development (Thesleff and Åberg, 1999).

Signalling molecules that mediate epithelial-mesenchymal interactions during tooth development mainly include, bone morphogenetic proteins (BMPs), fibroblast growth factors (FGFs), wntless- and int-related proteins (Wnts), and hedgehog proteins (Hhs) (Thesleff and Åberg, 1999; Nakashima and Reddi, 2003; Ajay Sharma et al., 2013).

Furthermore for successful engineered pulp tissue, the formation of blood vessels is essential for tissue survival (Nör, 2006; Janebodin et al., 2013). The formation of new blood vessels from pre-existing vessels, is termed angiogenesis (Folkman, 1995). Studies have linked angiogenesis to a number of growth factors including transforming growth factors (TGF; TGF- α , TGF- β), platelet-derived growth factor (PDGF), tumour necrotic factor- α (TNF- α), vascular endothelial growth factor (VEGF), and VEGF receptors (VEGFR-1 and VEGFR-2) (Matsushita et al., 2000; Grando Mattuella et al., 2007).

1.4.3 Scaffolds for dental pulp tissue regeneration:

In addition to the correct signalling cues and the appropriate stem cells, a three-dimensional scaffold that can support future cellular repopulation is required (Murray et al., 2007; Gotlieb et al., 2008; Waddington and Sloan, 2017). Scaffolds play an important role in future tissue regeneration, therefore the selection of an appropriate material is considered to be a crucial step for successful tissue regeneration (Yuan et al., 2011; Ajay Sharma et al., 2013; Nazzal and Duggal, 2017). Indeed, placement of a scaffold within the root canal has been shown to enhance revascularisation procedure and improve the quality of tissue formation (Garcia-Godoy and Murray, 2012).

Ideally scaffolds, when infiltrated with the desired cells, should facilitate cellular recruitment, attachment, growth and differentiation (Murray et al., 2007; Galler et al., 2010; Galler et al., 2011b; Yuan et al., 2011). Providing the conducive environment for cellular proliferation facilitates the secretion of ECM components. This is followed by constructive remodelling, scaffold degradation, and eventually replacement of the scaffold by the intended tissue (Galler et al., 2010; Galler et al., 2011b).

To promote future tissue engineering, several material requirements are considered. To prevent any unwanted tissue response, scaffolds should be biocompatible and non-immunogenic (Galler et al., 2010; Galler et al., 2011b; Yuan et al., 2011). They should possess the correct surface chemistry and structural framework to support cell attachment, organisation and vascularisation (Yang et al., 2001). A permeable material that effectively enables the transport of nutrients, oxygen and waste is highly desirable and crucial for cellular survival (Yang et al., 2001). Scaffolds should also be constructed from a biodegradable material, with a biodegradation rate in synchrony with constructive remodelling of newly formed tissues (Yang et al., 2001; Galler et al., 2010; Galler et al., 2011b). Furthermore, for future clinical translation, scaffolds should be easily applicable clinically and cost-effective (Yuan et al., 2011).

Despite the first attempt to engineer a pulp-like tissue on a synthetic scaffold dates back to the mid-90s by Mooney et al. (1996), it was not until the discovery of DPSCs by Gronthos et al. (2000) which further enhanced this field.

Biomaterials research has become of high scientific interest and several scaffold materials have been tested for their potential ability to support stem cell attachment, proliferation, and tissue formation (Conde et al., 2015). Several synthetic and natural scaffold materials are currently being developed for use in dental pulp regeneration.

1.4.3.1 Scaffolds constructed from synthetic materials:

Scaffolds constructed from synthetic materials are commercially attractive due to their unlimited supply and relative simple production (Galler et al., 2010; Colombo et al., 2014). These scaffolds offer a controlled and well-characterised composition with tailored handling characteristics (Galler et al., 2010; Song and Ott, 2011). Despite this tailored mechanical production, material degradation issues still exist (Lee and Mooney, 2001).

On the other hand, degradation of synthetic polymers causes the release of acidic by-products which impacts negatively on material biocompatibility (Yang et al., 2001). Furthermore, scaffolds constructed from synthetic materials lack the natural chemical structure of the ECM (Galler et al., 2011b). Several synthetic materials have been investigated for pulp-dentine complex regeneration as summarised in Table 1.3.

1.4.3.2 Scaffolds constructed from natural materials:

Scaffolds constructed from natural materials have the advantage of being, in most cases, biodegradable and biocompatible (Galler et al., 2010; Galler et al., 2011b). However, production issues mainly establishing control over specified features are challenging and can ultimately affect their biocompatibility and

structural integrity (Colombo et al., 2014). Furthermore, natural scaffolds lack standardisation with large batch variations (Yang et al., 2001; Conde et al., 2015), processing difficulties (Galler et al., 2010), and the risk of a possible immune response (Galler et al., 2010; Conde et al., 2015). Several natural materials have been investigated for pulp-dentine complex regeneration as summarised in Table 1.3.

Acellular biological scaffolds developed through tissue decellularisation have recently been advocated over other synthetic and natural scaffolds (Badylak, 2002; Gilbert et al., 2006; Crapo et al., 2011). These scaffolds have been introduced to overcome previous scaffold limitations mainly the poor resemblance to the natural tissue matrix, preservation of three-dimensional tissue architecture and natural ECM components consisting of a unique mixture of structural and functional proteins (Badylak, 2002; Badylak et al., 2009). Within the dental field attempts at decellularising different dental tissues for pulp-dentine complex regeneration have been summarised in Table 1.3 and further discussed below (Section 1.5).

Table 1.3: Scaffold performance used for pulp-dentine complex regeneration

Scaffold type	Evidence		Advantages	Disadvantages
	Experimental approach	Scaffold performance		
Synthetic scaffolds:				
Synthetic bioceramics:				
Hydroxyapatite / tricalcium phosphate	Scaffold seeded with DPSCs and transplanted into nude mice (Gronthos et al., 2000; Gronthos et al., 2002)	Formation of ectopic dentine-like structure	Biocompatible Biodegradable	Limited manufacturing ability to produce a porous structure Osteoconductive Brittle
Porous ceramic	Scaffold seeded with DPSCs and cultured <i>in vitro</i> in the presence of osteogenic differentiation medium and transplanted into nude mice (Zhang et al., 2006b)	Limited amount of hard tissue formation Poorly organised ECM Tissue resembled a more connective tissue than a dentine-like structure		

Synthetic polymers:				
Poly (lactic-co-glycolic acid)	Scaffold seeded with DPSCs, cultured <i>in vitro</i> and transplanted in rabbits (El-Backly et al., 2008)	<p>Early formation of patches of osteodentine-like matrix</p> <p>Tubular bi-layered structure</p> <p>Limited areas had well-organised appearance</p>	Inexpensive	<p>Lack of ECM specific environmental cues</p> <p>Acidic by-products on material degradation</p>
Poly- L -lactic acid	Scaffold seeded with SHED utilising tooth slice model and transplanted into nude mice (Cordeiro et al., 2008; Sakai et al., 2010)	<p>Formation of a vascularised dental pulp-like tissue</p> <p>Positive expression to DSPP</p> <p>Rapid degradation rate (due to low pH environment produced during polylactic acid degradation)</p>	<p>Standard reproducibility</p> <p>Adjustable chemical, mechanical, and physical properties</p>	
Poly- L -lactic acid	Scaffold seeded with DPSCs, bone morphogenetic protein-7, cultured within an odontogenic induction medium <i>in vitro</i> and transplanted into nude mice (Wang et al., 2010a)	<p>Positive expression to DSPP</p> <p>Hard tissue formation</p> <p>No resemblance to tubular dentine structure</p>		

Poly- L -lactic acid	Scaffold seeded with DPSCs utilising tooth slice model and transplanted into nude mice (Demarco et al., 2010)	Positive expression to DSPP and DMP-1		
Poly-D,L-lactide and glycolide	Scaffold seeded with SCAP and DPSCs and placed within root canal of extracted human teeth and transplanted into nude mice (Huang et al., 2010)	Formation of a vascularised pulp-like tissue Generated odontoblast-like cells were not well organised nor well aligned Scattered voids were seen throughout the formed tissues (remnants of un-resorbed synthetic scaffold)		
Synthetic hydrogels:				
Alginate hydrogels	Alginate hydrogels were either untreated, acid treated or combined with TGF- β 1 and cultured <i>in vitro</i> in human tooth slices (Dobie et al., 2002)	Both acid treated alginate and alginate hydrogels with TGF- β 1 showed signs of dentinogenesis Untreated alginate hydrogels showed no signs of dentinogenesis	Injectable materials Biocompatible Relative ease of production	Poor mechanical strength Early stage of research

<p>Puramatrix™ (self-assembling peptide hydrogel)</p>	<p>Scaffold seeded with DPSCs utilising tooth slice model and cultured <i>in vitro</i> (Cavalcanti et al., 2013)</p>	<p>Supported DPSCs survival and proliferation</p> <p>Positive expression to DSPP and DMP-1</p>	<p>Customised material</p> <p>Surface modification (addition of growth factors)</p>	
<p>Puramatrix™ (self-assembling peptide hydrogel)</p>	<p>Scaffold seeded with SHED and placed within root canal of extracted human teeth, cultured <i>in vitro</i> and transplanted into immunodeficient mice (Rosa et al., 2013)</p>	<p>Odontoblastic differentiation indicated by positive expression to DSPP and DMP-1</p> <p>Unable to support Odontoblastic differentiation in the absence of root canal (dentine derived growth factors)</p> <p>Formed tissue resembled a connective tissue-like appearance with a less dense ECM in comparison to the native pulps</p>		
<p>Self-assembling peptide nanofibres hydrogel</p>	<p>Scaffold seeded with DPSCs combined with several growth factors utilising tooth slice model and cultured <i>in vitro</i> and <i>in vivo</i> (Galler et al., 2011c).</p>	<p>Formation of a vascularised soft connective tissue resembling the native pulp tissue.</p>		

Natural scaffolds:				
Natural polymers:				
Collagen (produced from bovine hide)	Scaffold seeded with SHED combined with bone morphogenic protein-2 and TGF- β 1, placed within root canal of extracted human premolar teeth and cultured <i>in vitro</i> (Gotlieb et al., 2008)	Scaffold supported cell attachment Limited attachment of the pulp constructs to the surrounding root canal surfaces (less than 50 % contact)	Several diverse sources (animal, bacteria, crops and plant) Biodegradable Customised chemical properties	Processing difficulties Lack of standardisation (material properties may vary) Risk of pathogen transmission or immune response
Cross-linked collagen	Animal case study comparing the use of blood clot with/without collagen scaffold (Yamauchi et al., 2011)	The addition of a collagen scaffold increased amount of tissue formation compared to use of blood clot alone Formed tissue resembled cementum- and bone-like tissue		
Chitosan	Animal case study comparing the use of blood clot with/without chitosan scaffold (Palma et al., 2017)	The addition of a chitosan scaffold did not enhance tissue formation compared to use of blood clot alone		

Natural hydrogels:				
Recombinant human collagen type I hydrogels	Scaffold seeded with SHED and placed within root canal of extracted human teeth, cultured <i>in vitro</i> and transplanted into immunodeficient mice (Rosa et al., 2013)	<p>Odontoblastic differentiation indicated by positive expression to DSPP and DMP-1 when in contact with the root canal</p> <p>Unable to support odontoblastic differentiation in the absence of surrounding root canal</p> <p>Formed tissue resembled a connective tissue-like appearance with less dense ECM in comparison to the native pulps</p>	<p>Injectable materials</p> <p>Biocompatible</p> <p>Relative ease of production</p> <p>Customised material</p> <p>Surface modification (addition of growth factors)</p>	<p>Disadvantages of original material source</p> <p>Poor mechanical strength</p> <p>Early stage of research</p>
Hyaluronic acid cross-linked hydrogel	Scaffold seeded with tooth bud-derived dental mesenchymal cells combined with growth factors, utilising tooth slice model and cultured <i>in vitro</i> and transplanted into nude mice (Tan et al., 2015)	<p>Odontoblastic differentiation indicated by positive expression to DSPP and DMP-1</p> <p>Formed tissue resembled dentinal tubular structures, only in the presence of the growth factor</p> <p>The combined use of cells and scaffolds resulted in the formation of bone-like tissue</p>		

Platelet-rich plasma:				
Platelet-rich plasma	Human case report comparing the use of blood clot with/without platelet-rich plasma (Martin et al., 2013)	<p>Formed tissue resembled cementum- and bone-like tissue</p> <p>Calcifications, necrotic debris and dentine chips embedded within the mineralised tissue</p> <p>No evidence of odontoblasts or new dentine formation</p> <p>No difference between the use of blood clot alone or the addition of platelet-rich plasma</p>	<p>Autologous tissue</p> <p>Complex mixture of platelets and growth factors</p>	<p>Tissue repair not pulp regeneration was concluded as the clinical outcome</p> <p>Increase treatment cost</p> <p>Difficult handling properties</p> <p>Invasive procedure (especially young children as it requires drawing blood from the patient)</p>
Platelet-rich plasma	Animal case study testing several combinations of blood clot, pulp cells and platelet-rich plasma (Zhu et al., 2012)	<p>Formed tissue resembled cementum- and bone-like tissue</p> <p>No dentine-like tissue formation</p>		

Acellular biological scaffolds:				
Decellularised porcine tooth buds	Porcine molar tooth buds were demineralised and decellularised using a dual detergent based protocol, characterised and recellularised using porcine dental mesenchymal cells (Traphagen et al., 2012)	<p>Preservation of the ECM</p> <p>Positive expression of collagen, fibronectin and laminin proteins</p> <p>Recellularised scaffolds exhibited an increased collagen fibre density</p>	<p>Biocompatible</p> <p>Tissue specific ECM</p>	<p>Lack of optimised tissue specific decellularisation process</p> <p>Risk of immune response</p> <p>Early stage of research</p>
Decellularised miniature swine teeth	Tissue decellularised using a dual detergent based protocol, characterised and recellularised using DFSCs (Chen et al., 2015)	<p>Reduction in collagen type I and III</p> <p>Preservation of fibronectin and laminin proteins</p> <p>Supported cell survival</p>	<p>Favourable microenvironment for tissue engineering</p> <p>Spatial structure</p>	
Decellularised human root slices	Pulp-dentine disks (1.5 mm) were decellularised using a dual detergent based protocols, characterised and recellularised using SCAP (Song et al., 2017)	<p>Preservation of GAGs</p> <p>Reduced expression of fibronectin</p> <p>Scaffold supported cell viability with positive cellular expression to DSP and ALP</p>	<p>Preservation of vascular network</p>	

Abbreviations; (ALP) alkaline phosphatase, (DPSCs) dental pulp stem cells, (DSP) dentine sialoprotein, (DSPP) dentine sialophosphprotein, (DMP-1) dentine matrix protein-1, (DFSCs) dental follicle stem cells, (GAGs) glycosaminoglycans, (SCAP) stem cells from apical papilla and (TGF-β1) transforming growth factor beta-1.

1.5 Tissue decellularisation:

Tissue decellularisation is defined as the efficient removal of all cellular and nuclear contents within a given tissue without negatively affecting its composition, mechanical integrity and biological activity of the decellularised matrix (Gilbert et al., 2006; Badylak et al., 2009; Fu et al., 2014). Following decellularisation, the produced scaffold is composed of the tissues natural ECM components with preserved three-dimensional tissue architecture (Badylak et al., 2009; Wilshaw et al., 2012). ECM components consist of a unique mixture of structural and functional molecules that regulate several cellular activities. These molecules also contribute to ECM's strength and structural properties (Badylak, 2002; Badylak et al., 2009).

Although allogenic decellularised scaffolds are the preferred choice, they are largely limited by availability. Therefore, recent research has looked into xenogenic decellularised scaffolds as a readily available alternative. Decellularisation has been widely reported in the medical literature for various tissues and organs including, but not limited to, human pericardial matrix (Mirsadraee et al., 2006), human liver (Kajbafzadeh et al., 2013), human common femoral arteries (Wilshaw et al., 2012), human amniotic membrane (Wilshaw et al., 2006), porcine medial meniscus (Stapleton et al., 2008), porcine cornea (Yoeruek et al., 2012), porcine cartilage (Kheir et al., 2011), and porcine pulmonary valve (Luo et al., 2014).

Acellular biological scaffolds have also progressed to human trials and usage. Examples of commercially available ECM scaffolds in clinical usage include,

Acell Vet (porcine urinary bladder; Acell, Inc.), Alloderm (human dermis; Lifecell, Corp.), GraftJacket (human dermis; Wright Medical Technology), Restore (porcine small intestine; DePuy Orthopaedics), Oasis (porcine small intestine; Cook Biotech, Inc.), and Zimmer Collagen Repair Patch (porcine dermis; Zimmer, Inc.) (Gilbert et al., 2009). Within the dental field, decellularised tissues have been investigated as a suitable scaffold for pulp-dentine complex (Traphagen et al., 2012; Chen et al., 2015; Song et al., 2017) and whole tooth regeneration (Ikeda et al., 2009; Oshima et al., 2011; Zhang et al., 2017). These tissues were obtained from different sources (animal and human) and decellularised using various process.

1.5.1 Tissue decellularisation process:

In general terms, the decellularisation process involves single or combined usage of reagents and physical methods. These include: (i) Chemical agents (acids, bases, detergents, hypertonic and hypotonic solutions); (ii) Biological agents (enzymes, chelating agents and protease inhibitors); (iii) Physical methods (freeze-thaw cycle, snap freezing, mechanical force and agitation) (Gilbert et al., 2006; Crapo et al., 2011; Fu et al., 2014).

1.5.1.1 Chemical agents:

1.5.1.1.1 Acid and bases:

Acid and bases are known to solubilise cellular cytoplasmic components and aid the removal of nucleic acids. However, concerns regarding structural damage and removal of ECM components, such as collagen and GAG molecules, have been reported (Gilbert et al., 2006; Crapo et al., 2011).

Examples of commonly used acidic and alkaline reagents include acetic acid, peracetic acid, calcium hydroxide, and sodium hydroxide (De Filippo et al., 2002; Falke et al., 2004; Freytes et al., 2004).

Bases are incorporated in the early stages of decellularisation process to remove hair from the porcine dermis (Reing et al., 2010). However, they are generally considered harsh chemicals and are associated with significant reduction of growth factors and mechanical properties. Reduction of the ECM mechanical properties is linked to cleavage of collagen fibrils and damage to the collagen crosslinks (Gorschewsky et al., 2005).

Peracetic acid is commonly incorporated within the decellularisation process, mainly as a final step for tissue disinfection and sterilisation process. Peracetic acid acts as an oxidising agent leading to the microorganisms destruction (Pruss et al., 1999). Peracetic acid, at low concentrations of approximately 0.1 % (v/v), has been regarded as an effective disinfection and sterilisation agent for collagen-based biological scaffolds with no or minimal effect on the ECM structure and components (Hodde and Hiles, 2002; Hodde et al., 2007).

1.5.1.1.2 Detergents:

Detergents are water-soluble molecules composed of a polar head group and a hydrophobic tail or chain. Detergents are divided into ionic, non-ionic and zwitterionic based on their hydrophilic or hydrophobic characteristics and ionic groups (Seddon et al., 2004; Knight et al., 2008). They are widely used in tissue decellularisation and are regarded as an effective treatment for removal

of cellular material through dissociating DNA from proteins and solubilising cell membranes (Seddon et al., 2004; Cox and Emili, 2006).

Ionic detergents contain a charged cationic or anionic head group. Commonly used examples include sodium dodecyl sulphate (SDS), sodium deoxycholate and Triton X-200 are known to be effective at solubilising cytoplasmic and nuclear membranes (Seddon et al., 2004; Woods and Gratzer, 2005; Gilbert et al., 2006). In contrast to ionic detergents, non-ionic detergents contain an uncharged hydrophilic head group. Non-ionic detergents are known to be relatively mild and non-denaturing as they disrupt DNA-protein, lipid-lipid and lipid-protein interactions, however protein-protein interactions remains intact (Seddon et al., 2004; Woods and Gratzer, 2005; Crapo et al., 2011). Common example of this group in tissue decellularisation includes the use of Triton X-100. Zwitterionic detergent are known to combine properties of both ionic and non-ionic detergents, however able to cause more deactivation than the non-ionic detergents (Seddon et al., 2004). Example of this group include 3-[(3-cholamidopropyl) dimethylammonio]-1-propanesulfonate (CHAPS) (Seddon et al., 2004; Crapo et al., 2011).

1.5.1.1.3 Hypertonic and hypotonic solutions:

To further enhance the effect of the used detergent, hypertonic and/or hypotonic solutions are added to decellularisation protocols (Knight et al., 2008). The action of hypotonic solutions, in which the solute concentration in extracellular fluid is less than the cell cytosol, causes cell swelling and breakdown of cell membranes by means of osmotic shock. Hypotonic solutions have been reported to cause large influx of water with minimal disruption to ECM (Xu et al.,

2007). On the other hand, hypertonic solutions cause water movement out of the cell, as the solute concentration is higher than the cell cytosol. This leads to cell dehydration, shrinkage, probable death and cell detachment (Knight et al., 2008). Hypertonic solutions are also known to dissociate DNA from proteins (Cox and Emili, 2006). The addition of hypertonic and/or hypotonic rinses within a given decellularisation protocol has shown synergistic support aiding cell lysis, and removal of cell remnants and chemical residues within the treated tissue (Stapleton et al., 2008; Remlinger et al., 2012; Luo et al., 2014).

1.5.1.2 Biological agents:

1.5.1.2.1 Enzymes:

Enzymes are commonly used within decellularisation protocols for efficient removal of cellular and nuclear material. Examples include, but not limited to, collagenase, dispase, trypsin and nucleases (Bader et al., 2000; Chen et al., 2004; Rieder et al., 2004; Prasertsung et al., 2008). Nucleases (DNases and RNases) are known to catalyse the hydrolysis of DNA and RNA chain sequence, therefore aiding in the removal of nuclear material (Gilbert et al., 2006; Crapo et al., 2011). Within a given decellularisation protocol nucleases are, generally, used towards the final steps following disruption of cellular and nuclear membranes.

1.5.1.2.2 Chelating agents:

Chelating agents also aid in the removal of cellular contents from the treated tissue. They bind and congregate with metal ions present on cell adhesion sites, consequently disrupting cellular adhesions (Klebe, 1974; Gailit and

Ruoslahti, 1988). However, chelating agents are inadequate when used alone and typically used in combination with other enzymatic or detergent reagents (Hopkinson et al., 2008). Examples include EDTA and ethylene glycol tetraacetic acid (EGTA) (Gilbert et al., 2006; Crapo et al., 2011).

1.5.1.2.3 Protease inhibitors:

Protease inhibitors are frequently added to various decellularisation solutions in order to prevent undesirable ECM damage, that might occur due to the release of intracellular proteases following cell lysis (Gilbert et al., 2006; Crapo et al., 2011; Wilshaw et al., 2012). Examples of protease inhibitors include Aprotinin and leupeptin (Gilbert et al., 2006; Crapo et al., 2011). Aprotinin acts as a broad-spectrum protease inhibitor (Landis et al., 2001). EDTA, a chelating agent, also inhibits matrix metalloproteinase (Seltzer et al., 1976; Galis et al., 1994).

1.5.1.3 Physical methods:

The incorporation of physical methods within a decellularisation protocol is known to facilitate the efficiency of tissue decellularisation (Gilbert et al., 2006; Crapo et al., 2011; Fu et al., 2014). However, physical methods are insufficient alone in achieving complete cellular removal, therefore, used mainly in combination with other treatment steps. Examples include freeze-thaw cycles, snap freezing, mechanical force, and agitation (Gilbert et al., 2006; Crapo et al., 2011).

1.6 In summary:

The early optimism regarding regenerative endodontic procedures in the management of immature teeth with necrotic pulp tissues has now faded, with unpredictable results reported especially with regards to continuation of root development and increase dentine thickness. Furthermore, histological studies have shown cementum- and bone-like structures rather than pulp-like structure formation following such regeneration procedures. These procedures are unlikely to be successful unless basic principles of tissue engineering are followed and implemented in their clinical management. Such clinical protocols should be aimed at promoting and guiding the development of the desired structures using appropriate cells, signalling molecules, and scaffold material.

Although several scaffolds are currently being tested, to date, the ideal scaffold for pulp-dentine regeneration has not been identified. The production of acellular biological scaffolds composed of tissue specific ECM is highly promising in providing the ideal environment for selective tissue regeneration.

1.7 Aim and objectives:

We hypothesise that, therefore, an acellular dental pulp scaffold would facilitate regeneration of the dental pulp tissue for future use in clinical management of immature teeth with necrotic pulp tissues.

The overall aim of this research is to assess the feasibility of decellularising rat and human dental pulp tissues in producing a biocompatible acellular ECM scaffold with intact structural and biochemical components of the native dental pulp tissue.

The objectives of this project, therefore, are:

- To develop a reproducible decellularisation method capable in removing acceptable levels of rat and human pulp tissue cellular and nuclear material for use in pulp-dentine tissue regeneration.
- To determine the efficiency of the decellularisation method used in preserving the ECM structural histoarchitecture and components.
- To determine the decellularised scaffolds biocompatibility and ability to support recellularisation.

Chapter 2

General Materials and Methods

This chapter describes the general materials and methods used throughout the study, further details of specific experimental approaches are described in the upcoming chapters.

2.1 General materials:

2.1.1 Equipment and consumables:

Details of general laboratory equipment and consumables used throughout this study are listed in Table 2.1 and Table 2.2, respectively.

Table 2.1: General laboratory equipment used throughout the study

Equipment	Model	Manufacturer
Argon gas chamber	–	AGAR Auto Sputter Coater
Autoclave	–	Prestige medical
Balance	13204-S	College
Centrifuge	5804R	Eppendorf
Class II safety cabinet hood	N4-437-400E	NUAIRE
Confocal laser scanning microscope	SP2	Leica Microsystems
Electrical pressure cooker	Access retrieval unit	MenaPath

Fluorescence upright microscope	Axio imager Z1 with ApoTome	Zeiss
Freeze dryer	Alpha 2-4 LD plus	CHIST
Freezer	MDF-U20865	SANYO
Hand held drill	395	DREMEL
Handheld automated cell counter	Scepter™ 2.0 PHCC20060	Millipore
Histology water bath	HI1210	Leica
Hot plate	SH3	Stuart Scientific
Light inverted microscope	IX 71	Olympus
Light upright microscope	Axioplan	Zeiss
NanoDrop™ 2000 spectrophotometer	Nc/2000	Thermo Fisher Scientific Ltd.
Oven incubator	MCO-20 AIC	SANYO
Paraffin embedding machine	EG1150H	Leica Microsystems
Plate reader	Multiskan Spectrum	Thermo Fisher Scientific Ltd.
Polarised upright microscope	M2 Axio imager	Zeiss
Rotatory microtome	AS325	Leica Microsystems
Scanning electron microscope	S-3400N	Hitachi
Shaking incubator	C25	New Brunswick
Tissue processing machine	ASP200	Leica Microsystems
Vice clamp	-	-
Vortex	VXR 517	IKA-VIBRAX
Water bath	Grant / S4B	Scientific laboratory supplies

Table 2.2: General laboratory consumables used throughout the study

Consumables	Model/Size	Manufacturer
Bijou tubes	7 mL	Thermo Fisher Scientific Ltd.
Cell culture flasks	75 cm ² and 175 cm ²	Corning incorporated
CryoTube [®] vials	1.5 mL and 2 mL	Nunc [™]
Eppendorf tubes	Various sizes	Nunc [™]
Opsite flexigrid	4628	Smith & nephew
Optiplate [™] white plates	96-well	PerkinElmer [™]
Pipette tips	Various sizes	Star Labs
Plastic histology cassettes	M490-3	Simport
Silane coated microscopic slides	MDC-0102-54A	Cell path
Silicone embedding moulds	E4390	Sigma-Aldrich
Slides coverslips	COV12440S	Solmedia
Universal tubes	15 mL and 50 mL	Corning incorporated
Well plates (flat bottomed)	6-well, 12-well, 24-well, 48-well, 96-well	Corning incorporated
X-tra [®] adhesive microslides	3800200AE	Leica Biosystems

2.1.2 Chemicals, reagents and kits:

Details of all chemicals, reagents and kits used throughout the study are listed in Table 2.3.

Table 2.3: Chemicals, reagents and kits used throughout the study

Chemicals and reagents	Catalogue	Manufacturer
Agar	A-9915	Sigma-Aldrich
Alcian blue	RRSK400	Atom Scientific
Alpha-modified Eagle's medium	BE12-169F	Lonza
Antibody diluent	003218	Invitrogen
Antigen unmasking solution; citric acid based	H-3300	Vector Laboratories
Antigen unmasking solution; Tris-EDTA based	H-3301	Vector Laboratories
Aprotinin	A6279	Sigma-Aldrich
ATPLite™ assay	6016941	Perkin Elmer Life Sciences
Bond™ Enzyme Pretreatment kit	AR9551	Leica Biosystems
Bovine serum albumin	A7979	Sigma-Aldrich
Casein	Ssp-5020	Vector Laboratories
Cyanoacrylate adhesive glue	Z105902-1EA	Sigma-Aldrich
Dimethyl sulfoxide	D8418	Sigma-Aldrich
DNase I	AMPD1	Sigma-Aldrich
DNeasy Blood and Tissue Kit	69504	Qiagen
Synthetic mounting media (DPX mountant)	REA212	Solmedia
Dulbecco's modified Eagle's medium	D6546	Sigma-Aldrich

Endogenous peroxidase blocking with Bloxall (hydrogen peroxide)	SP-6000	Vector Laboratories
Eosin	RRSP35-D	Atom Scientific
Ethanol	32221-2	Sigma-Aldrich
Ethylene-diamine-tetra-acetic acid	03698	Sigma-Aldrich
Foetal bovine serum	DE14-802	Lonza
Giemsa solution	352603R	VWR International
Glacial acetic acid	27013	BDH
Glutaraldehyde solution	286824Q	Sigma-Aldrich
Horseradish peroxidase-conjugated secondary goat anti-rabbit antibody	XCP-P0100	MenaPath
ImmPACT 3,3'-diaminobenzidine (DAB) Peroxidase substrate	SK-4105	Vector Laboratories
ImmPRESS Excel staining kit	MP-7602	Vector Laboratories
L-glutamine solution	G7513	Sigma-Aldrich
LIVE/DEAD [®] stain kit	L3224	Molecular Probes [™]
Magnesium chloride solution	M1028	Sigma-Aldrich
Mayer's haematoxylin	RRSP60-D	Atom Scientific
Neutral buffered formalin	BAF-6000-08A	Cellpath
Nuclear Fast Red	RRSP4545-B	Atom Scientific
Penicillin-Streptomycin solution	P4333	Sigma-Aldrich
Peracetic acid	77240	Sigma-Aldrich
Phosphate-buffered saline	17-516F	Lonza
Phosphate-buffered saline (10X)	70013	Gibco by Life Technologies [™]

Picrosirius red stain	24901	Polysciences, Inc
RNase A	R4642	Sigma-Aldrich
Scott's tap water	EGW-0200-25A	CellPath
Sodium dodecyl sulphate	71736	Sigma-Aldrich
Sodium hydroxide	1310-73	Thermo Fisher Scientific Ltd.
Tris-buffer	T3038	Sigma-Aldrich
Tris-buffered saline	T5912	Sigma-Aldrich
Tris-buffered saline with 0.1 % Tween [®] 20	T9039	Sigma-Aldrich
Trizma [®] hydrochloride buffer solution	93313	Sigma-Aldrich
Trypsin / EDTA solution	T4049	Sigma-Aldrich
Type I collagen gel (rat tail)	A10483-01	Gibco by Life Technologies™
Vectashield antifade mounting medium with DAPI	H-1200	Vector Laboratories
Wiegert's haematoxylin	HS375	TCS Biosciences Ltd
Xylene	X/0250	Thermo Fisher Scientific Ltd.

2.1.3 Antibodies:

Details of primary antibodies, corresponding antigen retrieval method and secondary antibodies used for immunohistochemical labelling are listed in Table 2.4.

Table 2.4: Details of primary antibodies, the corresponding antigen retrieval method and isotypes used throughout the study

Antigen	Supplier	Source/ Clone/ Concentration supplied	Antigen retrieval Method	Secondary antibody	Dilution/ Concentration used	Isotype
Alkaline phosphatase	BioScience GTX100817	Rabbit polyclonal 48 $\mu\text{g.mL}^{-1}$	Heat induced with citric acid buffer	Horseradish peroxidase	1:1000 48 $\mu\text{g.mL}^{-1}$	IgG
Alpha-smooth muscle actin	Abcam ab7817	Mouse monoclonal 1A4 0.2 $\mu\text{g.mL}^{-1}$	Heat induced with citric acid buffer	ImmPRESS Excel	1:500 0.4 $\mu\text{g.mL}^{-1}$	IgG2a, Kappa
Collagen-I	Abcam ab90395	Mouse monoclonal COL-1 5-10 mg.mL^{-1}	Heat induced with Tris-EDTA buffer	ImmPRESS Excel	1:100 50-100 $\mu\text{g.mL}^{-1}$	IgG1
Collagen-III	Abcam ab6310	Mouse monoclonal FH-7A 3.300 mg.mL^{-1}	Heat induced with citric acid buffer	ImmPRESS Excel	1:200 16.5 $\mu\text{g.mL}^{-1}$	IgG1
Dentine matrix protein-1	Santa Cruz sc-73633	Mouse monoclonal LFMb-31 200 $\mu\text{l.mL}^{-1}$	Heat induced with citric acid buffer	ImmPRESS Excel	1:100 2 $\mu\text{g.mL}^{-1}$	IgG1, Kappa
Dentine sialoposphoprotein	Santa Cruz sc-73632	Mouse monoclonal LFMb-21 200 $\mu\text{l.mL}^{-1}$	Heat induced with citric acid buffer	ImmPRESS Excel	1:1000 0.2 $\mu\text{g.mL}^{-1}$	IgG2b, Kappa

Fibronectin	Abcam ab6328	Mouse monoclonal IST-9 1.140 mg.mL ⁻¹	Enzymatic antigen retrieval	ImmPRESS Excel	1:50 22.8 µg.mL ⁻¹	IgG1
Major histocompatibility class II RT1B	BIO-RAD MCA46R	Mouse monoclonal OX-6 1 mg.mL ⁻¹	Heat induced with citric acid buffer	ImmPRESS Excel	1:200 5 µg.mL ⁻¹	IgG1
Major histocompatibility class II, HLA-DR alpha-chain.	DAKO M0746	Mouse monoclonal TAL.1B5	Heat induced with citric acid buffer	ImmPRESS Excel	1:150 0.35 µg.mL ⁻¹	IgG1, Kappa.
Laminin	NovusBio NB300-144	Rabbit polyclonal LAMA1 1 mg.mL ⁻¹	Enzymatic antigen retrieval	Horseradish peroxidase	1:400 2.5 µg.mL ⁻¹	IgG
Vascular endothelial growth factor receptor-2	Cell Signaling 2479	Rabbit monoclonal KDR, Flk-1 100 µg.mL ⁻¹	Heat induced with Tris-EDTA buffer	Horseradish peroxidase	1:25 4 µg.mL ⁻¹	IgG
Vimentin	DAKO M0725	Mouse monoclonal V9 360 mg.mL ⁻¹	Heat induced with citric acid buffer	ImmPRESS Excel	1:10000 36 µg.mL ⁻¹	IgG1, Kappa
Vascular endothelial growth factor A	Abcam ab46154	Rabbit polyclonal 1 mg.mL ⁻¹	Heat induced with Tris-EDTA buffer	Horseradish peroxidase	1:200 (overnight) 5 µg.mL ⁻¹	IgG
Nestin	R&D Systems MAB1259	Mouse monoclonal 196908 0.5 mg.mL ⁻¹	Heat induced with Tris-EDTA buffer	ImmPRESS Excel	1:5000 0.1 µg.mL ⁻¹	IgG1

2.1.4 Isotype controls:

Details of isotype controls used for immunohistochemical labelling are listed in Table 2.5. The concentration used for isotype control was the same as the corresponding primary antibody.

Table 2.5: Isotype controls used throughout the study

Isotype	Supplier	Source/ Clone/ Concentration supplied
IgG	Abcam ab199507	Rabbit monoclonal EPR25A 0.5 mg.mL ⁻¹
IgG1	Abcam ab91353	Mouse monoclonal B11/6 0.1 mg.mL ⁻¹
IgG1 Kappa	Sigma-Aldrich M9269	Mouse monoclonal MOPC 21 1.0 mg.mL ⁻¹
IgG2a Kappa	Sigma-Aldrich M-7769	Mouse monoclonal UPC 10 5 mg.mL ⁻¹
IgG2b Kappa	DAKO X0944	Mouse monoclonal DAK-GO9 87 µg.mL ⁻¹

2.2 General methods:

2.2.1 Tissue procurement:

2.2.1.1 Rat teeth collection and pulp retrieval:

Wistar male rats, 28 days (\pm 2 days), were obtained from Central Biomedical Services (University of Leeds, UK) following appropriate methods of humane killing listed on Schedule 1 of the Animals (Scientific Procedures) Act 1986. All attempts were made to reduce the number of animals used. Rats were sacrificed with only rat heads collected. Two mandibular incisors were carefully extracted from each rat jaw. Rat pulp tissues were then carefully retrieved with a sterile scalpel and fine tweezers in a Class II safety cabinet.

2.2.1.2 Human teeth collection and pulp retrieval:

Human permanent molars and premolars free from any visible decay, fracture or developmental anomaly were included in this work. All teeth were collected within 48 hours following extraction from Leeds Dental Institute (University of Leeds, United Kingdom). Full written patient consent and appropriate ethical approval (Skeletal Research Tissue Bank; reference number 101013/MME/113; Appendix A) were obtained, according to the Human Tissue Act. Donors were both male and female with an age range between 11 - 30 years.

External tooth surfaces were cleaned with 70 % (v/v) ethanol and cleared from any remaining adhering external soft tissue using a sterile scalpel in Class II safety cabinet. Two methods were investigated for dental pulp retrieval as described below:

Method 1:

Teeth were initially decoronated (horizontally) followed by two longitudinal cuts on both sides of the root surface using a hand-held drill with a diamond disc. The root fragments were separated manually using sterile dental instruments (tweezers and a flat plastic instrument). The pulp tissue was then aseptically retrieved. Unfortunately, following testing the above method several times, the procedure was impractical. Holding the tooth stable while drilling was a challenge and possessed a significant hazard.

Method 2:

Teeth were placed in sterile gloves and broken using a screw vice clamp. The pulp tissues were carefully retrieved with sterile tweezers in a Class II safety cabinet. This method was more reliable and safer than Method 1. The extracted pulp tissue was carefully examined under strong light and magnification to remove any adhering dentine chips.

2.2.2 Tissue decellularisation:**2.2.2.1 Decellularisation solutions and reagents preparation:**

Solution preparation steps were carried out aseptically in a Class II safety cabinet and adjusted to the required pH using hydrochloric acid or sodium hydroxide. Non sterile solutions were sterile filtered through a 0.2 µm filter.

Hypotonic Tris buffer (10 mM Tris, 0.1 % w/v ethylene-diamine-tetra-acetic acid and 10 Kallikrein Inhibitor Unit (KIU).mL⁻¹ Aprotinin) was prepared by adding 1 mL of Tris solution (1 M Tris, pH 8.0), 680 µL of ethylene-diamine-tetra-acetic acid solution (EDTA, 500 mM), 96.2 µL of Aprotinin solution (10,400 KIU.mL⁻¹)

and completed to the total volume of 100 mL with distilled water. This buffer was made fresh before usage.

Hypotonic sodium dodecyl sulphate (SDS) buffer (0.03 % w/v SDS, 10 mM Tris, 0.1 % w/v EDTA and 10 KIU.mL⁻¹ Aprotinin) was prepared by adding 300 µL of SDS solution (10 % w/v) to 99.70 mL hypotonic buffer (prepared above), to make a final volume of 100 mL. This buffer was made fresh before usage.

Nuclease treatment solution (DNase 50 U.mL⁻¹, RNase 1 U.mL⁻¹) in buffer (50 mM Tris-hydrochloric acid, 10 mM magnesium chloride and 50 µg.mL⁻¹ bovine serum albumin; pH 7.5) was prepared by mixing 5 mL of Tris-hydrochloric acid (Tris-HCL) solution (1 M, pH 7.5), 1 mL of magnesium chloride solution (1 M) and 14.28 mL of bovine serum albumin solution. Followed by the addition of 5 mL DNase solution (1000 U.mL⁻¹) and 40 µL RNase solution (2523 U.mL⁻¹) and completed to a total volume of 100 mL with distilled water. This solution was made fresh before usage.

Phosphate buffered saline (PBS) wash buffer with Aprotinin (10 KIU.mL⁻¹) was prepared by adding 0.48 mL of Aprotinin solution (10,400 KIU.mL⁻¹) to 499.52 mL of PBS (pH 7.4) to make a total volume of 500 mL. This solution was made fresh before usage.

Peracetic acid solution (0.1 % v/v) was prepared by adding 225 µL of peracetic acid PBS without magnesium and calcium (pH 7.4) to a total volume of 100 mL. This solution was made fresh before usage.

2.2.2.2 Decellularisation protocol:

The decellularised protocol was carried out according to Wilshaw et al. (2006) as described below. All decellularisation treatments were carried out in 7 mL bijou tubes containing one pulp tissue in 4 mL solution. Tissue samples were initially washed in PBS (pH 7.4) containing Aprotinin (10 KIU.mL^{-1}) at room temperature, three times for 30 minutes. Samples were then placed into hypotonic Tris buffer (10 mM Tris, 0.1 % w/v EDTA and 10 KIU.mL^{-1} Aprotinin) at $4 \text{ }^{\circ}\text{C}$ for 16 hours. The following day samples were incubated in hypotonic SDS buffer (0.03 % w/v SDS, 10 mM Tris, 0.1 % w/v EDTA and 10 KIU.mL^{-1} Aprotinin) at $25 \text{ }^{\circ}\text{C}$ for 24 hours with agitation at 120 revolutions per minute (rpm). The next day samples were washed in TBS (pH 7.6) containing no protease inhibitors with agitation at 160 rpm, three times for 30 minutes before Incubation with nucleases treatment solution (DNase 50 U.mL^{-1} , RNase 1 U.mL^{-1}) in buffer (50 mM Tris-HCL, 10 mM magnesium chloride and $50 \text{ } \mu\text{g.mL}^{-1}$ bovine serum albumin; pH 7.5) at $37 \text{ }^{\circ}\text{C}$ for three hours with agitation at 80 rpm. Subsequently, samples were washed in TBS (pH 7.6) containing no protease inhibitors with agitation at 160 rpm twice for 20 minutes followed by one overnight wash (16 hours). Samples were then disinfected with 0.1 % (v/v) peracetic acid solution at room temperature for three hours with agitation at 160 rpm. Finally tissue samples were washed thrice in TBS (pH 7.6) with agitation at 160 rpm for 30 minutes each.

2.2.3 General histological technique:

2.2.3.1 Tissue fixation, processing and paraffin embedding:

Tissue samples were fully immersed in prefilled pots containing 10 % (v/v) neutral buffered formalin (4 % formaldehyde) for 24 hours followed by immersion in 70 % (v/v) ethanol. To avoid tissue loss during paraffin embedding and to facilitate the orientation of the samples, pulp tissues were carefully embedded in 2 % (w/v) agar (dissolved in PBS) using silicone embedding moulds.

The tissue-agar blocks were left to solidify for approximately 30 minutes at 4 °C. Tissue-agar blocks were placed in plastic histological cassettes and processed using an automated tissue processor using a routine protocol. Briefly, the specimens were dehydrated in series of ascending ethanol concentrations, cleared in three consecutive immersions of xylene and finally infused with paraffin wax (tissue processing protocol detailed below in Table 2.6).

The cassettes were transferred into paraffin within the wax embedding machine. Tissue-agar blocks were removed from the cassettes and embedded carefully in paraffin using stainless steel moulds. The histology cassettes were replaced on the top surface of the moulds, topped up with excess molten wax and left to solidify on a cold plate. Stainless steel moulds were then removed, excess wax trimmed and stored until future sectioning.

Table 2.6: Tissue processor protocol

Routine processing protocol	Time	Temperature
70 % (v/v) ethanol	30 minutes	37 °C
80 % (v/v) ethanol	30 minutes	37 °C
90 % (v/v) ethanol	30 minutes	37 °C
95 % (v/v) ethanol	30 minutes	37 °C
100 % (v/v) ethanol	60 minutes	37 °C
100 % (v/v) ethanol	60 minutes	37 °C
100 % (v/v) ethanol	90 minutes	37 °C
Xylene	60 minutes	37 °C
Xylene	90 minutes	37 °C
Xylene	90 minutes	37 °C
Wax	60 minutes	65 °C
Wax	60 minutes	65 °C
Wax	60 minutes	65 °C

2.2.3.2 Tissue sectioning and slide preparation:

Tissue embedded wax blocks were serial sectioned at 5 µm thickness for histology and immunohistochemistry staining using a rotatory microtome. Sections were placed to fluctuate on a hot water bath at 45 °C, collected on microscopic glass slides and left to dry overnight at 37 °C. Then every five in 20 sections were stained with haematoxylin and eosin to enable the selection of the most representative batch of slides to be stained for additional histology and

immunohistochemistry studies. All slides were heated for 20 minutes on a hot plate at 60 °C before dewaxing to maximise tissue adherence to glass slides.

2.2.3.3 Dewaxing and rehydration of paraffin embedded tissue sections:

The slides were immersed into four changes of xylene for five minutes each, rehydrated using descending ethanol series. This involved two changes of 100 % (v/v) ethanol, one change of 90 % (v/v) ethanol and one change of 75 % (v/v) ethanol for two minutes each. Finally the slides were gently rinsed using running tap water for an additional one minute.

2.2.3.4 Dehydration and clearing of stained tissue sections:

Following staining, the slides were dehydrated using ascending ethanol series. This involved one change of 75 % (v/v) ethanol for five minutes and three changes of 100 % (v/v) ethanol for 20 seconds. The slides were then cleared in four successive changes of xylene for five minute each. Finally, the slides were mounted using a synthetic resin mounting media (DPX mountant) and a cover slip.

2.2.4 Histological staining methods:

2.2.4.1 Haematoxylin and eosin staining:

Haematoxylin and eosin (H&E) staining was used to view general tissue histoarchitecture. Following dewaxing and rehydration (Section 2.2.3.3), tissue sections were immersed in Mayer's haematoxylin for three minutes and rinsed under a gentle flow of tap water for one minute. Sections were then immersed in Scott's tap water for one minute and rinsed with tap water for an additional

one minute. Subsequently, tissue sections were immersed in eosin for four minutes and rinsed with tap water for 30 seconds. Following staining, the slides were dehydrated, cleared and mounted (Section 2.2.3.4). Stained slides were kept overnight in a fume cupboard before viewing under bright-field microscopy using normal Köhler illumination. Images were captured digitally using an AxioPlan Zeiss light microscope fitted with AxioCam colour camera and AxioVision Rel. 4.8 software.

2.2.4.2 4',6-diamidino-2-phenylindole (DAPI) staining:

Vectashield Antifade Mounting Medium with DAPI was used to locate cell nuclei and/or residual nuclear material. Following dewaxing and rehydration (Section 2.2.3.3), the slides were washed in PBS (pH 7.4) and a drop of Vectashield Antifade Mounting Medium with DAPI was placed over the tissue section of each slide and mounted with a cover slip. Slides were viewed under fluorescence microscopy equipped with a DAPI filter set at 49 beamsplitter FT395 with excitation 365 nm and emission 445 / 450 nm wave lengths. Images were captured using a Zeiss Axio imager Z1 with ApoTome fitted with black and white AxioCam camera and AxioVision Rel. 4.7 software.

2.2.4.3 Alcian blue staining:

Alcian blue staining was used to view acidic mucosubstances and acetic mucins within the tissue. Following dewaxing and rehydration (Section 2.2.3.3), tissue sections were immersed in 3 % (v/v) Glacial acetic acid for three minutes, stained with 1 % (v/v) Alcian blue (pH 2.5) solution for 30 minutes and rinsed in distilled water. Sections were then counterstained in 0.1 % (w/v) nuclear fast

red solution for 10 minutes and rinsed under a gentle flow of tap water for one minute. Following staining, the slides were dehydrated, cleared and mounted (Section 2.2.3.4). Stained slides were kept overnight in a fume cupboard before viewing under bright-field microscopy using normal Köhler illumination. Images were captured digitally using an Axioplan Zeiss light microscope fitted with an AxioCam colour camera and AxioVision Rel. 4.8 software.

2.2.4.4 Picrosirius red staining:

Picrosirius red staining was used to visualise collagen in the tissue. Following dewaxing and rehydration (Section 2.2.3.3), tissue sections were immersed in Wiegert's hematoxylin for eight minutes and rinsed in distilled water. Sections were then immersed in phosphomolybdic acid for two minutes and rinsed in distilled water. Subsequently, tissue sections were immersed in Picrosirius red solution for 60 minutes, hydrochloric acid for two minutes and in 70 % (v/v) ethanol for 45 seconds. Following staining, the slides were dehydrated, cleared and mounted (Section 2.2.3.4). Stained slides were kept overnight in a fume cupboard before viewing under bright field and polarised light. Images were captured digitally using a Zeiss M2 Axio imager polarised microscopic and Zen Blue 2015 software.

2.2.5 Immunohistochemical labelling:

Immunohistochemical labelling was carried out on formalin fixed paraffin embedded samples. All immunohistochemistry slides were initially dewaxed and rehydrated (Section 2.2.3.3), subjected to specific antigen retrieval treatment followed by primary and secondary antibody staining procedure as described below and summarised in Table 2.4.

2.2.5.1 Antigen retrieval methods:

- i. Heat-induced antigen retrieval using citric acid buffer: This step involved a commercially available antigen unmasking solution consisting of citric acid buffer (pH 6.0). Slides were placed in a suitable slide rack container, fully immersed in citric acid buffer and inserted in a pressure cooker. The pressure cooker was heated to full pressure at 125 °C for two minutes and allowed to cool before removal of the slides.
- ii. Heat-induced antigen retrieval using Tris-EDTA buffer: This step involved a commercially available antigen unmasking solution consisting of Tris-EDTA buffer (pH 9.0). Slides were placed in a suitable slide rack container, fully immersed in Tris-EDTA buffer and inserted in a pressure cooker. The pressure cooker was heated to full pressure at 125 °C for two minutes and allowed to cool before removal of the slides.
- iii. Enzymatic antigen retrieval: Bond™ enzyme pretreatment kit was used following mixing enzyme concentrate and an enzyme diluent. Slides were placed in an air humidifier chamber with tissue sections covered with enzyme mix and incubated at 37 °C for 15 minutes.

2.2.5.2 Immunohistochemistry labelling procedure:

Following antigen retrieval, all tissue sections were subjected to endogenous hydrogen peroxidase blocking with Bloxall for 10 minutes. Tissue sections were washed once with TBS containing 0.1 % (v/v) Tween 20 (pH 7.6) for five minutes, subjected to protein blocking (1 / 10 casein) for 20 minutes and then incubated with the primary antibody or the appropriate isotype control at room temperature for one hour.

Subsequently, the slides were washed twice with TBS containing 0.1 % (v/v) Tween 20 (pH 7.6) for five minutes and then subjected to secondary antibody staining (immunolabelling) using either ImmPRESS Excel peroxidase anti-mouse or Horseradish peroxidase (HRP) anti-rabbit polymer following manufacturer's instructions at room temperature for 30 minutes.

Next, the slides were washed twice with TBS (pH 7.6) for five minutes and stained with ImmPACT 3,3'-diaminobenzidine (DAB) Peroxidase chromogen substrate at room temperature for five minutes. The slides were then rinsed under a gentle flow of tap water and counterstained with Mayer's haematoxylin for 30 seconds.

Following staining, the slides were then dehydrated, cleared and mounted (Section 2.2.3.4). Slides were left to dry overnight in a fume cupboard before viewing under bright-field microscopy using normal Köhler illumination. Images were captured digitally using an Axioplan Zeiss light microscope fitted with AxioCam colour camera and AxioVision Rel. 4.8 software.

2.2.6 DNA quantification assay:

DNA extraction was performed using DNeasy Blood and Tissue Kit following manufacturer's instructions (summarised in Figure 2.1). Dental pulp tissues were cut into small pieces, placed in a 1.5 mL DNase- and RNase-Free sterile microcentrifuge tube and lysed using proteinase K enzyme. Samples were incubated with proteinase K at 56 °C overnight until tissues were completely lysed. Pulse vortexing was regularly performed throughout the experimental steps as per manufacturer's instructions. The extracted DNA was collected in the flow-through of buffer AE and immediately quantified using a NanoDrop™ 2000 spectrophotometer with a measuring absorbance wavelength of 260 / 280 nm. The DNA content, of each sample, was normalised to the dry weight to determine the DNA content per tissue dry weight. Three readings per sample were taken and the mean of these readings was calculated.

To assess pulp tissue water content, randomly selected pulp tissues (in triplicates) were initially weighted (wet weight). Pulp tissues then underwent freeze-dry procedure and re-weighted (dry weight). The average pulp tissue water content was found to be approximately 70 % water (Appendix B). The percentage of pulp tissue water content was calculated based on the below equation:

$$\text{Percentage of pulp tissue water content} = \frac{\text{wet weight} - \text{dry weight}}{\text{wet weight}} \times 100$$

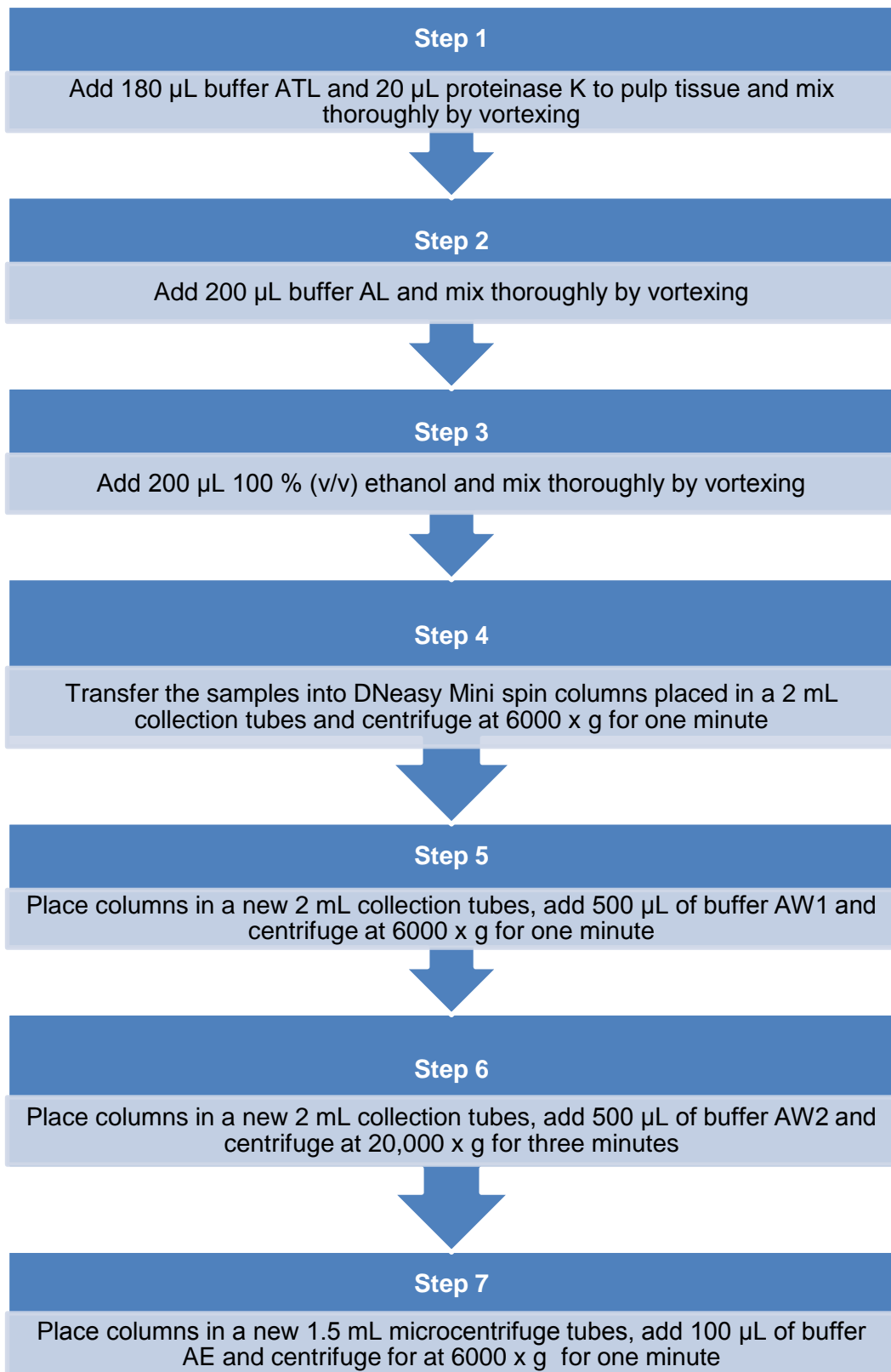


Figure 2.1: DNA extraction protocol.

2.2.7 Scanning electron microscope:

Sample preparation for scanning electron microscope (SEM) imaging initially involved tissue fixation in 2.5 % (v/v) glutaraldehyde solution overnight at 4 °C. Tissue samples were then washed thrice in distilled water for 10 minutes each, dehydrated in ascending concentrations of ethanol (30, 50, 70, 80, 90, and 95 % v/v) for 10 minutes each and a final concentration of 100 % (v/v) ethanol thrice for 20 minutes each. Fixed dehydrated samples were then exposed to 50 % (v/v) hexamethyldisilazane in ethanol solution for 10 minutes followed by 100 % (v/v) hexamethyldisilazane solution twice for 15 minutes each. Finally samples were placed in 100 % (v/v) hexamethyldisilazane solution and left to evaporate overnight in a fume hood. Before SEM viewing, samples were affixed to 1.2 mm aluminium stubs with adhesive carbon tape and gold sputter coated for 80 seconds in an argon gas chamber at 3 millibars.

2.2.8 Cell culture techniques:

As standard procedures, all cell culture work was performed aseptically in a Class II safety cabinet and incubated in a humidified atmosphere incubator containing 5 % (v/v) CO₂ and 95 % air at 37 °C. All tissue culture reagents and additives were equilibrated to 37 °C before usage.

2.2.8.1 Cell types used:

Cell types used throughout the study are listed in Table 2.7. Patient consent and ethical approval (Skeletal Research Tissue Bank; reference number 101013/MME/113; Appendix A) was obtained prior to the use of human dental pulp stem cells (DPSCs).

Table 2.7: Cell types used throughout the study

Cell	Type	Species	Supplier
L-929 cell line	Fibroblasts	Murine	Cell line reserve, Oral biology department, University of Leeds, UK.
Dental pulp stem cells	Primary cells	Human	Dr Matthew Tomlinson, Oral biology department, University of Leeds, UK.

Human DPSCs used in this work, kindly provided by Dr M Tomlinson, were isolated and cultured as described in (Tomlinson et al., 2015). Briefly, tooth surfaces were disinfected with 70 % (v/v) ethanol and any adherent soft tissue removed. The teeth were fractured and pulp tissue aseptically retrieved. Pulp tissues were mechanically disrupted and enzymatically digested in 3 mg.mL⁻¹ collagenase type I and 4 mg.mL⁻¹ dispase solution, incubated at 37 °C in 5 % (v/v) CO₂ and 95 % relative humidity with gentle agitation. Subsequently, the suspension was passed through a 70 µm cell strainer and centrifuged at 200 x g for five minutes. The collected cell pellet was then suspended in alpha-modified Eagle's medium supplemented with 15 % (v/v) foetal bovine serum (FBS), 1 % (v/v) 2 mM L-glutamine and antibiotics solutions (100 U.mL⁻¹ penicillin and 100 µg.mL⁻¹ streptomycin).

2.2.8.2 Cell specific culture medium:

L-929 cell line culture medium:

Dulbecco's modified Eagle's medium (DMEM) was used as a standard culture medium supplemented with 10 % (v/v) FBS, 1 % (v/v) 2 mM L-glutamine and antibiotics solutions (100 U.mL⁻¹ penicillin and 100 µg.mL⁻¹ streptomycin). The complete culture medium was stored at 4 °C for up to seven days.

Human dental pulp stem cells culture medium:

Alpha-modified Eagle's medium was used as a standard culture medium supplemented with 10 % (v/v) FBS, 1 % (v/v) 2 mM L-glutamine and antibiotics solutions (100 U.mL⁻¹ penicillin and 100 µg.mL⁻¹ streptomycin). The complete culture medium was stored at 4 °C for up to seven days.

2.2.8.3 Cell resurrection and maintenance:

Cells were removed from either liquid nitrogen (-196 °C) for long-time storage or -80 °C freezer for short-term storage, and rapidly thawed in the water bath set at 37 °C. The defrosted cell stock (1 mL) was immediately transferred in to 15 mL falcon tube and mixed with 9 mL of the cell specific medium. The cell suspension was then centrifuged at 150 x g for five minutes.

Following centrifugation, the supernatant was carefully aspirated and the cell pellet was initially resuspended in 1 mL followed by 9 mL of cell specific medium. The cell suspension solution was then divided into cell culture flasks as per volume and size required. Cell specific medium was changed every three days and cell growth, attachment, and proliferation was checked under phase contrast illumination using an inverted light microscope.

2.2.8.4 Cell passaging and counting:

Cells were passaged when they reached approximately 70 – 80 % confluency (density) within the cell culture flasks. Cell medium was aspirated from the cell culture flasks and the cell surface monolayer was washed twice with PBS (7.4) without calcium and magnesium (10 mL for T75 and 20 mL for T175, size flasks) for five minutes. Cells were then passaged by digestion with 0.25 % trypsin and 0.02 % EDTA solution, added to the cell culture flasks (5 mL for T75 and 10 mL for T175, size flasks) and incubated at 37 °C for three to five minutes. After the short incubation duration, cell detachment (floating cells) was assessed using an inverted microscope. On successful detachment, complete cell specific medium (10 mL for T75 and 20 mL for T175, size flasks) was added to each flask to deactivate trypsin / EDTA solution activity. Flask contents were then transferred into a universal tube and centrifuged at 150 x g for five minutes. Following centrifugation, the supernatant was discarded and the cell pellet was resuspended and homogenised in complete cell specific medium. A viable cell count was performed using a hand held automated cell counter fitted with 60 µL tips. The diluted cell suspension was reseeded into fresh cell culture flasks and incubated at 37 °C in 5 % (v/v) CO₂ and 95 % relative humidity.

2.2.8.5 Cell cryopreservation:

For future cell storage, cryopreserved medium consisting of 90 % (v/v) FBS and 10 % (v/v) filter sterilised Dimethyl sulfoxide (DMSO) was used. The cryopreserved medium was then added to the formed cell pellet. The cell suspension was aliquoted to 1 mL into CryoTube[®] vials and placed in

cryo-freezing pots containing isopropanol at -80 °C for a minimum of three hours for gradual temperature reduction. CryoTube[®] vials were stored at -80 °C or liquid nitrogen (-196 °C) for short or long term storage, respectively.

2.2.9 Cytotoxicity evaluation:

2.2.9.1 Contact cytotoxicity assay:

Contact cytotoxicity assay was performed with L-929 murine fibroblast cell lines in direct contact with the study samples and relevant controls. Controls used included cyanoacrylate adhesive glue as a positive control and type I collagen gel as a negative control.

All cell culture well plates were washed using three changes of sterile PBS (pH 7.4) without calcium and magnesium for 10 minutes. L-929 cell lines were cultured and maintained in their standard culture medium and diluted to a cell concentration of 2×10^5 cells.mL⁻¹. A volume of 2 mL of the diluted cell suspension, 4×10^5 cells per well, was added to the appropriate six-well cell culture plates and incubated for 48 hours in a humidified atmosphere incubator containing 5 % (v/v) CO₂ and 95 % air at 37 °C. Following incubation, the culture medium was carefully aspirated and the well plates were gently washed with PBS (pH 7.4) containing calcium and magnesium. Subsequently, the PBS was aspirated and the cells were fixed with 10 % (v/v) neutral buffered formalin for 10 minutes. The fixed cells were then stained with Giemsa solution for an additional five minutes. The plates were gently washed well with distilled water and left to air dry.

Type I collagen rat tail gel preparation protocol:

To form a firm collagen gel manufacturer's instructions were followed as described below:

Volume of collagen required (V1)

$$= \frac{\text{Final concentration of collagen} \times \text{Total volume (V)}}{\text{Initial collagen concentration}}$$

$$\text{Volume of PBS (10X) required (V2)} = \frac{V}{10}$$

$$\text{Volume of sodium hydroxide required (V3)} = V1 \times 0.025$$

$$\text{Volume of distilled water required (V4)} = (V) - (V1 + V2 + V3)$$

The required quantities of distilled water, sodium hydroxide, and PBS (10X) were added in a sterile Eppendorf tube. Collagen gel was slowly pipetted, added to the above and mixed well by gently pipetted up and down. The collagen mix was immediately placed on the desired plates and incubated at 37 °C for 30 to 40 minutes for a formation of a firm gel.

2.2.9.2 Extract cytotoxicity assay:

Extract cytotoxicity assay was performed with L-929 murine fibroblast cell lines incubated in test material extract and relevant controls. Controls used included 40 % (v/v) DMSO in DMEM as a positive control and serum-free DMEM as a negative control. For the test extract decellularised tissues were finely macerated and aseptically weighed. The macerated tissue were placed into sterile microcentrifuge tubes containing serum-free DMEM (ratio of 1 mL per 100 mg tissue) and incubated at 37 °C for 72 hours with agitation. Following

incubation, the microcentrifuge tubes were centrifuged at 500 x g for 15 minutes. The supernatants (test extract) were aseptically collected and sterility was assured by streaking onto fresh blood agar plates. The blood agar plates were checked for sterility following 48 hours incubation at 37 °C. The test extracts were stored at -20 °C until the experimental day.

L-929 cell lines were cultured and maintained in their standard culture medium and diluted to a concentration of 5×10^4 cells.mL⁻¹. A volume of 200 µL of the diluted cell suspension, 1×10^4 cells per well, was added to the appropriate wells of 96-well cell culture plates and incubated for overnight at 37 °C in 5 % (v/v) CO₂ and 95 % relative humidity.

On the day of the experiment, the test extracts and controls were warmed to 37 °C. At the same time, the medium from each well plate was gently aspirated and replaced with 100 µL of double strength DMEM containing 20 % (v/v) FBS, 2 % (v/v) 2 mM L-glutamine and antibiotics solutions (200 U.mL⁻¹ penicillin and 200 µ.mL⁻¹ streptomycin). Followed by, 100 µL of test extracts or control solutions. The cell culture plates were then incubated for 24 hours in a humidified atmosphere incubator containing 5 % (v/v) CO₂ and 95 % air at 37 °C. Following incubation, cell viability measuring the relative cellular adenosine triphosphate (ATP) content was determined using the ATPLite™ assay following manufacturer's instructions.

ATPLite™ assay:

The culture medium of test and control well plates were aspirated and 50 µL of fresh cell culture medium and 50 µL of mammalian cell lysis solution were added to each well and incubated at room temperature for five minutes with constant shaking. The contents of the each well were carefully transferred to white 96-well Optiplate™, supplemented with 50 µL of substrate solution and incubated for five minutes with constant shaking. The Optiplate™ was left to dark adapt at room temperature for 10 minutes and luminescence measured using TopCount™ plate reader.

2.2.10 Recellularisation of decellularised scaffold with dental pulp**stem cells:**

The decellularised scaffolds were individually placed in a sterile Eppendorf tube (200 µL capacity) supplemented with 180 µL of a diluted cell suspension. A hole was made in each Eppendorf lid and sealed with opsite flexigrid membrane, an adhesive polyurethane film that allows gas exchange, while keeping the contents of the tube sterile. The Eppendorf tubes were placed in an in-house rotator apparatus (Figure 2.2) set at 10 rpm, to allow dynamic seeding, and incubated for 24 hours in a humidified atmosphere incubator containing 5 % (v/v) CO₂ and 95 % air at 37 °C. The scaffolds were then carefully transferred into a 12-well cell culture plates, topped up with 2 mL of fresh cell culture medium. The culture medium was changed every three days throughout the duration of the experiment (7 and 14 days culture period).



Figure 2.2: Seeding rotator apparatus. The device consists of two rotating modules attached on rotating cylinders powered by a motor source.

2.2.11 Cell viability assay:

Cell viability of the recellularised scaffolds was assessed using a commercial Live/Dead[®] stain following manufacturer's instructions. A solution of 5 μ L calcein-AM and 20 μ L ethidium homodimer-1 in 10 mL in serum-free alpha-modified Eagle's medium was freshly prepared before usage. Scaffolds were individually placed in 48-well tissue culture plates and the prepared stain solution was added to each well plate to completely cover the scaffolds. The plates were covered and incubated for 45 minutes in a humidified atmosphere incubator containing 5 % (v/v) CO₂ and 95 % air at 37 °C. Stained scaffolds were washed on a plate rocker in serum-free alpha-modified Eagle's medium for 30 minutes followed by PBS (pH 7.4) for an additional five minute. The scaffolds were wet mounted using PBS and viewed using a confocal laser scanning microscope (SP2) with FITC and Texas red filters for dual-labelled samples.

2.2.12 Statistical analysis:

All numerical values were presented as means, standard deviations and 95 % confidence intervals for each set of results (n = sample number and $p = 0.05$). The independent student's t -tests were used for the comparison of groups of two means. One-way analysis of variance (ANOVA) with Bonferroni correction was used for the comparison of groups of more than two means. The differences between groups were considered significant with a p -value less than 0.05. All statistical analyses were analysed using GraphPad Prism (Software version 6).

Chapter 3

Decellularisation of the dental pulp tissues

3.1 Introduction:

Despite several scaffold materials currently being researched, in an attempt to regenerate the pulp-dentine complex, only limited success has been reported (Galler et al., 2011a). Limitations mainly include biodegradation, biocompatibility concerns (Murray et al., 2007) and poor control over newly formed tissue resembling more of a connective tissue than a dentine-like structure (Zhang et al., 2006a). Hence, the ideal scaffold for pulp regeneration is yet to be identified (Wang et al., 2010b; Song et al., 2017).

The natural tissue matrix is considered a vital component of all tissues and, possibly, the ideal scaffold for tissue regeneration (Badylak, 2002; Badylak, 2007; Ma, 2008). The extracellular matrix (ECM) is composed of a unique mixture of proteins, glycoproteins and proteoglycans organised in tissue specific structure (Badylak, 2002). Recently, the use of biological scaffolds composed of an acellular ECM derived through tissue decellularisation has been advocated and intensively researched in regenerative medicine (Gilbert et al., 2006; Crapo et al., 2011; Song and Ott, 2011).

Generally, the decellularisation process involves the combined usage of chemical and enzymatic agents in addition to physical methods. The procedure starts initially with lysis of the cell membrane, solubilisation of cytoplasmic and

nuclear components, ending with removal of cellular debris from the treated tissue. The incorporation of protease inhibitors in the early steps of the decellularisation process is known to protect the ECM against undesirable damage caused by the release of intracellular proteases during cell lysis (Gilbert et al., 2006; Crapo et al., 2011). Several washes with agitation are also incorporated throughout the decellularisation steps, to enhance the removal of chemical residues and cellular fragments from the ECM (Gilbert et al., 2006; Fu et al., 2014).

Several decellularisation protocols are available within the literature and vary widely dependent on the chemicals used, their concentration, duration of exposure, and most importantly the nature of treated tissue. The selection of a decellularising method is crucial in determining the success for developing an acellular pulp matrix. Ideally, the decellularisation process should aim at efficient removal of all its cellular and nuclear material while preserving the structural and functional matrix proteins (Badylak et al., 2009).

Detergents are commonly used for cell membrane lysis. Sodium dodecyl sulphate (SDS) is classified as an ionic detergent that is widely incorporated within various decellularisation protocols, it is considered to be an extremely effective detergent used for solubilising cytoplasmic and nuclear membranes (Seddon et al., 2004; Woods and Gratzer, 2005; Gilbert et al., 2006). However, concerns regarding the potential toxicity of residual SDS and tissue damage have been reported with 1 % (w/v) SDS. Bodnar et al. (1986) used 1 % (w/v) SDS as a treatment to porcine valves to prevent or delay calcification. The

results of their work demonstrated extreme structural damage causing tissue fragmentation, collagen swelling and significant loss of hydrothermal stability (Bodnar et al., 1986). Reducing the concentration of SDS to 0.1 % (w/v) resulted in acellular tissues with retained structural histoarchitecture following decellularisation of human pericardial tissue (Mirsadraee et al., 2006), human common femoral arteries (Wilshaw et al., 2012) and porcine urinary bladder (Rosario et al., 2008). Yoeruek et al. (2012) decellularised porcine corneas with 0.3 % (w/v) SDS with the addition of protease inhibitors within the decellularisation protocol. Furthermore, Wilshaw et al. (2006) decellularised human amniotic membrane using a low detergent protocol, 0.03 % (w/v) SDS, with added protease inhibitors. Results of the above studies, demonstrated complete cellular removal with preservation of the structural matrix (Wilshaw et al., 2006; Yoeruek et al., 2012). Indeed preservation of ECM following SDS detergent treatment has been directly linked to the low detergent concentration and the addition of protease inhibitors (Knight et al., 2008).

Triton X-100, non-ionic detergent, is also an effective detergent that is commonly used for cell membrane lysis. However, structural disruption of the ECM and removal of GAGs is reported with its usage (Gilbert et al., 2006; Crapo et al., 2011). Significant loss of GAG content was reported following the use of Triton X-100 to decellularise porcine aortic heart valves (Liao et al., 2008). Within the dental field, attempts to demineralise and decellularise porcine tooth buds (Traphagen et al., 2012), dental pulp tissues obtained from miniature swine teeth (Chen et al., 2015), and human tooth pulp tissues within root slices (Song et al., 2017) have been recently reported in the dental

literature. Although these protocols varied, they shared a similar dual detergent (combined use of SDS and Triton X-100) step. Despite these reported successful results, the use of decellularisation protocols with lower concentrations of toxic detergents such as SDS and Triton X-100 is advantageous for future cell proliferation and differentiation. Therefore, a low concentration detergent based decellularisation protocol utilising multiple gentle steps is of clinical interest.

Therefore, this chapter describes utilising a relatively mild method, composed of 0.03 % (w/v) SDS detergent, to decellularise the dental pulp tissues of both rat and human species. The efficiency of the decellularisation in terms of general histoarchitecture preservation and cellular removal were evaluated.

3.2 Aim and objectives:

3.2.1 Aim:

The aim of this chapter was to assess the feasibility of decellularising the whole dental pulp of both rat and human species through the use of a mild decellularisation method described by Wilshaw et al. (2006).

3.2.2 Objectives:

The above aim will be achieved through the following objectives:

- To determine the efficiency of decellularising the dental pulp on removal of cellular material in comparison to the native pulp tissue using histological qualitative assessment methods.
- To confirm the efficiency of decellularisation by evaluation of the total DNA content of the decellularised matrix in comparison to the native pulp tissue using DNA quantification assay.

3.3 Methods and experimental approaches:

This chapter describes the optimisation of the decellularisation protocol described by Wilshaw et al. (2006) for use on dental pulp tissues. The process of optimising the protocol involved two experiments. Experiment 1 involved the use of the Wilshaw decellularisation protocol on human dental pulp tissues. Based on the results obtained from experiment 1, the protocol was optimised through the inclusion of a freeze-thaw cycle prior to the start of decellularisation protocol (Experiment 2).

3.3.1 Experiment 1:

Human dental pulp tissues were retrieved as described in Section 2.2.1.2 and divided into native (control, n = 4) and decellularisation (study, n = 4) groups. The decellularisation process was performed as described in Section 2.2.2 and summarised in Figure 3.1. Images of human pulp tissue following decellularisation treatment are shown in Figure 3.2. Analysis of the native and decellularised pulp tissues were evaluated using H&E staining (Section 2.2.4.1) to view general tissue histoarchitecture and cell distribution and DAPI staining (Section 2.2.4.2) to identify cell nuclei and/or residual nuclear material. H&E stained sections were viewed using normal Köhler illumination, while, DAPI stained sections were viewed under reflected illumination equipped with a DAPI filter with all images captured digitally.

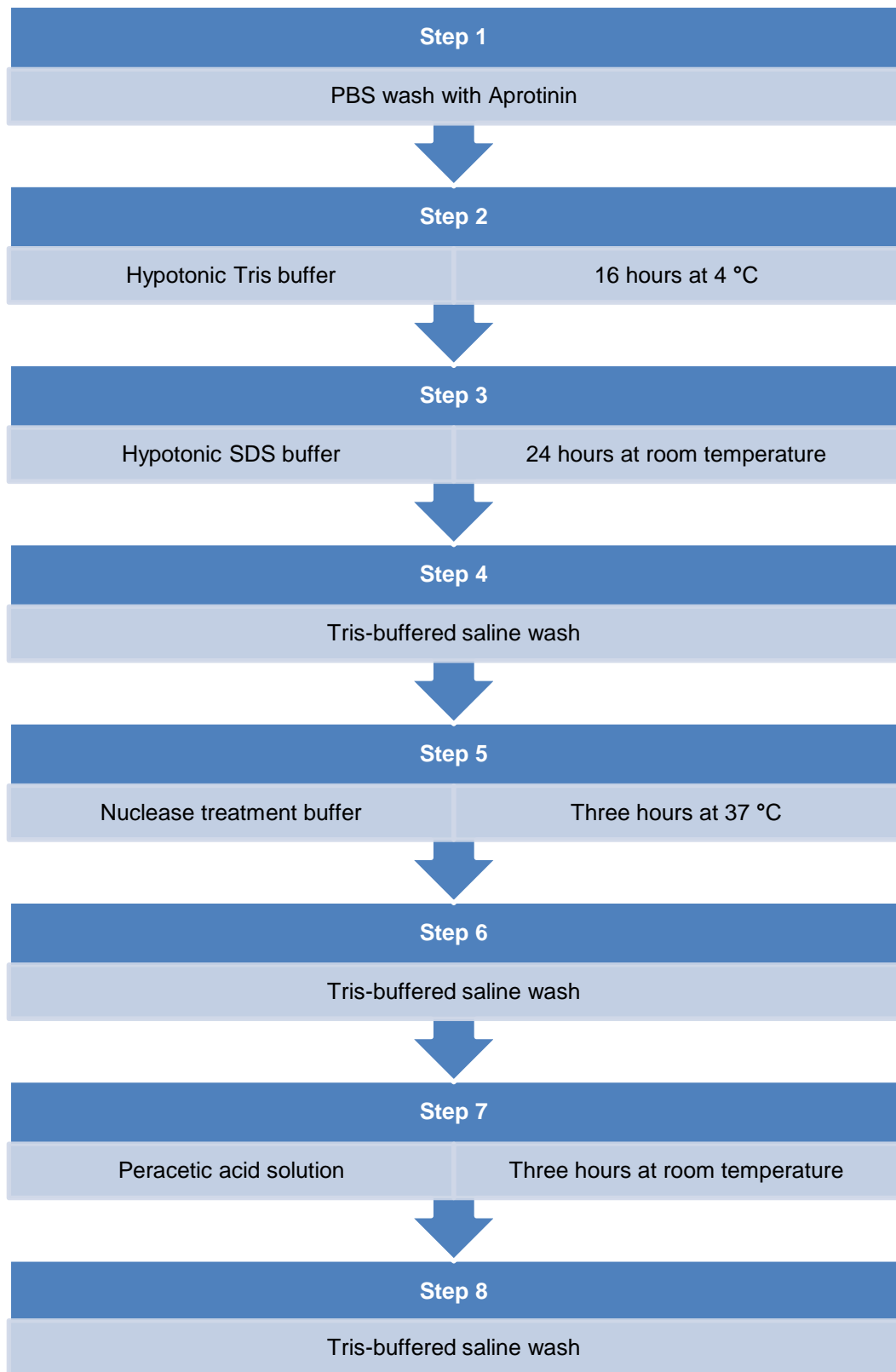


Figure 3.1: Process flow diagram of decellularisation experiment 1.

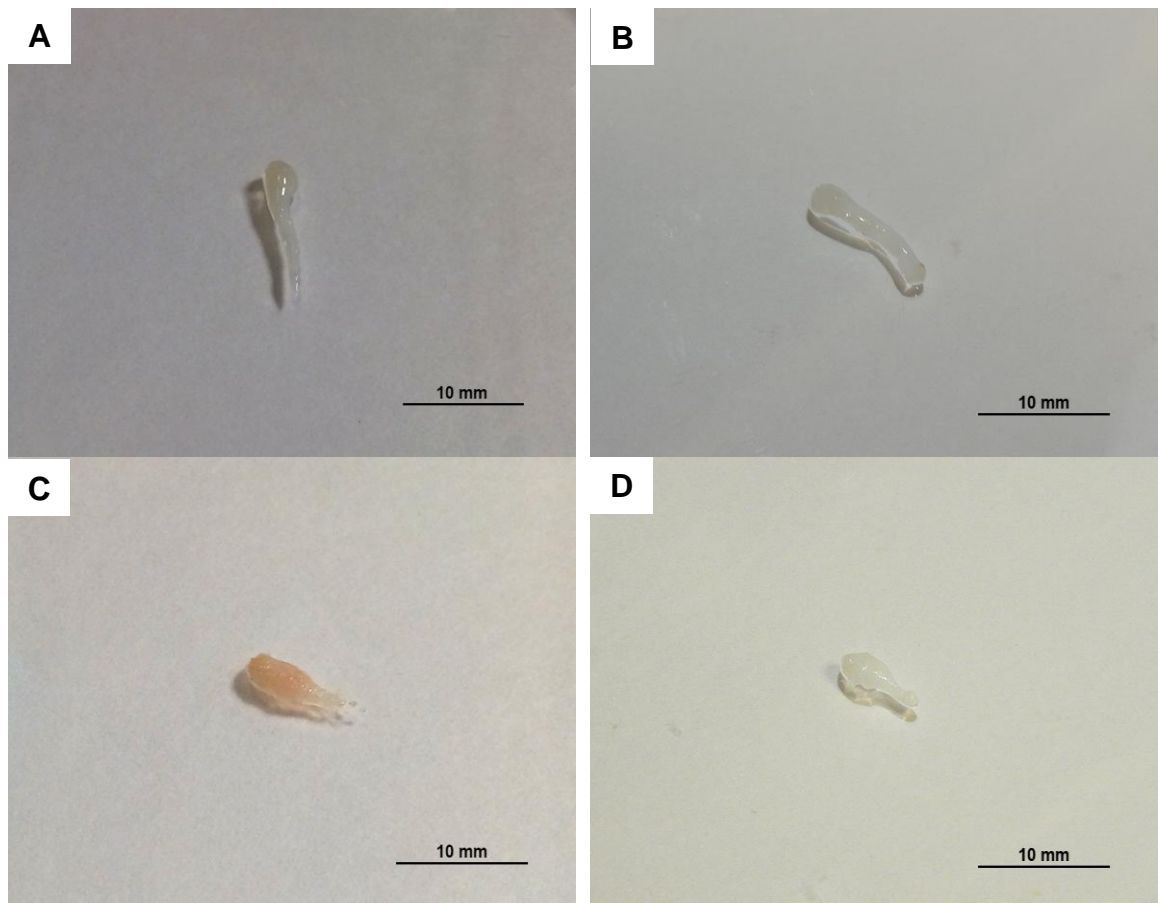


Figure 3.2: Representative images of decellularised human pulp tissues. (A and C) Human pulp tissues following step 1; washing with hypotonic Tris buffer containing (10 mM Tris, 0.1 % w/v EDTA and 10 KIU.mL⁻¹ Aprotinin) and (B and D) Human pulp tissues at completion of decellularisation steps.

3.3.2 Experiment 2:

Based on the results obtained from experiment 1 (Section 3.4.1), the decellularisation protocol was modified (as summarised in Figure 3.3) to include a single freeze-thaw cycle prior to decellularisation treatment to assist removal of residual cellular material. Retrieved rat (n = 8) and human (n = 8) pulp tissues were frozen at -80 °C until usage. Pulp tissues were divided into native (control) and decellularised (study) groups. Analysis of the native [rat (n = 4) and human (n = 4)] and decellularised [rat (n = 4) and human (n = 4)] dental pulp tissues were evaluated using H&E (Section 2.2.4.1) and DAPI

(Section 2.2.4.2) staining methods. H&E stained slides were viewed using normal Köhler illumination, while, DAPI stained slides were viewed under reflected illumination equipped with a DAPI filter with all images captured digitally.

Measurement of DNA content of the native and decellularised dental pulp tissues was also further performed as described in Section 2.2.6. Additional rat (n = 8) and human (n = 8) dental pulps were collected and equally divided into control and study groups. DNA extraction was performed using a DNeasy blood and Tissue Kit following manufacturer's instructions. Initially, tissue lyses were performed by adding proteinase K solution to each sample individually and incubated overnight at 56 °C until completely lysed. Samples were then loaded onto spin columns, washed and centrifuged in order to remove all proteins and other contaminating matters. Finally, the DNA was eluted into sterile DNase- and RNase-Free Eppendorf tubes. The extracted DNA was collected and quantified using a NanoDrop™ 2000 spectrophotometer with a measuring absorbance wavelength at 260 / 280 nm. Samples were normalised to 70 % dry weight with data analysis performed using independent student's *t*-test (*p*-value < 0.05).

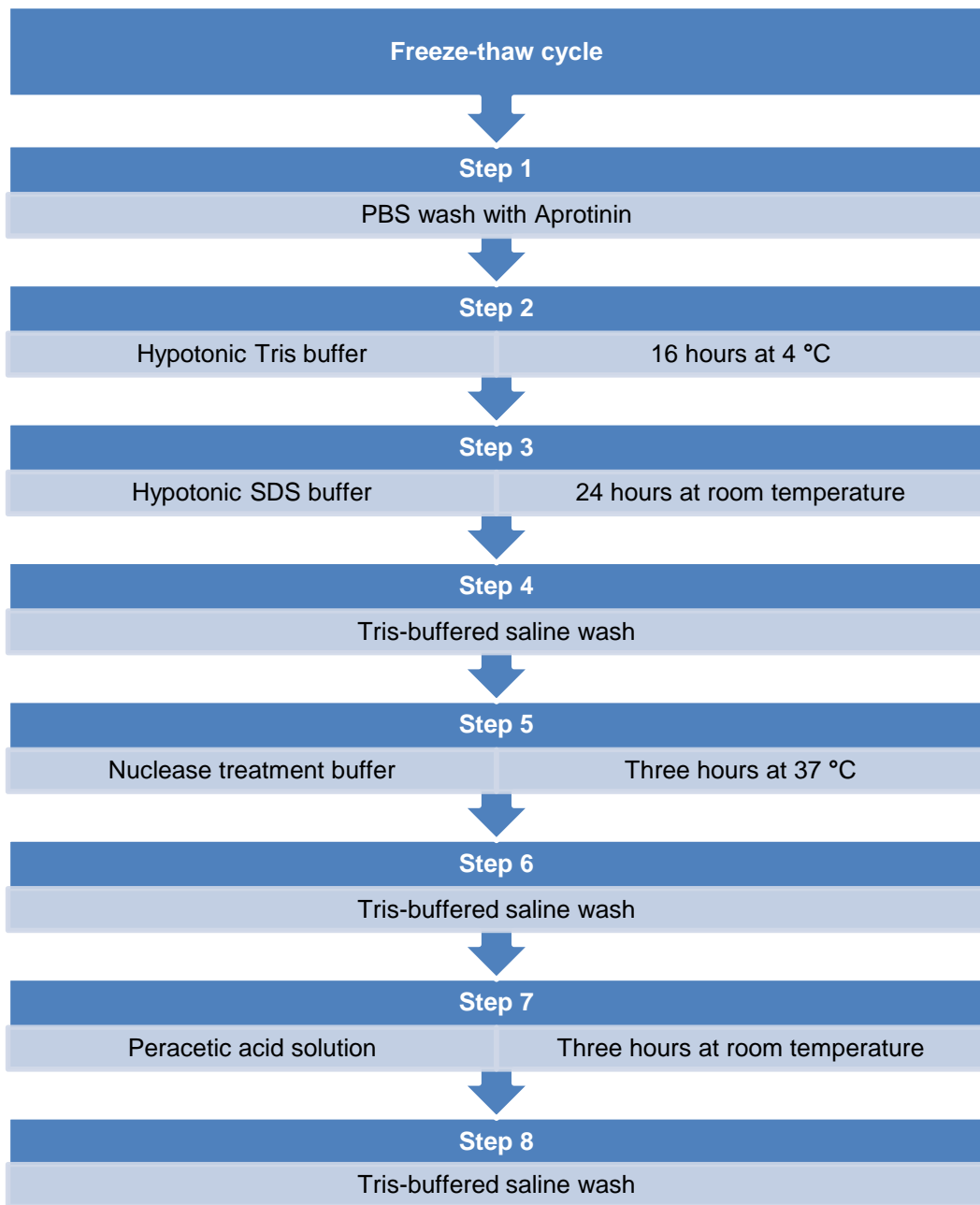


Figure 3.3: Process flow diagram of decellularisation experiment 2.

3.4 Results:

3.4.1 Results of experiment 1:

3.4.1.1 Histological analysis of native and decellularised dental pulp tissues:

Serial sections of the native and decellularised human pulp tissues based on experiment 1 were stained with H&E and DAPI to determine the efficiency of decellularisation.

Images of native H&E stained tissues viewed under light microscopy are shown in Figure 3.4 A and B. The native pulp tissues appeared as a highly cellular structure within a porous connective tissue stroma. The native human pulp connective tissue stroma appears pink following H&E staining, with various regions of matrix histoarchitecture clearly evident. The sub-odontoblastic layer was seen at the periphery of the pulp, followed by an acellular layer of Weil (cell-free area), a cell-rich layer and a central pulp core. A fine network of blood vessels, nerve fibres and capillaries was dispersed throughout the porous ECM. The native pulp tissues also appeared as a dense cellular structure, cells stained blue following H&E staining. The central pulp core contained spindle shaped fibroblasts-like cells and endothelial cells lining the blood vessels. Heterogeneity of pulp cells was visible throughout the pulp structure.

Images of native DAPI stained tissues viewed under fluorescence microscopy fitted with a DAPI filter are shown in Figure 3.5 A and B. DAPI stained native

tissues revealed highly cellular pulp tissues, with cell nuclei visible as bright blue dots on a black background.

Following decellularisation, images of decellularised tissue stained with H&E and DAPI are shown in Figure 3.4 C, D and Figure 3.5 C, D, respectively. No obvious cell nuclei were observed on the H&E stained sections. The pulp connective tissue stroma appeared, in some areas, more porous with the formation of larger spaces in the structural matrix. Despite this, preservation of the pulp tissue histoarchitecture composed of various histological regions and vascular channels were evident following decellularisation. However, blue nuclear fluorescent staining was seen in DAPI stained images. The fluorescence was not well defined and much smaller in size than that observed in the native tissues. From these observations it was concluded that the decellularisation protocol based on experiment 1 resulted in incomplete tissue decellularisation due to the presence of cells or, more likely, residual cellular material within the pulp matrix following decellularisation.

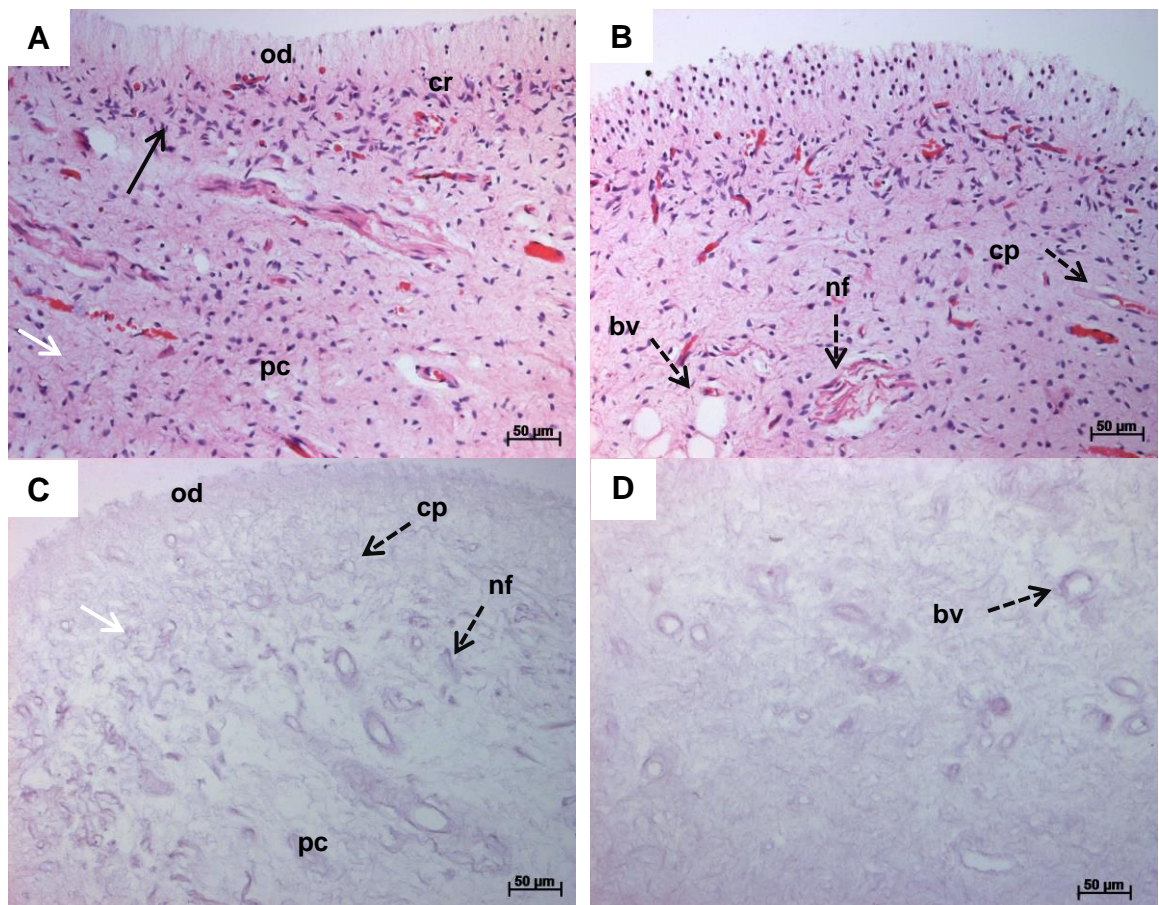


Figure 3.4: Representative images of H&E stained human tissues viewed under the light microscope. (A and B) Native pulp tissue showing a highly cellular structure within a porous connective tissue stroma and (C and D) Decellularised pulp tissue (experiment 1) showing an acellular structure with preservation of a surrounding stroma. (White arrow) Connective tissue stroma stained pink, (Solid black arrow) Cell nuclei stained blue, (od) Sub-odontoblastic layer, (cf) Cell-free layer, (cr) Cell-rich layer, (pc) Pulp core, (bv) Blood vessels, (nf) Nerve fibres and (cp) Capillaries. Scale bars are at 50 µm.

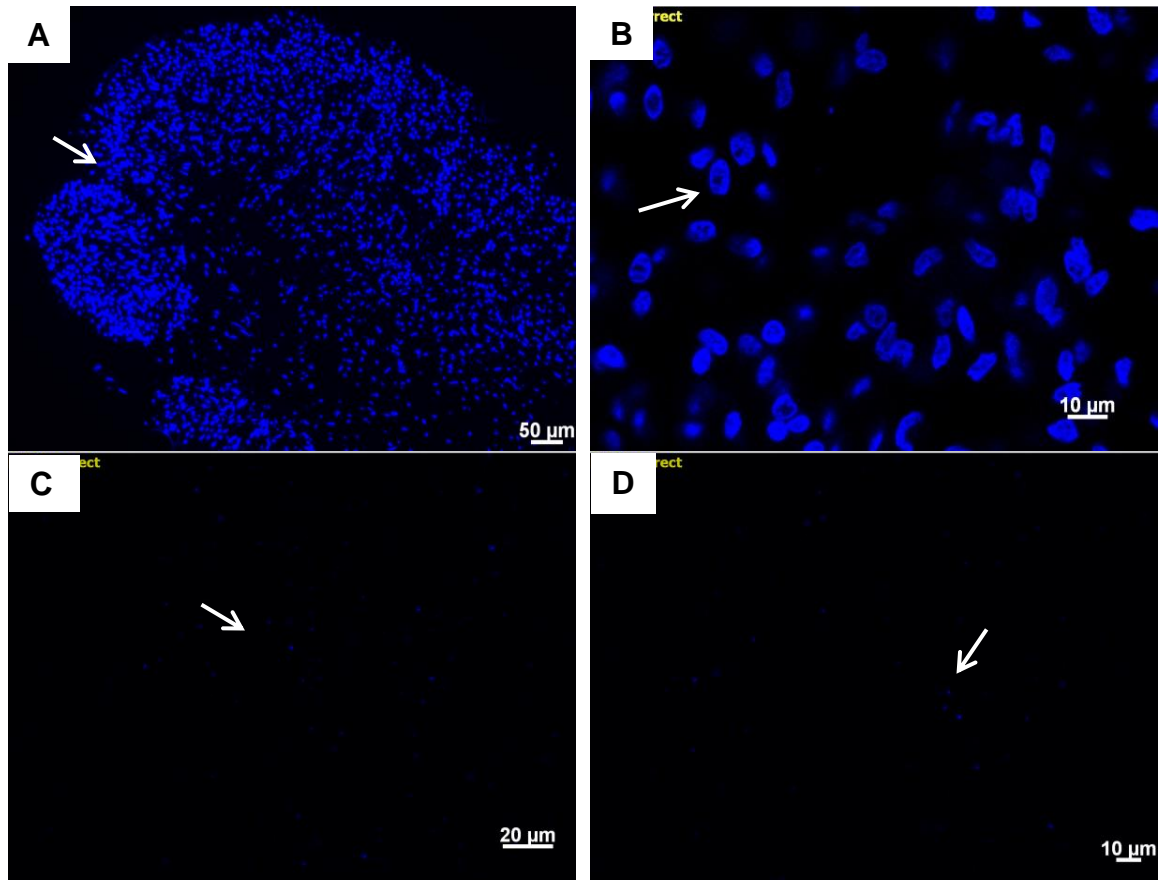


Figure 3.5: Representative images of DAPI stained human pulp tissues viewed under the fluorescent microscope. (A and B) Native pulp tissue showing a highly cellular matrix and (C and D) Decellularised pulp tissue (experiment 1) showing few remaining nucleic material. (White arrow) Cell nuclei stained blue. Scale bars (A) at 50 μm , (C) at 20 μm and (B and D) at 10 μm .

3.4.2 Results of experiment 2:

3.4.2.1 Histological analysis of native and decellularised dental pulp

tissues:

Serial sections of the native and decellularised rat and human pulp tissues based on experiment 2 were stained with H&E and DAPI to determine the efficiency of decellularisation.

H&E staining of the native rat (Figure 3.6 A, B) and human (Figure 3.8 A, B) pulp tissues appeared as a highly cellular connective tissue stroma. Various histological regions (sub-odontoblastic, cell rich, and central pulp core zones) were also clearly identified. DAPI stained images of native rat and human pulp tissues are shown in (Figure 3.7 A) and (Figure 3.9 A), respectively. Following staining, DAPI also revealed a highly cellular matrix in all native pulp tissues.

Following decellularisation, H&E staining of the rat (Figure 3.6 C, D) and human (Figure 3.8 C, D) pulp connective tissue stroma appeared, in some areas, more porous with the formation of larger spaces in the structural matrix. Despite this, preservation of the various histological regions and vascular channels were evident. No cell nuclei were observed on the H&E stained sections. This was further confirmed with DAPI as no blue nuclear fluorescent staining was visible in rat (Figure 3.7 B) and human (Figure 3.9 B) tissue sections. Collectively, observational results of this method indicated complete dental pulp tissue decellularisation with preservation of the ECM histoarchitecture.

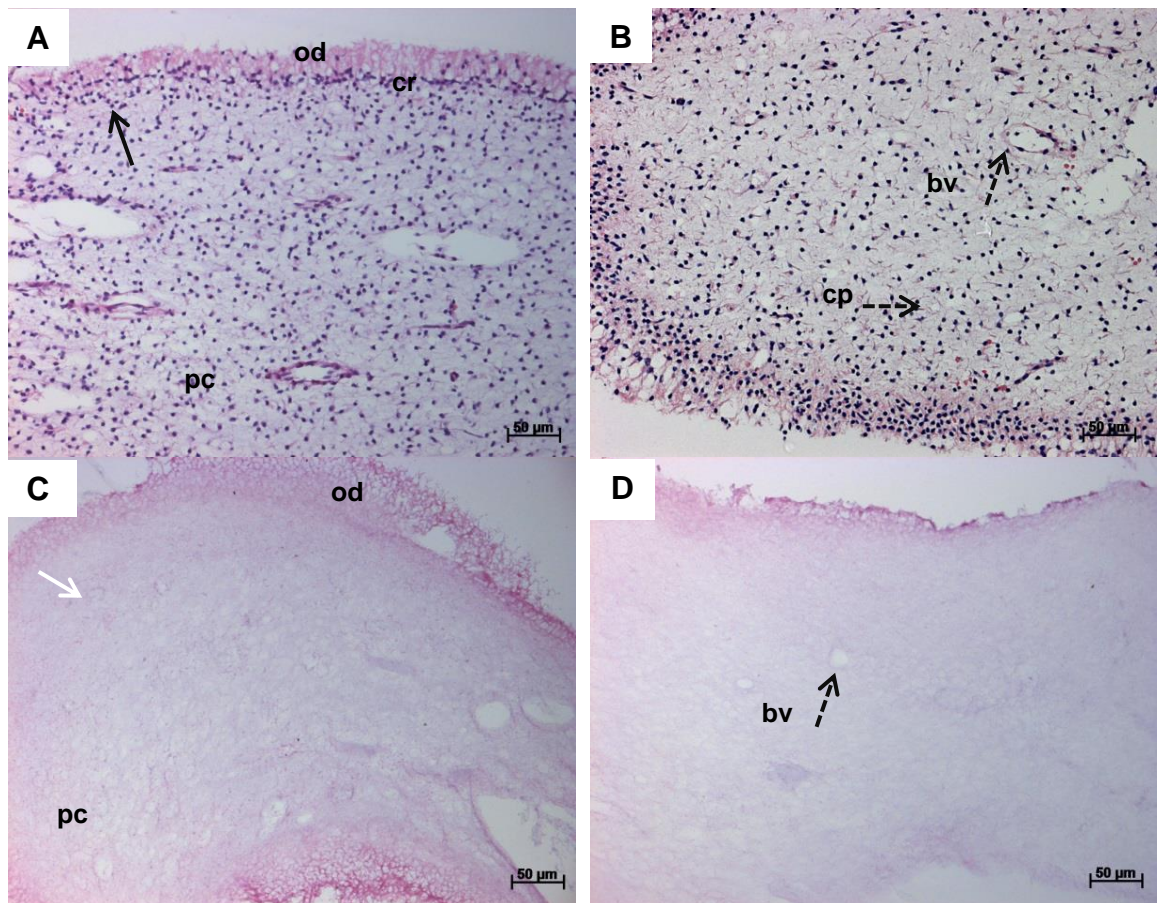


Figure 3.6: Representative images of H&E stained rat pulp tissues viewed under the light microscope. (A and B) Native pulp tissue showing a highly cellular structure within a porous connective tissue stroma and (C and D) Decellularised pulp tissue (experiment 2) showing an acellular structure with preservation of a surrounding stroma. (White arrow) Connective tissue stroma stained pink, (Solid black arrow) Cell nuclei stained blue, (od) Sub-odontoblastic layer, (cf) Cell-free layer, (cr) Cell-rich layer, (pc) Pulp core, (bv) Blood vessels, (nf) Nerve fibres and (cp) Capillaries. Scale bars are at 50 µm.

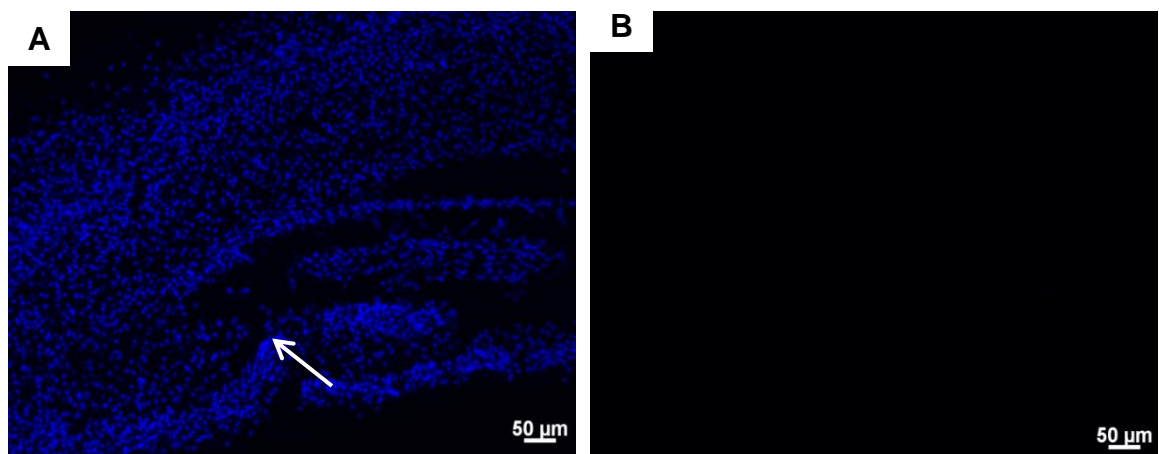


Figure 3.7: Representative images of DAPI stained rat pulp tissues viewed under the fluorescent microscope. (A) Native pulp tissue showing a highly cellular matrix and (B) Decellularised pulp tissue (experiment 2) showing no cell nuclei. (White arrow) Cell nuclei stained blue. Scale bars are at 50 µm.

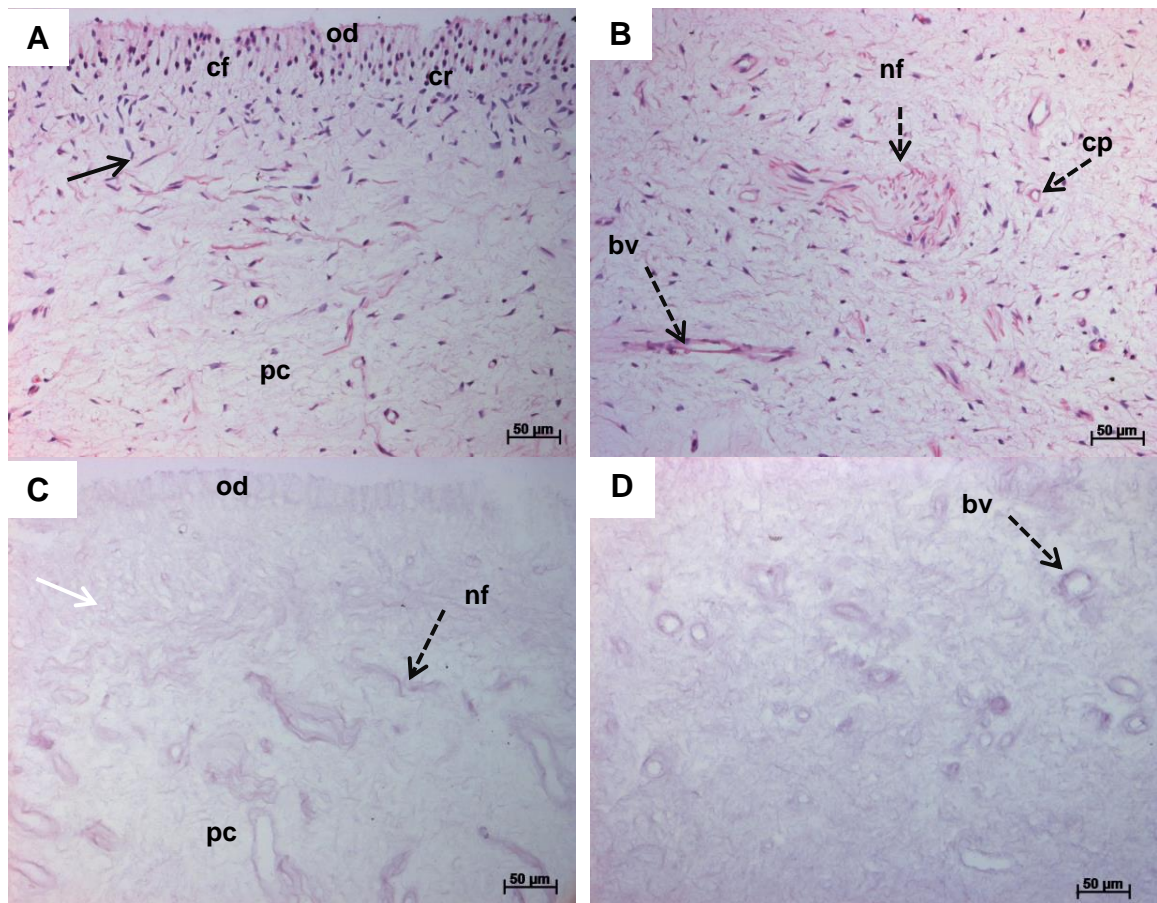


Figure 3.8: Representative images of H&E stained human pulp tissues viewed under the light microscope. (A and B) Native pulp tissue showing a highly cellular structure within a porous connective tissue stroma and (C and D) Decellularised pulp tissue (experiment 2) showing an acellular structure with preservation of a surrounding stroma. (White arrow) Connective tissue stroma stained pink, (Solid black arrow) Cell nuclei stained blue, (od) Subodontoblastic layer, (cf) Cell-free layer, (cr) Cell-rich layer, (pc) Pulp core, (bv) Blood vessels, (nf) Nerve fibres and (cp) Capillaries. Scale bars are at 50 µm.

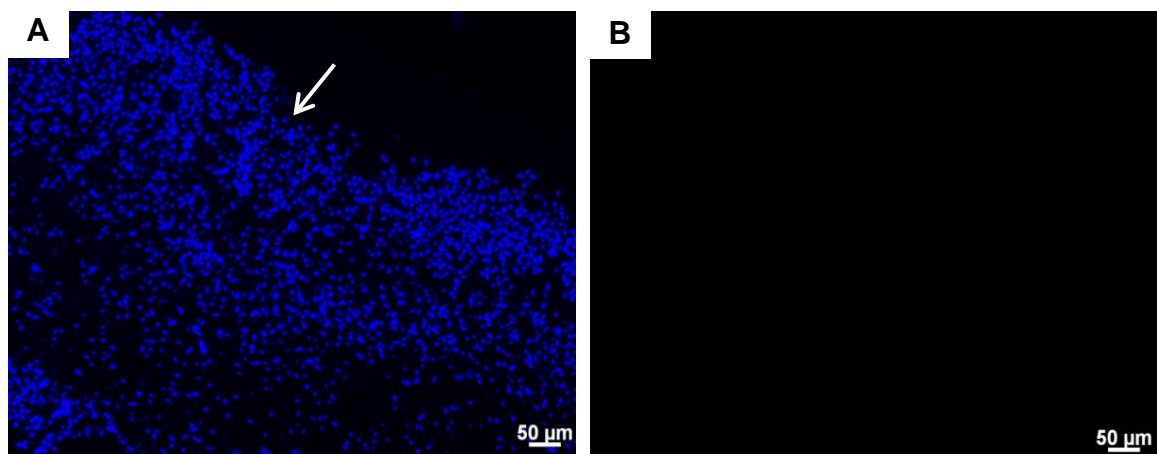


Figure 3.9: Representative images of DAPI stained human pulp tissues viewed under the fluorescent microscope. (A) Native pulp tissue showing a highly cellular matrix and (B) Decellularised pulp tissue (experiment 2) showing no cell nuclei. (White arrow) Cell nuclei stained blue. Scale bars are at 50 µm.

3.4.2.2 DNA content analysis of native and decellularised dental pulp tissues

Extracted native and decellularised pulp tissue DNA was quantified to determine the total DNA content present following decellularisation (experiment 2). Results of both rat and human tissues are shown in Figure 3.10 and Figure 3.11, respectively. Independent group student's *t*-test revealed significant differences between native and decellularised pulp tissues (p -value < 0.001) in both rat and human tissues. The mean DNA content in the decellularised tissues was $23.00 \pm 1.430 \text{ ng.mg}^{-1}$ in the rat tissues and $19.56 \pm 1.280 \text{ ng.mg}^{-1}$ in the human tissues. In comparison, the native tissue contained $1765 \pm 20.66 \text{ ng.mg}^{-1}$ and $1182 \pm 56.24 \text{ ng.mg}^{-1}$ in the rat and human tissues, respectively. The optimised decellularisation protocol used resulted in a negligible amount of remaining DNA content, with more than 98 % (dry weight) DNA content removal, in both rat and human dental pulp tissues (GraphPad Prism, Software 6).

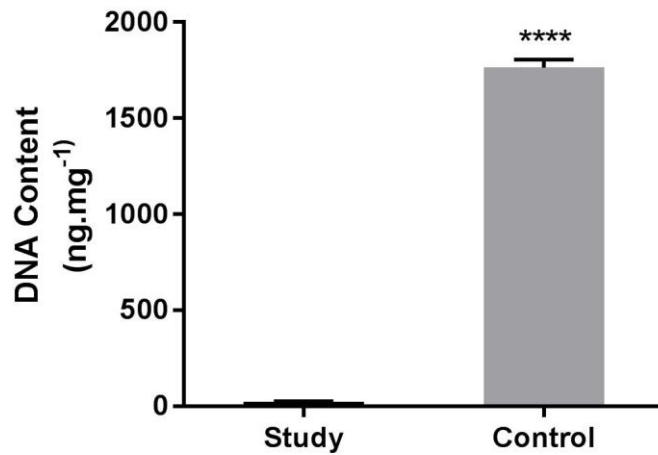


Figure 3.10: DNA content of native and decellularised rat pulp tissue following DNA extraction determined by NanoDrop™ 2000 spectrophotometer. Data represents mean values ($n = 4$) \pm 95 % confidence intervals. All samples were normalised to the ECM dry weight. The mean DNA content in the decellularised tissues was $23.00 \pm 1.430 \text{ ng.mg}^{-1}$ in comparison with $1765 \pm 20.66 \text{ ng.mg}^{-1}$ of the native tissues. Data analysis revealed significance difference between native and decellularised tissues (student's t -test, **** $p < 0.0001$).

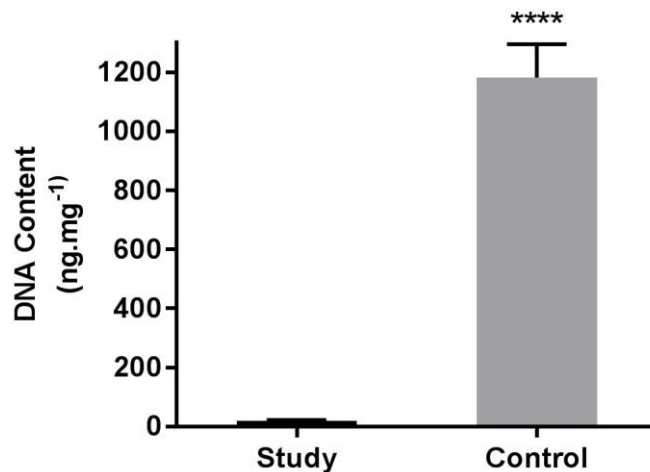


Figure 3.11: DNA content of native and decellularised human pulp tissues following DNA extraction determined by NanoDrop™ 2000 spectrophotometer. Data represents mean values ($n = 4$) \pm 95 % confidence intervals. All samples were normalised to the ECM dry weight. The mean DNA content in the decellularised tissues was $19.56 \pm 1.280 \text{ ng.mg}^{-1}$ in comparison to $1182 \pm 56.24 \text{ ng.mg}^{-1}$ in the native tissues. Data analysis revealed significance difference between native and decellularised tissues (student's t -test, **** $p < 0.0001$).

3.5 Discussion:

The development of a decellularised scaffold with complete elimination of donor cells and antigens while preserving ECM, could provide an excellent platform for regeneration (Badylak, 2002). Not only are these scaffolds non-immunogenic, the conserved native intact structures such as ECM proteins offer additional advantages. These proteins are known to be site specific and contribute towards future tissue regeneration (Song and Ott, 2011). Therefore, an acellular ECM with similar histological structure, composition and biological activity to the native tissue is beneficial for future tissue regeneration (Badylak et al., 2009).

Several decellularisation protocols are available and vary considerably. Wilshaw et al. (2006) used a relatively mild decellularisation protocol to decellularise human amniotic membrane. The protocol involved lysis of the cell membranes using hypotonic Tris buffer, followed by solubilisation of cytoplasmic and nuclear components using a single SDS detergent cycle, ending with removal of cellular material using a standard nuclease treatment. Several washing steps with agitation were also performed to ensure sufficient removal of residual cellular material and reagents used.

Different decellularisation protocols have been used in decellularising dental structures. In a chemically harsher decellularisation approach, several studies have utilised a combined detergent step, mainly SDS and Triton X-100. Traphagen et al. (2012) decellularised porcine tooth buds using a dual detergent approach. The Protocol included Tris hypotonic buffer treatment, five

cycles of SDS and Triton X-100 detergents (each cycle consisted of 1 or 5 % (w/v) SDS and 1 % (w/v) Triton X-100) followed by nuclease treatment. The authors concluded preservation of the tooth buds ECM with the removal of the majority of nuclei (Traphagen et al., 2012). A combined dual detergent based protocol, 1 % (w/v) SDS and 1 % (w/v) Triton X-100, was also performed by Chen et al. (2015) to decellularise dental pulp tissues obtained from miniature swine jaws. Morphological analysis following decellularisation revealed an acellular structure with preservation of natural shape of the pulp tissue. Despite, general preservation the odontoblastic layer was removed following treatment (Chen et al., 2015). More recently, Song et al. (2017) evaluated three different published protocols to decellularise human tooth slices (pulp-dentine disks of 1.5 mm thickness). They concluded the most efficient protocol with the minimal impact on the ECM composition involved treatment with a hypertonic buffer followed by three cycles of 1 % (w/v) SDS and one cycle of 1 % (w/v) Triton X-100 (Song et al., 2017).

The use of qualitative and quantitative DNA assessment methods is crucial in assessment of any decellularisation method. Indeed, residual cellular material can consequently elicit a host inflammatory response and inhibit future tissue remodelling (Brown et al., 2009; Keane et al., 2015). Therefore the combined use of H&E staining (showing a general view of tissue histoarchitecture and cellular content), DAPI staining (showing nuclei material) and DNA assays (quantitative assessment of DNA content) are essential criteria in assessing the used decellularisation protocols.

Histological analysis of experiment 1 samples showed an incomplete decellularisation of human pulpal tissues. H&E staining revealed an acellular matrix, however, residual cellular material was detected using DAPI staining.

These results could be explained based on the fact that H&E staining, although the gold standard for tissue histoarchitecture, is an insensitive method for DNA detection (Crapo et al., 2011). Furthermore, the additional use of DAPI staining revealed residual DNA material present within the matrix. Indeed, DAPI staining is regarded a sensitive and specific staining method for DNA detection, through the formation of fluorescent complexes on binding to specific clusters on the DNA surface (Kapuściński and Skoczylas, 1978; Kapuscinski, 1995).

Freeze-thaw cycles are known to cause cell lysis and reduce the amounts of chemical reagents needed to achieve effective decellularisation (Burk et al., 2014; Fu et al., 2014; Keane et al., 2015). Decellularisation protocols that combine the use of a freeze-thaw cycle and detergents have been successfully performed on various tissues including pulmonary valves (Luo et al., 2014), medial meniscus (Stapleton et al., 2008) and femoral arteries (Wilshaw et al., 2012). Therefore to improve the efficiency of decellularisation used in experiment 1 a slightly modified protocol in which a freeze-thaw cycle was used at the start of treatment (experiment 2). This temperature change opens up the structural matrix through the formation of ice crystals which consequently increases tissue permeability, and enhances the diffusion of decellularisation solutions (Gilbert et al., 2006; Crapo et al., 2011; Wilshaw et al., 2012). This

step can improve the consistency and practicality of future experiments allowing storage of several samples followed by batch decellularisation.

Histological analysis of experiment 2 samples resulted in complete decellularisation of rat and human pulp tissues. H&E staining revealed complete decellularisation with architectural preservation of the pulpal ECM. Preservation of the sub-odontoblastic layer and pulp core zone with retained vascular channels were evident. No nuclear material was stained with H&E and DAPI staining. Therefore, the addition of a single freeze-thaw cycle at the start of the process was found to be an essential step for a more successful procedure (complete decellularisation).

Evaluating the residual DNA content within an acellular biological scaffold is an important step following decellularisation (Gilbert et al., 2009; Wilshaw et al., 2012). Residual DNA material can be further extracted and quantified using specific kits. The United States Federal Drug Administration does not provide any regulatory limits to the amount of DNA material present in biological scaffolds (Gilbert et al., 2009). Substantial removal of DNA material is highly desirable for future clinical usage (Gilbert et al., 2009; Wilshaw et al., 2012). In this work, DNA content of both native and decellularised pulp tissues was extracted and quantified using a NanoDrop™ 2000 spectrophotometer with a peak absorbance at 260 / 280 nm. This simple and sensitive technique enables the detection of double and single stranded DNA material, and is commonly used for DNA quantification assessment (Wilshaw et al., 2012; Yoeruek et al., 2012; Song et al., 2017).

Following decellularisation, results of this work revealed significant reduction, greater than 98 %, in DNA content levels relative to the native tissues. These results are in agreement with a previous study which reported a reduction of greater than 97 % DNA content following decellularisation of pulp tooth slices (Song et al., 2017). The estimated remaining DNA content of $19.56 \pm 1.280 \text{ ng.mg}^{-1}$ in human and $23.00 \pm 1.430 \text{ ng.mg}^{-1}$ in rat tissues, is well below the considered maximum amount (50 ng.mg^{-1}) in a sufficiently decellularised tissue (Crapo et al., 2011; Kawecki et al., 2017). In a study by Gilbert et al. (2009) investigating DNA content in commercially available biological scaffolds, trace amounts of DNA material were found in several tested scaffolds (Gilbert et al., 2009). Despite this finding, it was concluded that such low residual DNA content is unlikely to cause any unwanted pro-inflammatory host response (Gilbert et al., 2009).

Collectively, results of this chapter describe complete decellularisation of the whole dental pulp tissues of rat and human tissues using the optimised decellularisation protocol (experiment 2). The results indicated a lack of cellular or nuclear material with general architectural preservation of a porous ECM embedded in a network of decellularised blood vessels, nerve fibres, and capillaries. Therefore further characterisation of the histoarchitecture of the decellularised pulp matrix of rat and human tissues was performed and described in the following chapter.

Chapter 4

Characterisation of the developed decellularised dental pulp tissue

4.1 Introduction:

The histological description of the dental pulp ECM is a loose highly hydrated viscous connective tissue matrix rich in proteoglycans and glycosaminoglycans (GAGs) held together within a network of collagen fibrils, reticular fibrils and adhesive proteins (Goldberg and Smith, 2004; Veis and Goldberg, 2014). This complex mixture of collagen and non-collagenous proteins are known to contribute to several tissue functions. These proteins provide structural function and binding sites for cell surface receptors (Badylak, 2002).

GAGs are essential components of dental pulp tissue ground substance. Within the pulp matrix, GAGs are attached to protein cores and exist as proteoglycans that contribute significantly to the matrix viscosity (Linde, 1985; Goldberg and Smith, 2004). GAGs play important roles in maintaining the structure of pulp tissue, regulate metabolism, water movement, attachment of growth factors and cytokines (Linde, 1973; Badylak, 2002). They are also implicated in collagen formation and mineralisation (Linde, 1973). The average GAG content in both rat and human pulp tissues was found to contain approximately 0.36 and 0.55 $\mu\text{g}\cdot\text{mg}^{-1}$ wet tissue weight, respectively (Linde, 1973).

Collagen fibres are the most abundant fibrous component of the pulp connective tissue matrix (Linde, 1985). They are known to largely contribute to the development and maintenance of the pulp matrix (Hillmann and Geurtsen, 1997). The collagen protein content varies between different teeth of the same species and also among the various species. Analysis of the dried pulp tissue revealed that human third molars contained the highest collagen content of 31.9 %, while human premolars contained 25.7 %. In comparison, rat pulp incisors contained a significantly lower collagen content of around 3.5 % (van Amerongen et al., 1983). Collagen type I and type III are fibril-forming collagens and represent the bulk of collagen within the dental pulp (van Amerongen et al., 1983; Martinez et al., 2000; Goldberg and Smith, 2004). In agreement with the above, positive immunohistochemical labelling of collagen type I and type III fibres were identified in the human dental pulp (Lukinmaa and Waltimo, 1992; Hillmann and Geurtsen, 1997; Martinez et al., 2000). Furthermore, a positive reactivity to procollagen (precursors of collagen) type I and type III were also expressed in the growing apical end of rat incisors (Cournil et al., 1979).

The Picrosirius red-polarisation method is documented as a reliable, specific and sensitive method for understanding the presence and distribution of various collagen types within a given tissue (Junqueira et al., 1979). It has been documented that both fibre thickness and packing of collagen molecules determine the wavelength pattern of polarisation colours following Picrosirius red-stained collagen tissue (Dayan et al., 1989). Collagen type I fibres are composed of thick bundles of collagen fibres ranging from 2 - 10 μm in

diameter. Microscopically, when viewed under the Picrosirius red-polarisation method, these closely packed thick fibres are strongly birefringent to light and appear as a yellow to red hue (Hillmann and Geurtsen, 1997). In contrast, collagen type III (reticulum fibres) are a loose network of individual thin fibres with a diameter of 0.5 - 1.5 μm . These thin fibres are weakly birefringent to light and appear green in colour under a polarised light (Montes and Junqueira, 1991; Hillmann and Geurtsen, 1997). Therefore, as the collagen fibres thickness increases the colour gradually moves from green (thinnest fibre) to yellow, orange ending with red (thickest fibre) (Junqueira et al., 1982). Having mentioned the above, scientifically it is inaccurate to conclude that all green fibres are collagen type III fibres (Rich and Whittaker, 2005). Indeed, newly deposited collagen type I fibres appear as immature thin fibres of a green hue colour (Rich and Whittaker, 2005). Furthermore, a recent study concluded the absorbed amount of light depends on the orientation of the collagen fibres (Lattouf et al., 2014). Hence the Picrosirius red-polarisation method is useful in revealing the organisation and heterogeneity of the collagen fibres present within the tissue (Lattouf et al., 2014).

Fibronectin is an extracellular adhesive protein present within the dental pulp matrix. It appears as a reticular pattern scattered throughout the pulp with dense concentrations around the blood vessels (Linde et al., 1982; van Amerongen et al., 1984). Fibronectin mediates several cellular and matrix interactions (Hynes, 1985). It assists the attachments of cellular and various extracellular components including collagen and proteoglycans (Linde et al., 1982).

The pulp matrix also contains a large family of glycoproteins termed laminin. Laminin is a major basement membrane protein with crucial roles in tissue development and regeneration (Aumailley et al., 2005; Fried et al., 2005). It is implicated in odontoblast differentiation (Yuasa et al., 2004) and migration of dental pulp stem cells (Howard et al., 2010). Laminin also exhibits a strong neurite promoting activity and is a key participant in neuronal outgrowth (Aumailley et al., 2005; Fried et al., 2005).

Cells expressing major histocompatibility complex class II molecules within the dental pulp have been documented (Jontell et al., 1987; Ohshima et al., 1999). These cells are present throughout the pulp tissue with a high localisation in the sub-odontoblastic layer (Ohshima et al., 1999). This group of cells serve as antigen-presenting cells and participate in the initial tissue recognition response (Jontell et al., 1987; Ohshima et al., 1999).

Following each decellularisation step undertaken alteration to the ECM composition and ultrastructure is inevitable. Attempts to reduce any structural loss and disruption are objectives of decellularisation (Gilbert et al., 2006; Crapo et al., 2011). The pulp tissues, rat and human, used in this chapter were decellularised using experiment 2. The extent of decellularisation, determined by further structural characterisation and identifying the presence and location of specific matrix molecules in the produced decellularised pulp tissues (namely those described above) were evaluated.

4.2 Aim and objectives:

4.2.1 Aim:

The aim of this chapter was to characterise and compare the compositions of the ECM of the native and decellularised dental pulp tissue of both rat and human species.

4.2.2 Objectives:

The above aim will be achieved through the following objectives:

- To determine the efficiency of the decellularised method used on the histoarchitecture of the decellularised matrix in comparison with native pulp tissue.
- To determine the efficiency of the decellularised method used on the preservation of specific structural proteins of the decellularised matrix in comparison with native pulp tissue.
- To determine the structural topography appearance of the decellularised matrix in comparison with native pulp tissue.

4.3 Methods and experimental approaches:

This chapter describes the structural characterisation of the decellularised dental pulp tissues utilising the protocol described in experiment 2. Structural characterisation initially involved histological staining methods using Alcian blue and Picrosirius red. Subsequent antibody immunolabelling of the main structural component (collagen fibres) and adhesive proteins was performed. Finally, scanning electron microscopy was used to visualise surface topography. All of the above methods were performed on rat and human tissues.

4.3.1 Histology characterisation of rat and human pulp tissues:

The histoarchitecture of the native [rat (n = 4) and human (n = 4)] and the decellularised [rat (n = 4) and human (n = 4)] dental pulp tissues were further characterised using Alcian blue (Section 2.2.4.3) and Picrosirius red (Section 2.2.4.4) staining methods. All stained sections were viewed using normal Köhler illumination and all images were captured digitally. Picrosirius red stained sections were additionally viewed using polarised microscopy.

4.3.2 Immunohistochemical labelling of rat and human pulp tissues:

Immunohistochemistry labelling of native [rat (n = 4) and human (n = 4)] and decellularised [rat (n = 4) and human (n = 4)] dental pulp tissues were further performed as described in Section 2.2.5. All immunohistochemical sections were subjected to the appropriate antigen retrieval method. Primary antibodies used in this chapter include monoclonal antibodies against anti-collagen type I, anti-collagen type III, anti-fibronectin and anti-histocompatibility complex class II

antigens, and polyclonal anti-laminin antigen. As negative controls, primary antibodies were omitted and replaced by isotype controls. Isotype control antibodies were used under the same conditions and concentrations as the corresponding primary antibody. Immunohistochemical stained sections were viewed using normal Köhler illumination and all images were captured digitally.

4.3.3 Scanning electron microscope evaluation:

The surface topography of native and decellularised dental pulp tissues were further examined using conventional high vacuum scanning electron microscopy (SEM). Dental pulp tissues [rat (n = 4) and human (n = 4)] were fixed in 2.5 % (v/v) glutaraldehyde, washed and dehydrated in a series of ethanol concentrations and hexamethyldisilazane solutions as described in Section 2.2.7. On completion, samples were affixed to 1.2 mm aluminium stubs with adhesive carbon tape, gold sputter coated for 80 seconds in an argon gas chamber at 3 millibars and visualised using high vacuum SEM.

4.4 Results:

4.4.1 Histological evaluation of native and decellularised dental pulp tissues:

Histological characterisation of native and decellularised pulp tissues were performed using Alcian blue and Picrosirius red staining. Images of the rat and human pulp tissues stained with Alcian blue are shown in Figure 4.1 and Figure 4.2, respectively. In the native tissues, a highly cellular tissue containing uniform distribution of GAGs within the tissue matrix was observed (Figure 4.2 A, B and Figure 4.2 A, B). Following decellularisation, preservation of a uniform distribution of GAGs was also observed in the tissue matrix (Figure 4.1 C, D and Figure 4.2 C, D). No visible differences in staining pattern between the native and the decellularised tissues could be seen.

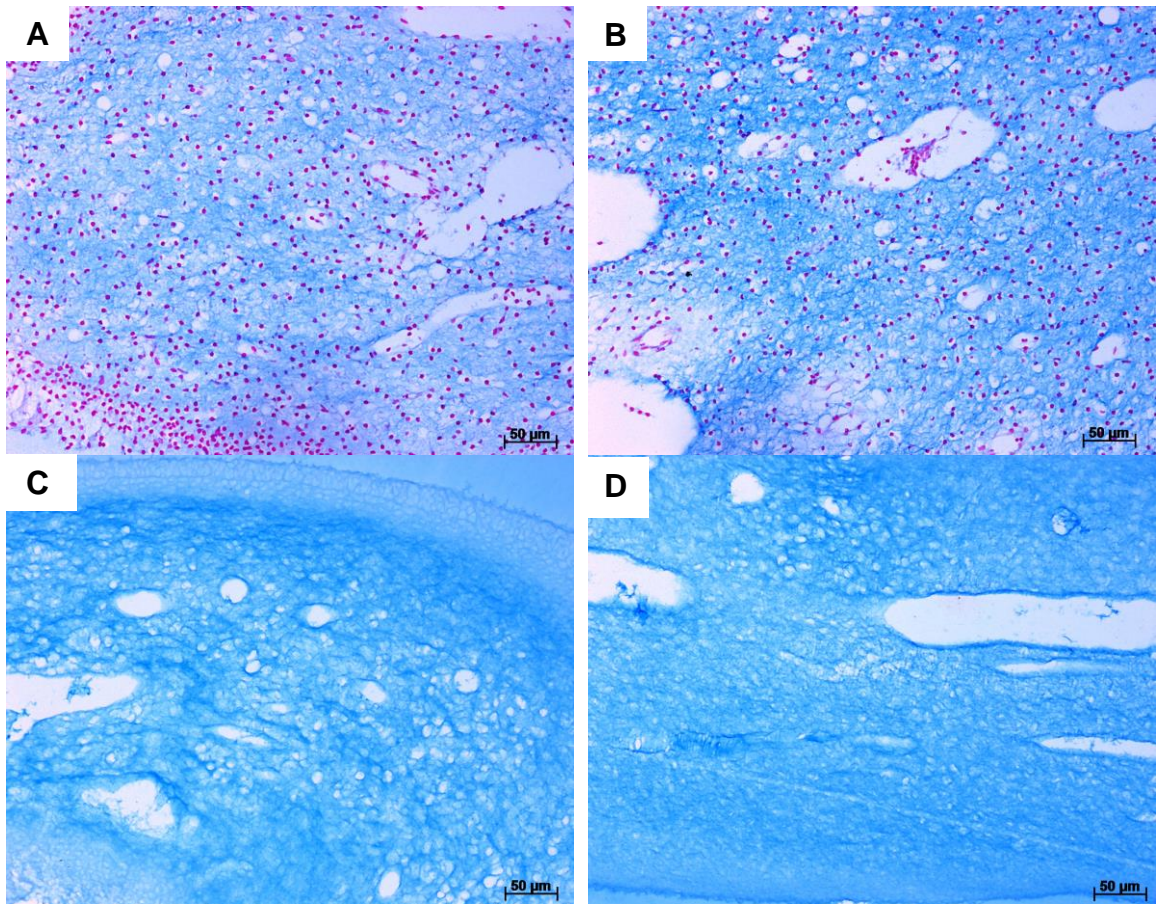


Figure 4.1: Representative images of Alcian blue stained rat pulp tissues viewed under the light microscope. (A and B) Native pulp tissues with abundant GAGs content in the matrix and (C and D) Decellularised pulp tissues with preserved GAGs content in the matrix. GAGs molecules stained blue and cell nuclei stained red. Scale bars are at 50 µm.

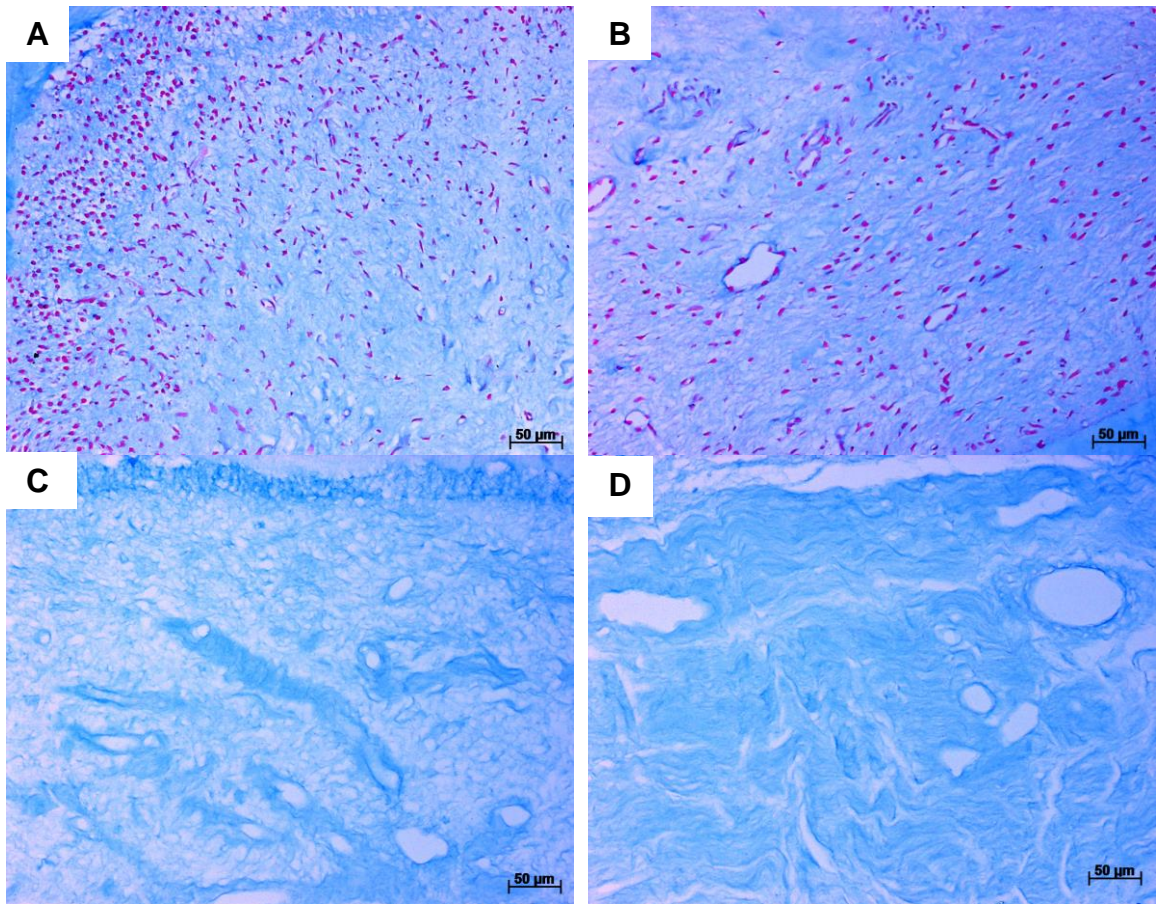


Figure 4.2: Representative images of Alcian blue stained human pulp tissues viewed under the light microscope. (A and B) Native pulp tissues with abundant GAGs content in the matrix and (C and D) Decellularised pulp tissues with preserved GAGs content in the matrix. GAGs molecules stained blue and cell nuclei stained red. Scale bars are at 50 μm .

Images of the rat and human pulp tissues stained with Picrosirius red and viewed under light microscopy are shown in Figure 4.3 and Figure 4.4, respectively. In the native rat tissues, a collagen network composed mainly of thin filaments and reticular fibrils occupied the matrix (Figure 4.3 A). In the native human tissues, a collagen rich matrix composed of thick fibre bundles surrounded by a network of thin filaments occupied the human pulp tissue matrix (Figure 4.4 A).

Under polarised light, rat pulp tissues were mainly composed of thin immature collagen fibres, which were weakly birefringent to polarised light and appeared green in colour (Figure 4.5 B). In contrast, thick mature fibre bundles appeared to be more dominant in human pulp tissues, these fibres were strongly birefringent to polarised light and appeared as a red, orange to yellow in colour (Figure 4.6 B). From these observations it is apparent that following decellularisation of rat and human tissues, a porous collagenous architecture consisting of abundant collagen fibres and fibrils were visible under light (Figure 4.3 B and Figure 4.4 B) and polarised (Figure 4.5 D and Figure 4.6 D) microscopy. The collagen fibres were well preserved and distributed throughout the entire tissue, largely concentrated around the vasculature structures. However, the tissue became slightly more porous in comparison to the native tissues.

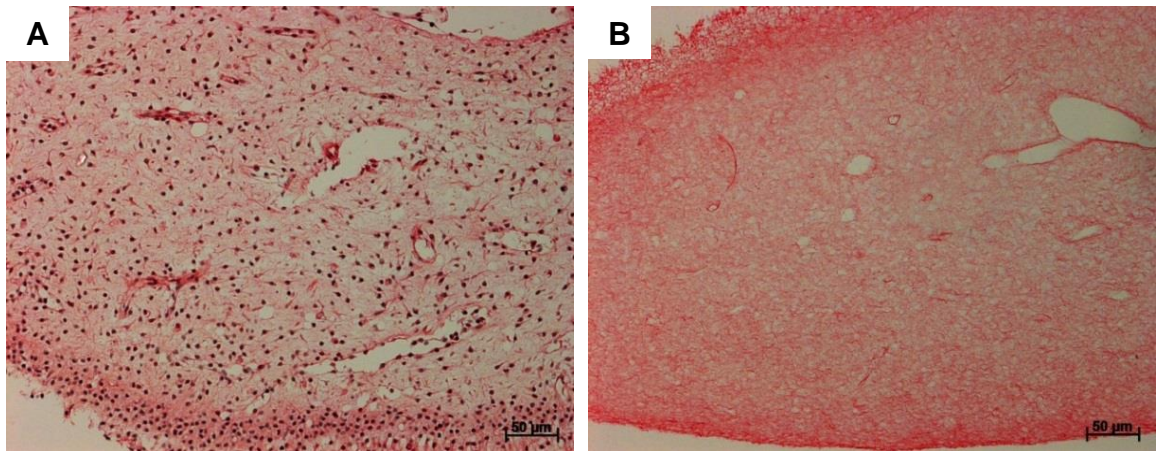


Figure 4.3: Representative images of Picrosirius red stained rat pulp tissues viewed under the light microscope. (A) Native tissues showing a porous collagen fibre network and (B) Decellularised tissues showing preservation of a porous collagen fibre network. Collagen fibres stained red and cell nuclei stained blue. Scale bars are at 50 µm.

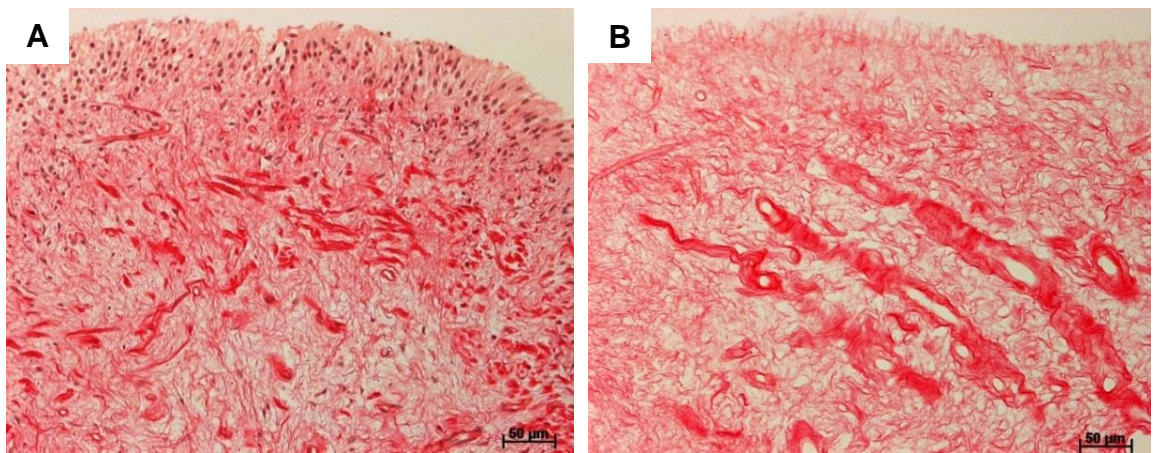


Figure 4.4: Representative images of Picrosirius red stained human pulp tissues viewed under the light microscope. (A) Native tissues showing a porous collagen fibre network and (B) Decellularised tissues showing preservation of a porous collagen fibre network. Collagen fibres stained red and cell nuclei stained blue. Scale bars are at 50 µm.

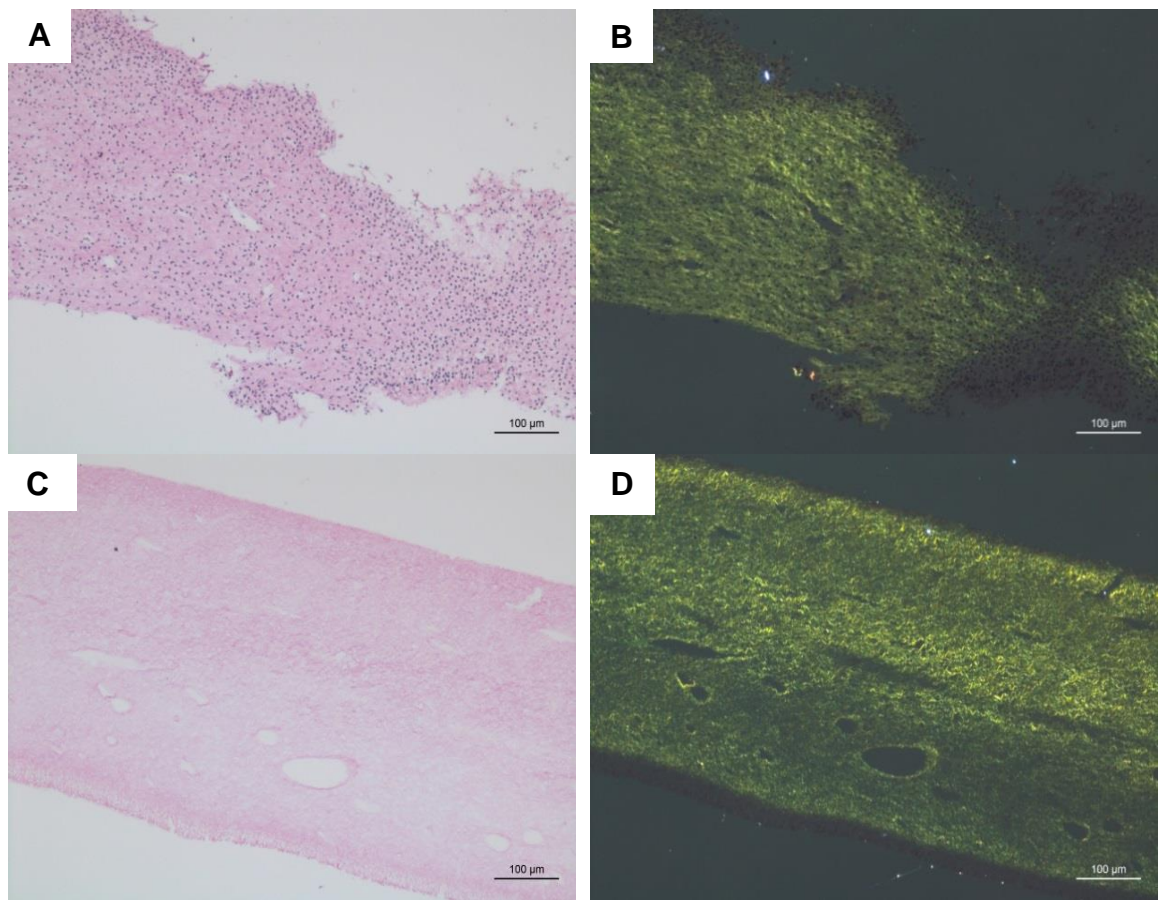


Figure 4.5: Representative images of Picrosirius red stained rat pulp tissues viewed under polarised microscope. (A) Native tissues appear as a cellular and porous collagen structure under bright field view, (B) Native tissues showing immature collagen fibres (green in colour) under the polarised light, (C) Decellularised tissues showing an acellular porous collagen structure under bright field view, (D) Decellularised tissues showing immature collagen fibres (green in colour) under the polarised light. Scale bars are at 100 µm.

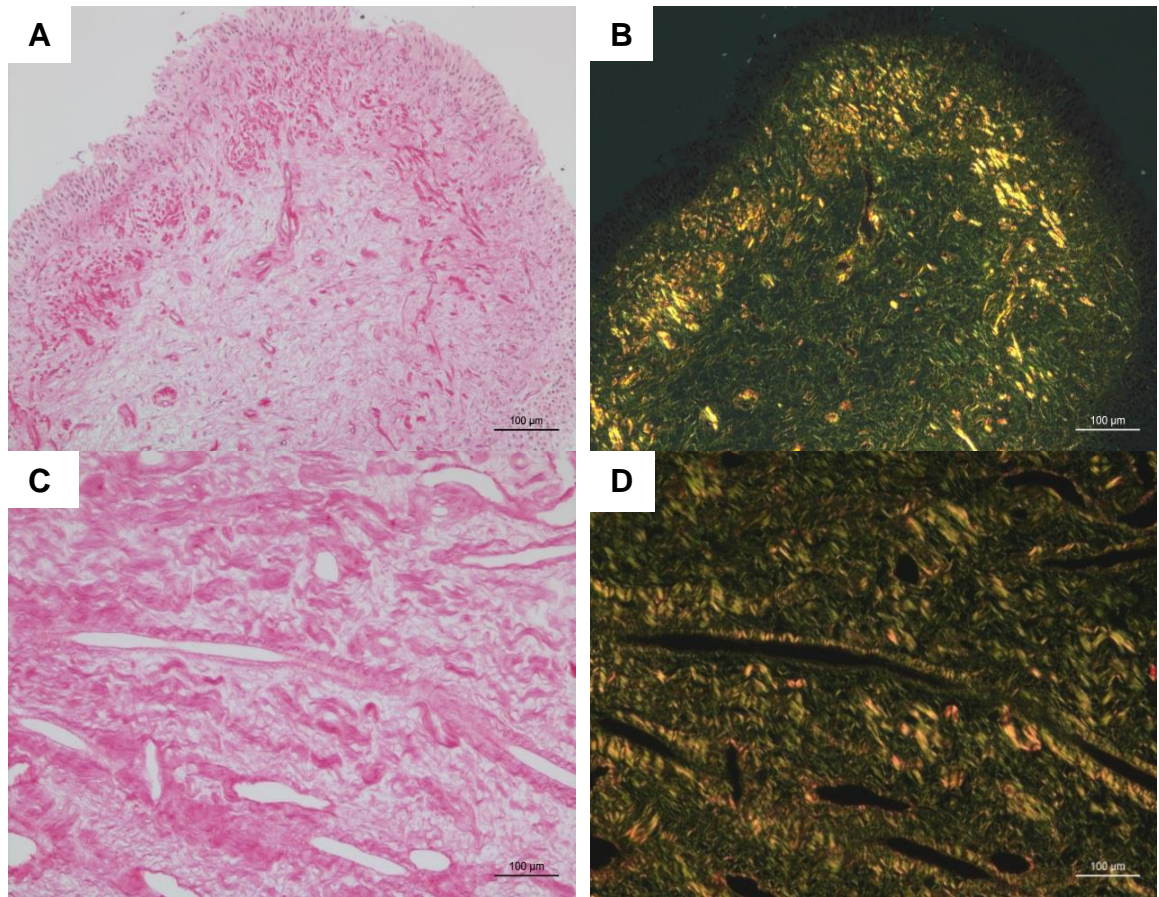


Figure 4.6: Representative images of Picrosirius red stained human pulp tissues viewed under the polarised microscope. (A) Native tissues appear as a cellular and porous collagen structure under bright filed view, (B) Native tissues showing heterogeneity of collagen fibres (various colours) under the polarised light, (C) Decellularised tissues showing an acellular porous collagen structure under bright filed view and (D) Decellularised tissues showing heterogeneity of collagen fibres (various colours) under the polarised light. Scale bars are at 100 µm.

4.4.2 Immunohistochemical evaluation of native and decellularised dental pulp tissues:

Antibody labelling was performed to localise specific ECM proteins present in the native and decellularised pulp tissue matrix.

4.4.2.1 Collagen type I:

Images of rat and human pulp tissues labelled with anti-collagen type I antibodies are shown in Figure 4.7 and Figure 4.8, respectively. The native rat pulp tissues were stained light brown, a weak positive immunoreactivity to collagen type I antigens (Figure 4.7 A). This less intense staining pattern consisting of thin fibres and fibrils was consistently seen in all examined native rat pulp tissues. In contrast, the native human pulp tissues were stained darker brown, a positive immunoreactivity to collagen type I antigens (Figure 4.8 A). The entire pulp depth extending from the sub-odontoblastic layer to the pulp core was strongly stained, representing a rich network of collagen type I fibres and bundles.

Following decellularisation, the pulp tissues of both rat (Figure 4.7 B) and human (Figure 4.8 B) samples revealed a positive slightly reduced staining pattern of collagen type I fibres in comparison to the relative native tissues. The distribution of the collagen type I fibres was mainly concentrated around the vasculature structures. No brown staining was observed in isotype control stained sections (Figure 4.7 C, D and Figure 4.8 C, D).

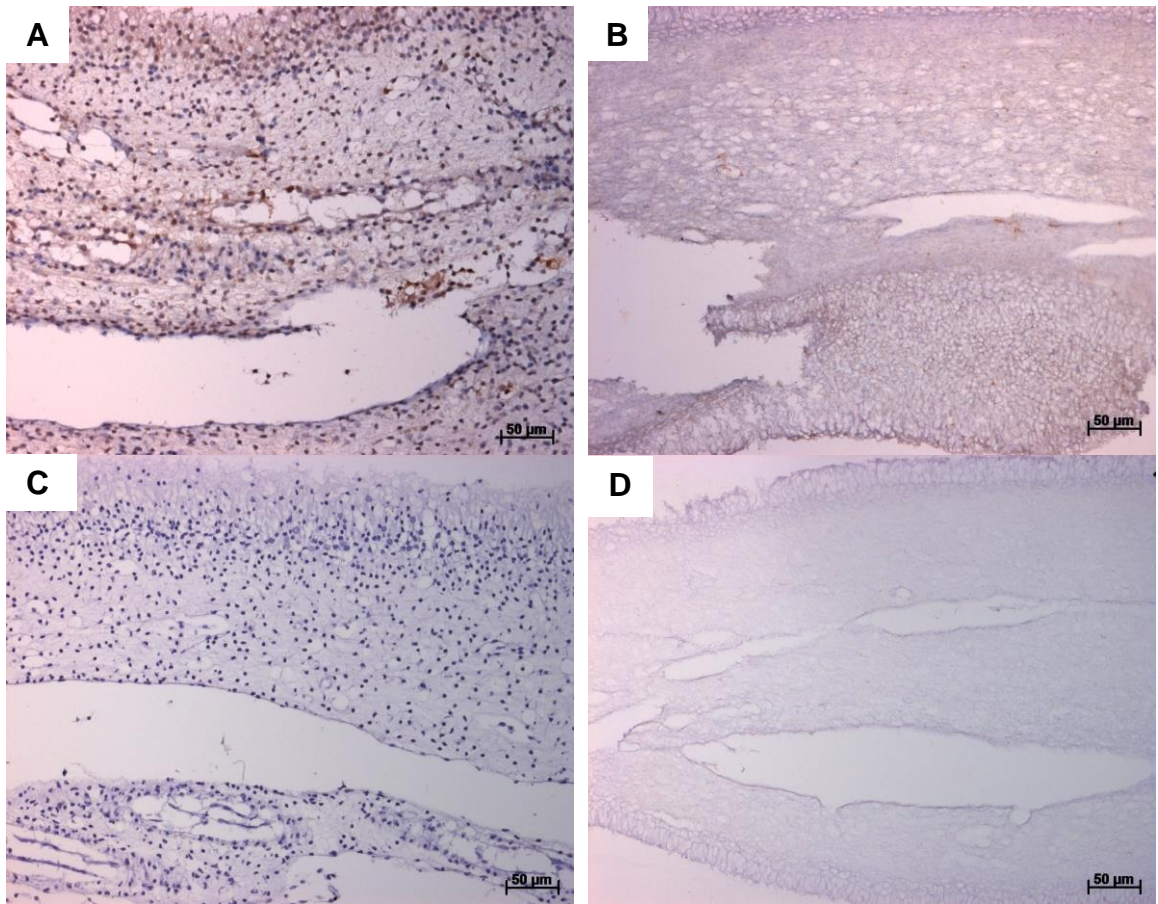


Figure 4.7: Representative images of rat pulp tissues labelled with collagen type I antigen viewed under the light microscope. (A) Native rat tissue, (B) Decellularised rat tissue, (C) Native rat tissue isotype and (D) Decellularised rat tissue isotype. Collagen type I fibres stained brown and cell nuclei stained blue. Scale bars are at 50 μm .

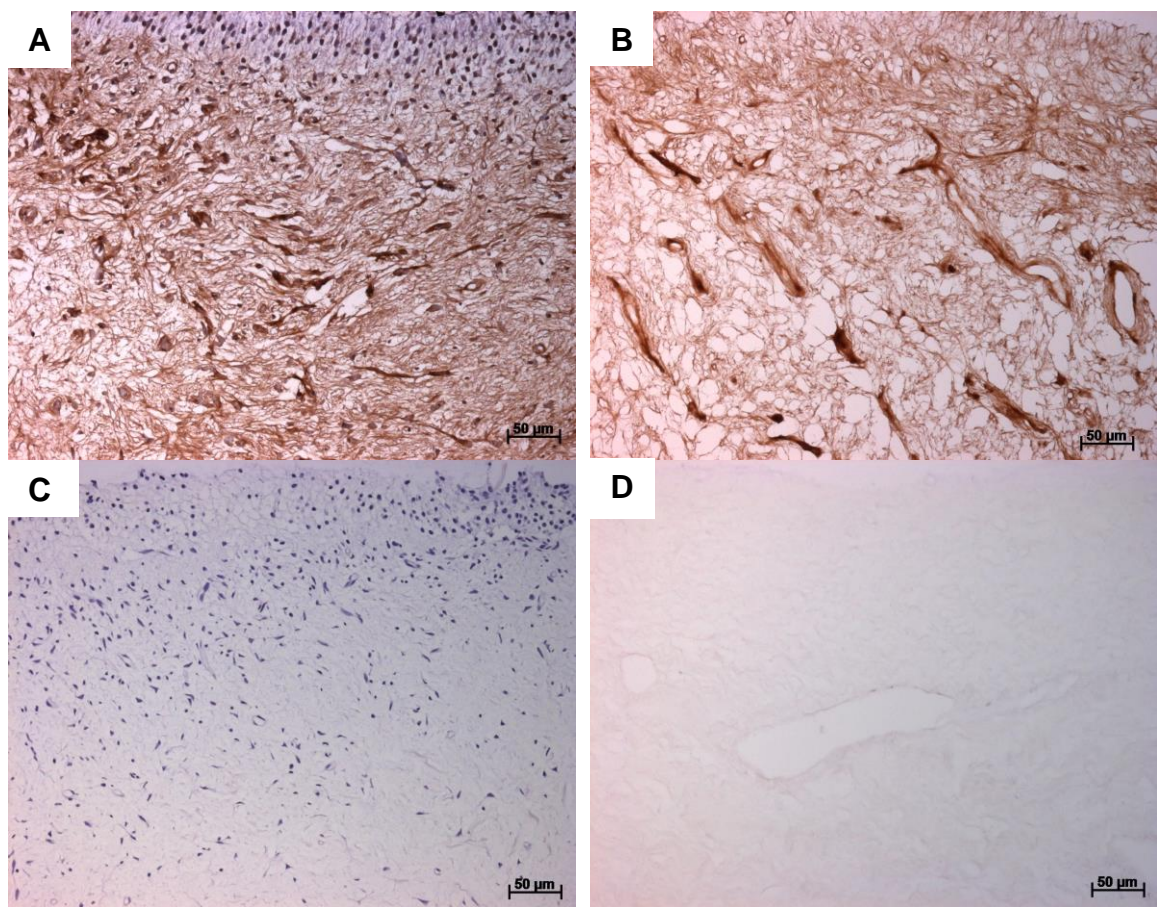


Figure 4.8: Representative images of human pulp tissues labelled with collagen type I antigen viewed under the light microscope. (A) Native human tissue, (B) Decellularised human tissue, (C) Native human tissue isotype control and (D) Decellularised human tissue isotype. Collagen type I fibres stained brown and cell nuclei stained blue. Scale bars are at 50 μm.

4.4.2.2 Collagen type III:

Images of rat and human pulp tissues labelled with anti-collagen type III antibodies are shown in Figure 4.9 and Figure 4.10, respectively. The native rat pulp tissues were stained light brown, a weak positive immunoreactivity to collagen type III antigens (Figure 4.9 A). This less intense staining pattern, resembling a reticular collagen network, was consistently seen in all examined native rat pulp tissues. In contrast, the native human pulp tissues were stained darker brown, a positive immunoreactivity to collagen type III antigens (Figure 4.10 A). The entire pulp depth extending from beneath the sub-odontoblastic layer to the pulp core was strongly stained, representing a rich network of collagen type III fibres and bundles.

Following decellularisation (in similarity to collagen type I) the pulp tissues of both rat (Figure 4.9 B) and human (Figure 4.10 B) samples revealed a positive and reduced staining pattern to collagen type III fibres in comparison to the relative native tissues. The distribution of the collagen type III fibres was mainly concentrated around and along the vasculature structures. No brown staining was observed in isotype control stained sections (Figure 4.9 C, D and Figure 4.10 C, D).

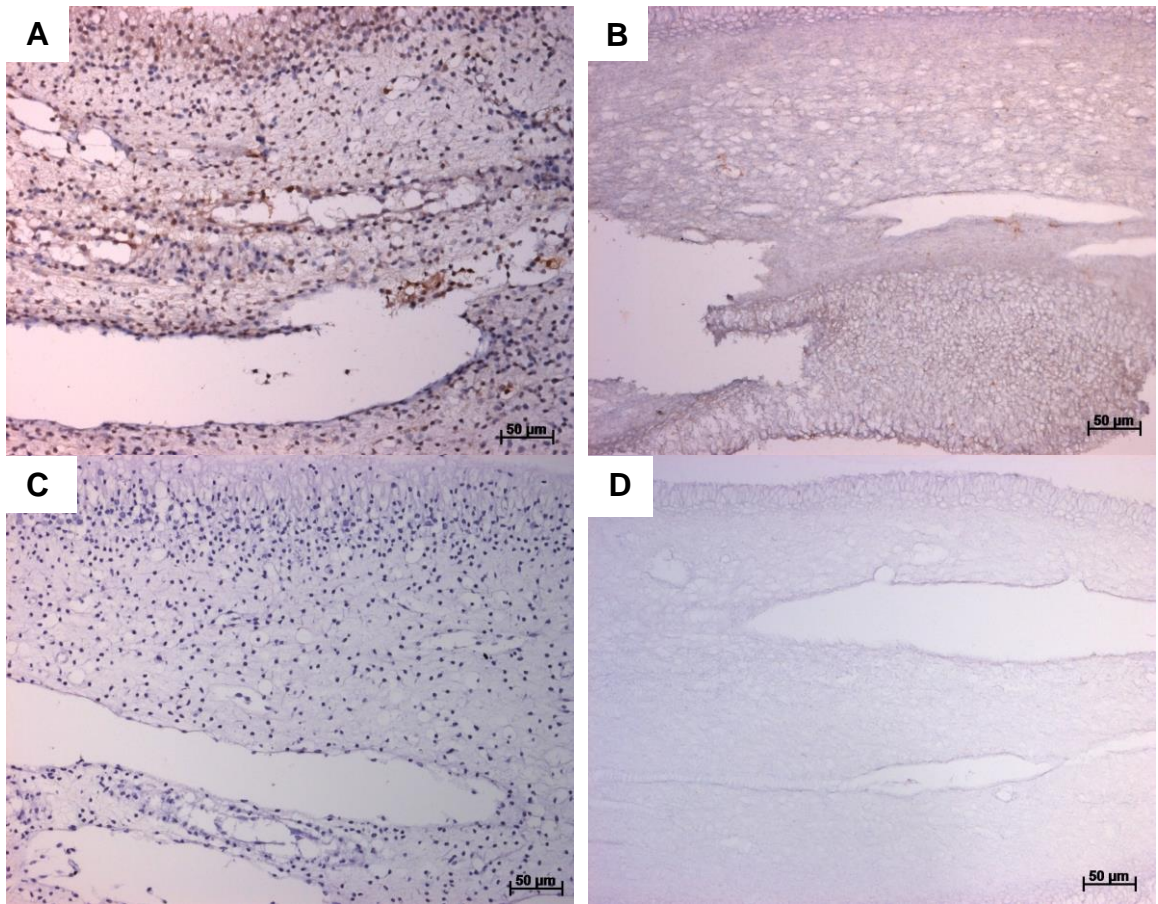


Figure 4.9: Representative images of rat pulp tissues labelled with collagen type III antigen viewed under the light microscope. (A) Native rat tissue, (B) Decellularised rat tissue, (C) Native rat tissue isotype and (D) Decellularised rat tissue isotype. Collagen type III fibres stained brown and cell nuclei stained blue. Scale bars are at 50 µm.

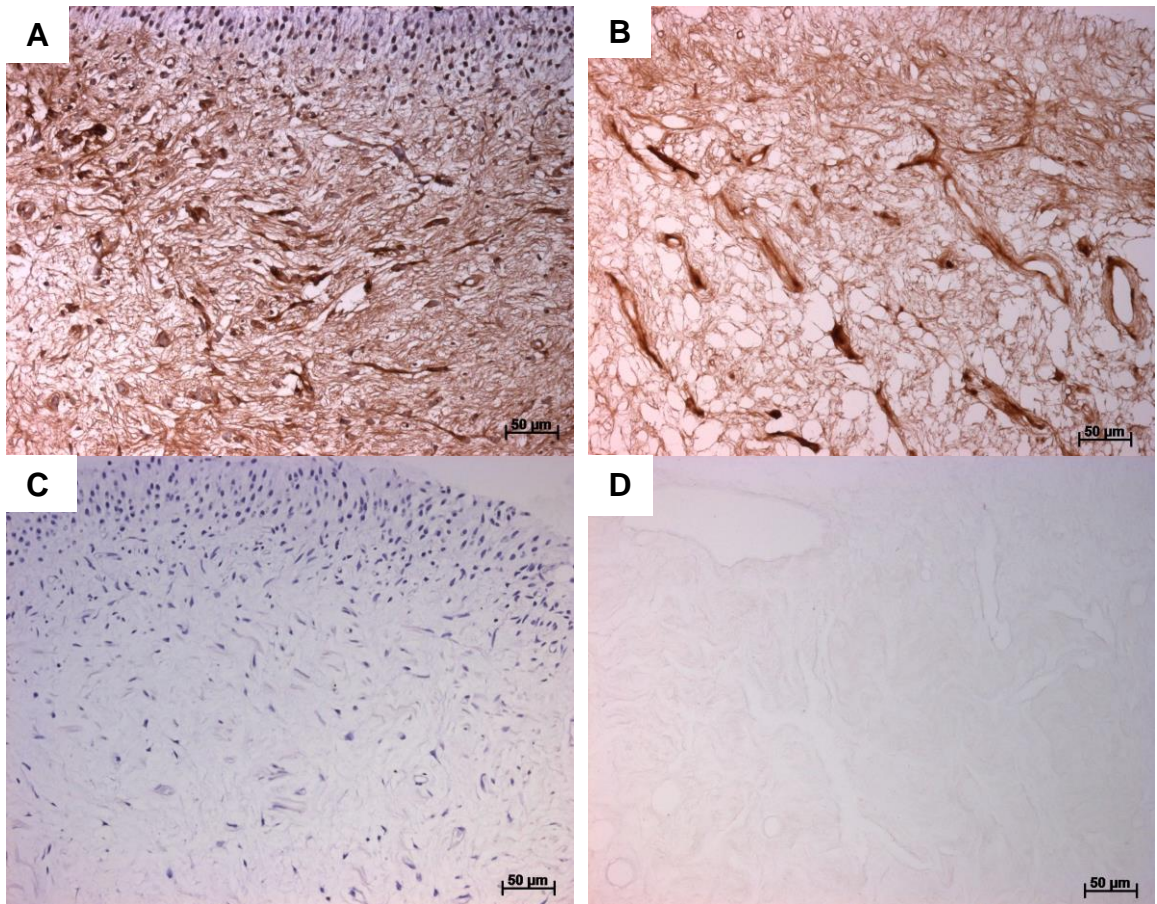


Figure 4.10: Representative images of human pulp tissues labelled with collagen type III antigen viewed under the light microscope. (A) Native human tissue, (B) Decellularised human tissue, (C) Native human tissue isotype control and (D) Decellularised human tissue isotype. Collagen type III fibres stained brown and cell nuclei stained blue. Scale bars are at 50 μm.

4.4.2.3 Fibronectin:

Images of rat and human pulp tissues labelled with anti-fibronectin antibodies are shown in Figure 4.11 and Figure 4.12, respectively. The native tissues of both rat (Figure 4.11 A) and human (Figure 4.12 A) samples were stained brown, a positive immunoreactivity to fibronectin antigens. Fibronectin staining appeared as a fibrous plexus mainly concentrating around blood vessels.

Following decellularisation, the pulpal tissues of both rat (Figure 4.11 B) and human (Figure 4.12 B) samples revealed a positive weak staining pattern to fibronectin fibres. As the native tissues, fibronectin positive fibres were mainly concentrated around blood vessels. No brown staining was observed in isotype control stained sections (Figure 4.11 C, D and Figure 4.12 C, D).

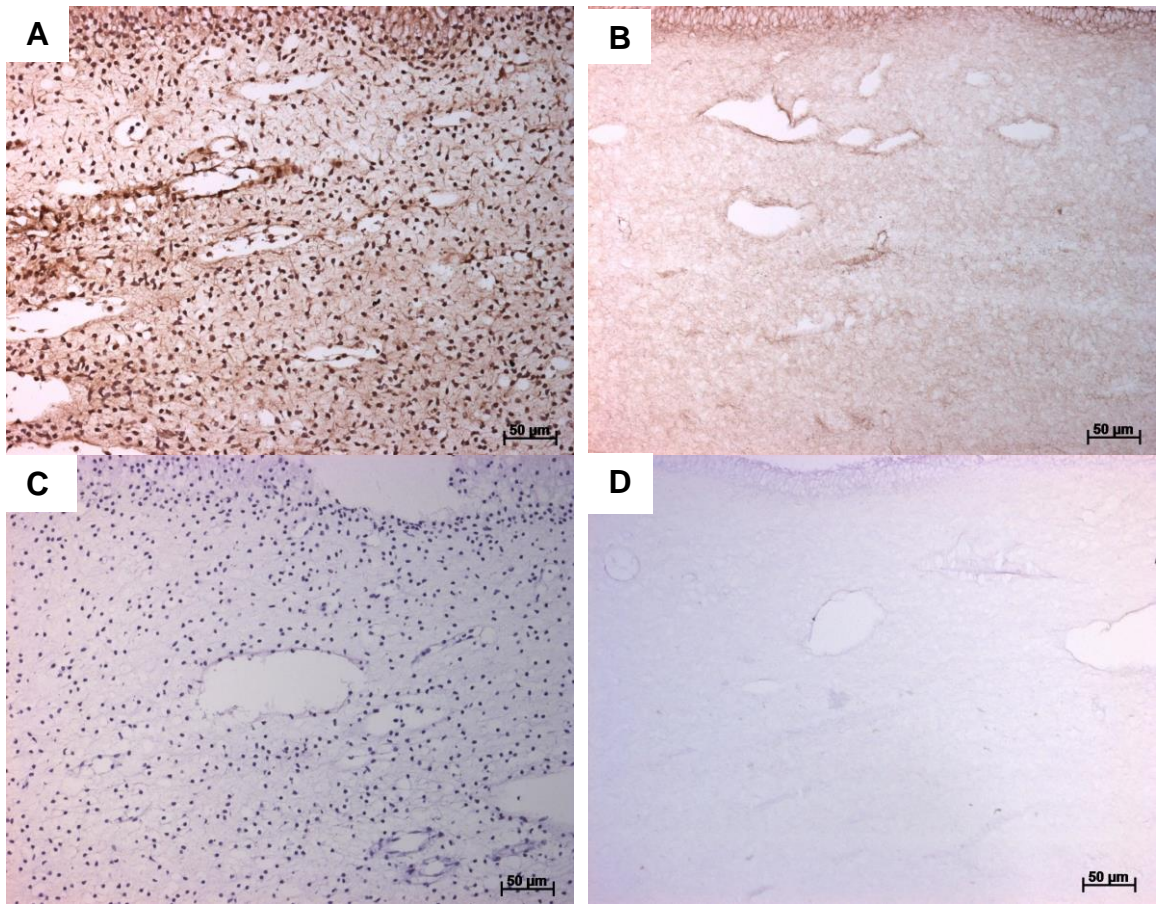


Figure 4.11: Representative images of rat pulp tissues labelled with fibronectin antigen and viewed under the light microscope. (A) Native rat tissue, (B) Decellularised rat tissue, (C) Native rat tissue isotype and (D) Decellularised rat tissue isotype. Fibronectin fibres stained brown and cell nuclei stained blue. Scale bars are at 50 µm.

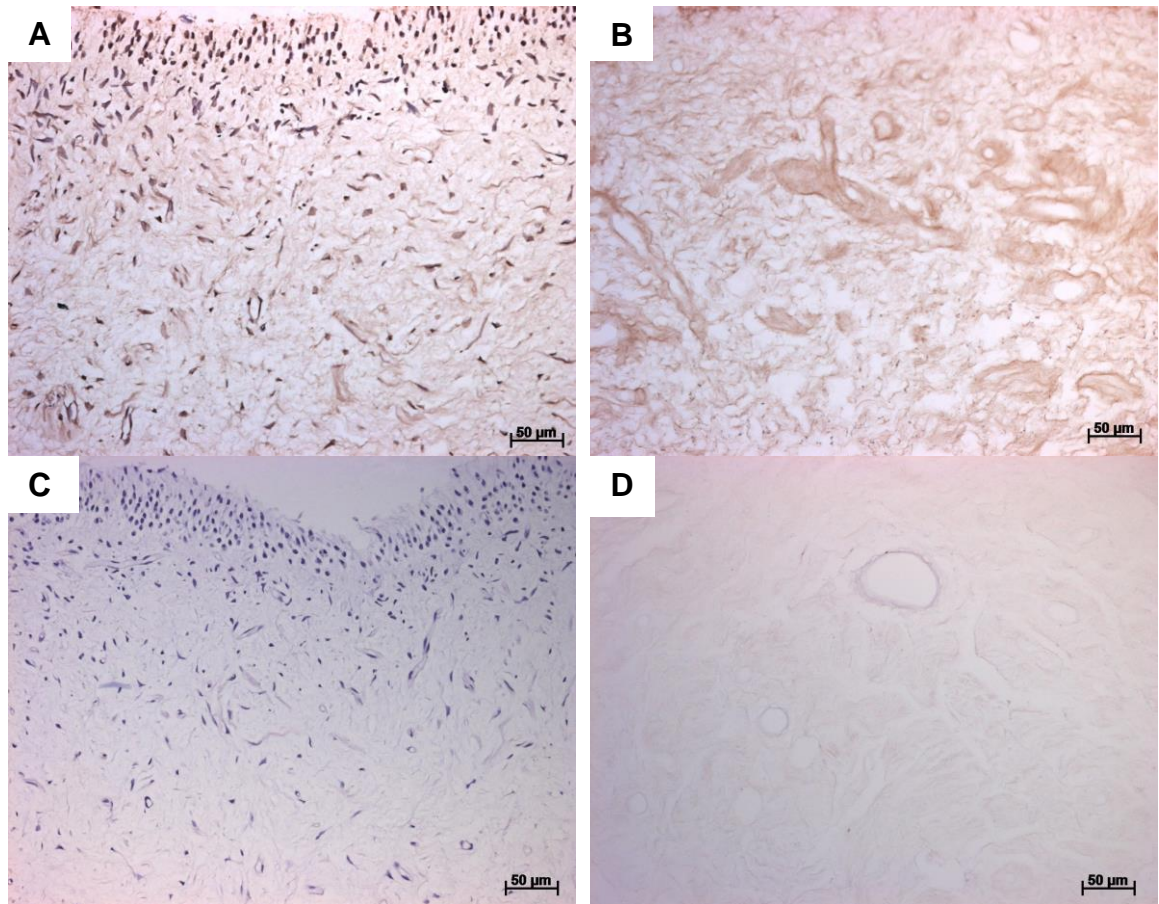


Figure 4.12: Representative images of human pulp tissues labelled with fibronectin antigen and viewed under the light microscope. (A) Native human tissue, (B) Decellularised human tissue, (C) Native human tissue isotype control and (D) Decellularised human tissue isotype. Fibronectin fibres stained brown and cell nuclei stained blue. Scale bars are at 50 µm.

4.4.2.4 Laminin:

Images of rat and human pulp tissues labelled with anti-laminin antibodies are shown in Figure 4.13 and Figure 4.14, respectively. The native tissues of both rat (Figure 4.13 A) and human (Figure 4.14 A) samples were stained brown, a positive immunoreactivity to laminin antigens. Laminin staining appeared as a fibrous plexus scattered throughout the entire ECM mainly concentrated around the basement membrane of vasculature structures.

Following decellularisation, the pulpal tissues of both rat (Figure 4.13 B) and human (Figure 4.14 B) samples revealed a positive staining pattern to laminin fibres. Although the staining of laminin was less intense in comparison to the relative native tissues, laminin fibres were also distributed throughout the entire ECM mainly concentrated around the vasculature structures. No brown staining was observed in isotype control stained sections (Figure 4.13 C, D and Figure 4.14 C, D).

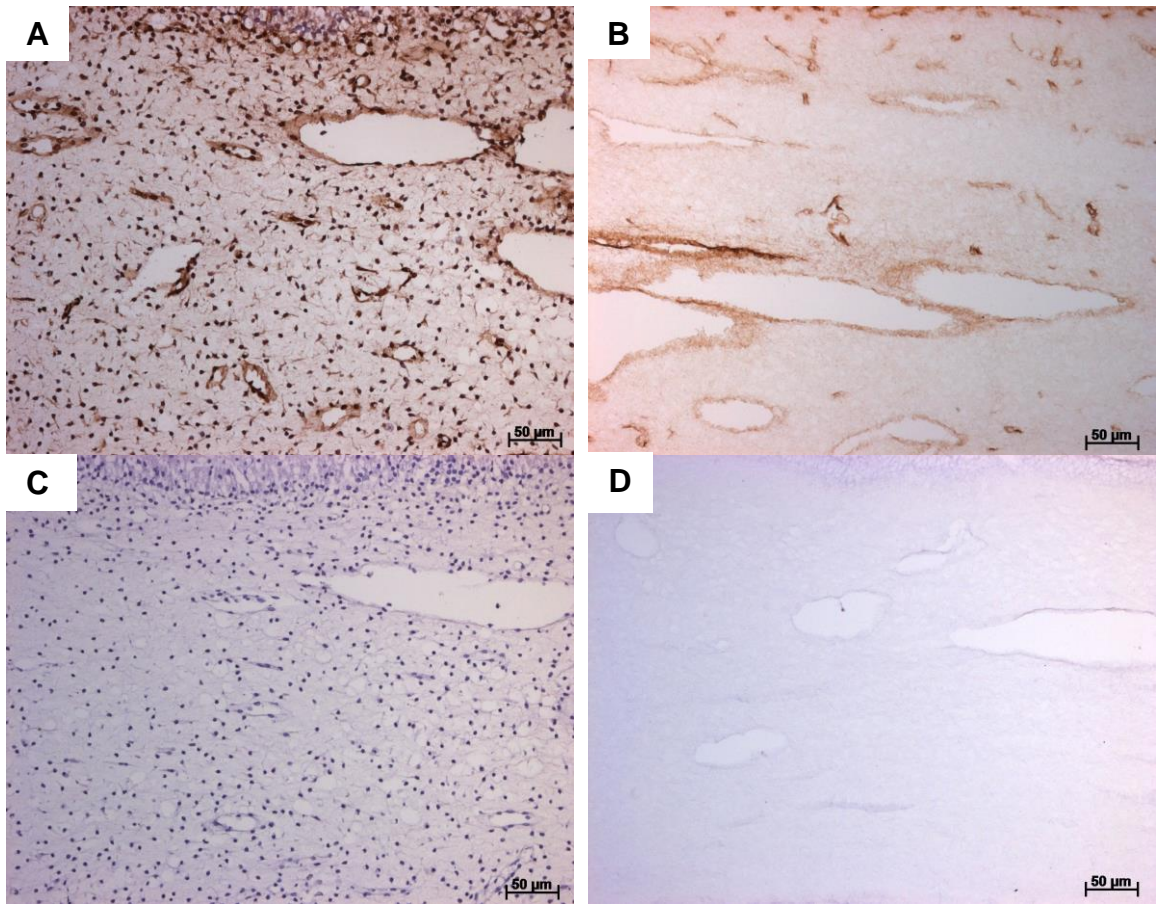


Figure 4.13: Representative images of rat pulp tissues labelled with laminin antigen viewed under the light microscope. (A) Native rat tissue, (B) Decellularised rat tissue, (C) Native rat tissue isotype and (D) Decellularised rat tissue isotype. Laminin fibres stained brown and cell nuclei stained blue. Scale bars are at 50 µm.

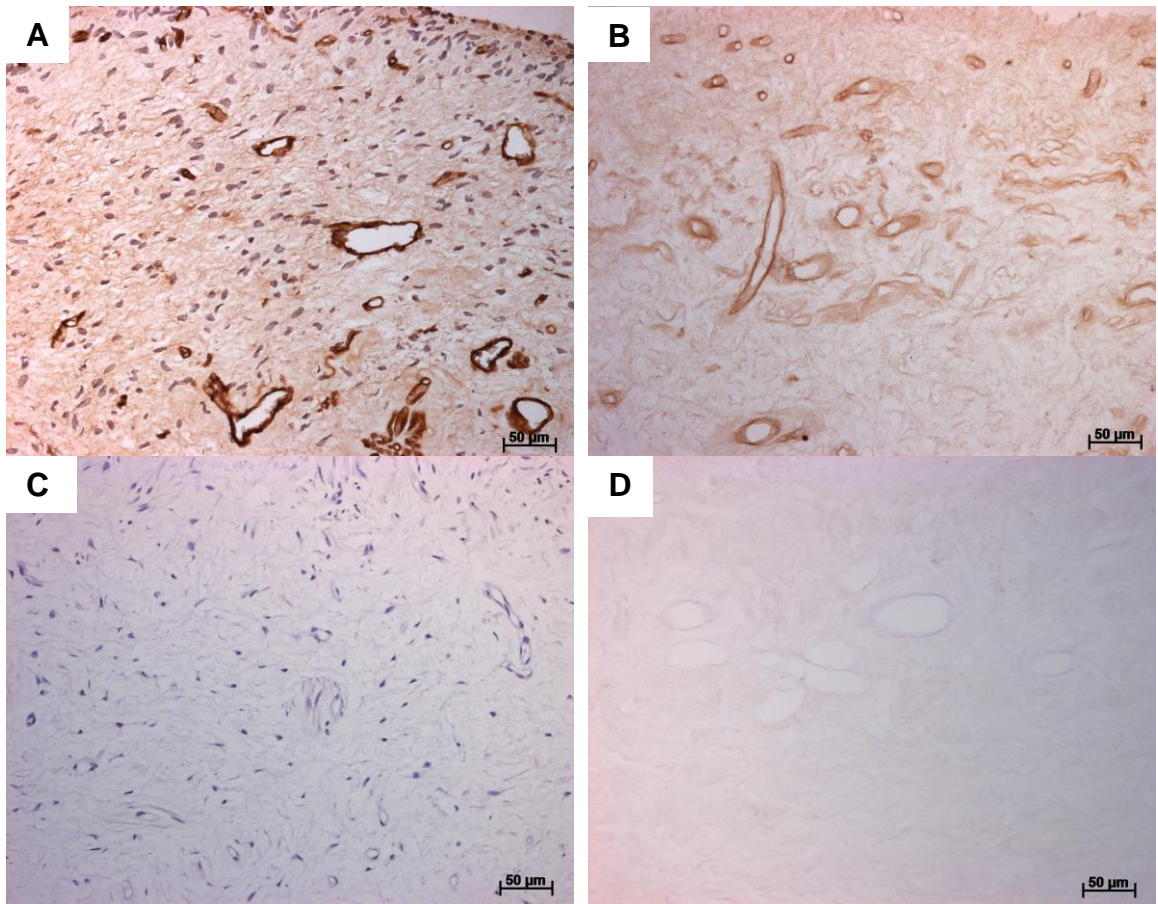


Figure 4.14: Representative images of human pulp tissues labelled with laminin antigen viewed under the light microscope. (A) Native human tissue, (B) Decellularised human tissue, (C) Native human tissue isotype control and (D) Decellularised human tissue isotype. Laminin fibres stained brown and cell nuclei stained blue. Scale bars are at 50 µm.

4.4.2.5 Major histocompatibility complex class II molecules:

Images of rat and human pulp tissues labelled with major histocompatibility complex class II antibodies are shown in Figure 4.15 and Figure 4.16, respectively. A positive immunoreactivity, stained brown, to major histocompatibility complex class II antigens was evident in the native pulp of both rat (Figure 4.15 A) and human (Figure 4.16 A) tissues. These antigens were located with specific cells, mainly concentrating within the sub-odontoblastic layer and around blood vessels in the pulp core, and appeared scattered throughout the ECM.

Following decellularisation, a negative immunoreactivity to major histocompatibility antigens was observed throughout both rat (Figure 4.15 B) and human (Figure 4.16 B) tissues. No brown staining was observed in isotype control stained sections (Figure 4.15 C, D and Figure 4.16 C, D).

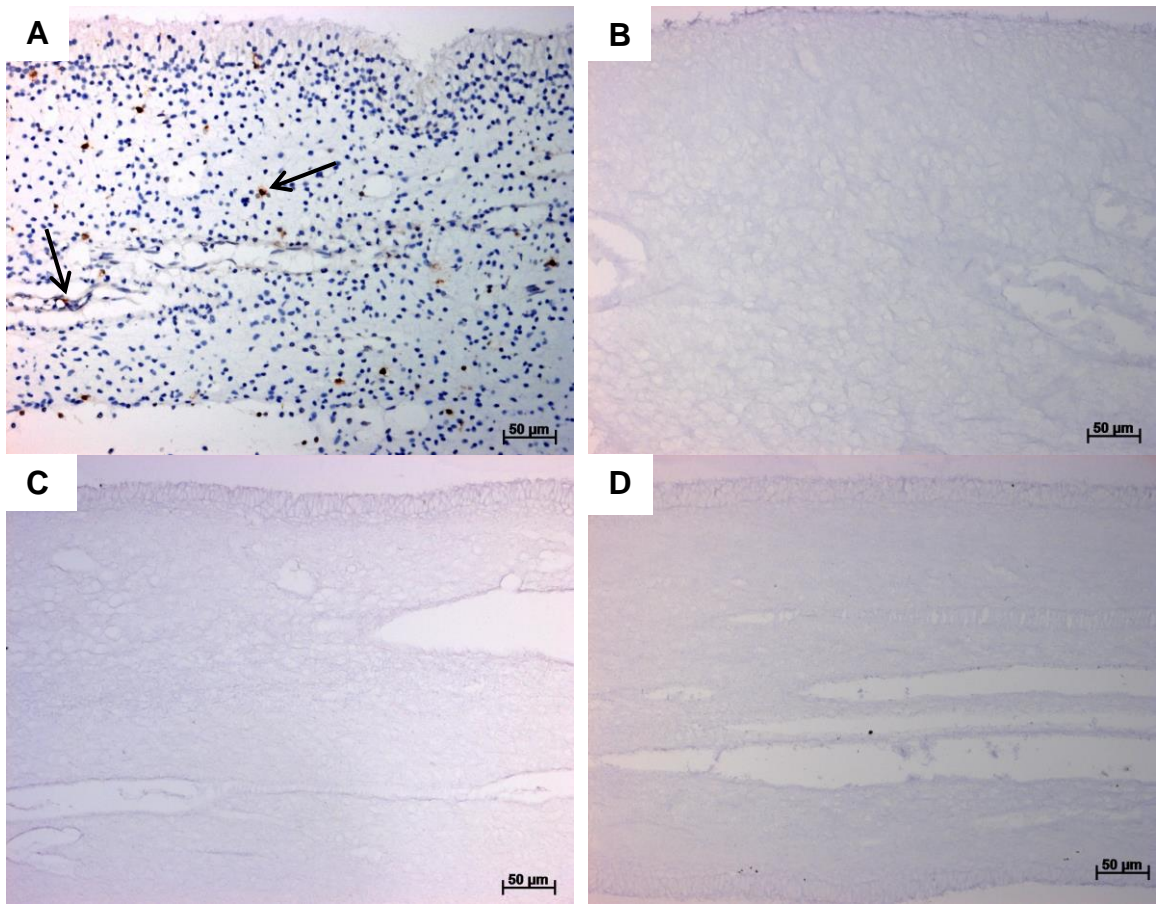


Figure 4.15: Representative images of rat pulp tissues labelled major histocompatibility complex class II antigen and viewed under the light microscope. (A) Native rat tissue, (B) Decellularised rat tissue, (C) Native rat tissue isotype and (D) Decellularised rat tissue isotype. Major histocompatibility complex class II positive cells stained brown (black arrow) and cell nuclei stained blue. Scale bars are at 50 µm.

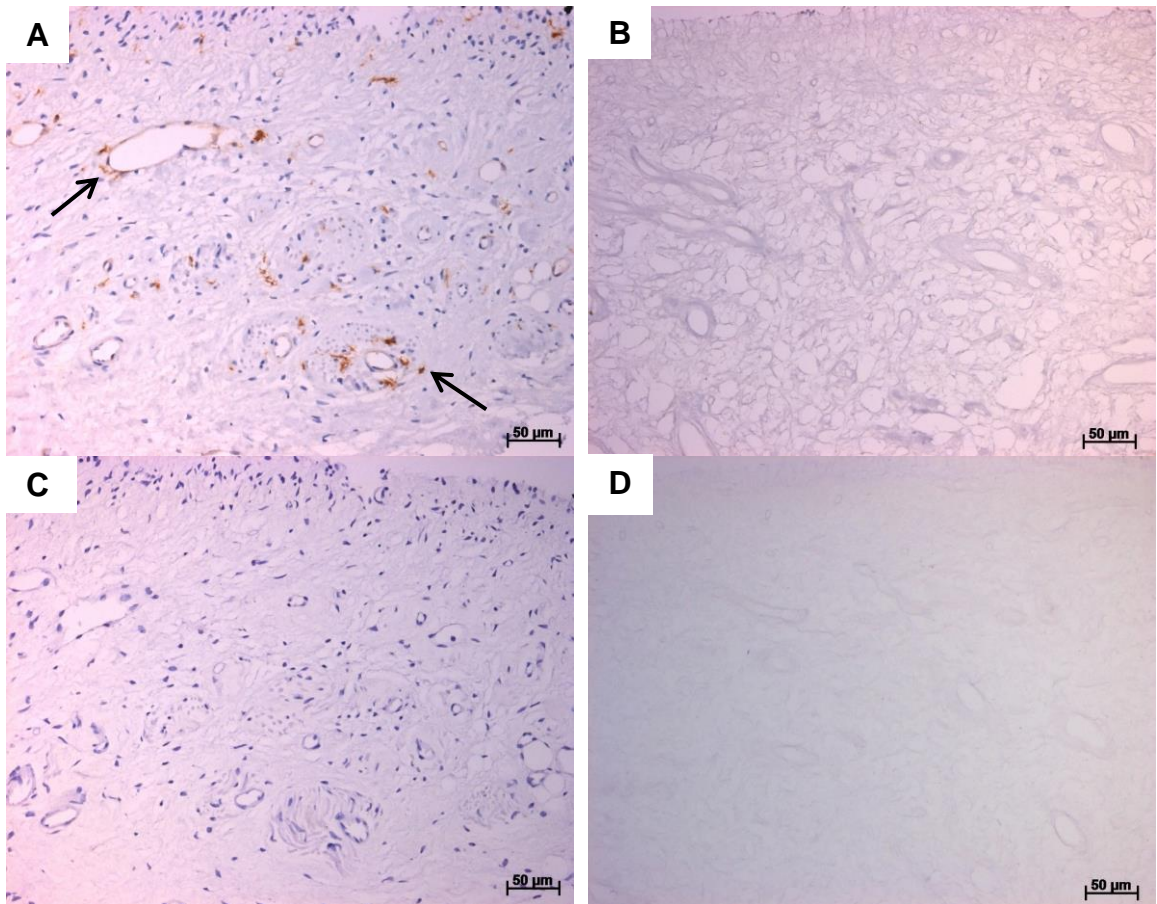


Figure 4.16: Representative images of human pulp tissues labelled major histocompatibility complex class II antigen and viewed under the light microscope. (A) Native human tissue, (B) Decellularised human tissue, (C) Native human tissue isotype control and (D) Decellularised human tissue isotype. Major histocompatibility complex class II positive cells stained brown (black arrow) and cell nuclei stained blue. Scale bars are at 50 µm.

4.4.3 Scanning electron microscope evaluation:

A conventional high vacuum SEM was used to view the surface topography of the dental pulp tissues. SEM generated images of the rat and human pulp tissues are shown in Figure 4.17 and Figure 4.18, respectively. Structural assessment of both native rat (Figure 4.17 A) and human (Figure 4.18 A) tissues revealed a dense irregular fibre mesh structure with interfibrillar spaces.

Following decellularisation, a loose fibre structure appeared to be denuded of some components (cells and more likely some of non-collagenous proteins). Despite the above alteration, preservation of complex entangled irregular fibre mesh was visible in both rat (Figure 4.17 B) and human (Figure 4.18 B) tissues.

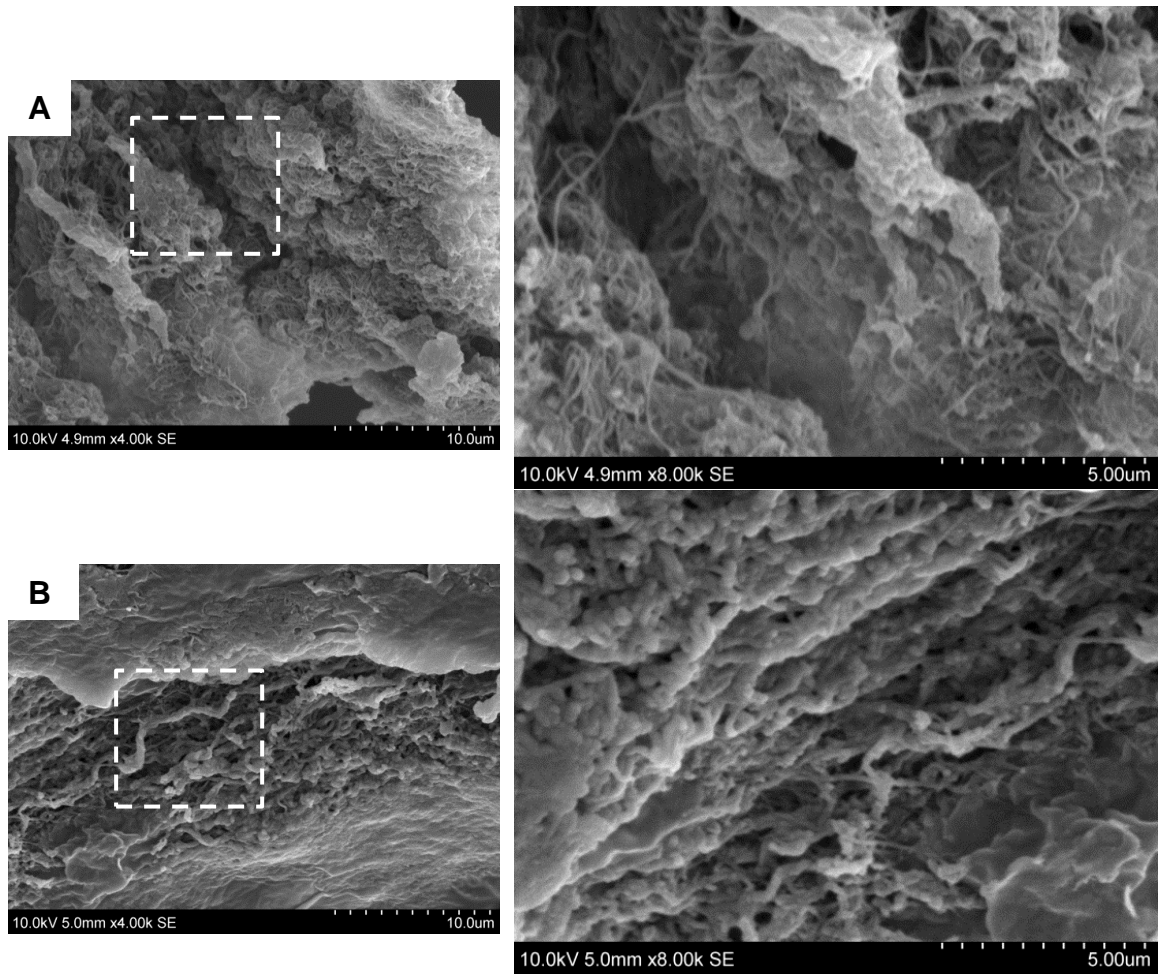


Figure 4.17: Representative images of rat pulp tissues viewed using the scanning electron microscope. (A) Native tissues with a dense irregular fibrous structure and (B) Decellularised tissues with a preserved porous fibrous structure. Scale bars A and B are at 10 µm. Right side images represent magnification of area delineated with dashed white rectangle, scale bar at 5 µm.

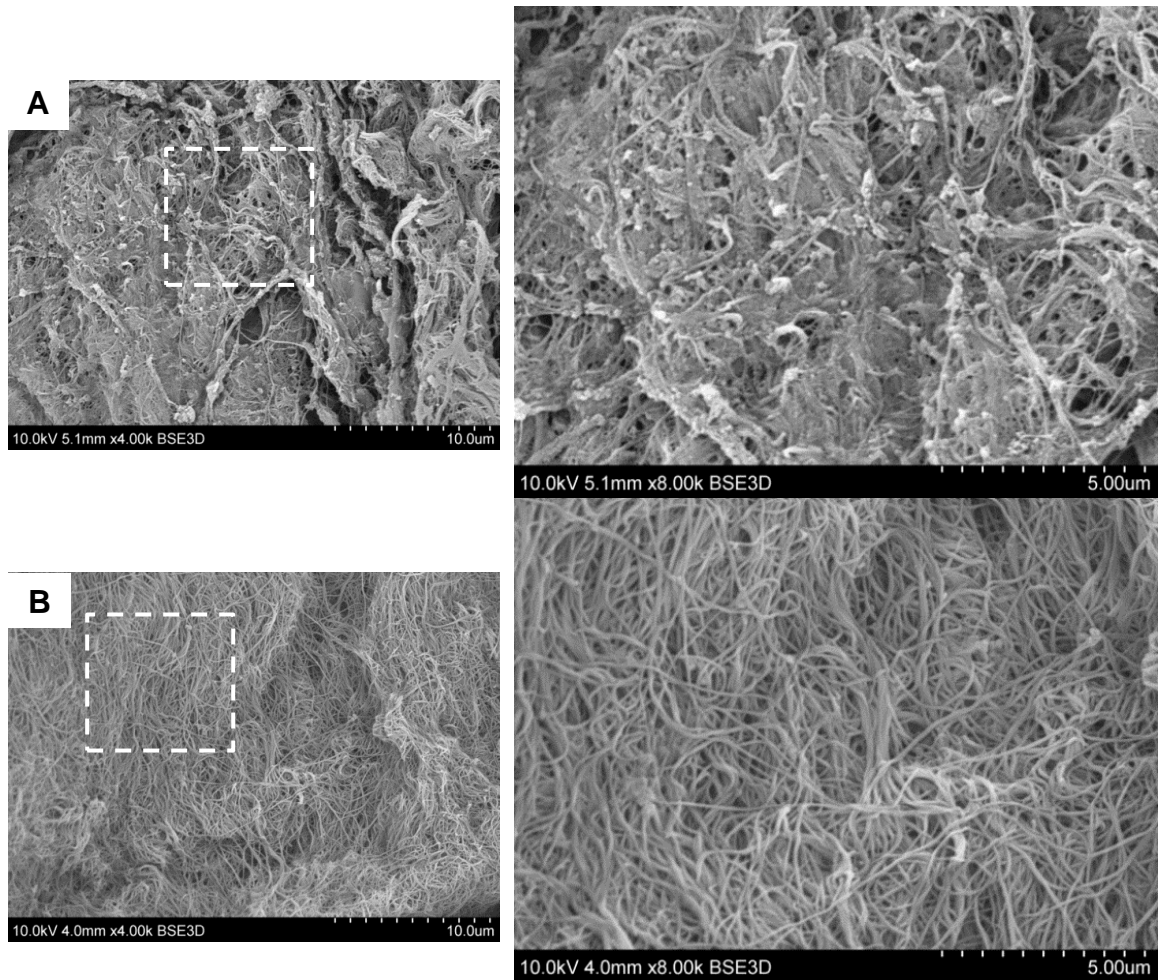


Figure 4.18: Representative images of human pulp tissues viewed using the scanning electron microscope. (A) Native tissues with a dense irregular fibre structure and (B) Decellularised tissues with a preserved porous fibre structure. Scale bars A and B are at 10 μm . Right side images represent magnification of area delineated with dashed white rectangle, scale bar at 5 μm .

4.5 Discussion:

The aim of the work presented in this chapter was to evaluate the effect of the optimised decellularisation protocol, experiment 2, on the natural pulpal ECM structural components. This method involved a freeze-thaw cycle followed by the use of a hypotonic Tris buffer, one cycle of 0.03 % (w/v) sodium dodecyl sulphate (SDS) hypotonic buffer and nuclease enzymatic treatment. Protease inhibitors and mechanical agitation were also incorporated.

The use of qualitative assessment methods is crucial for preliminary characterisation of the histoarchitecture of the produced decellularised matrix in comparison to corresponding native tissues. Therefore the combined use of histological (showing structural elements), immunohistochemical (identifying specific matrix components) and SEM (showing the surface topography of pulp tissues) analysis was essential in assessing the efficiency of decellularisation protocol (experiments 2).

Histological characterisation using Alcian blue staining in both rat and human decellularised tissues revealed no visible differences in GAGs distribution following decellularisation. There are conflicting results reported in the literature on the effect of SDS on tissue GAGs removal and/or preservation (Mirsadraee et al., 2006; Wilshaw et al., 2006; Kheir et al., 2011; Luo et al., 2014; Song et al., 2017). Results of this work are consistent with Mirsadraee et al. (2006) in human pericardial matrix decellularisation, Wilshaw et al. (2006) in human amniotic membrane matrix decellularisation and Wilshaw et al. (2012) in human common femoral arteries decellularisation. These studies used one cycle of

SDS as an ionic detergent step at either 0.1 % (w/v) or 0.03 % (w/v) SDS concentration in a hypotonic buffer for 24 hours at room temperature. Song et al. (2017) reported GAGs preservation following decellularisation of human tooth root slices, although, decellularisation was achieved using three cycles of 1 % (w/v) SDS and 1 % (w/v) Triton X-100 for 24 hours at room temperature.

In contrast, a significant reduction in GAGs content has been reported by Kheir et al. (2011) in porcine cartilage matrices decellularisation and Luo et al. (2014) in porcine pulmonary valve decellularisation when incubated with 0.1 % (w/v) SDS in a hypotonic buffer for 24 hours at 45 °C. Increasing the exposure temperature during decellularisation treatment might have negatively affected GAGs content. Furthermore, experimental work by Kheir et al. (2011) concluded that increasing the number of SDS cycles negatively effects the tissue GAGs content level (Kheir et al., 2011).

Preservation of collagen fibres was also assessed and characterised using histological and immunohistochemical staining methods. Picrosirius red staining is a specific method for collagen detection that can be analysed using light and polarised microscopy (Junqueira et al., 1979). Light microscopy analysis of both rat and human decellularisation tissues revealed a well preserved collagen structure. The collagen structure appeared slightly porous relative to the corresponding native tissues. This was consistent with Chen et al. (2015) following decellularisation of swine dental pulps. We also observed variability in pore size diameter throughout the scaffolds, which might act as a positive variable facilitating regeneration of heterogeneous tissues (pulp-dentine

complex). El-Backly et al. (2008) reported that small pore diameter facilitates tissue neovascularisation, while larger pores assist regeneration of mineralised tissue, cell migration and differentiation, in addition to waste and nutrition transportation (El-Backly et al., 2008). Further visual assessment of Picrosirius red staining under polarised light microscopy also revealed preservation of a complex heterogeneous porous collagen matrix following decellularisation.

For more specific assessment, collagen type I and III fibres were further labelled using monoclonal antibodies. The native human pulp tissue contained a rich network of collagen fibres, as evident with a strong brown staining pattern throughout the matrix. In contrast, an immature network of collagen fibres was evident in the native rat pulp tissues. The results from this work were in agreement van Amerongen et al. (1983) following a qualitative measurement of the collagen content of the dried pulp tissues. Human pulp tissues were found to contain 25.7 - 31.9 % collagen, while rat pulp incisors contained a significantly smaller content of 3.5 % collagen (van Amerongen et al., 1983). Following decellularisation collagen type I and III fibres were retained in both rat and human tissues, albeit expressing a slightly weak stain in comparison to relevant native tissues. In contrast to the present study results, Chen et al. (2015) reported a significant decline in both collagen type I and III fibres using immunohistochemical analysis on the decellularised miniature swine dental pulps with collagen fibres largely absent in the sub-odontoblastic layer. In their work, decellularisation was achieved based on a dual detergent method using 1 % (w/v) SDS and 1 % (w/v) Triton X-100 (Chen et al., 2015).

Conventional high vacuum SEM was performed to view the surface topography of the rat and human dental pulp tissues. Electron based signal images were produced through electron interaction with surface atoms of tissue samples. SEM generated images revealed that the decellularisation process seemed to preserve the irregular fibre mesh. The collagen fibres of the decellularised matrix appeared more exposed and an increase in matrix porosity. The formation of interfibrillar spaces within the matrix could be more evident due to the removal of cells from the tissue or as a consequence of exposure to several reagents and temperature changes during the decellularisation process. Oliveira et al. (2013) postulated that the vehiculating aqueous solutions used throughout the decellularisation treatment produced tissue swelling that consequently affected the tissue architecture (Oliveira et al., 2013).

To further evaluate matrix components immunohistochemical labelling against fibronectin and laminin adhesive proteins was performed. Fibronectin and laminin positive fibres in the native rat and human tissues showed similar distribution patterns. These fibres were mainly present within the sub-odontoblastic layer, around blood vessels and in the pulp core. This is in agreement with previous findings (Linde et al., 1982; van Amerongen et al., 1984). Following decellularisation, qualitative analysis of rat and human tissues revealed preservation of these fibres, albeit with a lower staining intensity. Preservation of fibronectin and laminin, as detected using immunohistochemical staining, was also reported by Chen et al. (2015) for the decellularisation of miniature swine pulps and by Traphagen et al. (2012) for the decellularisation of porcine tooth buds. A reduced expression of fibronectin, mainly within the

sub-odontoblastic layer, was found following the use of three cycles of 1 % (w/v) SDS and 1 % (w/v) Triton X-100 to decellularise tooth root slices (Song et al., 2017).

Furthermore, it was deemed appropriate to perform immunohistochemical labelling against major histocompatibility complex class II molecules. These molecules are expressed by immune cells including dendritic cells, monocytes and macrophages. These cells are commonly present in the native dental pulps, of rat and human tissues, and serve as initial defence cells (Jontell et al., 1987; Ohshima et al., 1999). Results of this work revealed negative reactivity to major histocompatibility complex class II molecules following decellularisation.

Collectively, qualitative analysis of this chapter show retention of porous collagen matrix with no obvious histoarchitecture disruption of ECM and preservation of essential adhesive proteins following decellularisation of the whole dental pulp tissues of rat and human species. Therefore, further analysis of the decellularised matrix cytotoxicity and ability to support recellularisation was performed and described in the following chapter.

Chapter 5

Cytotoxicity assessment and recellularisation of the decellularised scaffold

5.1 Introduction:

The decellularisation steps used in the optimised decellularisation protocol (experiment 2) involves the use of detergents, enzymes, and other reagents with the potential to negatively affect the tissues native extracellular matrix (ECM) structure and composition. Furthermore, any residual chemicals could be toxic to cells and ultimately result in a cytotoxic scaffold. Cytotoxicity is a commonly used term to describe a cascade of events which affect either direct cell membrane damage or the activation of natural cell suicide mechanisms. Cytotoxicity assessment of a given material is initially performed using *in vitro* cell culture methods. These *in vitro* cell culture based methods have the advantage of simplicity and reproducibility (Hensten-Pettersen, 1988).

The selection of the appropriate cell type for *in vitro* cytotoxicity assays remains debatable (Murray et al., 2000; Saw et al., 2005). Although primary cells are more clinically relevant, the use of established cell lines such as L-929 mouse fibroblasts are commonly used for dental material evaluation due to their high reproducibility, relatively standard growth, and morphology characteristics (Hensten-Pettersen, 1988; Torabinejad et al., 1995b; Thonemann et al., 2002; Saw et al., 2005; Ozdemir et al., 2009). *In vitro* cytotoxicity assays with established cell lines are also recommended by British and International

Organisation for Standardisation for cytotoxicity testing of medical devices (International Organisation for Standardisation, 2008; British Standard Institute, 2009). Therefore, in this work, *in vitro* contact and extract cytotoxicity assessment of the produced scaffolds were assessed using L-929 mouse fibroblast cell lines. Furthermore, to closely resemble the clinical setting, *in vitro* cell viability assays and recellularisation of the decellularised scaffolds were assessed using primary cell culture, dental pulp stem cells (DPSCs).

Preservation of specific matrix adhesive proteins within the decellularised scaffold is desirable due to their crucial roles in mediating cellular activities (Howard et al., 2010). It is this complex integration between the cells and the direct surrounding microenvironment (ECM proteins) that regulates future cell growth and differentiation (Martinez et al., 2000; Nakashima et al., 2013).

Several *in vitro* and *in vivo* studies have defined DPSCs as undifferentiated mesenchymal cells with the ability to differentiate into multiple lineages including odontoblastic cells (Gronthos et al., 2002; Zhang et al., 2006a; Prescott et al., 2008; Kim et al., 2009; Huang et al., 2010; Kawashima, 2012; Paduano et al., 2016). However, no known single molecule that specifically determines stem cell differentiation to odontoblast-like cells (Goldberg and Smith, 2004).

Nevertheless, the use of a panel of markers including dentine sialophosphoprotein (DSPP), dentine matrix protein-1 (DMP-1), and nestin to identify the odontogenic differentiation has been proposed (Goldberg and Smith, 2004). Other proof-of-principle studies also proposed the use of DSPP,

DMP-1 and alkaline phosphatase (ALP) as potential odontoblast markers (Almushayt et al. 2006; Prescott et al. 2008; Gronthos et al. 2000; Paduano et al. 2016). DSPP, a non-collagenous protein, is a precursor to two essential matrix proteins namely dentine sialoprotein and dentine sialophosphoprotein. DSPP is generally considered as a tooth specific gene and regarded as a phenotypic marker of dentine and secretory odontoblasts' (Gronthos et al., 2000; Goldberg and Smith, 2004). However, DSPP is also identified in bone, albeit a reduced expression level approximately 1 / 400 relative to dentine (Qin et al., 2002). DMP-1 is a non-collagenous protein that is primarily present in the mineralised matrix of bone and dentine (He et al., 2003; Narayanan et al., 2003). DMP-1 is regarded as an odontoblastic marker, secreted by pre-odontoblasts' as well as secretory odontoblasts' (Almushayt et al., 2005; Prescott et al., 2008). DMP-1 is subsequently exported, from the cells, to the surrounding matrix regulating the deposition of a mineralised matrix (He et al., 2003; Narayanan et al., 2003). Odontoblasts' cells also contain high levels of ALP enzyme. ALP enzymes are believed to contribute to the odontoblasts' ability to produce dentine and affect mineralisation (Yoshiki and Kurahashi, 1971; Goseki et al., 1990).

Furthermore, the characterisation of DPSCs, based on the expression of growth factors and cytoskeleton proteins (genes), is of equal importance. In general terms, the cellular cytoskeleton is composed of three types of structures including microfilaments, microtubuli and intermediate filaments. Several types of intermediate filaments are expressed in various cell types and are

functionally crucial for cellular and tissue organisation and function (About et al., 2000).

Vimentin is a major intermediate filament protein of mesenchymal cells and is known to participate in several protein functions mainly cell signalling, adhesion, and migration (Ivaska et al., 2007). Vimentin is expressed in the cytoplasm of pulp cell and extends peripherally from the central body to the cell processes (Murakami et al., 2012). Nestin, also an intermediate filament protein, is classified as neural progenitor marker and was originally identified in neuroepithelial stem cells (Sejersen and Lendahl, 1993; About et al., 2000). Nestin has also been identified in DPSCs and known as an early neuronal-associated marker (Arthur et al., 2008). In human and rodent teeth nestin was found to be expressed in functioning and newly differentiated odontoblast cells (Terling et al., 1995; Kuratate et al., 2008; Lee et al., 2012).

The expression of Alpha-smooth muscle actin (α -SMA), a cytoskeletal protein, in the vascular smooth muscle cells and pericytes of the normal dental pulp has been demonstrated (Shi and Gronthos, 2003; Yoshiba et al., 2012). During early stages of dental pulp healing, numerous α -SMA positive cells were expressed in newly differentiated odontoblast like cells (Yoshiba et al., 2012). It is also localised in various tissues during tissue repair and regeneration following injury (Yoshiba et al., 2012).

For successful pulp engineering, the formation of blood vessels via angiogenesis is a key factor (Gerhardt and Betsholtz, 2003; Nakashima et al., 2009; Janebodin et al., 2013; Saghiri et al., 2015). Studies have linked

angiogenesis to a number of growth factors including basic fibroblast growth factor (bFGF), transforming growth factor (TGF; TGF- α , TGF- β), platelet-derived growth factor (PDGF), tumour necrosis factor- α (TNF- α), and vascular endothelial growth factor (VEGF) (Grando Mattuella et al., 2007; Saghiri et al., 2015). VEGF, a heparin-binding glycoprotein of 45 kilodaltons, is regarded as the potent regulatory molecule controlling vascular permeability and angiogenesis (Ferrara, 2004; Grando Mattuella et al., 2007). VEGF family is composed of six members namely VEGF-A, B, C, D, E, and PDGF. Of these family members, VEGF-A is known as the key member that largely regulates angiogenesis (Ferrara, 2004; Grando Mattuella et al., 2007). In addition to the main molecule VEGF receptor tyrosine kinases, fms-like tyrosine kinase (Flt-1, also known as VEGFR-1) and kinase-insert domain containing receptor (KDR, also known as VEGFR-2) are present in the dental pulp. Although both receptors are present, VEGFR-2 is known to have the highest signalling activity and mediates human pulp cells proliferation, migration and vascular permeability (Matsushita et al., 2000; Grando Mattuella et al., 2007). According to Janebodin et al. (2013) the ability of DPSCs to function as pericyte-like cells and support angiogenesis is VEGFR-2 dependent (Janebodin et al., 2013).

The rat and human pulp tissues used in this chapter were decellularised using the optimised decellularisation protocol developed as previously described (experiment 2). The biocompatibility of the developed scaffolds was determined using cytotoxicity analysis. Furthermore, the differentiation ability of the DPSCs following recellularisation was evaluated by the identification of specific cellular molecules (namely those described above).

5.2 Aim and objectives:

5.2.1 Aim:

The aim of this chapter is to evaluate the decellularised scaffold cytotoxicity and to assess its potential to support human DPSCs attachment, proliferation and differentiation *in vitro*.

5.2.2 Objectives:

The above aim will be achieved through the following objectives:

- To determine the cytotoxicity of the decellularised rat and human scaffold using *in vitro* techniques.
- To evaluate the ability of human DPSCs to attach and migrate following recellularisation of the decellularised rat scaffolds.
- To evaluate the ability of human DPSCs to express odontoblast markers and molecular proteins following recellularisation of the decellularised rat scaffolds.

5.3 Methods and experimental approaches:

This chapter describes assessing the biocompatibility of the produced decellularised rat and human scaffolds using *in vitro* cytotoxicity evaluation methods with an established cell line. Subsequently, the produced decellularised rat and human scaffolds were recellularised with DPSCs and cell viability assessed following *in vitro* culture. Finally, the recellularised rat scaffolds were assessed for their ability to further support cell growth and differentiation using histology and immunohistochemistry staining methods. DPSCs were kindly provided by Dr M Tomlinson following patient consent and ethical approval (Skeletal Research Tissue Bank; reference number 101013/MME/113; Appendix A). DPSCs used in this work (passage 5) were harvested from a single donor and isolated via enzymatic digestion as described in Section 2.2.8.1.

5.3.1 Cytotoxicity evaluation of decellularised rat and human scaffolds:

To determine the *in vitro* cytotoxicity of the decellularised scaffolds, a new batch of rat and human dental pulp tissues were decellularised as described in experiment 2 (Section 3.3.2). Representative tissues were further checked using histological methods (H&E and DAPI) to ensure effective decellularisation. Decellularised tissues were obtained under aseptic conditions in a Class II safety cabinet and stored temporarily in PBS (pH 7.4) to avoid tissue dehydration. Cytotoxicity evaluations were undertaken using contact and extract cytotoxicity assays. Both assays were performed using L-929 murine

fibroblast cell line. Normal cell culture methods including cell resurrection, culturing and, passaging were performed as described in Section 2.2.8.

5.3.1.1 Contact cytotoxicity assay:

To assess the direct cytotoxicity of the decellularised scaffolds, contact cytotoxicity assays were performed as described in Section 2.2.9.1. Briefly, decellularised rat ($n = 4$) and human ($n = 4$) scaffolds were attached to the centre of six-well cell culture plates using collagen type I gel. Six-well plates containing collagen type I gel, as a negative control, and cyanoacrylate adhesive glue, as a positive control, were also prepared. L-929 cell lines were cultured in their standard culture medium and a cell concentration of 2×10^5 cells.mL⁻¹ (2 mL) was added to each well plate and incubated for 48 hours at 37 °C in 5 % (v/v) CO₂ and 95 % relative humidity. Following incubation, the cell layers were fixed and stained with Giemsa solution. Changes in cell growth and morphology were viewed using an inverted light microscope (Cell[^]B software) under bright field illumination with all images captured digitally.

5.3.1.2 Extract cytotoxicity assay:

To assess any potential extract cytotoxicity resulting from residual chemicals in decellularised scaffolds, extract cytotoxicity assays were performed as described in Section 2.2.9.2. Briefly, decellularised rat ($n = 8$) and human ($n = 8$) scaffolds were finely macerated and incubated with plain DMEM at 37 °C for 72 hours with agitation. The collected test extracts were used for this assay. Controls used included plain DMEM, as a negative control, and

40 % (v/v) DMSO in DMEM, as a positive control. L-929 cell lines were cultured in their standard culture medium and a diluted cell concentration of 5×10^4 cells.mL⁻¹ (200 μ L) was added to each well plate and incubated for 48 hours at 37 °C in 5 % (v/v) CO₂ and 95 % relative humidity. The cell viability was determined using ATPLite™ assay. Results were statistically analysed using one-way analysis of variance (ANOVA; *p*-value of < 0.05).

5.3.2 Cell seeding density:

Optimisation of a suitable cell seeding density was initially performed. Consistent scaffold lengths, approximately 5 - 6 mm, were dynamically seeded (Section 0) with two densities 5×10^3 and 1×10^4 cells per scaffold. Scaffolds were analysed using cell viability assay (Section 2.2.11) following 7 day culture. At the lower seeding density, 5×10^3 cells per scaffold, limited cells were populated within the scaffold. However, a seeding density of 1×10^4 cells per scaffold revealed adequate cell population throughout the scaffold. Based on these results (Figure 5.1), a cell seeding density of 1×10^4 cells per scaffold (5.55×10^4 cells.mL⁻¹) was selected as the most appropriate and used in future recellularisation experiments.

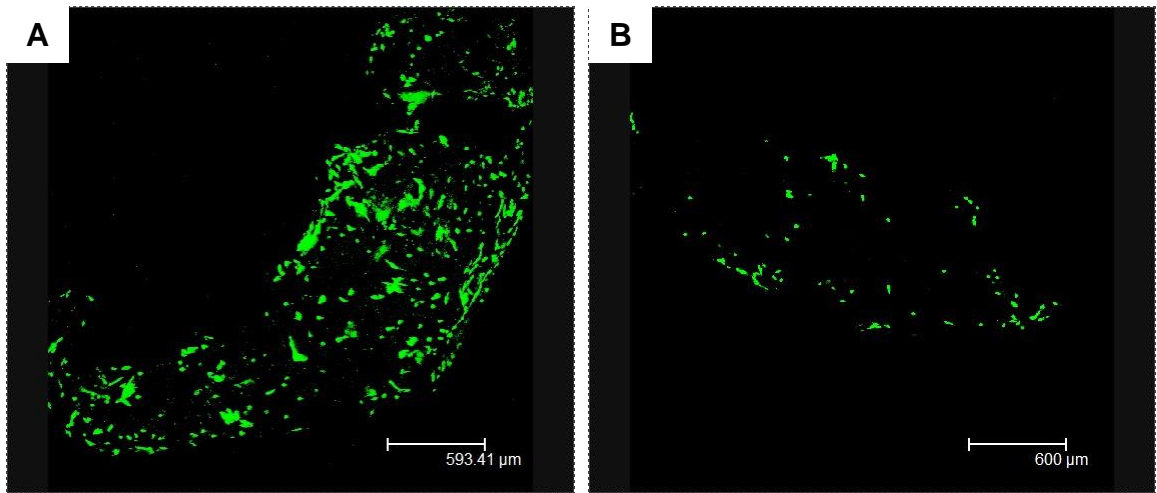


Figure 5.1: Optimisation of cell seeding density. (A) 1×10^4 cells per scaffold and (B) 5×10^3 cells per scaffold analysed with Live/Dead[®] stain using laser confocal microscopy.

5.3.3 Cell viability assay of rat and human scaffolds:

The decellularised scaffolds were recellularised with human DPSCs at a concentration of 1×10^4 cells per scaffold (5.55×10^4 cells.mL⁻¹). The ability of the decellularised rat ($n = 3$ / time point) and human ($n = 3$ / time point) scaffolds in supporting cell viability were assessed using Live/Dead[®] stain as described in Section 2.2.11. Stained scaffolds were analysed following 7 and 14 days culture under confocal laser scanning microscopy at excitation/emission wavelengths (calcein-AM = 494 / 517 nm and Ethidium homodimer-1 = 528 / 617 nm) using FITC and Texas red filters for dual-labelled samples. The signals of the two dyes were assessed at different depths of the scaffolds.

5.3.4 Recellularisation of rat scaffolds using DPSCs:

Decellularised rat scaffolds were recellularised with human DPSCs at a concentration of 1×10^4 cells per scaffold (5.55×10^4 cells.mL⁻¹). The ability of the decellularised rat scaffolds to support cell growth and differentiation

following recellularisation were analysed following 7 and 14 days culture using histological and immunohistochemical staining methods.

5.3.4.1 Histological evaluation of the recellularised rat scaffolds:

The attachment and migration of human DPSCs following recellularisation on the decellularised rat scaffolds (n = 3 / each time point) were analysed using H&E staining methods (Section 2.2.4.1). H&E stained sections were viewed using normal Köhler illumination and all images were captured digitally.

5.3.4.2 Immunohistochemical evaluation of the recellularised rat scaffolds:

Immunohistochemistry labelling of decellularised (n = 3 / each time point) and recellularised (n = 3 / each time point) rat scaffolds were performed as described in Section 2.2.5. All immunohistochemical sections were subjected the appropriate antigen retrieval method. Primary antibodies used in this chapter include monoclonal antibodies against α -SMA, DMP-1, DSPP, VEGFR-2, nestin and vimentin antigens, and polyclonal antibodies against ALP and VEGF-A antigens. As negative controls, primary antibodies were omitted and replaced by isotype controls. Isotype control antibodies were used under the same conditions and concentrations as the corresponding primary antibody. Immunohistochemical stained sections were viewed using normal Köhler illumination with all images captured digitally.

5.4 Results:

5.4.1 Cytotoxicity evaluation of decellularised rat and human scaffolds:

5.4.1.1 Contact cytotoxicity assay:

The contact cytotoxicity assays were performed to assess the cytotoxicity of the decellularised pulp scaffolds by culturing cells directly in contact with the scaffolds. Results of the rat (Figure 5.2) and human (Figure 5.3) decellularised scaffolds indicated no apparent cytotoxicity. L-929 cells exhibited standard morphology, vacuolisation and established an adherent monolayer on the seeded well plates. The cells grew in the area surrounding and in contact with all examined scaffolds.

Negative control, using collagen gel, indicated no apparent cytotoxicity with L-929 cells surrounding and in contact with the collagen gel (Figure 5.4 A). L-929 cells also, as above, exhibited standard morphology, vacuolisation and established an adherent monolayer on the seeded well plates. No differences in cell morphology and growth were also observed between cells cultured with the decellularised pulp scaffolds or solely with the collagen gel negative control.

On the contrary, positive controls, using cyanoacrylate glue, resulted in cell lysis with zones of no cell growth. L-929 cells exhibited a round morphology and were detached from the well plates (Figure 5.4 B).

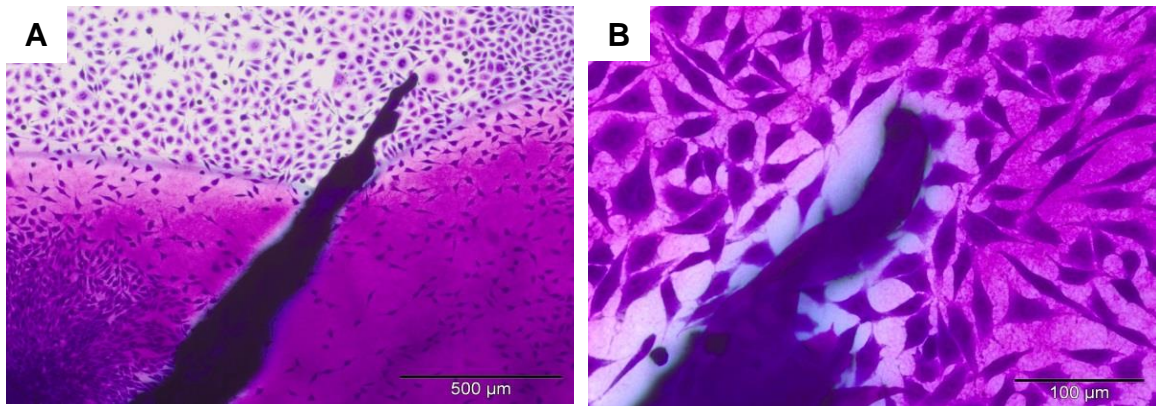


Figure 5.2: Contact cytotoxicity assays of decellularised rat scaffolds cultured with L-929 cell line for 48 hours, stained with Giemsa stain and viewed under brightfield illumination. Images representative of n = 4. (A and B) Rat decellularised scaffold showing no apparent cytotoxicity. Scale bars A at 500 µm and B at 100 µm.

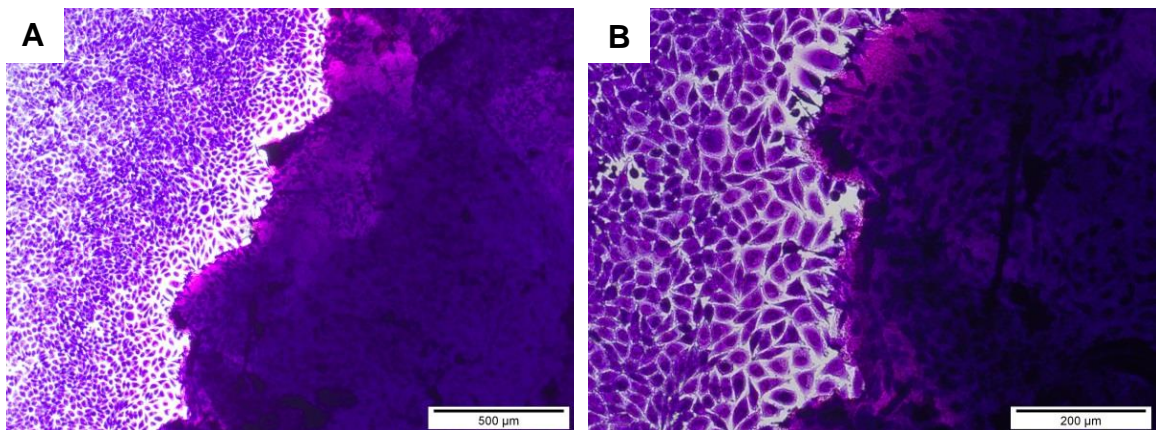


Figure 5.3: Contact cytotoxicity assays of decellularised human scaffolds cultured with L-929 cell line for 48 hours, stained with Giemsa stain and viewed under brightfield illumination. Images representative of n = 4. (A and B) Human decellularised scaffold showing no apparent cytotoxicity. Scale bars A at 500 µm and B at 200 µm.

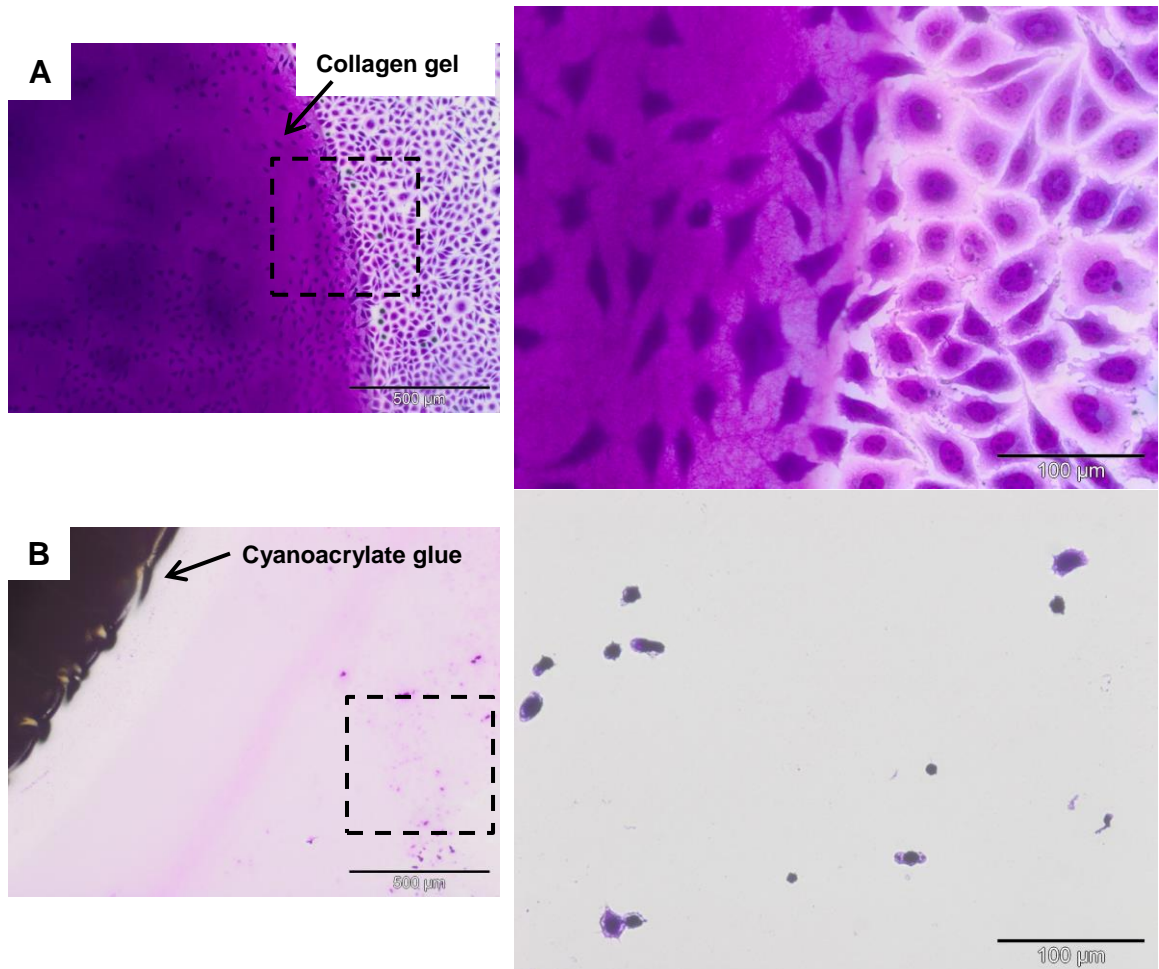


Figure 5.4: Controls used for contact cytotoxicity assays cultured with L-929 cell line for 48 hours, stained with Giemsa stain and viewed under brightfield illumination. I (A) Collagen gel (negative control) showing no apparent cytotoxicity, and (B) Cyanoacrylate glue (positive control) showing marked cytotoxicity with cell lysis. Scale bars A and B at 500 µm. Right side images represent magnification of area delineated with dashed black rectangle, scale bars at 100 µm.

5.4.1.2 Extract cytotoxicity assay:

The results of the relative cellular ATP content of rat and human scaffolds are presented in Figure 5.5 and Figure 5.6, respectively.

The relative cellular ATP content measurements were significantly lower in the positive control (DMSO) in comparison to the negative control (DMEM). In contrast, there was no significant difference in ATP content between the study group (decellularised extracts) and negative control (DMEM). This indicated that there wasn't any soluble extract cytotoxicity produced from the decellularised extracts. All statistical analyses was performed using ANOVA, $p < 0.05$, (GraphPad Prism, Software 6).

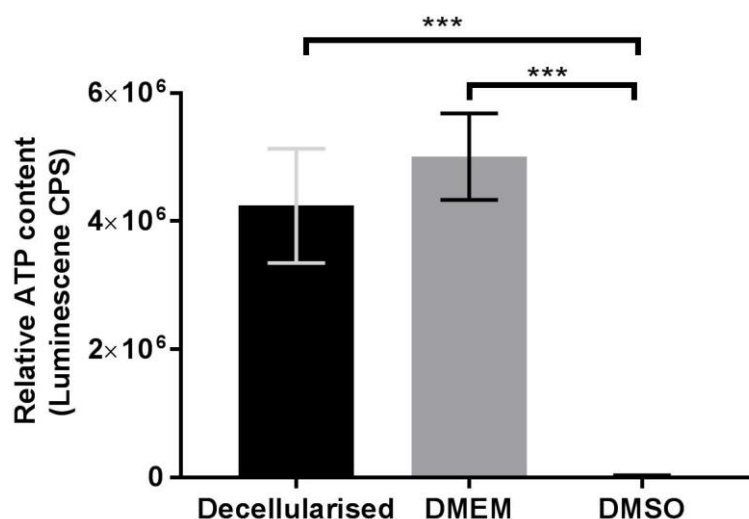


Figure 5.5: Extract cytotoxicity assay measuring the relative cellular ATP content of decellularised rat extracts following 24 hour culture. Data analysis revealed no significance difference between decellularised extracts and negative control (DMEM). Error bars represent $\pm 95\%$ confidence intervals. “***” indicates a significant difference when compared to positive control (DMSO); $p < 0.0002$, ANOVA; CPS, counts per second.

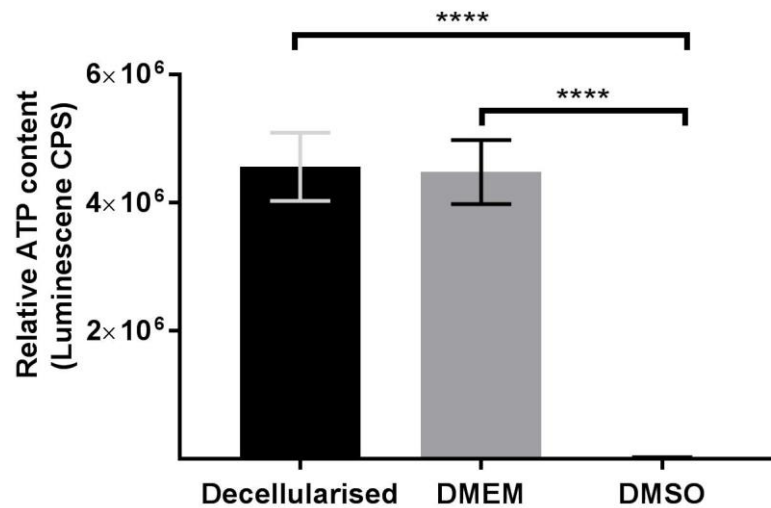


Figure 5.6: Extract cytotoxicity assay measuring the relative cellular ATP content of decellularised human extracts following 24 hour culture. Data analysis revealed no significance difference between decellularised extracts and negative control (DMEM). Error bars represent \pm 95 % confidence intervals. “****” indicates a significant difference when compared to positive control (DMSO); $p < 0.0001$, ANOVA; CPS, counts per second.

5.4.2 Cell viability assay of rat and human scaffolds:

The cell viability of human DPSCs following recellularisation of rat and human scaffolds were evaluated following 7 and 14 days culture using a commercial Live/Dead[®] stain. Confocal laser microscope images of rat and human recellularised scaffolds are presented in Figure 5.7 and Figure 5.8, respectively. These images represent a composite of merged Z-series laser images. The pulp constructs showed that most areas of the decellularised pulp scaffolds were populated with viable cells exhibiting an elongated morphology (stained green with calcein-AM) and only a few cells were dead (stained red with ethidium homodimer).

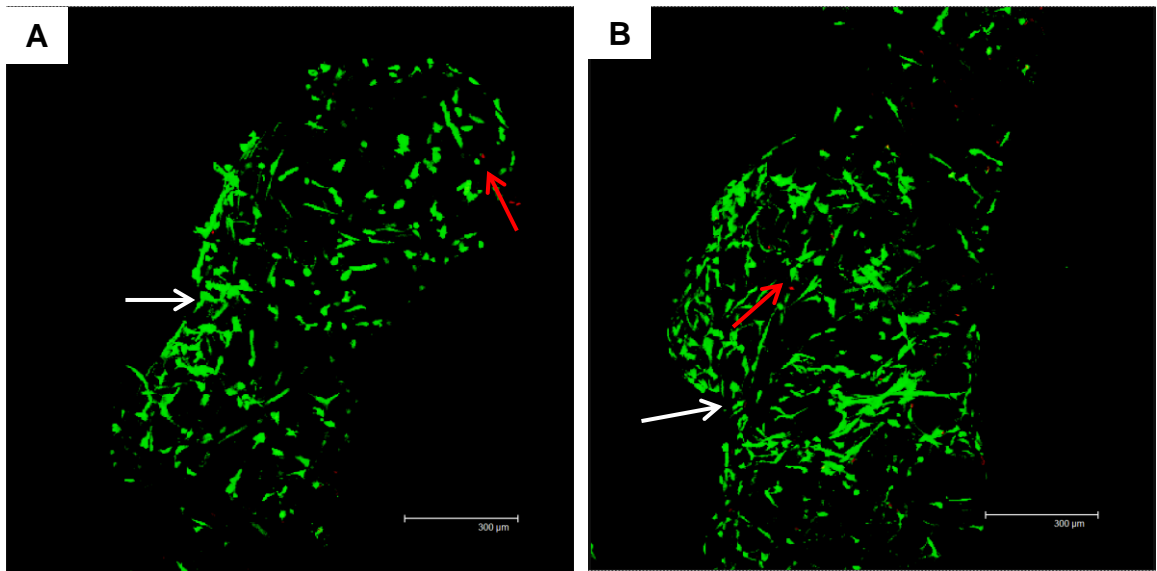


Figure 5.7: Cell viability assay of decellularised rat scaffolds seeded with DPSCs and analysed with Live/Dead[®] stain using laser confocal microscopy. Representative images of (A) Recellularised scaffolds (n = 3) following 7 day, and (B) Recellularised scaffolds (n = 3) following 14 day culture. Both images indicate scaffold populated with viable cells and only a few cells were dead. Live cells stained green (white arrow) and dead cells stained red (red arrow). Scale bars are at 300 µm.

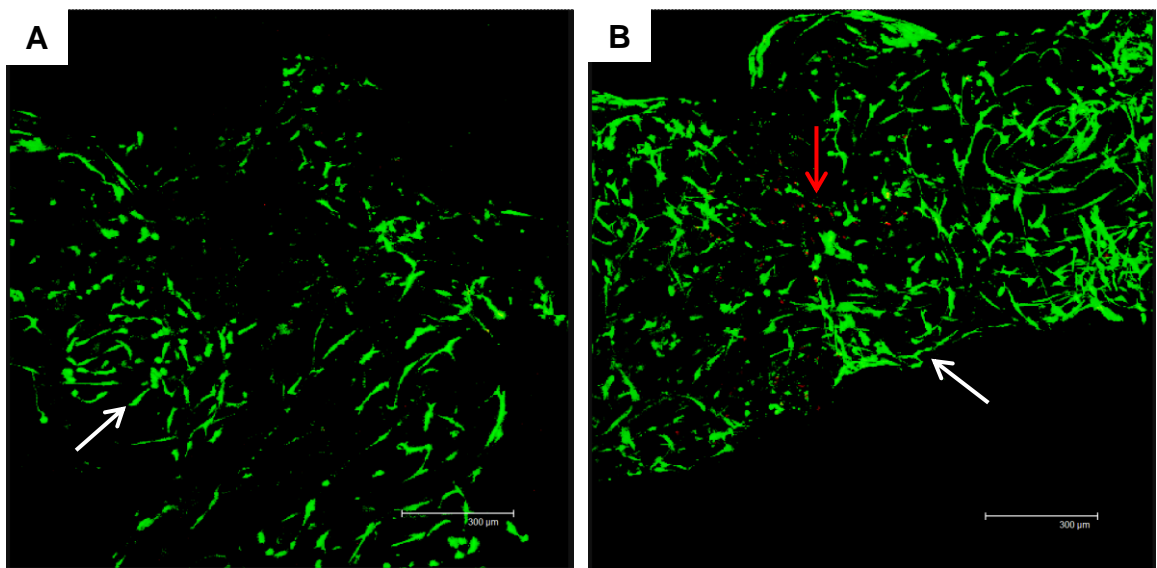


Figure 5.8: Cell viability assay of decellularised human scaffolds seeded with DPSCs and analysed with Live/Dead[®] stain using laser confocal microscope. Representative images of (A) Recellularised scaffolds (n = 3) following 7 day, and (B) Recellularised scaffolds (n = 3) following 14 day culture. Both images indicate scaffold populated with viable cells and only a few cells were dead. Live cells stained green (white arrow) and dead cells stained red (red arrow). Scale bars are at 300 µm.

5.4.3 Recellularisation of rat scaffolds using DPSCs:

5.4.3.1 Histological evaluation of the recellularised rat scaffolds:

Serial sections of the recellularised rat scaffolds stained with H&E (Figure 5.9 and Figure 5.10) were assessed to determine the ability of DPSCs to attach and migrate within the decellularised scaffold.

Following 7 and 14 days culture, DPSCs were attached to the outer surface and also migrated between the collagen fibres within the scaffold. Under the light microscope they appeared elongated, adherent and spindle-shaped morphology. Furthermore, as time elapsed, there was an apparent change in the scaffold shape from a longitudinal (7 days, Figure 5.9; A) to a contracted circular shape (14 days, Figure 5.10; A).

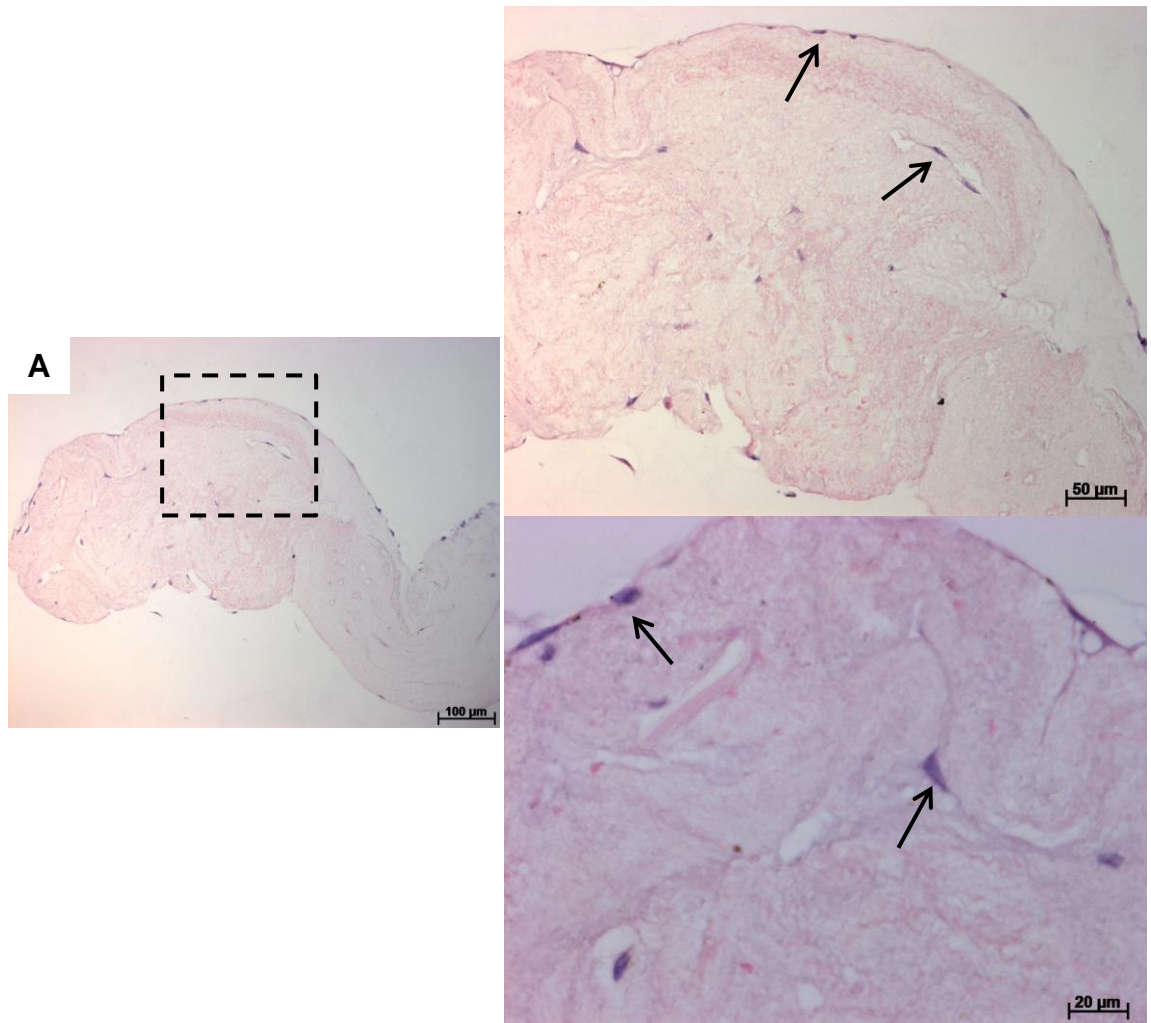


Figure 5.9: Representative images of H&E stained recellularised rat scaffolds seeded with DPSCs following 7 days culture viewed under the light microscope. (A) Seeded rat scaffold with apparent cell attachment and migration. Scale bar at 100 µm. Right side images represent magnification of area delineated with dashed black rectangle, with scales bars of 50 µm and 20 µm. Nuclei stained blue (black arrow) and ECM stained pink.

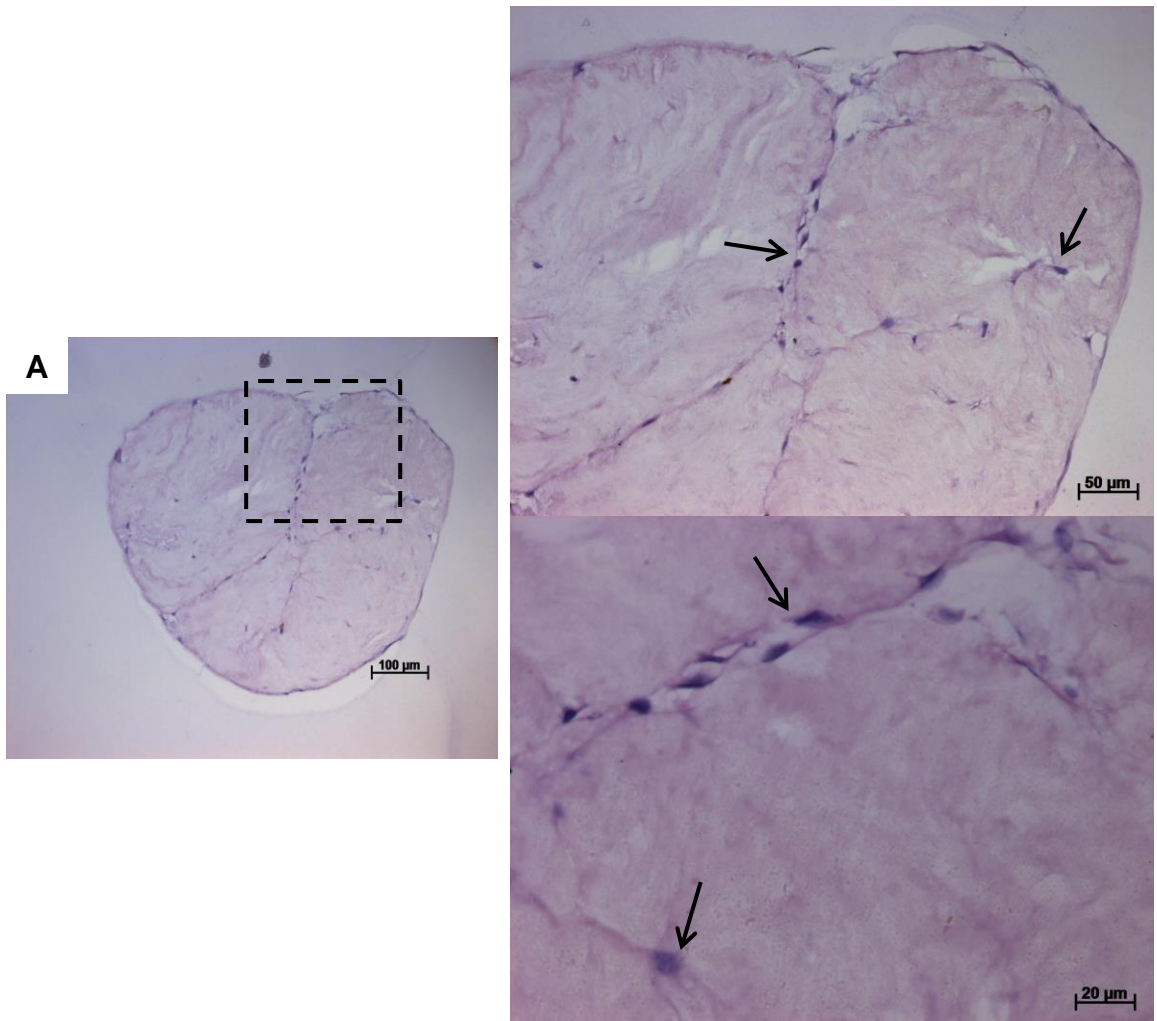


Figure 5.10: Representative images of H&E stained recellularised rat scaffolds seeded with DPSCs following 14 days culture viewed under the light microscope. (A) Seeded rat scaffold with apparent cell attachment and migration. Scale bar at 100 µm. Right side images represent magnification of area delineated with dashed black rectangle, with scales bars of 50 µm and 20 µm. Nuclei stained blue (black arrow) and ECM stained pink.

5.4.3.2 Immunohistochemical evaluation of the recellularised rat

scaffolds:

Antibody labelling was performed in order to assess the ability of the seeded stem cells to express odontoblastic markers and specific cellular cytoskeleton components. Odontoblastic markers evaluated in this work included DSPP, DMP-1, and ALP. To further assess the potential of the seeded DPSCs to differentiate and express various markers, a panel of genes were investigated. These included vimentin, nestin, α -SMA, VEGF-A, and VEGFR-2 genes.

5.4.3.2.1 DSPP:

Images of recellularised and non-seeded rat scaffolds labelled with anti-DSPP antibodies are shown in Figure 5.11. The seeded DPSCs were stained dark brown, indicating a strong positive cellular immunoreactivity to DSPP antigens (Figure 5.11 A and B). DSPP positive cells were evident in the cells scattered throughout the scaffold cultured for 7 and 14 days. In contrast, negative immunoreactivity was consistently evident in all non-seeded scaffolds (Figure 5.11 C). Also, the isotype control staining was negative (Figure 5.11 D).

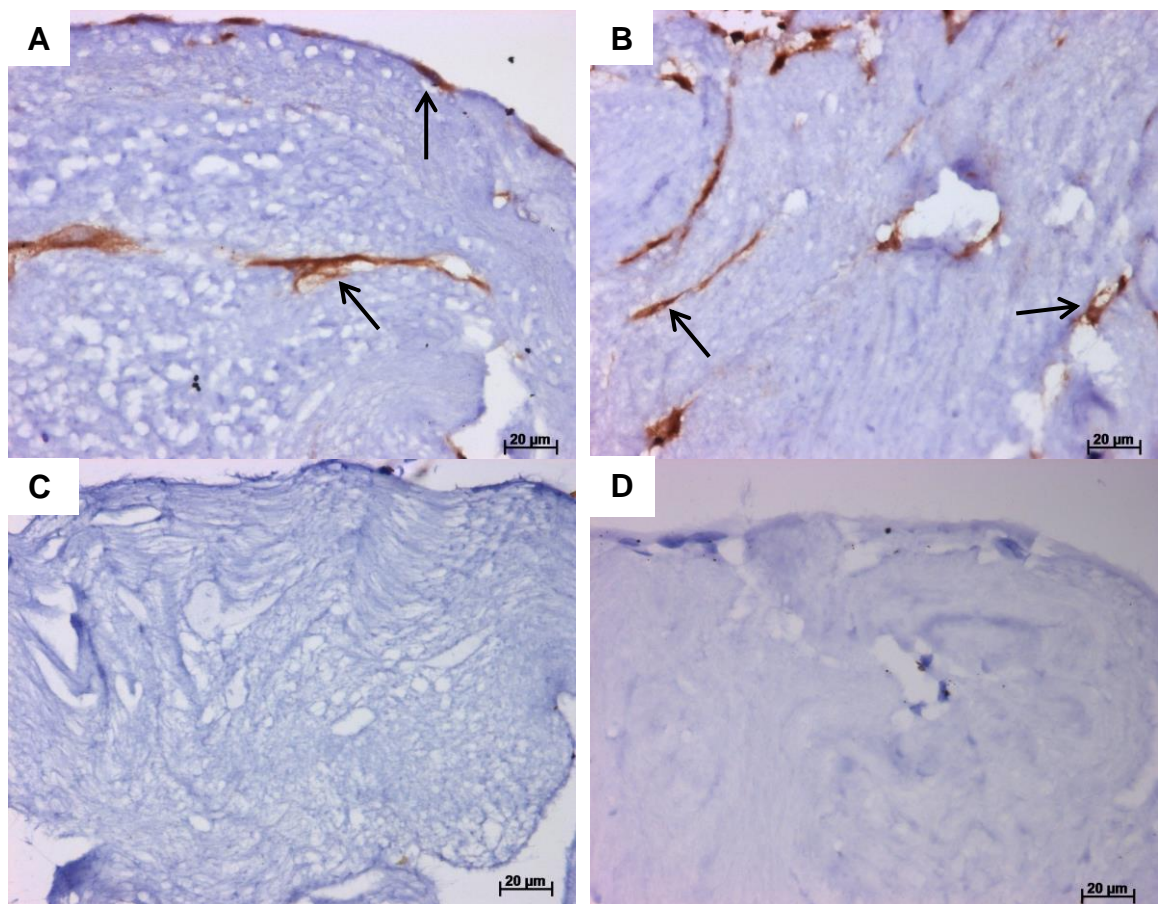


Figure 5.11: Representative images of recellularised rat scaffolds labelled with DSPP antigen and viewed under the light microscope. DSPP positive cells seen following (A) 7 and (B) 14 days culture, (C) Non-seeded scaffolds with negative expression and (D) Isotype controls with negative expression. DSPP positive cells stained brown (black arrow) and ECM stained purple. Scale bars are at 20 µm.

5.4.3.2.2 DMP-1:

Images of recellularised and non-seeded rat scaffolds labelled with anti-DMP-1 antibodies are shown in Figure 5.12. At 7 days, very few light brown stained cells were identified, indicating a weak positive immunoreactivity to DMP-1 antigens (Figure 5.12 A). Following 14 days culture, more cells were positively stained with a moderate intensity (Figure 5.12 B). A negative immunoreactivity was consistently evident in all non-seeded scaffolds (Figure 5.12 C). Also, the isotype control staining was negative (Figure 5.12 D).

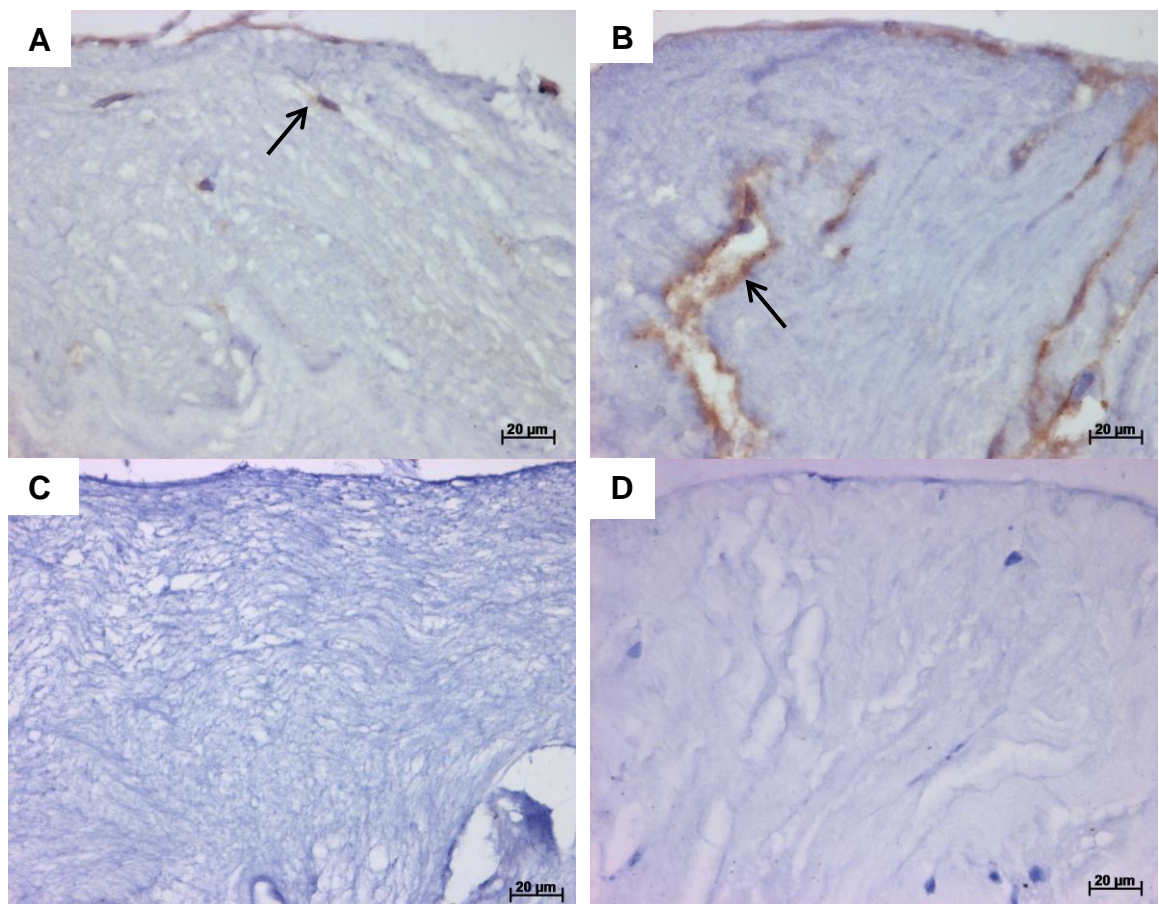


Figure 5.12: Representative images of recellularised rat scaffolds labelled with DMP-1 antigen and viewed under the light microscope. DMP-1 positive cells weakly expressed following (A) 7 and (B) 14 days culture, (C) Non-seeded scaffolds with negative expression and (D) Isotype controls with negative expression. DMP-1 positive cells stained brown (black arrow) and ECM stained purple. Scale bars are at 20 µm.

5.4.3.2.3 ALP:

Images of recellularised and non-seeded rat scaffolds labelled with anti-ALP antibodies are shown in Figure 5.13. At 7 days, the seeded DPSCs were not stained brown, indicating negative immunoreactivity to ALP antigens (Figure 5.13 A). Following 14 days culture, however, some ALP positive cells, although lightly stained, were observed within the scaffold (Figure 5.13 B). In contrast, negative immunoreactivity was consistently evident in all non-seeded scaffolds (Figure 5.13 C). Also, the isotype control staining was negative (Figure 5.13 D).

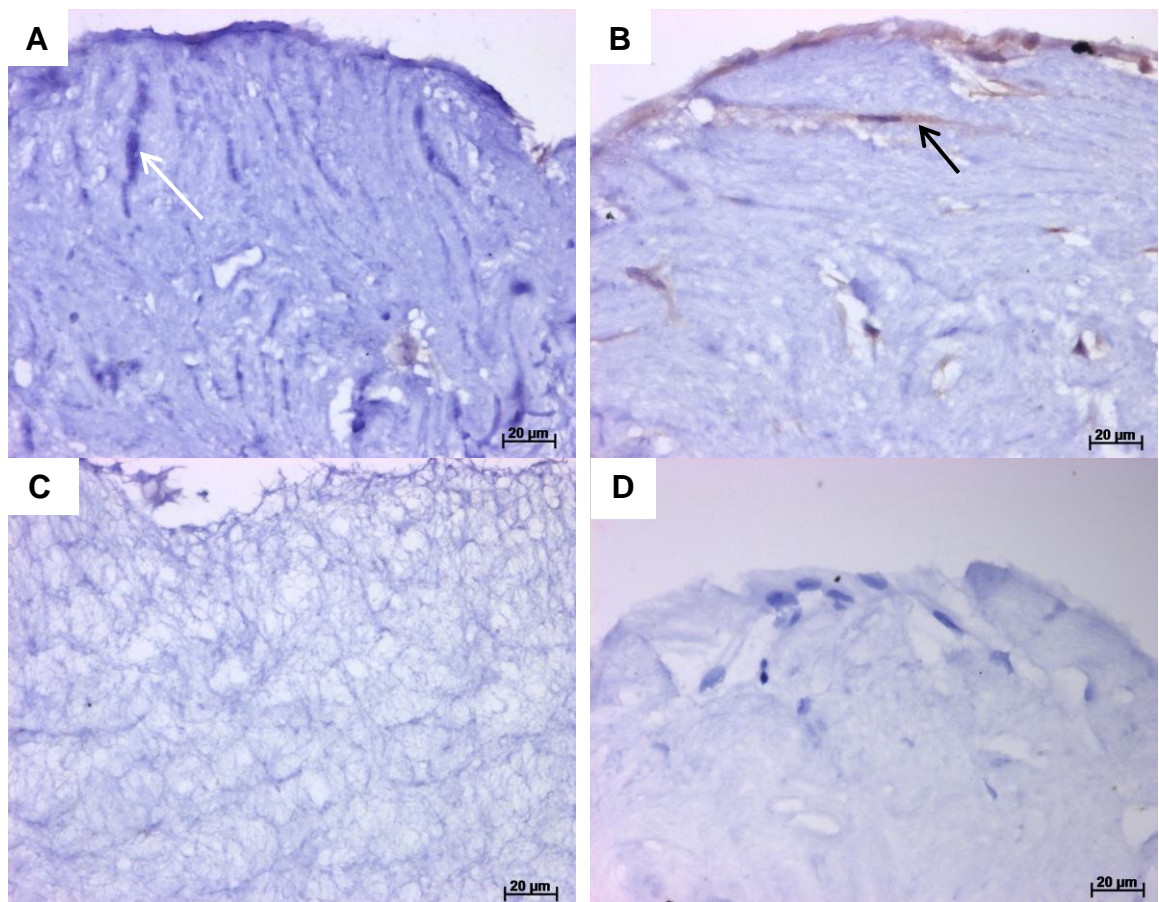


Figure 5.13: Representative images of recellularised rat scaffolds labelled with ALP antigen and viewed under the light microscope. (A) Negative expression to ALP seen at 7 days culture, (B) ALP positive cells weakly expressed at 14 days culture, (C) Non-seeded scaffold with negative expression and (D) Isotype controls with negative expression. ALP positive cells stained brown (black arrow), unstained DPSCs (white arrow) and ECM stained purple. Scale bars are at 20 µm.

5.4.3.2.4 Vimentin:

Images of recellularised and non-seeded rat scaffolds labelled with anti-vimentin antibodies are shown in Figure 5.14. The seeded DPSCs were stained brown, indicating a strong positive immunoreactivity to vimentin antigens. Vimentin positive cells were scattered throughout the scaffold cultured for 7 and 14 days (Figure 5.14 A and B). In contrast, negative immunoreactivity was consistently evident in all the non-seeded scaffolds (Figure 5.14 C). Also, the isotype control staining was negative (Figure 5.14 D).

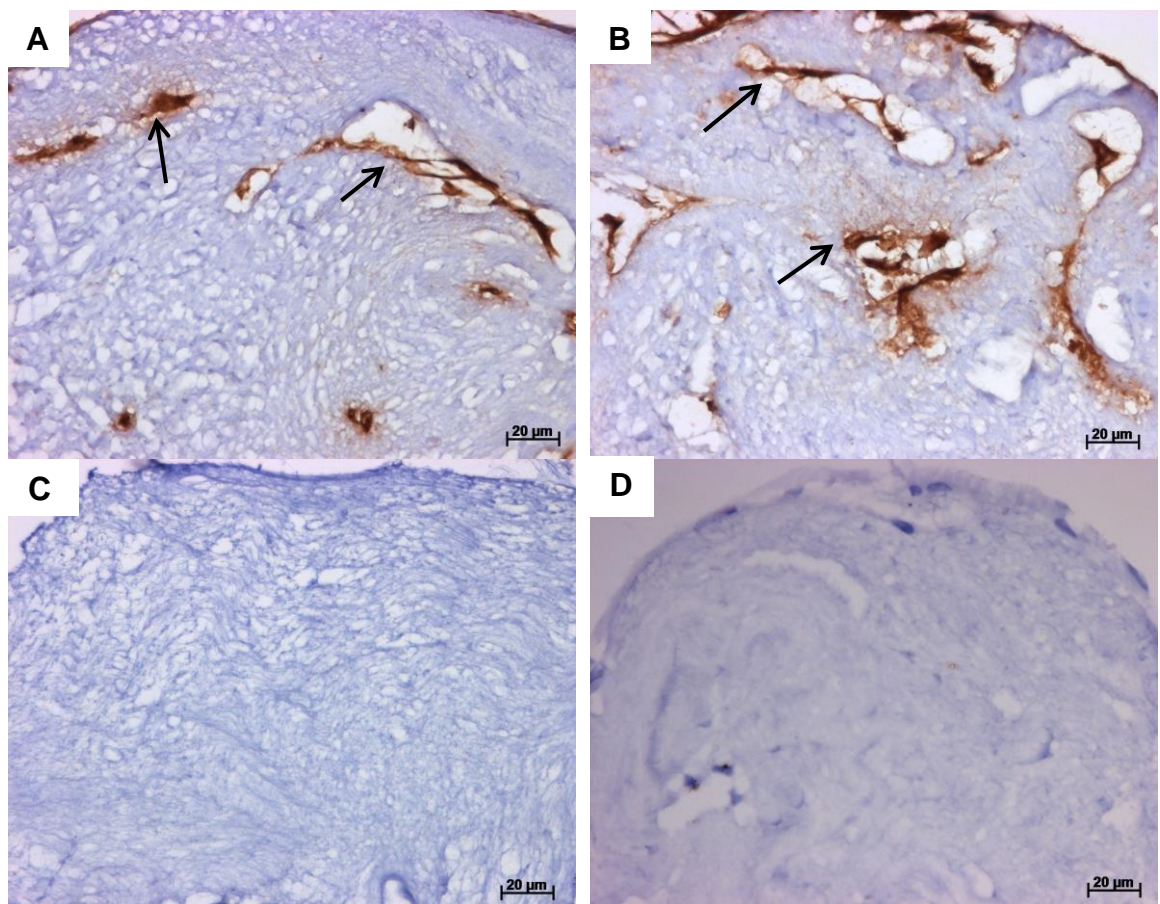


Figure 5.14: Representative images of recellularised rat scaffolds labelled with vimentin antigen and viewed under the light microscope. Vimentin positive cells seen following (A) 7 and (B) 14 days culture, (C) Non-seeded scaffolds with negative expression and (D) Isotype controls with negative expression. Vimentin positive cells stained brown (black arrow) and ECM stained purple. Scale bars are at 20 µm.

5.4.3.2.5 Nestin:

Images of recellularised and non-seeded rat scaffolds labelled with anti-nestin antibodies are shown in Figure 5.15. The seeded DPSCs were stained brown, indicating a positive immunoreactivity to nestin antigens. Nestin positive cells were evident in the majority of cells scattered throughout the scaffold cultured for 7 and 14 days (Figure 5.15 A and B). In contrast, negative immunoreactivity was consistently evident in all non-seeded rat scaffolds (Figure 5.15 C). Also, the isotype control staining was negative (Figure 5.15 D).

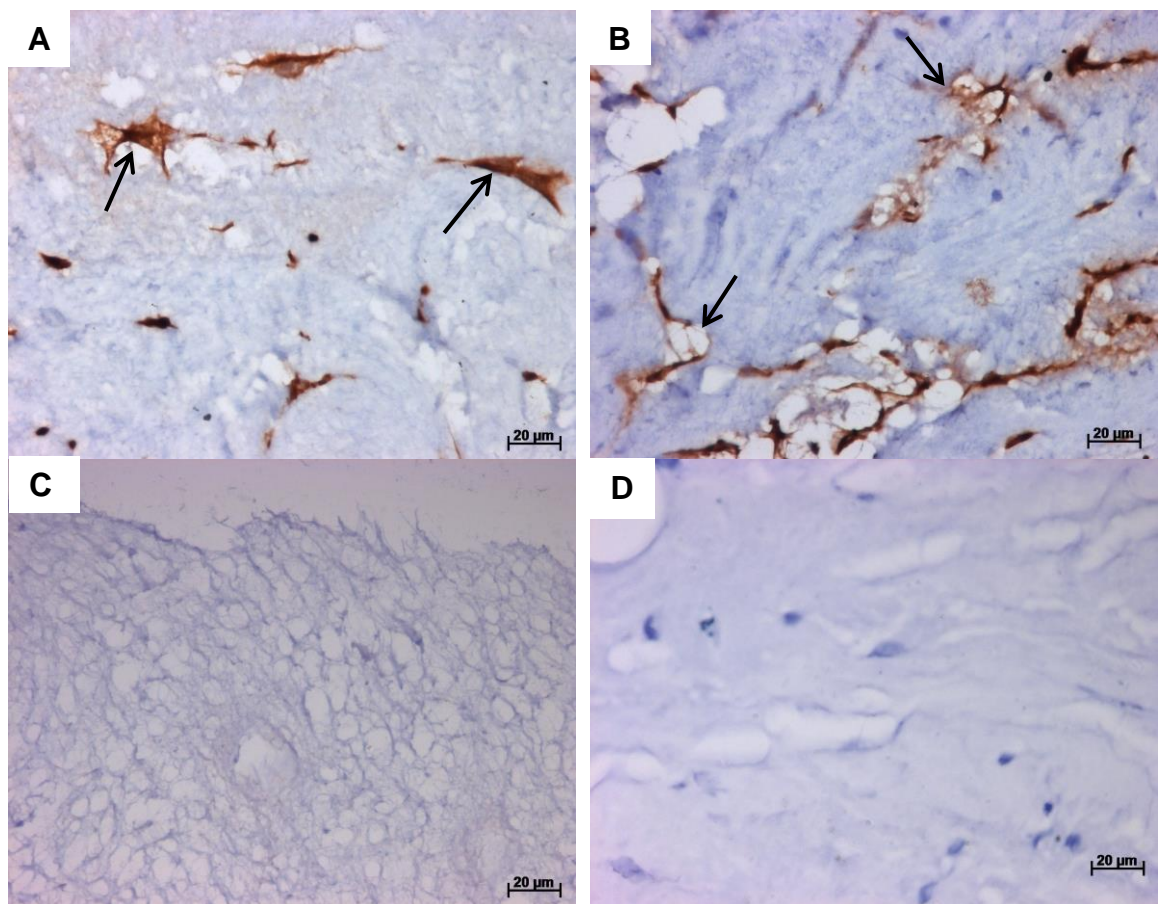


Figure 5.15: Representative images of recellularised rat scaffolds labelled with nestin antigen and viewed under the light microscope. Nestin positive cells seen following (A) 7 and (B) 14 days culture, (C) Non-seeded scaffolds with negative expression and (D) Isotype controls with negative expression. Nestin positive cells stained brown (black arrow) and ECM stained purple. Scale bars are at 20 µm.

5.4.3.2.6 Alpha-SMA:

Images of recellularised and non-seeded rat scaffolds labelled with anti- α -SMA antibodies are shown in Figure 5.16. At 7 days, the seeded DPSCs were not stained brown, indicating a negative immunoreactivity to α -SMA antigens (Figure 5.16 A). Following 14 days culture, however, some α -SMA positive cells, stained brown, were observed within the scaffold (Figure 5.16 B). A negative immunoreactivity was consistently evident in all non-seeded scaffolds (Figure 5.16 C). Also, the isotype control staining was negative (Figure 5.16 D).

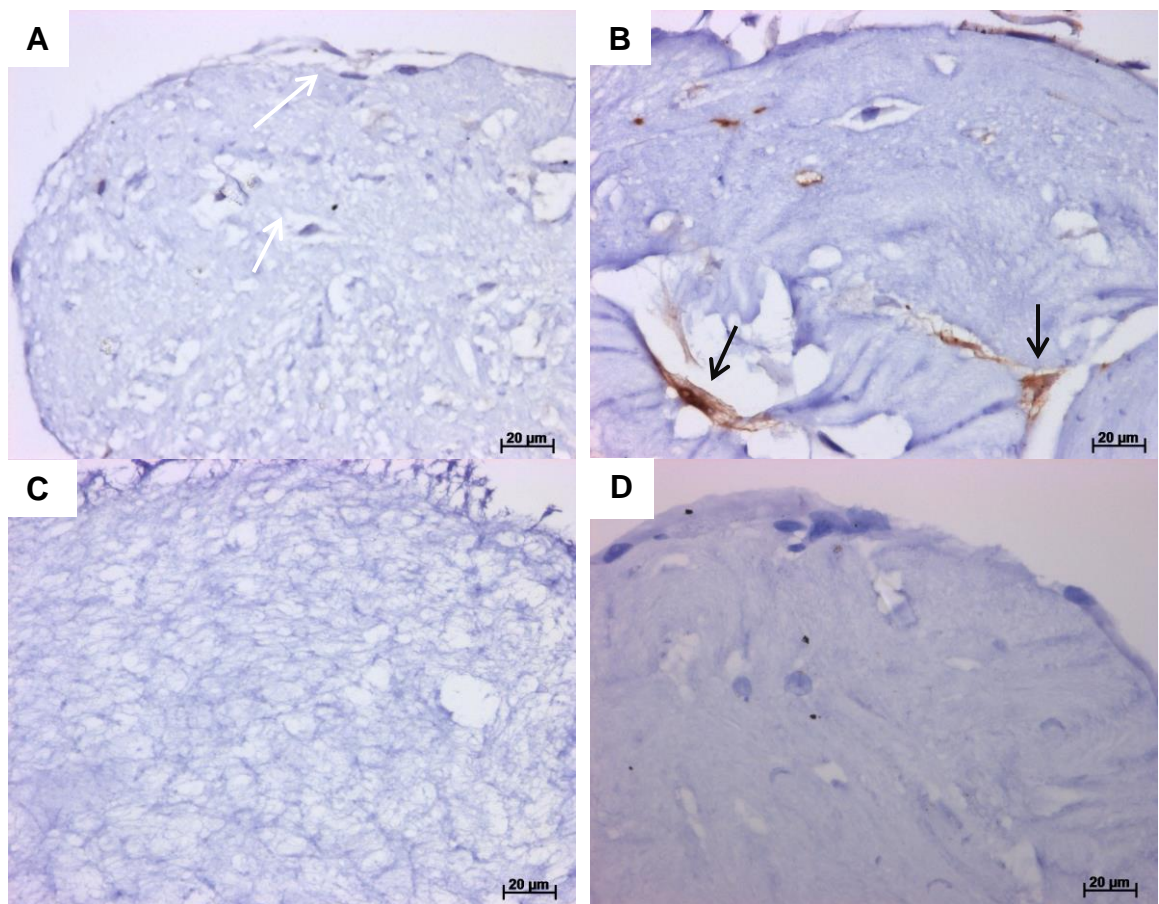


Figure 5.16: Representative images of recellularised rat scaffolds labelled with α -SMA antigen and viewed under the light microscope. (A) Negative expression to α -SMA seen at 7 days, (B) α -SMA positive cells seen at 14 days culture, (C) Non-seeded scaffolds with negative expression and (D) Isotype controls with negative expression. α -SMA positive cells stained brown (black arrow), unstained DPSCs (white arrow) and ECM stained purple. Scale bars are at 20 μ m.

5.4.3.2.7 VEGF-A and VEGFR-2:

Images of recellularised and non-seeded rat scaffolds labelled with anti-VEGF-A and anti-VEGFR-2 antibodies are shown in Figure 5.17 and Figure 5.18, respectively. The seeded DPSCs were stained brown, indicating a positive immunoreactivity to VEGF-A and VEGFR-2 antigens. VEGF-A and VEGFR-2 positive cells were evident in the majority of cells, cell body and process, scattered throughout the scaffold cultured for 7 and 14 days (Figure 5.17 A, B and Figure 5.18 A, B). In contrast, negative immunoreactivity was consistently evident in all non-seeded scaffolds (Figure 5.17 C and Figure 5.18 C). Also, the isotype control staining was negative (Figure 5.17 D and Figure 5.18 D).

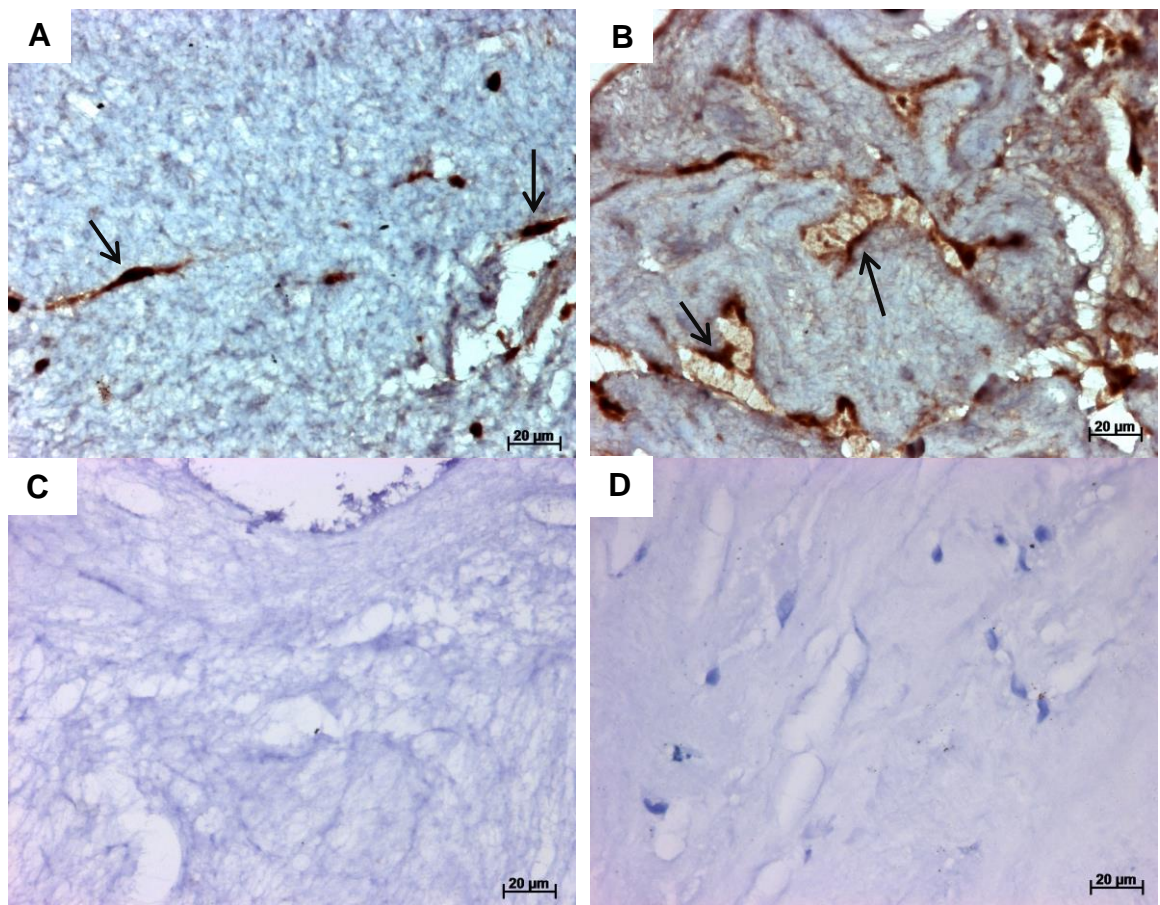


Figure 5.17: Representative images of recellularised rat scaffolds labelled with VEGF-A antigen and viewed under the light microscope. VEGF-A positive cells seen following (A) 7 and (B) 14 days culture, (C) Non-seeded scaffolds with negative expression, (D) Isotype controls with negative expression. VEGF-A positive cells stained brown (black arrow) and ECM stained purple. Scale bars are at 20 µm.

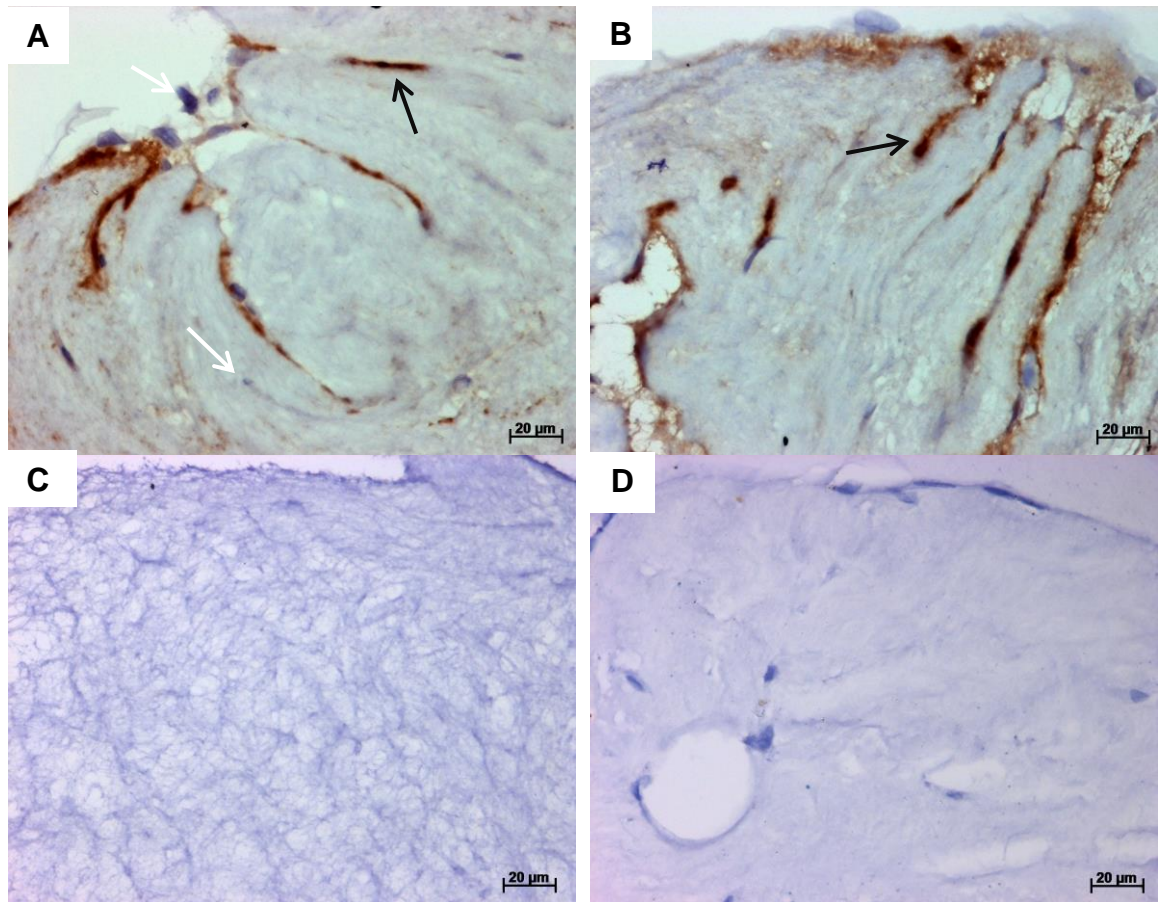


Figure 5.18: Representative images of recellularised rat scaffolds labelled with VEGFR-2 antigen and viewed under the light microscope. VEGFR-2 positive cells seen following (A) 7 and (B) 14 days culture, (C) Non-seeded scaffolds with negative expression, (D) Isotype controls with negative expression. VEGFR-2 positive cells stained brown (black arrow), unstained DPSCs (white arrow) and ECM stained purple. Scale bars are at 20 µm.

5.5 Discussion:

Results of previous chapters described the development of a decellularised pulp scaffold derived from both rat and human dental pulp tissues. The use of a mild decellularisation protocol that can produce a biocompatible ECM scaffold able to support cell attachment and proliferation is desirable. To achieve tissue decellularisation, low concentration detergents are incorporated within the modified protocol to achieve efficient cellular removal.

Sodium dodecyl sulphate (SDS), an ionic detergent, is widely used within various decellularisation protocols for efficient cellular and nuclear membrane solubilisation (Gilbert et al., 2006; Crapo et al., 2011). Despite efficient cellular removal, concerns regarding residual SDS toxicity and tissue damage are reported when using concentrations at or above 1 % (w/v) SDS (Bodnar et al., 1986; Courtman et al., 1994). Indeed, residual detergents that remain within the scaffold following decellularisation could be cytotoxic and ultimately inhibit scaffold function and recellularisation (Rieder et al., 2004).

No cytotoxicity was apparent following the use of 0.03 % (w/v) SDS for decellularisation of rat and human pulp tissues. Contact cytotoxicity results indicated a non-toxic tissue with cell growth surrounding and in direct contact with the decellularised tissues. Extract cytotoxicity assays also found no reduction in cellular viability following incubation in decellularised tissue extracts in comparison to the negative controls. These results are in line with other biocompatible studies including decellularised human pericardial matrix (Mirsadraee et al., 2006), human amniotic membrane (Wilshaw et al., 2008),

porcine medial meniscus (Stapleton et al., 2008), human arteries (Wilshaw et al., 2012), and porcine pulmonary valves (Luo et al., 2014). The lack of tissue toxicity observed has been linked to the low concentration of SDS, the use of extensive washing cycles and mechanical agitation (Wilshaw et al., 2012). Indeed, extensive washing with agitation between decellularisation steps and at the end of treatment has been advocated by several authors to wash out residual chemicals and cellular remnants (Stapleton et al., 2008; Luo et al., 2014).

As the decellularised dental pulp revealed a biocompatible scaffold, it was deemed necessary to investigate if the decellularised dental pulp offers an appropriate environment to support the growth and differentiation of DPSCs. The Live/Dead[®] assay uses two compounds, calcein-AM and ethidium homodimer, that provide a distinguishing colour between live and dead cells. Calcein-AM is transported across a cell membrane, only entering live cells producing a bright green colour. In contrast, ethidium homodimer is membrane impermeable, only entering dead cells and binds to nucleic acid due to damaged cell membrane producing a bright red colour. Live/Dead[®] staining of the pulp constructs showed that most areas of the decellularised pulp scaffolds were populated with viable cells exhibiting elongated spindle morphology. Dead cells, small round morphology, were present in low numbers within the scaffold.

Notably in this work, the recellularised rat and human scaffolds (SDS-treated pulp tissue) were able to support DPSCs viability and attachment following 14 days culture *in vitro*. This result is in agreement with several other studies demonstrating cell attachment and proliferation on SDS-treated decellularised scaffolds (Wilshaw et al., 2008; Song et al., 2017).

Furthermore, H&E stained serial sections of the recellularised rat scaffolds revealed that DPSCs were attached to the outer surface and migrated within the scaffold. As time elapsed, a decrease in the overall size of the seeded scaffolds was apparent, changing from original tubular shape observed at day 7 to a circular shape at day 14. Contraction of a pulp cell-seeded scaffold has been documented as early as mid-90s when Mooney et al. (1996) utilised cultured human fibroblast cells seeded on a synthetic polyglycolic acid matrix (Mooney et al., 1996). A marked contraction of a collagen-glycosaminoglycan ECM seeded with DPSCs was also reported (Brock et al., 2002). This matrix contraction was reported to be linked to the expression of α -SMA positive dental pulp cells and their ability to contract a collagen based matrix (Brock et al., 2002), which was linked with myofibroblasts contractility activity (Yoshida et al., 2012). In the light of the above reported studies, the expression of α -SMA by DPSCs cultured on rat decellularised dental pulp scaffolds demonstrated herein this work, more likely, contributed to the contraction of the scaffold. Further work is needed to shed light on this observation and its long term effect on pulp tissue engineering.

The differentiation of DPSCs was characterised based on the expression of odontoblastic markers, cytoskeleton proteins, and growth factors. In this work, immunohistochemical labelling of recellularised rat scaffolds revealed high differentiation ability in standard culture media. DPSCs seeded within the decellularised scaffolds expressed several putative markers of odontoblastic differentiation including DSPP, DMP-1, and ALP. These markers, although non-specific, are commonly used by several researchers to identify cell differentiation towards odontoblastic lineage (Cordeiro et al., 2008; Prescott et al., 2008; Huang et al., 2010; Rosa et al., 2013). The present study observations revealed ALP positive cells, weakly stained, by day 14 and a negative expression at day 7. Negative ALP expression has been linked to the developmental stage of odontoblasts' or to the ambiguous location of the enzyme (Yoshiki and Kurahashi, 1971).

Furthermore, cytoskeleton proteins, vimentin and nestin positive cells were strongly expressed following recellularisation. Although vimentin is not considered as a pulp tissue specific protein, it has been suggested as a dental pulp quality standard protein for characterisation of pulp regeneration (Murakami et al., 2012). Vimentin is expressed by neuronal precursor cells and has been linked to neurogenesis (neuronal differentiation) (Yabe et al., 2003). In a study by Arthur et al. (2008) DPSCs expressed nestin following incubation in specific neuronal inductive medium. They further concluded, that exposure of DPSCs to the correct environment cues was crucial for their ultimate differentiation into active neurons (Arthur et al., 2008).

Growth factors are synthesised by cells and, when binding occurs to their specific receptors, consequently guide cell behaviour (Matsushita et al., 2000; Grando Mattuella et al., 2007). Vascular endothelium growth factor and its receptor are known to be potent regulators of angiogenesis within the dental pulp tissue, which subsequently leads to sprouting of blood vessels (Ferrara, 2004; Grando Mattuella et al., 2007; Saghiri et al., 2015). Importantly, the development of a vascularised pulp construct is required for the maintenance of a vital engineered tissue (Cordeiro et al., 2008). In this work, a positive cellular immunoreactivity to VEGF-A and VEGFR-2 antigens was evident following recellularisation.

In summary, this chapter described the development of a non-cytotoxic scaffold that is able to support human DPSCs viability and attachment following *in vitro* culture. Although the potential of the scaffold to support DPSCs growth and differentiation in this work is based on qualitative analysis, it was clearly evident that the seeded DPSCs co-expressed several genes following incubation in standard cell culture medium with no added specific inductive reagents.

Chapter 6

General discussion, future work, and conclusions

6.1 General discussion:

The dental pulp is a specialised loose connective tissue surrounded by a hard dentine structure. The function of a vital dental pulp contributes to tooth function, vitality, sensibility, and nutrition. Dental pulp also offers protection with the ability to respond to injury through repair or regeneration (Yu and Abbott, 2007; Pashley et al., 2008; Kumar, 2014). Loss of vitality (necrosis) of the dental pulp halts normal tooth development in young patients with incomplete root formation (immature teeth). Clinically these teeth suffer from a reduced crown to root ratio and thin dentinal walls, hence highly liable to fracture (Cvek, 1992). Despite improved clinical management of non-vital immature permanent teeth throughout the years, the long term prognosis remains compromised. Unfortunately, the gold standard MTA apical plug treatment does not contribute to any further root development nor does it restore the pulp tissue function (Torabinejad and Abu-Tahun, 2010; Diogenes et al., 2016).

More recently, the use of regenerative endodontic procedures for the treatment of non-vital immature permanent teeth has increased. The main fundamental step of these procedures is the cell influx within the canal following evoked periapical bleeding. Indeed, the preapical area contains stem cells of a high regenerative ability (Sonoyama et al., 2006; Sonoyama et al., 2008; Lovelace et al., 2011). Despite the available stem cells, regenerative endodontic

procedures in their current format have been associated with unpredictable results and non-specific tissue formation (Sloan and Smith, 2007; Wang et al., 2010b; Shimizu et al., 2013; Nosrat et al., 2014; European Society of Endodontology, 2016). The main reason, thought to be, behind the formation of bone- and cementum-like tissue is the non-specific surrounding environment caused by the formed blood clot acting as a temporary scaffold. In line with the above, it is well known that cell growth and differentiation is strongly influenced by the surrounding microenvironment (Martinez et al., 2000; Nakashima et al., 2013).

Therefore, to address these limitations, researchers have focused on combining the principles of tissue engineering within the clinical practice of regenerative endodontics. Of these principles, scaffold development is subject to intense research. A recent systematic review highlighted a large heterogeneity of results on several tested dental scaffold materials (Conde et al., 2015; Tong et al., 2017), with the need to develop a new scaffold material with close resemblance to the natural pulp matrix (Dissanayaka et al., 2014; Conde et al., 2015). More recently, the use of biological scaffolds composed of an acellular ECM derived through tissue decellularisation is intensively researched in regenerative medicine (Gilbert et al., 2006; Crapo et al., 2011; Song and Ott, 2011). Ideally, the produced decellularised scaffold is composed of natural ECM components with preserved three-dimensional tissue architecture (Badylak et al., 2009; Wilshaw et al., 2012). The ECM is regarded as a vital component of all tissues and, possibly, the ideal scaffold for tissue regeneration (Badylak, 2002; Badylak, 2007; Ma, 2008). Therefore, the concept of a

decellularised pulp tissue scaffold, with preserved structural components, is an attractive alternative material that might enhance the clinical outcome (Nazzal and Duggal, 2017). The overall aim of this research was to assess the feasibility of decellularising rat and human dental pulp tissues using a mild decellularisation method to produce a biocompatible acellular ECM scaffold which retains the structural and biochemical components of native dental pulp.

In this work, decellularisation of rat and human pulp tissues for future scaffold development in regenerative endodontics was investigated. Rat pulp tissues were used for proof of concept prior to the assessment of human pulp tissues due mainly to the limited availability of extracted sound human permanent teeth.

The use of laboratory rats is inevitable part of biomedical research applications, with over 80 % of published studies performed on rodents (Sengupta, 2013). The laboratory rats are considered to be particularly useful in: cardiovascular research, experimental oncology, immunology, toxicology and dental research (Sengupta, 2013). Indeed, multiple researchers studying the pulp tissue have been performed on rat incisors and molars. These studies include, but not limited to, pulp tissue response following pulp capping (Hu et al., 1998; Lovschall et al., 2001), bleaching application (Cintra et al., 2013), chronic exposure to sodium fluoride (Centeno et al., 2015) and to evaluate treatment options in necrotic immature teeth (Scarparo et al., 2011). Rat pulp tissues share similar histological structures to human dental pulp tissue and its structural composition has been widely studied (Linde, 1973; Cournil et al., 1979; van Amerongen et al., 1983). The use of rat tissue also allows for future

ex vivo and *in vivo* animal transplantation work to be conducted on the same species, hence reducing variables and cross-species reactions.

Decellularisation within the dental field has recently been attempted, with most studies published during the course of this work. These studies included decellularisation of porcine tooth buds (Traphagen et al., 2012), miniature swine pulp tissues (Chen et al., 2015) and human tooth slices (Song et al., 2017) using various decellularisation protocols. Although, in general terms, the above decellularisation protocols varied, the use of sodium dodecyl sulphate (SDS) and Triton X-100 as a detergent step was a common step in these protocols, however, with different concentrations, number of cycles, temperature, and duration of exposure.

Chen et al. (2015) developed an acellular matrix with preservation of native pulp shape using 1 % (w/v) SDS and 1 % (w/v) Triton X-100. In contrast, Song et al. (2017) reported incomplete decellularisation following one cycle of 1 % (w/v) SDS and one cycle of 1 % (w/v) Triton X-100. These authors achieved complete decellularisation of the pulp tissue within tooth slices through increasing the number of SDS cycles to three cycles.

Despite the above methods resulting in complete decellularisation of the dental tissues, harsh decellularisation protocols (mainly utilising chemicals of high concentration, multiple cycles, and long exposure duration) are more likely to alter the ECM. Consequently, this may negatively affect the ECM properties, cellular activity and long term outcome. SDS, an ionic detergent, at a concentration of 1 % (w/v), has been found to cause structural damage to

treated porcine valves (Bodnar et al., 1986). Gratzner et al. (2006) also reported alteration to matrix structure and reduced GAGs content following use of 1 % SDS to decellularise bone–anterior cruciate ligament. Furthermore, the use of Triton X-100, a non-ionic detergent, was linked to major loss of GAGs content in porcine aortic heart valves (Liao et al., 2008). Therefore, a low concentration detergent based decellularisation protocol utilising multiple gentle steps is of clinical interest.

The protocol used in this work was previously described by Wilshaw et al. (2006) and involved cell membrane lysis using hypotonic Tris buffer, solubilisation of cytoplasmic and nuclear components using a single detergent cycle of 0.03 % (w/v) SDS in a hypotonic buffer, followed by removal of cellular material using a nuclease treatment. Protease inhibitors were added to various steps of the protocol, to assist matrix preservation. Several washing steps with agitation were also performed to ensure sufficient removal of residual cellular material and reagents used. The choice of using this protocol was, therefore, based on the lower concentrations of SDS used with no incorporation of Triton X-100. These authors were able to successfully decellularise human amniotic membrane (Wilshaw et al., 2006; Wilshaw et al., 2008). Histologically the amniotic membrane consists of a single epithelial layer and a thick basement membrane. In similarity with the pulp matrix, the ECM of the amniotic basement membrane is composed predominantly of collagen fibre bundles (types I and III) and non-collagen proteoglycans and glycoproteins, including fibronectin and laminin (Parry and Strauss, 1998; Niknejad et al., 2008). The initial work of the present study in developing this protocol for use in decellularisation of human

dental pulp tissues showed incomplete decellularisation of the pulp tissue. H&E staining revealed an acellular matrix, however, residual cellular materials were detected using more sensitive and specific staining methods, DAPI staining. Therefore to enhance tissue decellularisation without the addition of reagents or increasing exposure time/temperature (Burk et al., 2014; Fu et al., 2014; Keane et al., 2015), freeze-thaw cycles were incorporated at the start of treatment (experiment 2). The temperature change, following freeze-thaw, leads to the formation of ice crystals opening up the structural matrix, consequently enhances tissue permeability and the diffusion of decellularisation solutions (Gilbert et al., 2006; Crapo et al., 2011; Wilshaw et al., 2012). In line with the above, several decellularisation protocols that utilise freeze-thaw cycles and detergents have been successfully performed on various tissues including medial meniscus (Stapleton et al., 2008), femoral arteries (Wilshaw et al., 2012), and pulmonary valves (Luo et al., 2014).

Following the incorporation of freeze-thaw cycles into the Wilshaw protocol, results of experiment 2 showed complete decellularisation of both rat and human dental pulp tissues. H&E staining revealed complete decellularisation with architectural preservation of the pulpal ECM zones, including sub-odontoblastic and pulp core zone with retained vascular channels. Furthermore, no nuclear material was visible following nuclear specific DAPI staining. Additionally, further evaluation of the residual DNA content within the decellularised scaffold is of utmost importance and a commonly used assessment method by several researchers (Mirsadraee et al., 2006; Kheir et al., 2011; Traphagen et al., 2012; Wilshaw et al., 2012; Yoeruek et al., 2012;

Song et al., 2017). Notably, residual DNA material within a decellularised matrix could consequently elicit a host inflammatory response and inhibit future tissue remodelling (Brown et al., 2009; Keane et al., 2015). In this work, DNA quantification analysis confirmed the qualitative results and revealed significant reduction, greater than 98 %, in DNA content levels relative to the control tissues. These results are in line with several previous studies which reported a reduction of greater than 96 % DNA content following tissue decellularisation (Wilshaw et al., 2012; Luo et al., 2014; Song et al., 2017).

The residual DNA content was approximately $23.00 \pm 1.430 \text{ ng.mg}^{-1}$ in rat and $19.56 \pm 1.280 \text{ ng.mg}^{-1}$ in human tissues. These results are well below the benchmark criteria for the maximum amount (50 ng.mg^{-1}) of DNA content in sufficiently decellularised tissues (Crapo et al., 2011; Kawecki et al., 2017), however, there was no given evidence behind the proposed criteria and the selected maximum threshold. Furthermore, the United States Federal Drug Administration, to date, does not provide any regulatory limits to the amount of DNA material present in biological scaffolds (Gilbert et al., 2009). To further understand the DNA content of biological scaffolds, Gilbert et al. (2009) analysed the DNA content of several commercially available biological scaffolds which were reported to be clinically successful. Interesting, their results indicated trace amounts of DNA material in most tested scaffolds. However, they further explained that the presence of small amounts of residual DNA material was unlikely to cause any unwanted pro-inflammatory host response (Gilbert et al., 2009).

Major histocompatibility complex class II molecules evaluation of the decellularised scaffold was also considered necessary. These molecules are expressed by immune cells (dendritic cells, monocytes and macrophages) that are commonly present throughout the pulp tissue (Jontell et al., 1987; Ohshima et al., 1999). This group of cells serve as antigen-presenting cells and participate in initial tissue recognition response (Jontell et al., 1987; Ohshima et al., 1999). In this work, immunohistochemical labelling against major histocompatibility complex class II molecules revealed negative expression following decellularisation.

Preservation of the ECM structure and composition was essential in the development of the decellularised pulp tissue scaffold. Histologically, the pulp matrix is composed of a complex mixture of collagen and non-collagenous proteins that contribute to several tissue functions. Collagen fibres, the main structural component, contribute to the development and maintenance of the pulp matrix (Hillmann and Geurtsen, 1997). GAG molecules provide crucial functions in regulating metabolism, water movement, and attachment sites for growth factors and cytokines (Linde, 1973; Badylak, 2002). Fibronectin adhesive proteins are known to mediate several cellular and matrix interactions (Hynes, 1985), including the attachments of cellular and various extracellular components (Linde et al., 1982). Laminin proteins are also implicated in tissue development and regeneration (Aumailley et al., 2005; Fried et al., 2005), odontoblast differentiation (Yuasa et al., 2004), and migration of dental pulp stem cells (Howard et al., 2010).

Preservation of the collagen structure was assessed qualitatively using Picrosirius red staining method, SEM imaging, and specific immunolabelling detection. Picrosirius red staining viewed under the polarised microscope indicated collagen fibre preservation following decellularisation. Collagen fibre structure, tissue porosity, and interfibrillar space preservation were also confirmed through the use of SEM imaging. Specific antibody labelling against collagen type I and III fibres also revealed fibre preservation, albeit expressing a slightly weak stain in comparison to the native tissues. In contrast, Chen et al. (2015) reported a significant decline in both collagen type I and III fibres following decellularisation of miniature swine dental pulps (Chen et al., 2015). The results of the above study could be a consequence of high SDS concentration used and/or the additional use of Triton X-100. Indeed, structural disruption of the ECM has been reported following the use of Triton X-100 (Gilbert et al., 2006; Crapo et al., 2011), and/or SDS concentrations of 1 % (w/v) SDS (Bodnar et al., 1986; Gratzner et al., 2006).

Additional characterisation of the pulp tissue matrix composition (non-collagen proteins) was assessed qualitatively using specific histological staining methods and immunolabelling detection. Alcian blue staining method is widely used as a specific stain to localise acidic polysaccharides present within the tissue matrix. Results of this work indicated preservation of GAG molecules following decellularisation with no visible difference in staining pattern, in comparison to the control tissues.

Antibody labelling against fibronectin and laminin adhesive proteins indicated preservation following decellularisation, albeit at a lower staining intensity. Preservation of fibronectin and laminin was also reported by Chen et al. (2015) and Traphagen et al. (2012) following decellularisation of miniature swine pulps and porcine tooth buds, respectively. In contrast, reduced expression of fibronectin was reported following the use of three cycles of 1 % (w/v) SDS and 1 % (w/v) Triton X-100 to decellularise tooth root slices (Song et al., 2017).

Subsequently, following efficient decellularisation it was necessary to assess the scaffolds biocompatibility and ability to support cell growth and differentiation. Scaffold disinfection or sterilisation is also essential prior to cell seeding. Incubation in antibiotic (Chen et al., 2015) or peracetic acid (Hodde et al., 2007) solutions are reported as effective initial disinfection steps. Tissue sterilisation through the use of antibiotic solutions had been reported as a successful sterilisation method by Chen et al. (2015) in the decellularisation of swine dental pulps using a combination of 100 U.mL^{-1} penicillin and 100 mg.mL^{-1} streptomycin over 48 hours. However, residues of antibiotics that remain in the decellularised scaffold present a potential regulatory hurdle for future clinical approval. These produced scaffolds would be classified as a drug rather than a clinical biological scaffold (Gilbert et al., 2006; Crapo et al., 2011).

Peracetic acid is known to rapidly penetrate microorganisms causing the release of oxygens and free radicals. This oxidation process leads to the inactivation and destruction of a wide range microorganisms (Pruss et al., 1999). Furthermore, it is regarded as a successful disinfection agent for

collagen-based biological scaffolds (Hodde and Hiles, 2002; Hodde et al., 2007) and in line with several decellularisation protocols of various tissues (Wilshaw et al., 2006; Stapleton et al., 2008; Wilshaw et al., 2008; Kheir et al., 2011; Luo et al., 2014). Therefore, in this work, peracetic acid was used in the final step of the decellularisation process.

The biocompatibility of produced decellularised rat and human scaffolds were assessed using *in vitro* cytotoxicity assays. Although, the appropriate cell type for *in vitro* cytotoxicity assays remains debatable (Murray et al., 2000; Saw et al., 2005), the use of established cell lines (L-929 murine fibroblasts) are commonly used in dental research due to their relatively standard growth, morphology characteristics, and high reproducibility (Hensten-Pettersen, 1988; Torabinejad et al., 1995b; Thonemann et al., 2002; Saw et al., 2005; Ozdemir et al., 2009). Established cell lines are also recommended by the International Organisation for Standardisation and the British Standard Institute for cytotoxicity testing of medical devices (International Organisation for Standardisation, 2008; British Standard Institute, 2009). Therefore, in this work, *in vitro* contact and extract cytotoxicity assessment of the produced scaffolds were assessed using L-929 cell lines. Furthermore, to closely resemble the clinical environment, dental pulp stem cells (DPSCs) were chosen for cell viability assays and recellularisation of the decellularised scaffolds.

Both contact and extract cytotoxicity assays using L-929 fibroblasts demonstrated a non-cytotoxic material with similar rates of cell growth and proliferation in comparison to the relevant controls. Cell viability assay

(Live/Dead[®] staining) also indicated that both rat and human decellularised scaffolds supported DPSCs viability and attachment following 14 days culture. Furthermore, the ability of the produced scaffold to support cell differentiation was also determined. Immunohistochemical labelling of recellularised rat scaffolds revealed high differentiation ability. DPSCs survived and expressed cytoskeleton genes, growth factors, and markers of odontoblastic differentiation.

In this work, the recellularised scaffolds expressed dentine sialophosphoprotein (DSPP), dentine matrix protein-1 (DMP-1), and alkaline phosphatase (ALP) antigens, markers of odontoblastic differentiation, as early as 7 and 14 days in standard culture media. *In vivo* studies by Cavalcanti et al. (2013) and Rosa et al. (2013) assessed the odontoblastic differentiation of stem cells on different potential scaffolds. Their results indicated a positive expression of DSPP and DMP-1 markers at 21 days culture following the use of Puramatrix[™] seeded with DPSCs placed in tooth slice model (Cavalcanti et al., 2013) and Puramatrix[™] seeded with SHED placed in full length root canals (Rosa et al., 2013). Furthermore, human recombinant collagen seeded with SHED and placed in full length root canals resulted in a positive expression for DSPP at 14 days culture, while DMP-1 expression was only evident following 28 days culture (Rosa et al., 2013).

Notably in both above studies, neither seeded scaffolds were able to induce odontoblastic differentiation of stem cells without the surrounding dentine structure. Decellularised pulp tooth slice model performed by Song et al. (2017) also demonstrated the ability of SCAP to survive and express odontoblastic markers, ALP and dentine sialoprotein, following 14 days culture. Indeed, it has

been shown that environmental cues generated by the tooth slice model have a direct impact on DPSCs and SHED differentiation into odontoblastic cell lineages (Cordeiro et al., 2008; Demarco et al., 2010; Sakai et al., 2010). In comparison, this work demonstrated the ability of DPSCs to express markers of odontoblastic differentiation solely within the decellularised ECM. Therefore, it could be hypothesised, that placement of the decellularised ECM in contact with the surrounding dentine structure results in enhanced stem cell differentiation, matrix deposition, and ultimately engineering a pulp-dentine complex with close resemblance to the native tissue.

Immunolabelling of cellular cytoskeleton proteins and growth factors, expressed within the recellularised scaffolds, was also performed, due to their crucial roles in future tissue regeneration. Vimentin, a major intermediate filament protein, regulates several functions including cell signalling, adhesion, and migration (Ivaska et al., 2007). Alpha-smooth muscle actin (α -SMA), a cytoskeletal protein, is positively expressed in various tissues during repair and regeneration (van Beurden et al., 2005), including the dental pulp tissue (Shi and Gronthos, 2003; Yoshida et al., 2012). Alpha-SMA also regulates various cell-cell interactions, including cell proliferation and differentiation (Saunders and D'Amore, 1992). In this work, immunohistochemical analysis revealed a positive cellular expression against vimentin and α -SMA within the recellularised rat scaffolds.

Furthermore, successful pulp-dentine complex regeneration also depends on neurogenesis and angiogenesis. Nestin, a neural progenitor marker, has been identified in DPSCs (Arthur et al., 2008). Positive nestin expression in newly

differentiated and functioning odontoblast cells has been reported in several studies utilising both rodent and human teeth (Terling et al., 1995; Kuratate et al., 2008; Lee et al., 2012). The formation of blood vessels aids transport of oxygen and nutrient and attracts prevascular stem cells to the regenerated site, thereby preventing tissue necrosis (Nakashima et al., 2009; Bronckaers et al., 2013; Saghiri et al., 2015).

Notably, several studies have highlighted the ability of DPSCs to induce angiogenesis and express proangiogenic factors including vascular endothelial growth factor (VEGF) (Matsushita et al., 2000; Nakashima et al., 2009; Bronckaers et al., 2013). VEGF-A and vascular kinase-insert domain containing receptor (VEGFR-2) are potent regulators of angiogenesis within the dental pulp tissue (Ferrara, 2004; Grando Mattuella et al., 2007; Janebodin et al., 2013). They aid the differentiation of DPSCs into endothelial-like cells, subsequently leading to sprouting of blood vessels (Grando Mattuella et al., 2007; Saghiri et al., 2015). Immunolabelling results of this work also revealed a positive cellular expression against nestin, VEGF-A, and VEGFR-2 antigens in standard culture media.

Although results of the regenerative potential of the recellularised scaffolds are derived from qualitative analysis, immunohistochemical labelling, the absence of quantitative data is a limitation in the interpretation of results. The need for quantitative techniques such as Enzyme-linked Immunosorbent Assay (ELISA), western blotting, and reverse-transcription/polymerase-chain-reaction (RT-PCR) are required for further validation of results. Scaffold implantation in

well-established *ex vivo* and *in vivo* clinical models are also necessary to further evaluate and understand the scaffold recellularisation and tissue regeneration ability within environments closely resembling the human body.

6.2 Conclusions:

The data presented in this thesis reports the results of a novel approach in decellularising rat and human dental pulp tissues using a mild single detergent based decellularisation protocol. This data confirmed the feasibility of decellularising both rat and human pulp tissues while preserving dental pulp structural components and adhesive proteins. Using this protocol, the decellularised scaffolds elicited no apparent cytotoxicity to cell growth and proliferation. The recellularised scaffolds also demonstrated the ability to support dental pulp stem cells viability and differentiation, with a positive cellular expression against odontoblastic markers, cytoskeleton proteins, and growth factors. Overall, the results of the work presented in this thesis lay the foundation for developing decellularised dental pulp tissue scaffold for use in regenerative endodontics.

6.3 Recommendations for future work and clinical translation:

For future use of decellularised scaffolds in regenerative endodontics, the following aspects should be addressed in developing this scaffold further:

- i. Scaffold structure: The work presented in this thesis involved qualitative assessment of the scaffolds ECM using histological and immunohistochemical methods. Additional quantification assessment of the presented ECM using a range of commercially available biochemical assays including: hydroxyproline, denatured collagen, and glycosaminoglycans assays are required. Further structural assessment including pore size measurements and the investigation of the rheology (viscosity) properties can provide important information. According to Rosa et al. (2013) scaffold viscosity properties may directly impact cell migration and the diffusion of signalling molecules, consequently affecting tissue regeneration.

- ii. Stem cell source: The production of a laboratory made cell seeded scaffold is clinically attractive (cell transplantation approach) (Galler, 2016). Therefore the choice of stem cells is crucial if *in vitro* cell seeding is to be used. Autologous stem cells are immunocompatible and the preferred choice for tissue engineering. However, variability in the isolated cell properties exist which ultimately could affect a reproducible standardised clinical product (Sensebé et al., 2010; Wall et al., 2017).

Allogenic stem cells, on the other hand, are utilised with caution as they carry a risk of immunorejection (Wall et al., 2017). Unfortunately, this approach is afflicted with excessive cost and regulatory hurdles that may hinder future clinical approval (Yuan et al., 2011; Galler et al., 2014; Galler, 2016).

An alternative approach is cell homing, a cell-free approach (Hou et al., 2004; Yuan et al., 2011; Galler et al., 2014; Galler, 2016). Clinically, this involves placement of a cell free scaffold which relies on subsequent endogenous cells repopulating the scaffolds (Hou et al., 2004; Galler, 2016). Cellular migration within the canal space is triggered by inducing apical bleeding, as currently practiced during regenerative endodontic procedures. The biological acellular scaffold, in such a technique, is inserted into the root canal to provide a more controlled environment for cellular activity. This approach has the advantage of reducing cost, as it eliminates laboratory handling of stem cells and therefore provides a less complicated pathway for regulatory approval and clinical translation (Yuan et al., 2011).

- iii. Optimal tissue source: Although a successful decellularised matrix was developed from the dental pulp tissues retrieved from human permanent teeth and rat incisors, limited availability of human permanent tissues and difficult retrieval of rat tissues require addressing in any future work. The use of pulp tissues obtained from exfoliated primary teeth is a possible approach, as these teeth naturally exfoliate. An alternative

direction could involve the use of a larger animal source such as bovine or porcine dental pulp tissues. The main advantages of such sources include better availability, simpler tissue retrieval techniques, larger tissues, and less ethical consideration as such animals are usually sacrificed for dietary requirements. The development of bovine, porcine, and human primary tooth scaffolds are currently being investigated by the Leeds research group.

- iv. Delivery methods: An intact porous scaffold or an injectable hydrogel are the main delivery methods and require further development. The use of an intact porous scaffold that can be directly inserted into the root canal, replicating endodontic treatment with gutta-percha cones or MTA placement is a possible direction. This method, if successful, offers a simple clinical pathway. A second method of delivery, involves transforming the acellular scaffold into an injectable hydrogel. The ability of the injectable material, in its initial liquid state, to closely adapt to the variable root canal shapes is an attractive property (Cavalcanti et al., 2013). It also offers clinicians an easy scaffold delivery method, especially in narrow and curved root canals (Demarco et al., 2011; Rosa et al., 2013).
- v. Scaffold sterilisation: The selection of the appropriate method to sterilise the final decellularised scaffolds without affecting its structural, mechanical and biological properties requires testing (Sun and Leung,

2008). Aseptic production of a human acellular ECM may be acceptable for clinical use, in conjunction with routine medical history and serological screening. The national screening criteria for donor suitability against Human Immunodeficiency Virus types 1 and 2, Hepatitis B, Hepatitis C, Syphilis and Human T-cell Lymphotropic Virus must be assessed. In contrast, scaffolds derived from animal tissues must be sterilised. Terminal sterilisation methods include electron beam irradiation, ethylene oxide gas and gamma E-beam irradiation. Incubation in acids has also been reported. These methods have been tested individually or through a combined approach (hybrid) on several tissues/organs. Changes in the mechanical properties of porcine urinary bladder were reported following use of either ethylene oxide, gamma irradiation or electron beam irradiation (Freytes et al., 2008). The use of peracetic acid within an ethanol solution resulted in a non-cross linked viral free porcine small intestine scaffold (Hodde and Hiles, 2002). Hybrid sterilisation methods using ethylene oxide gas combined with either peracetic acid or gamma irradiation resulted in efficient sterilisation of human-sized liver tissue (Kajbafzadeh et al., 2012). The combined use of peracetic acid with ethylene oxide gas on porcine small intestine submucosa retained a bioactive scaffold that was able to support cellular activity (Hodde et al., 2007).

- vi. Host immune response: The produced final product must undergo thorough immunological evaluation *in vitro*. A major hurdle for tissue

transplantation of allogenic or xenogenic source is immune rejection (Galili, 2001; Wong and Griffiths, 2014). This immune response of the transplanted tissues, if present, plays a pivotal role in the upcoming regeneration process (Daly et al., 2009; Wong and Griffiths, 2014). Previous attempts to overcome tissue antigenicity involved chemical fixation, mainly utilising cross-linking process, by masking the implanted tissue antigens (Okamura et al., 1980). Unfortunately, chemical cross linking might negatively affect tissue function and biocompatibility (Manji et al., 2006; Williams, 2008). More recently, tissue decellularisation has been advocated to eliminate the immune rejection, based on efficient removal of cellular material. Indeed, scaffold acellularity has been regarded as an immunological measurement outcome and efficient assessment of the scaffold cellularity must be undertaken (Wong and Griffiths, 2014). Furthermore, xenogenic hyperacute rejection is reported to be mediated by complement activation of antibodies against Alpha-1,3 Galactose (α -gal) epitope (Galili, 2001; Daly et al., 2009). The α -gal epitope has been found to be expressed in non-primate mammals and New World monkeys. Exceptions include apes, humans and Old World monkeys which lack the presence of α -gal epitope and produce anti-Gal antibodies. Upon exposure, the circulating anti-Gal antibodies in humans bind to α -gal epitope leading to a hyperacute rejection (Galili, 2001; Daly et al., 2009). Therefore, assessing the complete removal of α -gal epitope from the xenogenic tissue is essential and can be assessed qualitatively through immunohistochemical labelling methods or

quantitatively using ELISA assay. Indeed, the efficient removal of α -gal has been reported in several studies utilising animal tissues. These results indicated no evidence of α -gal expression following decellularisation of porcine medial meniscus (Stapleton et al., 2008), porcine bone cartilage (Kheir et al., 2011) and porcine pulmonary valve (Luo et al., 2014).

- vii. Scaffold environment: To test the efficacy of the produced scaffold to regenerate and interact with the surrounding environment, *ex vivo* culture models have been introduced within this field (Sloan et al., 1998). These *ex vivo* models aim to provide clinical relevant models that can be performed in a controlled laboratory setting. These models take into account similar *in vivo* spatial organisation, thereby providing cells with a three-dimensional environment (Sloan et al., 2017). The use of a tooth slice *ex vivo* culture model involves placement of a scaffold within prepared dentine disks of 1 – 2 mm thickness. These dentine disks can be obtained from human or rodent teeth (Sloan et al., 2017). The utilisation of ectopic root transplantation models has also been reported (Gotlieb et al., 2008; Huang et al., 2010). This involves scaffold placement within empty full length root canal spaces. The use of ectopic root transplantation models closely replicates the clinical environment and provides pivotal information regarding the shape and quality of the engineered pulp tissue (Gotlieb et al., 2008; Huang et al., 2010). The

mandible slice *ex vivo* culture model could also be used for pulp tissue regeneration (Sloan et al., 2017).

Following laboratory testing, the designed scaffolds should be tested using the gold standard *in vivo* studies using functional animal models and large animal studies. If successful results are obtained from the above studies, the final step of this work would ultimately involve well controlled human clinical trials. The scalability of a new treatment strategy from the laboratory bench to the chair side ideally should require early manufacturing considerations. Protocol standardisation, reduced contamination risk, and in-process control are the minimal manufacturing demands that should be carefully addressed before using such scaffolds in human pulp regeneration (Wall et al., 2017).

References

- Abe, S., Yamaguchi, S., Watanabe, A., Hamada, K. and Amagasa, T. 2008. Hard Tissue Regeneration Capacity of Apical Pulp Derived Cells (Apdcs) from Human Tooth with Immature Apex. *Biochemical and Biophysical Research Communications*. **371**(1), pp.90-93.
- About, I., Laurent-Maquin, D., Lendahl, U. and Mitsiadis, T. A. 2000. Nestin Expression in Embryonic and Adult Human Teeth under Normal and Pathological Conditions. *The American Journal of Pathology*. **157**(1), pp.287-295.
- Ajay Sharma, L., Sharma, A. and Dias, G. J. 2013. Advances in Regeneration of Dental Pulp—a Literature Review. *Journal of Investigative and Clinical Dentistry*. **6**(2), pp.85-92.
- Al Ansary, M. A., Day, P. F., Duggal, M. S. and Brunton, P. A. 2009. Interventions for Treating Traumatized Necrotic Immature Permanent Anterior Teeth: Inducing a Calcific Barrier & Root Strengthening. *Dental Traumatology*. **25**(4), pp.367-379.
- Almushayt, A., Narayanan, K., Zaki, A. E. and George, A. 2005. Dentin Matrix Protein 1 Induces Cytodifferentiation of Dental Pulp Stem Cells into Odontoblasts. *Gene Therapy*. **13**, pp.611.
- American Association of Endodontists. 2013. *Scope of Endodontics: Regenerative Endodontics Position Statement* [Online]. American Association of Endodontists. Available: http://www.aae.org/uploadedfiles/clinical_resources/guidelines_and_position_statements/scopeofendo_regendo.pdf [Accessed 28/05/2017].
- Andreasen, J. O., Farik, B. and Munksgaard, E. C. 2002. Long-Term Calcium Hydroxide as a Root Canal Dressing May Increase Risk of Root Fracture. *Dental Traumatology*. **18**(3), pp.134-137.
- Arthur, A., Rychkov, G., Shi, S., Koblar, S. A. and Gronthos, S. 2008. Adult Human Dental Pulp Stem Cells Differentiate toward Functionally Active Neurons under Appropriate Environmental Cues. *Stem Cells*. **26**(7), pp.1787-1795.
- Aumailley, M., Bruckner-Tuderman, L., Carter, W. G., Deutzmann, R., Edgar, D., Ekblom, P., et al., 2005. A Simplified Laminin Nomenclature. *Matrix Biology*. **24**(5), pp.326-332.

Bader, A., Steinhoff, G., Strobl, K., Schilling, T., Brandes, G., Mertsching, H., et al., 2000. Engineering of Human Vascular Aortic Tissue Based on a Xenogeneic Starter Matrix. *Transplantation*. **70**(1), pp.7-14.

Badylak, S. F. 2002. The Extracellular Matrix as a Scaffold for Tissue Reconstruction. *Seminars in Cell and Developmental Biology*. **13**(5), pp.377-383.

Badylak, S. F. 2007. The Extracellular Matrix as a Biologic Scaffold Material. *Biomaterials*. **28**(25), pp.3587-3593.

Badylak, S. F., Freytes, D. O. and Gilbert, T. W. 2009. Extracellular Matrix as a Biological Scaffold Material: Structure and Function. *Acta biomaterialia*. **5**(1), pp.1-13.

Banchs, F. and Trope, M. 2004. Revascularization of Immature Permanent Teeth with Apical Periodontitis: New Treatment Protocol? *Journal of Endodontics*. **30**(4), pp.196-200.

Becerra, P., Ricucci, D., Loghin, S., Gibbs, J. L. and Lin, L. M. 2014. Histologic Study of a Human Immature Permanent Premolar with Chronic Apical Abscess after Revascularization/Revitalization. *Journal of Endodontics*. **40**(1), pp.133-139.

Bodnar, E., Olsen, E. G. J., Florio, R. and Dobrin, J. 1986. Damage of Porcine Aortic Valve Tissue Caused by the Surfactant Sodiumdodecylsulphate. *Thoracic and Cardiovascular Surgeon*. **34**(2), pp.82-85.

British Standard Institute 2009. *Bs En Iso 10993-5. Biological Evaluation of Medical Devices—Part 5: Tests for in Vitro Cytotoxicity*. London: BSI.

Brock, D. P., Marty-Roix, R. and Spector, M. 2002. α -Smooth-Muscle Actin in and Contraction of Porcine Dental Pulp Cells. *Journal of Dental Research*. **81**(3), pp.203-208.

Bronckaers, A., Hilkens, P., Fanton, Y., Struys, T., Gervois, P., Politis, C., et al., 2013. Angiogenic Properties of Human Dental Pulp Stem Cells. *PloS One*. **8**(8), pp.e71104.

Brown, B. N., Valentin, J. E., Stewart-Akers, A. M., McCabe, G. P. and Badylak, S. F. 2009. Macrophage Phenotype and Remodeling Outcomes in Response to Biologic Scaffolds with and without a Cellular Component. *Biomaterials*. **30**(8), pp.1482-1491.

- Burk, J., Erbe, I., Berner, D., Kacza, J., Kasper, C., Pfeiffer, B., et al., 2014. Freeze-Thaw Cycles Enhance Decellularization of Large Tendons. *Tissue Engineering. Part C, Methods*. **20**(4), pp.276-284.
- Cavalcanti, B. N., Zeitlin, B. D. and Nör, J. E. 2013. A Hydrogel Scaffold That Maintains Viability and Supports Differentiation of Dental Pulp Stem Cells. *Dental Materials*. **29**(1), pp.97-102.
- Cehreli, Z. C., Isbitiren, B., Sara, S. and Erbas, G. 2011. Regenerative Endodontic Treatment (Revascularization) of Immature Necrotic Molars Medicated with Calcium Hydroxide: A Case Series. *Journal of Endodontics*. **37**(9), pp.1327-1330.
- Centeno, V. A., Fontanetti, P. A., Interlandi, V., Ponce, R. H. and Gallará, R. V. 2015. Fluoride Alters Connexin Expression in Rat Incisor Pulp. *Archives of Oral Biology*. **60**(2), pp.313-319.
- Chen, G., Chen, J., Yang, B., Li, L., Luo, X., Zhang, X., et al., 2015. Combination of Aligned PIIg/Gelatin Electrospun Sheets, Native Dental Pulp Extracellular Matrix and Treated Dentin Matrix as Substrates for Tooth Root Regeneration. *Biomaterials*. **52**, pp.56-70.
- Chen, M. H., Chen, K. L., Chen, C. A., Tayebaty, F., Rosenberg, P. and Lin, L. 2012. Responses of Immature Permanent Teeth with Infected Necrotic Pulp Tissue and Apical Periodontitis/Abscess to Revascularization Procedures. *International Endodontic Journal*. **45**(3), pp.294-305.
- Chen, R.-N., Ho, H.-O., Tsai, Y.-T. and Sheu, M.-T. 2004. Process Development of an Acellular Dermal Matrix (Adm) for Biomedical Applications. *Biomaterials*. **25**(13), pp.2679-2686.
- Cintra, L. T. A., Benetti, F., da Silva Facundo, A. C., Ferreira, L. L., Gomes-Filho, J. E., Ervolino, E., et al., 2013. The Number of Bleaching Sessions Influences Pulp Tissue Damage in Rat Teeth. *Journal of Endodontics*. **39**(12), pp.1576-1580.
- Cognato, H. and Yurchenco, P. D. 2000. Form and Function: The Laminin Family of Heterotrimers. *Developmental Dynamics*. **218**(2), pp.213-234.
- Colombo, J. S., Moore, A. N., Hartgerink, J. D. and D'Souza, R. N. 2014. Scaffolds to Control Inflammation and Facilitate Dental Pulp Regeneration. *Journal of Endodontics*. **40**(4), pp.S6-S12.
- Conde, M. C. M., Chisini, L. A., Demarco, F. F., Nör, J. E., Casagrande, L. and Tarquinio, S. B. C. 2015. Stem Cell-Based Pulp Tissue Engineering: Variables

Enrolled in Translation from the Bench to the Bedside, a Systematic Review of Literature. *International Endodontic Journal*. **49**(6), pp.543-550.

Cordeiro, M. M., Dong, Z., Kaneko, T., Zhang, Z., Miyazawa, M., Shi, S., et al., 2008. Dental Pulp Tissue Engineering with Stem Cells from Exfoliated Deciduous Teeth. *Journal of Endodontics*. **34**(8), pp.962-969.

Cournil, I., Leblond, C. P., Pomponio, J., Hand, A. R., Sederlof, L. and Martin, G. R. 1979. Immunohistochemical Localization of Procollagens. I. Light Microscopic Distribution of Procollagen I, Iii and Iv Antigenicity in the Rat Incisor Tooth by the Indirect Peroxidase-Anti-Peroxidase Method. *Journal of Histochemistry and Cytochemistry*. **27**(7), pp.1059-1069.

Courtman, D. W., Pereira, C. A., Kashef, V., McComb, D., Lee, J. M. and Wilson, G. J. 1994. Development of a Pericardial Acellular Matrix Biomaterial: Biochemical and Mechanical Effects of Cell Extraction. *Journal of Biomedical Materials Research*. **28**(6), pp.655-666.

Cox, B. and Emili, A. 2006. Tissue Subcellular Fractionation and Protein Extraction for Use in Mass-Spectrometry-Based Proteomics. *Nature Protocols*. **1**(4), pp.1872.

Crapo, P. M., Gilbert, T. W. and Badylak, S. F. 2011. An Overview of Tissue and Whole Organ Decellularization Processes. *Biomaterials*. **32**(12), pp.3233-3243.

Cvek, M. 1992. Prognosis of Luxated Non-Vital Maxillary Incisors Treated with Calcium Hydroxide and Filled with Gutta-Percha. A Retrospective Clinical Study. *Dental Traumatology*. **8**(2), pp.45-55.

Daly, K. A., Stewart-Akers, A. M., Hara, H., Ezzelarab, M., Long, C., Cordero, K., et al., 2009. Effect of the Agal Epitope on the Response to Small Intestinal Submucosa Extracellular Matrix in a Nonhuman Primate Model. *Tissue Engineering Part A*. **15**(12), pp.3877-3888.

Dayan, D., Hiss, Y., Hirshberg, A., Bubis, J. and Wolman, M. 1989. Are the Polarization Colors of Picrosirius Red-Stained Collagen Determined Only by the Diameter of the Fibers? *Histochemistry*. **93**(1), pp.27-29.

De Filippo, R. E., Yoo, J. J. and Atala, A. 2002. Urethral Replacement Using Cell Seeded Tubularized Collagen Matrices. *The Journal of Urology*. **168**(4, Supplement), pp.1789-1793.

Demarco, F. F., Casagrande, L., Zhang, Z., Dong, Z., Tarquinio, S. B., Zeitlin, B. D., et al., 2010. Effects of Morphogen and Scaffold Porogen on the

Differentiation of Dental Pulp Stem Cells. *Journal of Endodontics*. **36**(11), pp.1805-1811.

Demarco, F. F., Conde, M. C. M., Cavalcanti, B. N., Casagrande, L., Sakai, V. T. and Nör, J. E. 2011. Dental Pulp Tissue Engineering. *Brazilian Dental Journal*. **22**(1), pp.3-13.

Ding, R. Y., Cheung, G. S.-p., Chen, J., Yin, X. Z., Wang, Q. Q. and Zhang, C. F. 2009. Pulp Revascularization of Immature Teeth with Apical Periodontitis: A Clinical Study. *Journal of Endodontics*. **35**(5), pp.745-749.

Diogenes, A., Henry, M. A., Teixeira, F. B. and Hargreaves, K. M. 2013. An Update on Clinical Regenerative Endodontics. *Endodontic Topics*. **28**(1), pp.2-23.

Diogenes, A. and Ruparel, N. B. 2017. Regenerative Endodontic Procedures. *Dental Clinics of North America*. **61**(1), pp.111-125.

Diogenes, A., Ruparel, N. B., Shiloah, Y. and Hargreaves, K. M. 2016. Regenerative Endodontics. *The Journal of the American Dental Association*. **147**(5), pp.372-380.

Diogenes, A. R., Ruparel, N. B., Teixeira, F. B. and Hargreaves, K. M. 2014. Translational Science in Disinfection for Regenerative Endodontics. *Journal of Endodontics*. **40**(4), pp.S52-S57.

Dissanayaka, W. L., Zhu, L., Hargreaves, K. M., Jin, L. and Zhang, C. 2014. Scaffold-Free Prevascularized Microtissue Spheroids for Pulp Regeneration. *Journal of Dental Research*. **93**(12), pp.1296-1303.

Dobie, K., Smith, G., Sloan, A. J. and Smith, A. J. 2002. Effects of Alginate Hydrogels and Tgf-B1 on Human Dental Pulp Repair in Vitro. *Connective Tissue Research*. **43**(2-3), pp.387-390.

Dominguez Reyes, A., Muñoz Muñoz, L. and Aznar Martín, T. 2005. Study of Calcium Hydroxide Apexification in 26 Young Permanent Incisors. *Dental Traumatology*. **21**(3), pp.141-145.

Dominici, M., Le Blanc, K., Mueller, I., Slaper-Cortenbach, I., Marini, F. C., Krause, D. S., et al., 2006. Minimal Criteria for Defining Multipotent Mesenchymal Stromal Cells. The International Society for Cellular Therapy Position Statement. *Cytotherapy*. **8**(4), pp.315-317.

Doyon, G. E., Dumsha, T. and von Fraunhofer, J. A. 2005. Fracture Resistance of Human Root Dentin Exposed to Intracanal Calcium Hydroxide. *Journal of Endodontics*. **31**(12), pp.895-897.

Duggal, M., Tong, H. J., Al-Ansary, M., Twati, W., Day, P. F. and Nazzal, H. 2017. Interventions for the Endodontic Management of Non-Vital Traumatized Immature Permanent Anterior Teeth in Children and Adolescents: A Systematic Review of the Evidence and Guidelines of the European Academy of Paediatric Dentistry. *European Archives of Paediatric Dentistry*. **18**(3), pp.139-151.

Egusa, H., Sonoyama, W., Nishimura, M., Atsuta, I. and Akiyama, K. 2012. Stem Cells in Dentistry – Part I: Stem Cell Sources. *Journal of Prosthodontic Research*. **56**(3), pp.151-165.

El-Backly, R. M., Massoud, A. G., El-Badry, A. M., Sherif, R. A. and Marei, M. K. 2008. Regeneration of Dentine/Pulp-Like Tissue Using a Dental Pulp Stem Cell/Poly (Lactic-Co-Glycolic) Acid Scaffold Construct in New Zealand White Rabbits. *Australian Endodontic Journal*. **34**(2), pp.52-67.

El Meligy, O. A. S. and Avery, D. R. 2006. Comparison of Apexification with Mineral Trioxide Aggregate and Calcium Hydroxide. *Pediatric Dentistry*. **28**(3), pp.248-253.

European Society of Endodontology 2016. *European Society of Endodontology Position Statement: Revitalization Procedures*. *International Endodontic Journal*.

Falke, G., Yoo, J. J., Kwon, T. G., Moreland, R. and Atala, A. 2004. Formation of Corporal Tissue Architecture in Vivo Using Human Cavernosal Muscle and Endothelial Cells Seeded on Collagen Matrices *Tissue Engineering. Part C, Methods*. **9**(5), pp.871-879.

Ferrara, N. 2004. Vascular Endothelial Growth Factor: Basic Science and Clinical Progress. *Endocrine Reviews*. **25**(4), pp.581-611.

Folkman, J. 1995. Angiogenesis in Cancer, Vascular, Rheumatoid and Other Disease. *Nature Medicine*. **1**(1), pp.27-30.

Freytes, D. O., Badylak, S. F., Webster, T. J., Geddes, L. A. and Rundell, A. E. 2004. Biaxial Strength of Multilaminated Extracellular Matrix Scaffolds. *Biomaterials*. **25**(12), pp.2353-2361.

Freytes, D. O., Stoner, R. M. and Badylak, S. F. 2008. Uniaxial and Biaxial Properties of Terminally Sterilized Porcine Urinary Bladder Matrix Scaffolds.

Journal of Biomedical Materials Research Part B: Applied Biomaterials. **84B**(2), pp.408-414.

Fried, K., Sime, W., Lillesaar, C., Virtanen, I., Tryggvasson, K. and Patarroyo, M. 2005. Laminins 2 (A2 β 1 γ 1, Lm-211) and 8 (A4 β 1 γ 1, Lm-411) Are Synthesized and Secreted by Tooth Pulp Fibroblasts and Differentially Promote Neurite Outgrowth from Trigeminal Ganglion Sensory Neurons. *Experimental Cell Research.* **307**(2), pp.329-341.

Fu, R.-H., Wang, Y.-C., Liu, S.-P., Shih, T.-R., Lin, H.-L., Chen, Y.-M., et al., 2014. Decellularization and Recellularization Technologies in Tissue Engineering. *Cell Transplantation.* **23**(4-5), pp.621-630.

Gailit, J. and Ruoslahti, E. 1988. Regulation of the Fibronectin Receptor Affinity by Divalent Cations. *Journal of Biological Chemistry.* **263**(26), pp.12927-12932.

Galili, U. 2001. The A-Gal Epitope (Gal α 1-3gal β 1-4glcnac-R) in Xenotransplantation. *Biochimie.* **83**(7), pp.557-563.

Galis, Z. S., Sukhova, G. K., Lark, M. W. and Libby, P. 1994. Increased Expression of Matrix Metalloproteinases and Matrix Degrading Activity in Vulnerable Regions of Human Atherosclerotic Plaques. *Journal of Clinical Investigation.* **94**(6), pp.2493-2503.

Galler, K., D'souza, R., Hartgerink, J. and Schmalz, G. 2011a. Scaffolds for Dental Pulp Tissue Engineering. *Advances in Dental Research.* **23**(3), pp.333-339.

Galler, K. M. 2016. Clinical Procedures for Revitalization: Current Knowledge and Considerations. *International Endodontic Journal.* **49**(10), pp.926-936.

Galler, K. M., D'Souza, R. N. and Hartgerink, J. D. 2010. Biomaterials and Their Potential Applications for Dental Tissue Engineering. *Journal of Materials Chemistry.* **20**(40), pp.8730-8746.

Galler, K. M., D'Souza, R. N., Hartgerink, J. D. and Schmalz, G. 2011b. Scaffolds for Dental Pulp Tissue Engineering. *Advances in Dental Research.* **23**(3), pp.333-339.

Galler, K. M., Eidt, A. and Schmalz, G. 2014. Cell-Free Approaches for Dental Pulp Tissue Engineering. *Journal of Endodontics.* **40**(4, Supplement), pp.S41-S45.

Galler, K. M., Hartgerink, J. D., Cavender, A. C., Schmalz, G. and D'Souza, R. N. 2011c. A Customized Self-Assembling Peptide Hydrogel for Dental Pulp Tissue Engineering. *Tissue Engineering Part A*. **18**(1-2), pp.176-184.

Garcia-Godoy, F. and Murray, P. E. 2012. Recommendations for Using Regenerative Endodontic Procedures in Permanent Immature Traumatized Teeth. *Dental Traumatology*. **28**(1), pp.33-41.

Gelse, K., Pöschl, E. and Aigner, T. 2003. Collagens—Structure, Function, and Biosynthesis. *Advanced Drug Delivery Reviews*. **55**(12), pp.1531-1546.

Gerhardt, H. and Betsholtz, C. 2003. Endothelial-Pericyte Interactions in Angiogenesis. *Cell and Tissue Research*. **314**(1), pp.15-23.

Gilbert, T. W., Freund, J. M. and Badylak, S. F. 2009. Quantification of DNA in Biologic Scaffold Materials. *Journal of Surgical Research*. **152**(1), pp.135-139.

Gilbert, T. W., Sellaro, T. L. and Badylak, S. F. 2006. Decellularization of Tissues and Organs. *Biomaterials*. **27**(19), pp.3675-3683.

Glossary of Endodontic Terms 9th edition. 2016. *American Association of Endodontists*, [Online]. Chicago. Available: <http://www.nxtbook.com/nxtbooks/aae/endodonticglossary2016/#/2> [Accessed 17/2/2016].

Goldberg, M. 2014a. Dentin, Pulp, and Tooth Pain. In: HAND, A. R. and FRANK, M. E. (eds.) *Fundamentals of Oral Histology and Physiology*. First ed.: John Wiley & Sons.

Goldberg, M. 2014b. Pulp Anatomy and Characterization of Pulp Cells. In: GOLDBERG, M. (ed.) *The Dental Pulp*. Berlin: Springer.

Goldberg, M. and Smith, A. J. 2004. Cells and Extracellular Matrices of Dentin and Pulp: A Biological Basis for Repair and Tissue Engineering. *Critical Reviews in Oral Biology and Medicine*. **15**(1), pp.13-27.

Gorschewsky, O., Puetz, A., Riechert, K., Klakow, A. and Becker, R. 2005. Quantitative Analysis of Biochemical Characteristics of Bone-Patellar Tendon-Bone Allografts *Bio-Medical Materials and Engineering*. **15**(6), pp.403 - 411.

Goseki, M., Oida, S., Nifuji, A. and Sasaki, S. 1990. Properties of Alkaline Phosphatase of the Human Dental Pulp. *Journal of Dental Research*. **69**(3), pp.909-912.

Gotlieb, E. L., Murray, P. E., Namerow, K. N., Kuttler, S. and Garcia-Godoy, F. 2008. An Ultrastructural Investigation of Tissue-Engineered Pulp Constructs Implanted within Endodontically Treated Teeth. *The Journal of the American Dental Association*. **139**(4), pp.457-465.

Grando Mattuella, L., Westphalen Bento, L., Poli de Figueiredo, J. A., Eduardo Nör, J., Borba de Araujo, F. and Christina Medeiros Fossati, A. 2007. Vascular Endothelial Growth Factor and Its Relationship with the Dental Pulp. *Journal of Endodontics*. **33**(5), pp.524-530.

Gratzer, P. F., Harrison, R. D. and Woods, T. 2006. Matrix Alteration and Not Residual Sodium Dodecyl Sulfate Cytotoxicity Affects the Cellular Repopulation of a Decellularized Matrix. *Tissue Engineering*. **12**(10), pp.2975-2983.

Gronthos, S., Brahim, J., Li, W., Fisher, L. W., Cherman, N., Boyde, A., et al., 2002. Stem Cell Properties of Human Dental Pulp Stem Cells. *Journal of Dental Research*. **81**(8), pp.531-535.

Gronthos, S., Mankani, M., Brahim, J., Robey, P. G. and Shi, S. 2000. Postnatal Human Dental Pulp Stem Cells (Dpscs) in Vitro and in Vivo. *Proceedings of the National Academy of Sciences*. **97**(25), pp.13625-13630.

He, G., Dahl, T., Veis, A. and George, A. 2003. Dentin Matrix Protein 1 Initiates Hydroxyapatite Formation in Vitro. *Connective Tissue Research*. **44**(1), pp.240-245.

Hensten-Pettersen, A. 1988. Comparison of the Methods Available for Assessing Cytotoxicity. *International Endodontic Journal*. **21**(2), pp.89-99.

Hillmann, G. and Geurtsen, W. 1997. Light-Microscopical Investigation of the Distribution of Extracellular Matrix Molecules and Calcifications in Human Dental Pulps of Various Ages. *Cell and Tissue Research*. **289**(1), pp.145-154.

Hodde, J. and Hiles, M. 2002. Virus Safety of a Porcine-Derived Medical Device: Evaluation of a Viral Inactivation Method. *Biotechnology and Bioengineering*. **79**(2), pp.211-216.

Hodde, J., Janis, A. and Hiles, M. 2007. Effects of Sterilization on an Extracellular Matrix Scaffold: Part II. Bioactivity and Matrix Interaction. *Journal of Materials Science: Materials in Medicine*. **18**(4), pp.545-550.

Hopkinson, A., Shanmuganathan, V. A., Gray, T., Yeung, A. M., Lowe, J., James, D. K., et al., 2008. Optimization of Amniotic Membrane (Am) Denuding for Tissue Engineering. *Tissue Engineering Part C: Methods*. **14**(4), pp.371-381.

Hou, Q., De Bank, P. A. and Shakesheff, K. M. 2004. Injectable Scaffolds for Tissue Regeneration. *Journal of Materials Chemistry*. **14**(13), pp.1915-1923.

Howard, C., Murray, P. E. and Namerow, K. N. 2010. Dental Pulp Stem Cell Migration. *Journal of Endodontics*. **36**(12), pp.1963-1966.

Hu, C. C., Zhang, C., Qian, Q. and Tatum, N. B. 1998. Reparative Dentin Formation in Rat Molars after Direct Pulp Capping with Growth Factors. *Journal of Endodontics*. **24**(11), pp.744-751.

Huang, G. T.-J., Yamaza, T., Shea, L. D., Djouad, F., Kuhn, N. Z., Tuan, R. S., et al., 2010. Stem/Progenitor Cell-Mediated De Novo Regeneration of Dental Pulp with Newly Deposited Continuous Layer of Dentin in an in Vivo Model. *Tissue Engineering Part A*. **16**(2), pp.605-615.

Huang, G. T. J., Sonoyama, W., Liu, Y., Liu, H., Wang, S. and Shi, S. 2008. The Hidden Treasure in Apical Papilla: The Potential Role in Pulp/Dentin Regeneration and Bioroot Engineering. *Journal of Endodontics*. **34**(6), pp.645-651.

Hynes, R. 1985. Molecular Biology of Fibronectin. *Annual Review of Cell Biology*. **1**(1), pp.67-90.

Ikeda, E., Morita, R., Nakao, K., Ishida, K., Nakamura, T., Takano-Yamamoto, T., et al., 2009. Fully Functional Bioengineered Tooth Replacement as an Organ Replacement Therapy. *Proceedings of the National Academy of Sciences*. **106**(32), pp.13475-13480.

International Organisation for Standardisation 2008. *Dentistry Preclinical Evaluation of Biocompatibility of Medical Devices in Dentistry—Test Methods for Dental Materials*. Geneva: ISO 7405.

Ivaska, J., Pallari, H.-M., Nevo, J. and Eriksson, J. E. 2007. Novel Functions of Vimentin in Cell Adhesion, Migration, and Signaling. *Experimental Cell Research*. **313**(10), pp.2050-2062.

Iwaya, S.-i., Ikawa, M. and Kubota, M. 2001. Revascularization of an Immature Permanent Tooth with Apical Periodontitis and Sinus Tract. *Dental Traumatology*. **17**(4), pp.185-187.

Janebodin, K., Zeng, Y., Buranaphatthana, W., Ieronimakis, N. and Reyes, M. 2013. Vegfr2-Dependent Angiogenic Capacity of Pericyte-Like Dental Pulp Stem Cells. *Journal of Dental Research*. **92**(6), pp.524-531.

Jeeruphan, T., Jantararat, J., Yanpiset, K., Suwannapan, L., Khewsawai, P. and Hargreaves, K. M. 2012. Mahidol Study 1: Comparison of Radiographic and Survival Outcomes of Immature Teeth Treated with Either Regenerative Endodontic or Apexification Methods: A Retrospective Study. *Journal of Endodontics*. **38**(10), pp.1330-1336.

Jontell, M., Gunraj, M. and Bergenholtz, G. 1987. Immunocompetent Cells in the Normal Dental Pulp. *Journal of Dental Research*. **66**(6), pp.1149-1153.

Jung, I.-Y., Lee, S.-J. and Hargreaves, K. M. 2008. Biologically Based Treatment of Immature Permanent Teeth with Pulpal Necrosis: A Case Series. *Journal of Endodontics*. **34**(7), pp.876-887.

Junqueira, L. C. U., Bignolas, G. and Brentani, R. 1979. Picrosirius Staining Plus Polarization Microscopy, a Specific Method for Collagen Detection in Tissue Sections. *The Histochemical Journal*. **11**(4), pp.447-455.

Junqueira, L. C. U., Montes, G. S. and Sanchez, E. M. 1982. The Influence of Tissue Section Thickness on the Study of Collagen by the Picrosirius-Polarization Method. *Histochemistry*. **74**(1), pp.153-156.

Kahler, B., Rossi-Fedele, G., Chugal, N. and Lin, L. M. 2017. An Evidence-Based Review of the Efficacy of Treatment Approaches for Immature Permanent Teeth with Pulp Necrosis. *Journal of Endodontics*. **43**(7), pp.1052-1057.

Kajbafzadeh, A.-M., Javan-Farazmand, N., Monajemzadeh, M. and Baghayee, A. 2012. Determining the Optimal Decellularization and Sterilization Protocol for Preparing a Tissue Scaffold of a Human-Sized Liver Tissue. *Tissue Engineering Part C: Methods*. **19**(8), pp.642-651.

Kajbafzadeh, A.-M., Javan-Farazmand, N., Monajemzadeh, M. and Baghayee, A. 2013. Determining the Optimal Decellularization and Sterilization Protocol for Preparing a Tissue Scaffold of a Human-Sized Liver Tissue. *Tissue Engineering Part C: Methods*. **19**(8), pp.642-651.

Kapuscinski, J. 1995. Dapi: A DNA-Specific Fluorescent Probe. *Biotechnic and Histochemistry*. **70**(5), pp.220-233.

Kapuściński, J. and Skoczylas, B. 1978. Fluorescent Complexes of DNA with Dapi 4',6-Diamidine-2-Phenyl Indole 2hcl or Dci 4',6-Dicarboxyamide-2-Pheanyl Indole. *Nucleic Acids Research*. **5**(10), pp.3775-3800.

Kawashima, N. 2012. Characterisation of Dental Pulp Stem Cells: A New Horizon for Tissue Regeneration? *Archives of Oral Biology*. **57**(11), pp.1439-1458.

Kawecki, M., Łabuś, W., Klama-Baryla, A., Kitala, D., Kraut, M., Glik, J., et al., 2017. A Review of Decellurization Methods Caused by an Urgent Need for Quality Control of Cell-Free Extracellular Matrix' Scaffolds and Their Role in Regenerative Medicine. *Journal of Biomedical Materials Research Part B: Applied Biomaterials*. pp.DOI: 10.1002/jbm.b.33865.

Keane, T. J., Swinehart, I. T. and Badylak, S. F. 2015. Methods of Tissue Decellularization Used for Preparation of Biologic Scaffolds and in Vivo Relevance. *Methods*. **84**, pp.25-34.

Kheir, E., Stapleton, T., Shaw, D., Jin, Z., Fisher, J. and Ingham, E. 2011. Development and Characterization of an Acellular Porcine Cartilage Bone Matrix for Use in Tissue Engineering. *Journal of Biomedical Materials Research Part A*. **99**(2), pp.283-294.

Kim, N. R., Lee, D. H., Chung, P.-H. and Yang, H.-C. 2009. Distinct Differentiation Properties of Human Dental Pulp Cells on Collagen, Gelatin, and Chitosan Scaffolds. *Oral Surgery, Oral Medicine, Oral Pathology, Oral Radiology, and Endodontology*. **108**(5), pp.e94-e100.

Klebe, R. J. 1974. Isolation of a Collagen-Dependent Cell Attachment Factor. *Nature*. **250**(5463), pp.248-251.

Knight, R. L., Wilcox, H. E., Korossis, S. A., Fisher, J. and Ingham, E. 2008. The Use of Acellular Matrices for the Tissue Engineering of Cardiac Valves. *Proceedings of the Institution of Mechanical Engineers, Part H: Journal of Engineering in Medicine*. **222**(1), pp.129-143.

Kodonas, K., Gogos, C., Papadimitriou, S., Kouzi-Koliakou, K. and Tziafas, D. 2012. Experimental Formation of Dentin-Like Structure in the Root Canal Implant Model Using Cryopreserved Swine Dental Pulp Progenitor Cells. *Journal of Endodontics*. **38**(7), pp.913-919.

Kontakiotis, E. G., Filippatos, C. G. and Agrafioti, A. 2014. Levels of Evidence for the Outcome of Regenerative Endodontic Therapy. *Journal of Endodontics*. **40**(8), pp.1045-1053.

Kumar, G. 2014. *Orban's Oral Histology & Embryology*, Elsevier Health Sciences.

Kuratate, M., Yoshiba, K., Shigetani, Y., Yoshiba, N., Ohshima, H. and Okiji, T. 2008. Immunohistochemical Analysis of Nestin, Osteopontin, and Proliferating Cells in the Reparative Process of Exposed Dental Pulp Capped with Mineral Trioxide Aggregate. *Journal of Endodontics*. **34**(8), pp.970-974.

Lader, D., Chadwick, B., Chestnutt, I., Harker, R., Morris, J., Nuttall, N., et al., 2003. *Children's Dental Health Survey* [Online]. Office for National Statistics, Social Survey Division. Available: Accessed 19/07/2016 from <http://dx.doi.org/10.5255/UKDA-SN-6764-1>.

Landis, R. C., Haskard, D. O. and Taylor, K. M. 2001. New Antiinflammatory and Platelet-Preserving Effects of Aprotinin. *The Annals of Thoracic Surgery*. **72**(5), pp.S1808-S1813.

Langer, R. and Vacanti, J. 1993. Tissue Engineering. *Science*. **260**(5110), pp.920-926.

Lattouf, R., Younes, R., Lutomski, D., Naaman, N., Godeau, G., Senni, K., et al., 2014. Picrosirius Red Staining a Useful Tool to Appraise Collagen Networks in Normal and Pathological Tissues. *Journal of Histochemistry and Cytochemistry*. **62**(10), pp.751-758.

Lee, K. Y. and Mooney, D. J. 2001. Hydrogels for Tissue Engineering. *Chemical Reviews*. **101**(7), pp.1869-1880.

Lee, S.-M., Zhang, Q. and Le, A. D. 2014. Dental Stem Cells: Sources and Potential Applications. *Current Oral Health Reports*. **1**(1), pp.34-42.

Lee, Y., Go, E. J., Jung, H. S., Kim, E., Jung, I. Y. and Lee, S. J. 2012. Immunohistochemical Analysis of Pulpal Regeneration by Nestin Expression in Replanted Teeth. *International Endodontic Journal*. **45**(7), pp.652-659.

Lenzi, R. and Trope, M. 2012. Revitalization Procedures in Two Traumatized Incisors with Different Biological Outcomes. *Journal of Endodontics*. **38**(3), pp.411-414.

Liao, J., Joyce, E. M. and Sacks, M. S. 2008. Effects of Decellularization on the Mechanical and Structural Properties of the Porcine Aortic Valve Leaflet. *Biomaterials*. **29**(8), pp.1065-1074.

Lin, L. M., Shimizu, E., Gibbs, J. L., Loghin, S. and Ricucci, D. 2014. Histologic and Histobacteriologic Observations of Failed Revascularization/Revitalization Therapy: A Case Report. *Journal of Endodontics*. **40**(2), pp.291-295.

Linde, A. 1973. A Study of the Dental Pulp Glycosaminoglycans from Permanent Human Teeth and Rat and Rabbit Incisors. *Archives of Oral Biology*. **18**(1), pp.49-59.

Linde, A. 1985. Session Ii: Cells and Extracellular Matrices of the Dental Pulp — C.T. Hanks, Chairman. *Journal of Dental Research*. **64**(4), pp.523-529.

Linde, A., Johansson, S., Jonsson, R. and Jontell, M. 1982. Localization of Fibronectin During Dentinogenesis in Rat Incisor. *Archives of Oral Biology*. **27**(12), pp.1069-1073.

Lovelace, T. W., Henry, M. A., Hargreaves, K. M. and Diogenes, A. 2011. Evaluation of the Delivery of Mesenchymal Stem Cells into the Root Canal Space of Necrotic Immature Teeth after Clinical Regenerative Endodontic Procedure. *Journal of Endodontics*. **37**(2), pp.133-138.

Lovschall, H., Fejerskov, O. and Flyvbjerg, A. 2001. Pulp-Capping with Recombinant Human Insulin- Like Growth Factor I (Rhigf-I) in Rat Molars. *Advances in Dental Research*. **15**(1), pp.108-112.

Lukinmaa, P.-L. and Waltimo, J. 1992. Immunohistochemical Localization of Types I, V, and Vi Collagen in Human Permanent Teeth and Periodontal Ligament. *Journal of Dental Research*. **71**(2), pp.391-397.

Luo, J., Korossis, S. A., Wilshaw, S. P., Jennings, L. M., Fisher, J. and Ingham, E. 2014. Development and Characterization of Acellular Porcine Pulmonary Valve Scaffolds for Tissue Engineering. *Tissue Eng Part A*. **20**(21-22), pp.2963-2974.

Ma, P. X. 2008. Biomimetic Materials for Tissue Engineering. *Advanced Drug Delivery Reviews*. **60**(2), pp.184-198.

Manji, R. A., Zhu, L. F., Nijjar, N. K., Rayner, D. C., Korbutt, G. S., Churchill, T. A., et al., 2006. Glutaraldehyde-Fixed Bioprosthetic Heart Valve Conduits Calcify and Fail from Xenograft Rejection. *Circulation*. **114**(4), pp.318-327.

Marão, H. F., Panzarini, S. R., Aranega, A. M., Sonoda, C. K., Poi, W. R., Esteves, J. C., et al., 2012. Periapical Tissue Reactions to Calcium Hydroxide and Mta after External Root Resorption as a Sequela of Delayed Tooth Replantation. *Dental Traumatology*. **28**(4), pp.306-313.

Martin, D. E., De Almeida, J. F. A., Henry, M. A., Khaing, Z. Z., Schmidt, C. E., Teixeira, F. B., et al., 2014. Concentration-Dependent Effect of Sodium Hypochlorite on Stem Cells of Apical Papilla Survival and Differentiation. *Journal of Endodontics*. **40**(1), pp.51-55.

Martin, G., Ricucci, D., Gibbs, J. L. and Lin, L. M. 2013. Histological Findings of Revascularized/Revitalized Immature Permanent Molar with Apical Periodontitis Using Platelet-Rich Plasma. *Journal of Endodontics*. **39**(1), pp.138-144.

Martinez, E. F., de Souza, S. O. M., Corrêa, L. and de Araújo, V. C. 2000. Immunohistochemical Localization of Tenascin, Fibronectin, and Type Iii Collagen in Human Dental Pulp. *Journal of Endodontics*. **26**(12), pp.708-711.

Matsushita, K., Motani, R., Sakutal, T., Yamaguchi, N., Koga, T., Matsuo, K., et al., 2000. The Role of Vascular Endothelial Growth Factor in Human Dental Pulp Cells: Induction of Chemotaxis, Proliferation, and Differentiation and Activation of the Ap-1-Dependent Signaling Pathway. *Journal of Dental Research*. **79**(8), pp.1596-1603.

Miller, E. K., Lee, J. Y., Tawil, P. Z., Teixeira, F. B. and Vann, W. F. 2012. Emerging Therapies for the Management of Traumatized Immature Permanent Incisors. *Pediatric Dentistry*. **34**(1), pp.66-69.

Mirsadraee, S., Wilcox, H. E., Korossis, S. A., Kearney, J. N., Watterson, K. G., Fisher, J., et al., 2006. Development and Characterization of an Acellular Human Pericardial Matrix for Tissue Engineering. *Tissue Engineering*. **12**(4), pp.763-773.

Miura, M., Gronthos, S., Zhao, M., Lu, B., Fisher, L. W., Robey, P. G., et al., 2003. Shed: Stem Cells from Human Exfoliated Deciduous Teeth. *Proceedings of the National Academy of Sciences*. **100**(10), pp.5807-5812.

Mohammadi, Z. and Dummer, P. M. H. 2011. Properties and Applications of Calcium Hydroxide in Endodontics and Dental Traumatology. *International Endodontic Journal*. **44**(8), pp.697-730.

Montes, G. and Junqueira, L. 1991. The Use of the Picrosirius-Polarization Method for the Study of the Biopathology of Collagen. *Memorias do Instituto Oswaldo Cruz*. **86**, pp.1-11.

Mooney, D. J., Powell, C., Piana, J. and Rutherford, B. 1996. Engineering Dental Pulp-Like Tissue in Vitro. *Biotechnology Progress*. **12**(6), pp.865-868.

Moreno-Hidalgo, M. C., Caleza-Jimenez, C., Mendoza-Mendoza, A. and Iglesias-Linares, A. 2014. Revascularization of Immature Permanent Teeth with Apical Periodontitis. *International Endodontic Journal*. **47**(4), pp.321-331.

Morsczeck, C., Götz, W., Schierholz, J., Zeilhofer, F., Kühn, U., Möhl, C., et al., 2005. Isolation of Precursor Cells (Pcs) from Human Dental Follicle of Wisdom Teeth. *Matrix Biology*. **24**(2), pp.155-165.

Moule, A. and Moule, C. 2007. The Endodontic Management of Traumatized Permanent Anterior Teeth: A Review. *Australian Dental Journal*. **52**(s1), pp.S122-S137.

Murakami, M., Imabayashi, K., Watanabe, A., Takeuchi, N., Ishizaka, R., Iohara, K., et al., 2012. Identification of Novel Function of Vimentin for Quality Standard for Regenerated Pulp Tissue. *Journal of Endodontics*. **38**(7), pp.920-926.

Murray, P. E., Garcia-Godoy, F. and Hargreaves, K. M. 2007. Regenerative Endodontics: A Review of Current Status and a Call for Action. *Journal of Endodontics*. **33**(4), pp.377-390.

Murray, P. E., Lumley, P. J., Ross, H. F. and Smith, A. J. 2000. Tooth Slice Organ Culture for Cytotoxicity Assessment of Dental Materials. *Biomaterials*. **21**(16), pp.1711-1721.

Nagata, J. Y., de Almeida Gomes, B. P. F., Lima, T. F. R., Murakami, L. S., de Faria, D. E., Campos, G. R., et al., 2014. Traumatized Immature Teeth Treated with 2 Protocols of Pulp Revascularization. *Journal of Endodontics*. **40**(5), pp.606-612.

Nakashima, M. and Akamine, A. 2005. The Application of Tissue Engineering to Regeneration of Pulp and Dentin in Endodontics. *Journal of Endodontics*. **31**(10), pp.711-718.

Nakashima, M. and Iohara, K. 2011. Regeneration of Dental Pulp by Stem Cells. *Advances in Dental Research*. **23**(3), pp.313-319.

Nakashima, M., Iohara, K. and Murakami, M. 2013. Dental Pulp Stem Cells and Regeneration. *Endodontic Topics*. **28**(1), pp.38-50.

Nakashima, M., Iohara, K. and Sugiyama, M. 2009. Human Dental Pulp Stem Cells with Highly Angiogenic and Neurogenic Potential for Possible Use in Pulp Regeneration. *Cytokine and Growth Factor Reviews*. **20**(5), pp.435-440.

Nakashima, M. and Reddi, A. H. 2003. The Application of Bone Morphogenetic Proteins to Dental Tissue Engineering. *Nat Biotech*. **21**(9), pp.1025-1032.

Narayanan, K., Ramachandran, A., Hao, J., He, G., Park, K. W., Cho, M., et al., 2003. Dual Functional Roles of Dentin Matrix Protein 1: Implications in Biomineralization and Gene Transcription by Activation of Intracellular Ca²⁺ Store. *Journal of Biological Chemistry*. **278**(19), pp.17500-17508.

Nazzal, H. and Duggal, M. S. 2017. Regenerative Endodontics: A True Paradigm Shift or a Bandwagon About to Be Derailed? *European Archives of Paediatric Dentistry*. **18**(1), pp.3-15.

Nicoloso, G. F., Pötter, I. G., Rocha, R. d. O., Montagner, F. and Casagrande, L. 2017. A Comparative Evaluation of Endodontic Treatments for Immature Necrotic Permanent Teeth Based on Clinical and Radiographic Outcomes: A Systematic Review and Meta-Analysis. *International Journal of Paediatric Dentistry*. **27**(3), pp.217-227.

Niknejad, H., Peirovi, H., Jorjani, M., Ahmadiani, A., Ghanavi, J. and Seifalian, A. 2008. Properties of the Amniotic Membrane for Potential Use in Tissue Engineering. *European Cells & Materials Journal*. (15), pp. 88-99.

Nör, J. E. 2006. Buonocore Memorial Lecture: Tooth Regeneration in Operative Dentistry. *Operative Dentistry*. **31**(6), pp.633-642.

Nosrat, A., Homayounfar, N. and Oloomi, K. 2012. Drawbacks and Unfavorable Outcomes of Regenerative Endodontic Treatments of Necrotic Immature Teeth: A Literature Review and Report of a Case. *Journal of Endodontics*. **38**(10), pp.1428-1434.

Nosrat, A., Kim, J. R., Verma, P. and Chand, P. S. 2014. Tissue Engineering Considerations in Dental Pulp Regeneration. *Iranian endodontic journal*. **9**(1), pp.30-40.

Ohshima, H., Maeda, T. and Takano, Y. 1999. The Distribution and Ultrastructure of Class II MHC-Positive Cells in Human Dental Pulp. *Cell and Tissue Research*. **295**(1), pp.151-158.

Okamura, K., Chiba, C., Iriyama, T., Itoh, T., Maeta, H., Ijima, H., et al., 1980. Antigen Depressant Effect of Glutaraldehyde for Aortic Heterografts with a Valve, with Special Reference to a Concentration Right Fit for the Preservation of Grafts. *Surgery*. **87**(2), pp.170-176.

Oliveira, A. C., Garzón, I., Ionescu, A. M., Carriel, V., de la Cruz Cardona, J., González-Andrades, M., et al., 2013. Evaluation of Small Intestine Grafts Decellularization Methods for Corneal Tissue Engineering. *PloS One*. **8**(6), pp.e66538.

Oshima, M., Mizuno, M., Imamura, A., Ogawa, M., Yasukawa, M., Yamazaki, H., et al., 2011. Functional Tooth Regeneration Using a Bioengineered Tooth Unit as a Mature Organ Replacement Regenerative Therapy. *PloS One*. **6**(7), pp.e21531.

- Östby, B. N. 1961. The Role of the Blood Clot in Endodontic Therapy an Experimental Histologic Study. *Acta Odontologica Scandinavica*. **19**(3-4), pp.323-353.
- Ozdemir, K. G., Yilmaz, H. and Yilmaz, S. 2009. In Vitro Evaluation of Cytotoxicity of Soft Lining Materials on L929 Cells by Mtt Assay. *Journal of Biomedical Materials Research Part B: Applied Biomaterials*. **90B**(1), pp.82-86.
- Paduano, F., Marrelli, M., White, L. J., Shakesheff, K. M. and Tatullo, M. 2016. Odontogenic Differentiation of Human Dental Pulp Stem Cells on Hydrogel Scaffolds Derived from Decellularized Bone Extracellular Matrix and Collagen Type I. *PloS One*. **11**(2), pp.e0148225.
- Palma, P. J., Ramos, J. C., Martins, J. B., Diogenes, A., Figueiredo, M. H., Ferreira, P., et al., 2017. Histologic Evaluation of Regenerative Endodontic Procedures with the Use of Chitosan Scaffolds in Immature Dog Teeth with Apical Periodontitis. *Journal of Endodontics*. **43**(8), pp.1279-1287.
- Parirokh, M. and Torabinejad, M. 2010. Mineral Trioxide Aggregate: A Comprehensive Literature Review—Part I: Chemical, Physical, and Antibacterial Properties. *Journal of Endodontics*. **36**(1), pp.16-27.
- Parry, S. and Strauss, J. F. 1998. Premature Rupture of the Fetal Membranes. *New England Journal of Medicine*. **338**(10), pp.663-670.
- Pashley, D. H., Walton, R. E. and Slavkin, H. C. 2008. Histology and Physiology of the Dental Pulp. In: INGLE, J. I. (ed.) *Ingle's Endodontics 6*. PMPH-USA.
- Petrino, J. A., Boda, K. K., Shambarger, S., Bowles, W. R. and McClanahan, S. B. 2010. Challenges in Regenerative Endodontics: A Case Series. *Journal of Endodontics*. **36**(3), pp.536-541.
- Pradhan, D. P., Chawla, H. S., Gauba, K. and Goyal, A. 2006. Comparative Evaluation of Endodontic Management of Teeth with Unformed Apices with Mineral Trioxide Aggregate and Calcium Hydroxide. *Journal of Dentistry for Children*. **73**(2), pp.79-85.
- Prasertsung, I., Kanokpanont, S., Bunaprasert, T., Thanakit, V. and Damrongsakkul, S. 2008. Development of Acellular Dermis from Porcine Skin Using Periodic Pressurized Technique. *Journal of Biomedical Materials Research Part B: Applied Biomaterials*. **85B**(1), pp.210-219.
- Prescott, R. S., Alsanea, R., Fayad, M. I., Johnson, B. R., Wenckus, C. S., Hao, J., et al., 2008. In Vivo Generation of Dental Pulp-Like Tissue by Using Dental Pulp Stem Cells, a Collagen Scaffold, and Dentin Matrix Protein 1 after

- Subcutaneous Transplantation in Mice. *Journal of Endodontics*. **34**(4), pp.421-426.
- Pruss, A., Kao, M., Kiesewetter, H., Von Versen, R. and Pauli, G. 1999. Virus Safety of Avital Bone Tissue Transplants: Evaluation of Sterilization Steps of Spongiosa Cuboids Using a Peracetic Acid–Methanol Mixture. *Biologicals*. **27**(3), pp.195-201.
- Qin, C., Brunn, J. C., Cadena, E., Ridall, A., Tsujigiwa, H., Nagatsuka, H., et al., 2002. The Expression of Dentin Sialophosphoprotein Gene in Bone. *Journal of Dental Research*. **81**(6), pp.392-394.
- Rafter, M. 2005. Apexification: A Review. *Dental Traumatology*. **21**(1), pp.1-8.
- Reing, J. E., Brown, B. N., Daly, K. A., Freund, J. M., Gilbert, T. W., Hsiong, S. X., et al., 2010. The Effects of Processing Methods Upon Mechanical and Biologic Properties of Porcine Dermal Extracellular Matrix Scaffolds. *Biomaterials*. **31**(33), pp.8626-8633.
- Remlinger, N. T., Wearden, P. D. and Gilbert, T. W. 2012. Procedure for Decellularization of Porcine Heart by Retrograde Coronary Perfusion. *Journal of Visualized Experiments*. (70), pp.e50059.
- Ricard-Blum, S. and Ruggiero, F. 2005. The Collagen Superfamily: From the Extracellular Matrix to the Cell Membrane. *Pathologie Biologie*. **53**(7), pp.430-442.
- Rich, L. and Whittaker, P. 2005. Collagen and Picrosirius Red Staining: A Polarized Light Assessment of Fibrillar Hue and Spatial Distribution. *Braz J Morphol Sci*. **22**(2), pp.97-104.
- Rieder, E., Kasimir, M.-T., Silberhumer, G., Seebacher, G., Wolner, E., Simon, P., et al., 2004. Decellularization Protocols of Porcine Heart Valves Differ Importantly in Efficiency of Cell Removal and Susceptibility of the Matrix to Recellularization with Human Vascular Cells. *The Journal of Thoracic and Cardiovascular Surgery*. **127**(2), pp.399-405.
- Rosa, V., Zhang, Z., Grande, R. H. M. and Nör, J. E. 2013. Dental Pulp Tissue Engineering in Full-Length Human Root Canals. *Journal of Dental Research*. **92**(11), pp.970-975.
- Rosario, D. J., Reilly, G. C., Ali Salah, E., Glover, M., Bullock, A. J. and MacNeil, S. 2008. Decellularization and Sterilization of Porcine Urinary Bladder Matrix for Tissue Engineering in the Lower Urinary Tract. *Regenerative Medicine*. **3**(2), pp.145–156.

Saghiri, M. A., Asatourian, A., Sorenson, C. M. and Sheibani, N. 2015. Role of Angiogenesis in Endodontics: Contributions of Stem Cells and Proangiogenic and Antiangiogenic Factors to Dental Pulp Regeneration. *Journal of Endodontics*. **41**(6), pp.797-803.

Sakai, V. T., Zhang, Z., Dong, Z., Neiva, K. G., Machado, M. A. A. M., Shi, S., et al., 2010. Shed Differentiate into Functional Odontoblasts and Endothelium. *Journal of Dental Research*. **89**(8), pp.791-796.

Saoud, T. M. A., Zaazou, A., Nabil, A., Moussa, S., Lin, L. M. and Gibbs, J. L. 2014. Clinical and Radiographic Outcomes of Traumatized Immature Permanent Necrotic Teeth after Revascularization/Revitalization Therapy. *Journal of Endodontics*. **40**(12), pp.1946-1952.

Sarris, S., Tahmassebi, J. F., Duggal, M. S. and Cross, I. A. 2008. A Clinical Evaluation of Mineral Trioxide Aggregate for Root-End Closure of Non-Vital Immature Permanent Incisors in Children-a Pilot Study. *Dental Traumatology*. **24**(1), pp.79-85.

Saunders, K. B. and D'Amore, P. A. 1992. An in Vitro Model for Cell-Cell Interactions. *In Vitro Cellular & Developmental Biology - Animal*. **28**(7), pp.521.

Saw, T. Y., Cao, T., Yap, A. U. J. and Lee Ng, M. M. 2005. Tooth Slice Organ Culture and Established Cell Line Culture Models for Cytotoxicity Assessment of Dental Materials. *Toxicology in Vitro*. **19**(1), pp.145-154.

Scarparo, R. K., Dondoni, L., Böttcher, D. E., Grecca, F. S., Rockenbach, M. I. B. and Batista, E. L. 2011. Response to Intracanal Medication in Immature Teeth with Pulp Necrosis: An Experimental Model in Rat Molars. *Journal of Endodontics*. **37**(8), pp.1069-1073.

Seddon, A. M., Curnow, P. and Booth, P. J. 2004. Membrane Proteins, Lipids and Detergents: Not Just a Soap Opera. *Biochimica et Biophysica Acta (BBA) - Biomembranes*. **1666**(1–2), pp.105-117.

Sejersen, T. and Lendahl, U. 1993. Transient Expression of the Intermediate Filament Nestin During Skeletal Muscle Development. *Journal of Cell Science*. **106**(4), pp.1291-1300.

Seltzer, J. L., Welgus, H. G., Jeffrey, J. J. and Eisen, A. Z. 1976. The Function of Ca²⁺ in the Action of Mammalian Collagenases. *Archives of Biochemistry and Biophysics*. **173**(1), pp.355-361.

Sengupta, P. 2013. The Laboratory Rat: Relating Its Age with Human's. *International Journal of Preventive Medicine*. **4**(6), pp.624-630.

Sensebé, L., Bourin, P. and Tarte, K. 2010. Good Manufacturing Practices Production of Mesenchymal Stem/Stromal Cells. *Human Gene Therapy*. **22**(1), pp.19-26.

Seo, B.-M., Miura, M., Gronthos, S., Mark Bartold, P., Batouli, S., Brahim, J., et al., 2004. Investigation of Multipotent Postnatal Stem Cells from Human Periodontal Ligament. *The Lancet*. **364**(9429), pp.149-155.

Shi, S. and Gronthos, S. 2003. Perivascular Niche of Postnatal Mesenchymal Stem Cells in Human Bone Marrow and Dental Pulp. *Journal of Bone and Mineral Research*. **18**(4), pp.696-704.

Shimizu, E., Ricucci, D., Albert, J., Alobaid, A. S., Gibbs, J. L., Huang, G. T. J., et al., 2013. Clinical, Radiographic, and Histological Observation of a Human Immature Permanent Tooth with Chronic Apical Abscess after Revitalization Treatment. *Journal of Endodontics*. **39**(8), pp.1078-1083.

Simon, S., Rilliard, F., Berdal, A. and Machtou, P. 2007. The Use of Mineral Trioxide Aggregate in One-Visit Apexification Treatment: A Prospective Study. *International Endodontic Journal*. **40**(3), pp.186-197.

Sloan, A. J., Colombo, J., Riberts, J., Waddington, R. J. and Ayre, W. N. 2017. Tissue Culture Models and Approaches for Dental Tissue Regeneration. In: WADDINGTON, R. J. and SLOAN, A. J. (eds.) *Tissue Engineering and Regeneration in Dentistry: Current Strategies*. John Wiley & Sons.

Sloan, A. J., Shelton, R. M., Hann, A. C., Moxham, B. J. and Smith, A. J. 1998. An in Vitro Approach for the Study of Dentinogenesis by Organ Culture of the Dentine–Pulp Complex from Rat Incisor Teeth. *Archives of Oral Biology*. **43**(6), pp.421-430.

Sloan, A. J. and Smith, A. J. 2007. Stem Cells and the Dental Pulp: Potential Roles in Dentine Regeneration and Repair. *Oral Diseases*. **13**(2), pp.151-157.

Sloan, A. J. and Waddington, R. J. 2009. Dental Pulp Stem Cells: What, Where, How? *International Journal of Paediatric Dentistry*. **19**(1), pp.61-70.

Song, J. J. and Ott, H. C. 2011. Organ Engineering Based on Decellularized Matrix Scaffolds. *Trends in Molecular Medicine*. **17**(8), pp.424-432.

Song, J. S., Takimoto, K., Jeon, M., Vadakekalam, J., Ruparel, N. B. and Diogenes, A. 2017. Decellularized Human Dental Pulp as a Scaffold for Regenerative Endodontics. *Journal of Dental Research*. **96**(6), pp.640-646.

Sonoyama, W., Liu, Y., Fang, D., Yamaza, T., Seo, B.-M., Zhang, C., et al., 2006. Mesenchymal Stem Cell-Mediated Functional Tooth Regeneration in Swine. *PLoS One*. **1**(1), pp.e79.

Sonoyama, W., Liu, Y., Yamaza, T., Tuan, R. S., Wang, S., Shi, S., et al., 2008. Characterization of the Apical Papilla and Its Residing Stem Cells from Human Immature Permanent Teeth: A Pilot Study. *Journal of Endodontics*. **34**(2), pp.166-171.

Sonoyama, W., Seo, B.-M., Yamaza, T. and Shi, S. 2007. Human Hertwig's Epithelial Root Sheath Cells Play Crucial Roles in Cementum Formation. *Journal of Dental Research*. **86**(7), pp.594-599.

Stapleton, T. W., Ingram, J., Katta, J., Knight, R., Korossis, S., Fisher, J., et al., 2008. Development and Characterization of an Acellular Porcine Medial Meniscus for Use in Tissue Engineering. *Tissue Engineering Part A*. **14**(4), pp.505-518.

Sun, W. Q. and Leung, P. 2008. Calorimetric Study of Extracellular Tissue Matrix Degradation and Instability after Gamma Irradiation. *Acta Biomaterialia*. **4**(4), pp.817-826.

Tan, L., Wang, J., Yin, S., Zhu, W., Zhou, G., Cao, Y., et al., 2015. Regeneration of Dentin-Pulp-Like Tissue Using an Injectable Tissue Engineering Technique. *RSC Advances*. **5**(73), pp.59723-59737.

Terling, C., Rass, A., Mitsiadis, T. A., Fried, K., Lendahl, U. and Wroblewski, J. 1995. Expression of the Intermediate Filament Nestin During Rodent Tooth Development. *International Journal of Developmental Biology*. **39**, pp.947 - 956.

Thesleff, I. and Åberg, T. 1999. Molecular Regulation of Tooth Development. *Bone*. **25**(1), pp.123-125.

Thesleff, I. and Sharpe, P. 1997. Signalling Networks Regulating Dental Development. *Mechanisms of Development*. **67**(2), pp.111-123.

Thibodeau, B. and Trope, M. 2007. Pulp Revascularization of a Necrotic Infected Immature Permanent Tooth: Case Report and Review of the Literature. *Pediatric Dentistry*. **29**(1), pp.47-50.

Thomson, A. and Kahler, B. 2010. Regenerative Endodontics—Biologically-Based Treatment for Immature Permanent Teeth: A Case Report and Review of the Literature. *Australian Dental Journal*. **55**(4), pp.446-452.

Thomson, J. A., Itskovitz-Eldor, J., Shapiro, S. S., Waknitz, M. A., Swiergiel, J. J., Marshall, V. S., et al., 1998. Embryonic Stem Cell Lines Derived from Human Blastocysts. *Science*. **282**(5391), pp.1145-1147.

Thonemann, B., Schmalz, G., Hiller, K. A. and Schweikl, H. 2002. Responses of L929 Mouse Fibroblasts, Primary and Immortalized Bovine Dental Papilla-Derived Cell Lines to Dental Resin Components. *Dental Materials*. **18**(4), pp.318-323.

Tomlinson, M. J., Dennis, C., Yang, X. B. and Kirkham, J. 2015. Tissue Non-Specific Alkaline Phosphatase Production by Human Dental Pulp Stromal Cells Is Enhanced by High Density Cell Culture. *Cell and Tissue Research*. **361**(2), pp.529-540.

Tong, H. J., Rajan, S., Bhujel, N., Kang, J., Duggal, M. and Nazzal, H. 2017. Regenerative Endodontic Therapy in the Management of Nonvital Immature Permanent Teeth: A Systematic Review-Outcome Evaluation and Meta-Analysis. *Journal of Endodontics*. **43**(9), pp.1453- 1464.

Torabinejad, M. and Abu-Tahun, I. 2010. Management of Teeth with Necrotic Pulps and Open Apices. *Endodontic Topics*. **23**(1), pp.105-130.

Torabinejad, M. and Chivian, N. 1999. Clinical Applications of Mineral Trioxide Aggregate. *Journal of Endodontics*. **25**(3), pp.197-205.

Torabinejad, M., Hong, C. U., McDonald, F. and Pitt Ford, T. R. 1995a. Physical and Chemical Properties of a New Root-End Filling Material. *Journal of Endodontics*. **21**(7), pp.349-353.

Torabinejad, M., Hong, C. U., Pitt Ford, T. R. and Kettering, J. D. 1995b. Cytotoxicity of Four Root End Filling Materials. *Journal of Endodontics*. **21**(10), pp.489-492.

Torabinejad, M., Nosrat, A., Verma, P. and Udochukwu, O. 2017. Regenerative Endodontic Treatment or Mineral Trioxide Aggregate Apical Plug in Teeth with Necrotic Pulps and Open Apices: A Systematic Review and Meta-Analysis. *Journal of Endodontics*. **In press**.

Traebert, J., de Lacerda, J. T., Foster Page, L. A., Thomson, W. M. and Bortoluzzi, M. C. 2012. Impact of Traumatic Dental Injuries on the Quality of Life of Schoolchildren. *Dental Traumatology*. **28**(6), pp.423-428.

Traphagen, S. B., Furligas, N., Xylas, J. F., Sengupta, S., Kaplan, D. L., Georgakoudi, I., et al., 2012. Characterization of Natural, Decellularized and Reseeded Porcine Tooth Bud Matrices. *Biomaterials*. **33**(21), pp.5287-5296.

Trope, M. 2008. Regenerative Potential of Dental Pulp. *Journal of Endodontics*. **34**(7), pp.S13-S17.

Twati, W., Wood, D., Liskiewicz, T. and Duggal, M. 2009a. Effect of Nonsetting Calcium Hydroxide and MTA on Human Dentine Following Long Term Application. *International Journal of Paediatric Dentistry*. **19**(S1), pp.43 (abstract O16-117).

Twati, W., Wood, D., Liskiewicz, T., Willmott, N. and Duggal, M. 2009b. An Evaluation of the Effect of Non-Setting Calcium Hydroxide on Human Dentine: A Pilot Study. *European Archives of Paediatric Dentistry*. **10**(2), pp.104-109.

van Amerongen, J. P., Lemmens, I. G. and Tonino, G. J. M. 1983. The Concentration, Extractability and Characterization of Collagen in Human Dental Pulp. *Archives of Oral Biology*. **28**(4), pp.339-345.

van Amerongen, J. P., Lemmens, I. G. and Tonino, G. J. M. 1984. Immunofluorescent Localization and Extractability of Fibronectin in Human Dental Pulp. *Archives of Oral Biology*. **29**(2), pp.93-99.

van Beurden, H. E., Von den Hoff, J. W., Torensma, R., Maltha, J. C. and Kuijpers-Jagtman, A. M. 2005. Myofibroblasts in Palatal Wound Healing: Prospects for the Reduction of Wound Contraction after Cleft Palate Repair. *Journal of Dental Research*. **84**(10), pp.871-880.

Veis, A. and Goldberg, M. 2014. Pulp Extracellular Matrix. *In: GOLDBERG, M. (ed.) The Dental Pulp*. Berlin: Springer.

Waddington, R. J. and Sloan, A. J. 2017. Research Advances in Tissue Regeneration by Dental Pulp Stem Cells. *In: WADDINGTON, R. J. and SLOAN, A. J. (eds.) Tissue Engineering and Regeneration in Dentistry: Current Strategies*. John Wiley & Sons.

Walia, T., Singh Chawla, H. and Gauba, K. 2001. Management of Wide Open Apices in Non-Vital Permanent Teeth with Ca (OH) 2 Paste. *Journal of Clinical Pediatric Dentistry*. **25**(1), pp.51-56.

Wall, I., Thompson, D., Peticone, C. and Perez, R. 2017. Industrial Translation Requirements for Manufacture of Stem Cell-Derived and Tissue-Engineered Products. *In: WADDINGTON, R. J. and SLOAN, A. J. (eds.) Tissue Engineering and Regeneration in Dentistry: Current Strategies*. John Wiley & Sons.

Wang, J., Liu, X., Jin, X., Ma, H., Hu, J., Ni, L., et al., 2010a. The Odontogenic Differentiation of Human Dental Pulp Stem Cells on Nanofibrous Poly(L-Lactic Acid) Scaffolds in Vitro and in Vivo. *Acta Biomaterialia*. **6**(10), pp.3856-3863.

Wang, X., Thibodeau, B., Trope, M., Lin, L. M. and Huang, G. T. J. 2010b. Histologic Characterization of Regenerated Tissues in Canal Space after the Revitalization/Revascularization Procedure of Immature Dog Teeth with Apical Periodontitis. *Journal of Endodontics*. **36**(1), pp.56-63.

Wigler, R., Kaufman, A. Y., Lin, S., Steinbock, N., Hazan-Molina, H. and Torneck, C. D. 2013. Revascularization: A Treatment for Permanent Teeth With necrotic Pulp and Incomplete Root Development. *Journal of Endodontics*. **39**(3), pp.319-326.

Williams, D. F. 2008. On the Mechanisms of Biocompatibility. *Biomaterials*. **29**(20), pp.2941-2953.

Wilshaw, S. P., Kearney, J., Fisher, J. and Ingham, E. 2008. Biocompatibility and Potential of Acellular Human Amniotic Membrane to Support the Attachment and Proliferation of Allogeneic Cells. *Tissue Engineering Part A*. **14**(4), pp.463-472.

Wilshaw, S. P., Kearney, J. N., Fisher, J. and Ingham, E. 2006. Production of an Acellular Amniotic Membrane Matrix for Use in Tissue Engineering. *Tissue Engineering*. **12**(8), pp.2117-2129.

Wilshaw, S. P., Rooney, P., Berry, H., Kearney, J. N., Homer-Vanniasinkam, S., Fisher, J., et al., 2012. Development and Characterization of Acellular Allogeneic Arterial Matrices. *Tissue Engineering Part A*. **18**(5-6), pp.471-483.

Witherspoon, D. E., Small, J. C., Regan, J. D. and Nunn, M. 2008. Retrospective Analysis of Open Apex Teeth Obturated with Mineral Trioxide Aggregate. *Journal of Endodontics*. **34**(10), pp.1171-1176.

Wong, M. L. and Griffiths, L. G. 2014. Immunogenicity in Xenogeneic Scaffold Generation: Antigen Removal Vs. Decellularization. *Acta Biomaterialia*. **10**(5), pp.1806-1816.

Woods, T. and Gratzner, P. F. 2005. Effectiveness of Three Extraction Techniques in the Development of a Decellularized Bone–Anterior Cruciate Ligament–Bone Graft. *Biomaterials*. **26**(35), pp.7339-7349.

Xu, C. C., Chan, R. W. and Tirunagari, N. 2007. A Biodegradable, Acellular Xenogeneic Scaffold for Regeneration of the Vocal Fold Lamina Propria. *Tissue Engineering*. **13**(3), pp.551-566.

Yabe, J. T., Chan, W. K. H., Wang, F.-S., Pimenta, A., Ortiz, D. D. and Shea, T. B. 2003. Regulation of the Transition from Vimentin to Neurofilaments During Neuronal Differentiation. *Cell Motility and the Cytoskeleton*. **56**(3), pp.193-205.

Yamauchi, N., Yamauchi, S., Nagaoka, H., Duggan, D., Zhong, S., Lee, S. M., et al., 2011. Tissue Engineering Strategies for Immature Teeth with Apical Periodontitis. *Journal of Endodontics*. **37**(3), pp.390-397.

Yang, S., Leong, K.-F., Du, Z. and Chua, C.-K. 2001. The Design of Scaffolds for Use in Tissue Engineering. Part I. Traditional Factors. *Tissue Engineering*. **7**(6), pp.679-689.

Yoeruek, E., Bayyoud, T., Maurus, C., Hofmann, J., Spitzer, M. S., Bartz-Schmidt, K. U., et al., 2012. Decellularization of Porcine Corneas and Repopulation with Human Corneal Cells for Tissue-Engineered Xenografts. *Acta Ophthalmologica*. **90**(2), pp.e125-e131.

Yoshida, N., Yoshida, K., Ohkura, N., Shigetani, Y., Takei, E., Hosoya, A., et al., 2012. Immunohistochemical Analysis of Two Stem Cell Markers of A-Smooth Muscle Actin and Stro-1 During Wound Healing of Human Dental Pulp. *Histochemistry and Cell Biology*. **138**(4), pp.583-592.

Yoshiki, S. and Kurahashi, Y. 1971. A Light and Electron Microscopic Study of Alkaline Phosphatase Activity in the Early Stage of Dentinogenesis in the Young Rat. *Archives of Oral Biology*. **16**(10), pp.1143-1145.

Yu, C. and Abbott, P. V. 2007. An Overview of the Dental Pulp: Its Functions and Responses to Injury. *Australian Dental Journal*. **52**, pp.S4-S6.

Yuan, Z., Nie, H., Wang, S., Lee, C. H., Li, A., Fu, S. Y., et al., 2011. Biomaterial Selection for Tooth Regeneration. *Tissue Engineering Part B: Reviews*. **17**(5), pp.373-388.

Yuasa, K., Fukumoto, S., Kamasaki, Y., Yamada, A., Fukumoto, E., Kanaoka, K., et al., 2004. Laminin A2 Is Essential for Odontoblast Differentiation Regulating Dentin Sialoprotein Expression. *Journal of Biological Chemistry*. **279**(11), pp.10286-10292.

Zhang, Q., Shi, S., Liu, Y., Uyanne, J., Shi, Y., Shi, S., et al., 2009. Mesenchymal Stem Cells Derived from Human Gingiva Are Capable of Immunomodulatory Functions and Ameliorate Inflammation-Related Tissue Destruction in Experimental Colitis. *The Journal of Immunology*. **183**(12), pp.7787-7798.

Zhang, W., Frank Walboomers, X., van Kuppevelt, T. H., Daamen, W. F., Bian, Z. and Jansen, J. A. 2006a. The Performance of Human Dental Pulp Stem Cells on Different Three-Dimensional Scaffold Materials. *Biomaterials*. **27**(33), pp.5658-5668.

Zhang, W., Vazquez, B., Oreadi, D. and Yelick, P. C. 2017. Decellularized Tooth Bud Scaffolds for Tooth Regeneration. *Journal of Dental Research*. **96**(5), pp.516-523.

Zhang, W., Walboomers, X. F., Shi, S., Fan, M. and Jansen, J. A. 2006b. Multilineage Differentiation Potential of Stem Cells Derived from Human Dental Pulp after Cryopreservation. *Tissue Engineering*. **12**(10), pp.2813-2823.

Zhu, X., Zhang, C., Huang, G. T. J., Cheung, G. S. P., Dissanayaka, W. L. and Zhu, W. 2012. Transplantation of Dental Pulp Stem Cells and Platelet-Rich Plasma for Pulp Regeneration. *Journal of Endodontics*. **38**(12), pp.1604-1609.

Appendices

Appendix (A): Tissue bank approval form for teeth collection and the use of dental pulp stem cells.



Tissue Sample Form for School of Dentistry Research Tissue Bank

Applicant: Manal Matoug-Elwerfelli

DREC No: 101013/MME/113

Research Tissue:

Bank ID No:.....
Age of patient (time of collection):.....
Sex:
Ethnic Origin:.....
Signed (Recipient):
Signed (Supplier):.....
Date sample taken:.....

Please ensure Bank ID number is recorded on all samples created from tissue received from the LDI Tissue Bank.

This is a requirement of the Human Tissue Act. By receiving tissue from the bank you are agreeing to abide by the HTA regulations.

Useful links:

<http://www.hta.gov.uk/> Human Tissue Authority website

http://www.opsi.gov.uk/acts/acts2004/ukpga_20040030_en_1 Human Tissue Act 2004

Appendix (B): Percentage of pulp tissue water content

Pulp tissue wet weight	Pulp tissue dry weight	Percentage of water content
13.15 mg	4.2 mg	68.06 %
14.81 mg	4.05 mg	72.65 %
12.85 mg	3.22 mg	74.94 %
13.82 mg	4.9 mg	64.54 %
11.82 mg	3.92 mg	66.83 %
10.65 mg	3.15 mg	70.42 %
10.50 mg	3.15 mg	69.01 %
11.55 mg	3.66 mg	68.31 %

Appendix (C): National and international poster/oral presentations and awards achieved.

Poster awards:

Image A1: Matoug-Elwerfelli, Monty Duggal, El-Mostafa Raif, Stacey-Paul Wilshaw, Hani Nazzal (2017). *A biocompatible acellular extracellular matrix scaffold for regenerative endodontics*. Arabian Academy of Paediatric Dentistry (ArAcPD) Cairo congress. Prof Monty Duggal Trauma Award-first prize.

Image A2: Manal Matoug-Elwerfelli, Hani Nazzal, Monty Duggal, Filomena Esteves, El-Mostafa Raif (2016). *Decellularised dental pulp as a suitable scaffold for regenerative endodontic techniques*. School Of Dentistry Research day, University of Leeds, UK. Awarded-first prize.

Image A3: Manal Matoug-Elwerfelli, Hani Nazzal, Monty Duggal, Jennifer Graham, El-Mostafa Raif (2015). *Decellularisation of dental pulp for use as a scaffold in regenerative endodontics*. International Association of Paediatric Dentistry (IAPD), Glasgow congress. NuSmile Restorative Dentistry Research Award-first prize, combined oral and poster presentation.

Presentation awards:

Oral presentation: Manal Matoug-Elwerfelli, Hani Nazzal, Monty Duggal, Filomena Esteves, Mostafa El-Raif (2016). *Decellularised dental pulp as a suitable scaffold for regenerative endodontic techniques*. European Academy of Paediatric Dentistry (EAPD), Belgrade congress. Young Researcher of the Year Award-first prize

Other presentations/posters:

Oral presentation: Manal Matoug-Elwerfelli, El-Mostafa Raif, Hani Nazzal, Filomena Esteves, Monty Duggal (2015). *Decellularisation of dental pulp for use as a scaffold in regenerative endodontics*. School Of Dentistry Research day, University of Leeds, UK.

Image A4: Manal Matoug-Elwerfelli, Hani Nazzal, Monty Duggal, Jennifer Graham, El-Mostafa Raif (2015). *Developing an acellular dental pulp scaffold*. LIMMs Symposium, University of Leeds, UK.

A Biocompatible Acellular Extracellular Matrix Scaffold For Regenerative Endodontics

Matoug-Elwerfelli M¹, Duggal M², Raif EM¹, Wilshaw S-P³, Nazzal H⁴

¹Department of Oral Biology, University of Leeds, UK. ²Discipline of Orthodontics and Paediatric Dentistry, National University Singapore, Singapore. ³Faculty of Biological sciences, University of Leeds, U.K. ⁴Department of Paediatric Dentistry, University of Leeds, UK.

INTRODUCTION

- Our previous work has shown that the extracellular matrix components were preserved following decellularisation of the human dental pulp tissues (Matoug-Elwerfelli *et al.*, 2015).
- Therefore, further assessment of the acellular scaffold biocompatibility is needed to evaluate the feasibility for future clinical use in regenerative endodontic techniques.

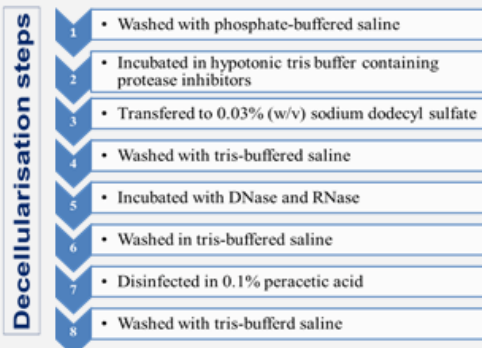


AIM

The aim of this work is to assess the acellular human scaffold biocompatibility and ability to support human dental pulp stem cells (HDPSCs) attachment and growth.

METHODS

Following informed patient consent and ethical approval, human dental pulps, retrieved from sound permanent premolar teeth, were decellularised as below:



Biocompatibility assessment

- Contact cytotoxicity assay was assessed using mouse fibroblast cell line (L929) in direct contact with the acellular scaffold (n=4) for 48 hours.
- Extract cytotoxicity assay was assessed by incubation of L929 cells with acellular scaffold extracts (n=4) and measurement of relative cellular adenosine triphosphate (ATP) activity using ATPLite™ assay.
- Further cell viability was assessed using Live/Dead® staining of dynamically seeded acellular scaffolds (n=3). Scaffolds were seeded with HDPSCs in standard culture medium for two weeks.

RESULTS

1. Contact cytotoxicity assay

Acellular scaffolds were found to be biocompatible. Cells proliferated up to and in contact with acellular scaffolds, no change in cell morphology was observed (Figure 1).

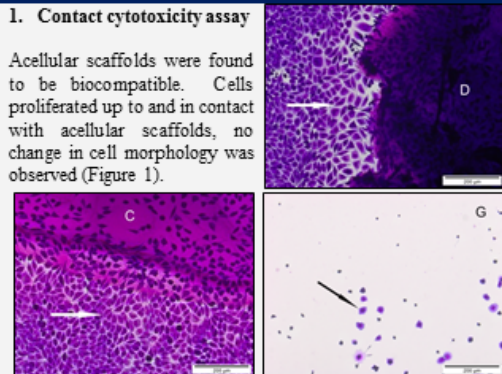


Figure 1: Photomicrographs illustrating contact cytotoxicity assay cultured with L929 cell line for 48 hours and stained with Giemsa stain. Decellularised human pulp tissue (D) and collagen gel (C; negative control) showed no cytotoxicity with cell growth and proliferation (white arrow). Cyanoacrylate glue (G; positive control) showed cytotoxicity with cell lysis and necrosis (black arrow).

2. Extract cytotoxicity assay

No significant differences in cellular ATP activity were found following incubation in acellular scaffold extracts in comparison to DMEM (negative control) (Figure 2).

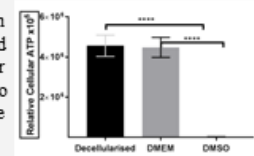


Figure 2: Relative cellular ATP content of L929 cells incubated in decellularised tissue extracts, DMEM (negative control) and DMSO (positive control) following 24 hour culture. Data represents mean values \pm 95% confidence limits. Analysis revealed no significance difference between decellularised extracts and DMEM (ANOVA, $p > 0.05$) and significance in comparison to DMSO (**** $p < 0.0001$).

3. Live/Dead® assay

Confocal laser imaging showed HDPSCs colonising the acellular scaffold, a high majority of live (green) cells was seen following two weeks culture. Therefore, the scaffold was able to support HDPSCs attachment and growth (Figure 3).

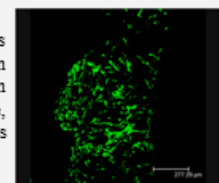


Figure 3: Photomicrographs of acellular scaffolds seeded with HDPSCs and stained with Live/Dead®. Images show large areas of staining with calcein-AM (green, live cells) and minimal areas of staining with ethidium homodimer (red, dead cells) on the scaffold.

CONCLUSIONS

The decellularisation technique resulted in a biocompatible scaffold. Further *in-Vivo* studies are needed to confirm these results before translation to clinical practice.

ACKNOWLEDGMENTS

Extended thanks goes to Filomena Esteves, Ali Maria, Rachel Bell the Libyan Embassy and the Academy of Medical Sciences for their valuable support.

REFERENCES

Matoug-Elwerfelli M, H Nazzal, J Graham, M Duggal and E Raif (2015). Decellularisation of dental pulp for use as a scaffold in regenerative endodontics. Abstracts from the 25th Congress of the International Journal of Paediatric Dentistry. Glasgow, UK. 25: 70.

Decellularised dental pulp as a suitable scaffold for regenerative endodontic techniques



UNIVERSITY OF LEEDS

Manal Matoug-Elwerfelli¹, Hani Nazzal², Monty Duggal², Filomena Esteves³, El-Mostafa Raif¹

1- Department of Oral Biology, 2- Department of Paediatric Dentistry, University of Leeds, UK.
3- Leeds Institute of Cancer and Pathology, St James University Hospital, Leeds, UK.

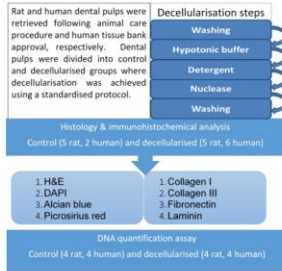
BACKGROUND

The early optimism regarding regenerative endodontic techniques for non-vital immature teeth has now faded. These techniques are unlikely to be successful unless basic principles of tissue engineering are followed and implemented in their clinical management. To date, the ideal scaffold for dentine-pulp complex regeneration has not been identified.

AIM

Assess the feasibility of decellularising human dental pulp tissues for use as a scaffold in regenerative endodontic techniques.

METHODS



RESULTS

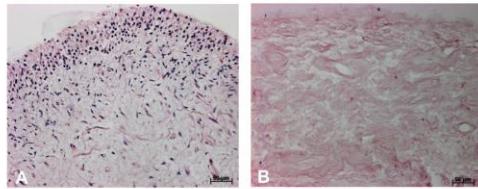


Figure 1: Photomicrographs illustrating a comparison between H&E stained control and study human pulp tissues. (A) Control tissues showing a dense cell population within an ECM. (B) Study tissues showing an acellular porous matrix after decellularisation. Similar results were seen in rat tissues.

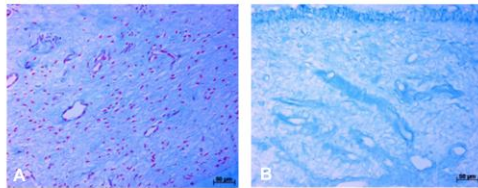


Figure 2: Photomicrographs illustrating a comparison between alcian blue stained control and study human pulp tissues. (A) Control tissues showing normal appearance of acidic polysaccharides. (B) Study tissues showing preservation of polysaccharides after decellularisation. Similar results were seen in rat tissues.

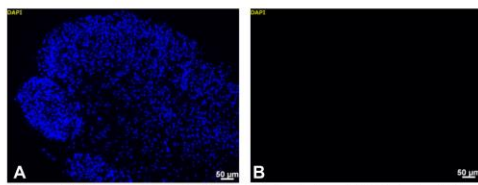


Figure 3: Photomicrographs illustrating a comparison between DAPI stained control and study human pulp tissues. (A) Control tissues showing a highly cellular tissue (nuclei stained blue). (B) Study tissues with no whole nuclei present. Similar results were seen in rat tissues.

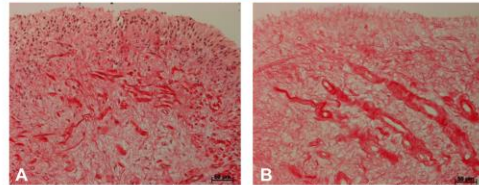


Figure 4: Photomicrographs illustrating a comparison between picrosirius red stained control and study human pulp tissues. (A) Control tissues showing a porous rich collagen structure. (B) Study tissues showing preservation of collagen structure after decellularisation. Similar results were seen in rat tissues.

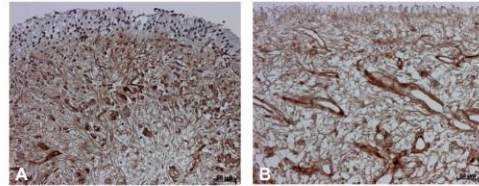


Figure 5: Photomicrographs of immunohistochemically stained control and study human pulp tissues labelled using a monoclonal antibody against collagen type I. (A) Control tissues showing a rich collagen type I matrix. (B) Study tissues showing preservation of collagen type I fibres after decellularisation. Similar results were seen in rat tissues.

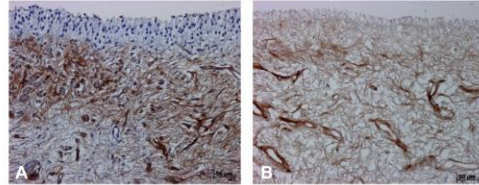
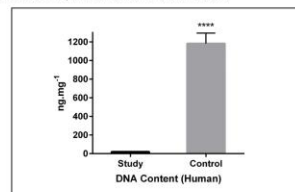


Figure 6: Photomicrographs of immunohistochemically stained control and study human pulp tissues labelled using a monoclonal antibody against collagen type III. (A) Control tissues showing a dense collagen type III matrix. (B) Study tissues showing preservation of collagen type III fibres after decellularisation. Similar results were seen with fibronectin & Laminin (images not shown) in both human and rat tissues.



Graph 1: DNA content of fresh and decellularised human dental pulp tissues (n=8). Average mean DNA content in the decellularised pulp tissue was 23.00±1.430 ng/mg in comparison to 1765±20.66 ng/mg in the control pulp tissue. Results indicate that there was a greater than 98.4% reduction in DNA content (*P* value < 0.0001). Similar results were seen in rat tissues.

CONCLUSION

This study shows promising results with regards to decellularising dental pulp tissues and producing an acellular pulp matrix with preserved extracellular structure and composition. In the future this scaffold could be seeded with stem cells for the regeneration of the dentine-pulp complex.

REFERENCES

Wilshaw, S. P., Kearney, J. N., Fisher, J. & Ingham, E. 2006. Production of an acellular amniotic membrane matrix for use in tissue engineering. *Tissue engineering*, 12, 2117-2129.

DECELLULARISATION OF DENTAL PULP FOR USE AS A SCAFFOLD IN REGENERATIVE ENDODONTICS

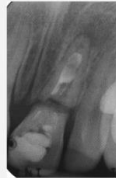


Manal Matoug-Elwerfelli¹, Hani Nazzal², Jennifer Graham³, Monty Duggal², El Mostafa Raif¹

CLINICAL PROBLEM

The current endodontic management techniques for non-vital immature teeth is associated with poor long term prognosis and a high risk for cervical root fractures.

The early optimism regarding regenerative endodontic techniques for non-vital immature has now faded, with unpredictable results especially with regards to continuation of root development and increase dentine thickness.



These are unlikely to be successful unless basic principles of tissue engineering are followed and implemented in their clinical management.

Novel tissue engineering approaches to produce a biocompatible acellular extracellular matrix through decellularisation of a complete pulp tissue could serve as an ideal scaffold that could be seeded with stem cells to facilitate pulp-dentine regeneration and treatment outcomes.

AIM

To develop an acellular dental pulp scaffold in order to produce an effective extracellular matrix that is able to promote and facilitate regeneration of pulp-dentine complex for non-vital immature teeth.

MATERIAL AND METHODS

Human dental pulp tissues were retrieved. The study pulp tissue was decellularised using a well established decellularisation protocol by Wilshaw and co-workers (2006), while the control pulp tissue was left untreated.

Histological sections were then prepared and stained using hematoxylin and eosin, picrosirius red, alcian blue and 4',6-diamidino-2-phenylindole (DAPI) stain in order to assess tissue histological architecture, collagen distribution, glycosaminoglycans (GAGs) and DNA detection respectively.

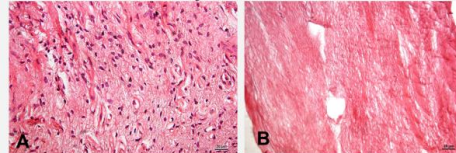
Decellularisation steps	1	Washed with phosphate-buffered saline
	2	Hypotonic tris buffer with protease inhibitors
	3	Transferred to 0.03% (w/v) sodium dodecyl sulfate
	4	Washed with tris-buffered saline
	5	Incubated with DNase and RNase
	6	Washed in tris-buffered saline

RESULTS

The decellularised pulp showed a well preserved acellular tissue structure with no obvious disruption to the overall matrix histological architecture and no whole nuclei were identified following decellularisation.

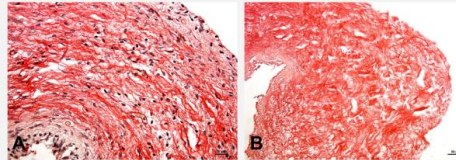
HISTOLOGICAL ASSESSMENT

Hematoxylin and eosin stain



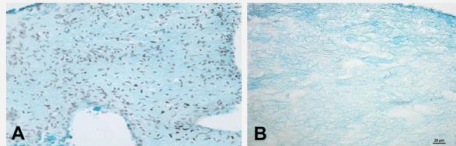
(A) Control tissues showing a highly cellular tissue (nuclei stained purple and extracellular matrix stained pink).
(B) Study tissues showing an acellular porous matrix after decellularisation.

Picrosirius red stain



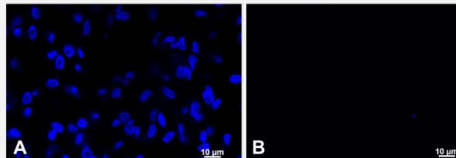
(A) Control tissues showing cellular material within a collagen structure (nuclei stained purple and collagen stained red).
(B) Study tissues after decellularisation showing no cellular material but preservation of collagen structure.

Alcian blue stain



(A) Control tissues showing normal appearance of GAGs in a highly cellular tissue.
(B) Study tissues showing preservation of GAGs within an acellular matrix after decellularisation.

DAPI stain



(A) Control tissues showing a highly cellular tissue (nuclei stained blue).
(B) Study tissues with no whole nuclei present.

CONCLUSION

The decellularisation technique used showed promising results with regards to eliminating cellular materials while maintaining the extracellular matrix needed for stem cell growth and differentiation. Further development of this method could provide a simple, safe, effective and a clinically usable scaffold for regeneration of the pulp-dentine complex.

ACKNOWLEDGMENTS

Mrs Jackie Hudson for histology training and Sarah Perry for obtaining DAPI images. Many thanks to Libyan Embassy for funding this project.

Image A4

School of Dentistry
 FACULTY OF MEDICINE AND HEALTH

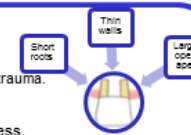

UNIVERSITY OF LEEDS

Developing an acellular dental pulp scaffold

Manal Matoug-Ewerfell¹, Hanl Nazza², Jennifer Graham³, Monty Duggal², El Mostafa Raifi¹
¹Oral Biology, School of Dentistry, University of Leeds, LS2 9LU, UK
²Paediatric Dentistry, School of Dentistry, University of Leeds, LS2 9LU, UK
³Department of Histopathology, University of Leeds, LS2 9LU, UK

BACKGROUND

- > Developmentally, when teeth erupt into the oral cavity the root formation is far from complete. This on average takes approximately 3 years for root to complete its growth.
- > Unfortunately, root development can be interrupted following pulp tissue necrosis as a result of caries or dental trauma.
- > These non-vital teeth are termed immature and pose a difficult challenge to the clinician.
- > The current regenerative endodontic techniques of non-vital immature teeth offer less than an ideal approach, with unpredictable results especially with regards to continuation of root development and increase dentin thickness.
- > With greater knowledge and improvements within the field of tissue engineering, novel approaches to produce a biocompatible acellular extracellular matrix through decellularisation process could be developed to improve treatment outcome.



AIM

To develop an acellular dental pulp scaffold

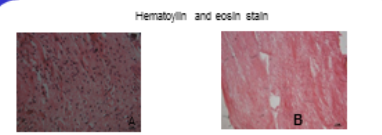
METHODS

Two human dental pulp tissues were extracted. The study pulp tissue was decellularised using a well-established decellularisation protocol (Wilshaw *et al*, 2006), while the control pulp tissue was left untreated. Histological sections were then prepared and stained using hematoxylin and eosin, alcian blue, picrosirius red and 4',6-diamidino-2-phenylindole (DAPI) stain in order to assess tissue histological architecture, GAG content, collagen distribution, DNA detection respectively.

RESULTS

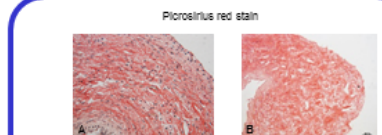
The decellularised tissue showed well preserved acellular tissue structure with no obvious disruption to the overall matrix histological architecture and no whole nuclei following decellularisation.

Hematoxylin and eosin stain



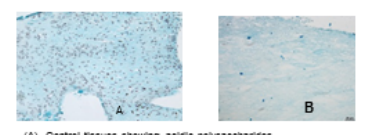
(A) Control tissue showing a highly cellular tissue.
(B) Study tissues showing an acellular porous tissue.

Picrosirius red stain



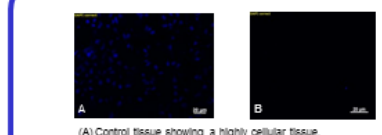
(A) Control tissue showing a porous collagen structure.
(B) Study tissue showing preservation of collagen structure.

Alcian blue stain



(A) Control tissues showing acidic polysaccharides.
(B) Study tissues showing preservation of acidic polysaccharides.

DAPI stain



(A) Control tissue showing a highly cellular tissue.
(B) Study tissues showing no whole nuclei are present.

CONCLUSION

The decellularisation technique used showed promising results with regards to eliminating cellular materials while maintaining the extracellular matrix needed for stem cell growth and differentiation.

FUTURE WORK

- > Immunohistochemistry analysis
- > Collagen and GAG analysis
- > In vitro biocompatibility assays
- > Cell seeding of new scaffold

ACKNOWLEDGMENTS

Mrs Jackie Hudson for histology training and Sarah Perry for obtaining DAPI Images.

REFERENCES

WILSHAW, B.P., KEARNEY, J.N., FISHER, J. & INGHAM, E. 2006. Production of an acellular amniotic membrane matrix for use in tissue engineering. *Tissue engineering*, 12, 2117-2129.